2020

Toward the Mechanism Underlying Latanoprost- and Benzalkonium Chloride-Induced Meibomian Gland Dysfunction in Patients Treated for Glaucoma

Jillian Ziemanski
University of Alabama at Birmingham

TOWARD THE MECHANISM UNDERLYING LATANOPROST- AND BENZALKONIUM CHLORIDE-INDUCED MEIBOMIAN GLAND DYSFUNCTION IN PATIENTS TREATED FOR GLAUCOMA

by

JILLIAN F. ZIEMANSKI

KELLY K. NICHOLS, COMMITTEE CHAIR
JIANZHONG CHEN
JASON J. NICHOLS
STEVEN PITTLER
MARK WILLCOX

A DISSERTATION

Submitted to the graduate faculty of The University of Alabama at Birmingham,
in partial fulfillment of the requirements for the degree of
Doctor of Philosophy

BIRMINGHAM, ALABAMA

2020

TOWARD THE MECHANISM UNDERLYING LATANOPROST- AND BENZALKONIUM CHLORIDE-INDUCED MEIBOMIAN GLAND DYSFUNCTION IN PATIENTS TREATED FOR GLAUCOMA

JILLIAN F. ZIEMANSKI

VISION SCIENCE GRADUATE PROGRAM

ABSTRACT

Once thought to be no more than a vexing eye condition, ocular surface disease (OSD) is now being viewed as a differentiating factor between sight and no sight. In the setting of glaucoma, OSD can interfere with treatment success, potentially allowing the visually devastating pathology of glaucoma to plow onward with little restraint. Compounding the clinical challenge is the growing awareness that glaucoma-associated OSD appears to be iatrogenically induced by topical ophthalmic medications. Daily, topical instillation of preserved prostaglandin analogs (PGAs), the most common first-line treatment for glaucoma, has been linked to a variety of OSD subtypes, including meibomian gland dysfunction (MGD). The mechanisms that underlie these associations are poorly understood.

The purpose of this dissertation project was to test the hypothesis that prostaglandins (PGE_2 and $PGF_{2\alpha}$), a representative PGA (latanoprost), and its preservative system (benzalkonium chloride [BAK]) impose cytotoxic effects on and modulate lipid expression from immortalized human meibomian gland epithelial cells (HMGECs). To accomplish these goals, experimental methodology needed to be refined to optimize nonpolar lipid extraction from cell lysates, to adapt harvesting protocols to

improve efficiency, and to test the differentiating capacity (as measured by lipidomic expression) of purported differentiating agents.

Chapter One provides a comprehensive overview of background information pertinent to glaucoma-associated MGD and presents pilot work that supports the design of this project. Chapters Two through Four describe the development of experimental methodology specific to lipid analysis from HMGECs. Chapters Five and Six, building upon this formative work, apply these methods to the crux of this research project: elucidating the mechanisms of iatrogenic MGD in glaucoma. Chapter Five evaluates the physiologic effects of PGE_2 and $PGF_{2\alpha}$ on HMGEC viability and lipid expression. Chapter Six explores the pathophysiologic effects of latanoprost, BAK, and the combination of the two on the same parameters. The final chapter, Chapter Seven, summarizes and integrates the results of this work, placing it within the context of current literature. Chapter Seven, as well as this dissertation as a whole, closes with forward-looking statements, new hypotheses, new research directions, and applications to clinical practice.

Keywords: glaucoma, meibomian gland dysfunction, ocular surface disease, prostaglandins, latanoprost, benzalkonium chloride

DEDICATION

For Marshall—*You are the sunshine of my every day.*

For Brooklyn—*You can.*

ACKNOWLEDGMENTS

First, I would like to thank my advisor, Kelly Nichols, for her guidance and support over the (many) years. There are few people for whom I would uproot my life and move to another state, let alone do it twice. The decision to follow her across institutions has allowed me to reach new heights professionally and personally. I am both grateful and honored to have been able to learn from her how to excel as a clinician scientist, faculty member, leader, and working mom. Above all else, I am thankful for her friendship, the early-morning runs, and the celebration of milestones. *Thank you.*

I would also like to thank Jason Nichols, an unofficial co-mentor yet official committee member, for always broadening my perspective, for occasionally challenging me when I didn't want to be challenged, and motivating me—even when he didn't realize it—to be better. I appreciate each of my committee members and acknowledge their contribution to this work, even beyond what is listed here: Jianzhong Chen for his expertise in lipidomics and mass spectrometry, Steve Pittler for his expertise with fluorescent microscopy and image processing, and Mark Willcox for his broad topical expertise in nearly every aspect of dry eye disease that I am interested in. I am fortunate to have had the support of this group to shape me throughout this process.

Special recognition is owed to former lab mates, William Ngo and Shyam Panthi, for their selfless assistance in the lab with tasks that a pregnant lady was forbidden to do.

I am grateful for Landon Wilson and Steve Barnes for their technical and analytical expertise with mass spectrometry. Without their involvement, this project would not have been possible. I am thankful for Jose Luis Roig-Lopez for his constant willingness to teach and help troubleshoot.

I would also like to thank my first and forever best friend, Sharon Meadows, for being the best mom and Mimi around. This dissertation wouldn't have come to fruition in the middle of a global pandemic without her willingness to drive from several states away to care for and play with her granddaughter. Brooklyn and I adore you.

Lastly, on a more personal note, I am beyond grateful for the amazing support of my incredible husband, Marshall. He has walked through many stages of this PhD with me. Whether it was keeping me company during mundane lab tasks, lending an ear at the end of trying days, inviting me on walks to get some fresh air, cooking me (very) impressive dinners, or taking on nearly all childcare responsibilities, he has been a constant source of encouragement and has made this PhD journey borderline pleasurable. I truly am thankful for you and everything you do for our family each day. And to our baby girl, your sweet giggles and tight hugs around the neck were a much-needed respite after long days in the lab, hours upon hours of data analysis, and hard-fought pages. When the words didn't come, you always did, exuding your innocence and lightness, allowing me to realign, refocus, and resume. You two make everything worthwhile.

TABLE OF CONTENTS

LIST OF TABLES

Table *Page*

CHAPTER ONE: INTRODUCTION

CHAPTER THREE: SATURATION OF CHOLESTERYL ESTERS PRODUCED BY HUMAN MEIBOMIAN GLAND EPITHELIAL CELLS AFTER TREATMENT WITH ROSIGLITAZONE

CHAPTER FOUR: TRIACYLGLYCEROL LIPIDOME FROM HUMAN MEIBOMIAN GLAND EPITHELIAL CELLS: DESCRIPTION, RESPONSE TO CULTURE CONDITIONS, AND PERSPECTIVE ON FUNCTION

LIST OF FIGURES

Figure *Page*

CHAPTER ONE: INTRODUCTION

CHAPTER TWO: EVALUATION OF CELL HARVESTING TECHNIQUES TO OPTIMIZE LIPIDOMIC ANALYSIS FROM HUMAN MEIBOMIAN GLAND EPITHELIAL CELLS IN CULTURE

CHAPTER SEVEN: DISCUSSION

CHAPTER ONE: INTRODUCTION

Once thought to be no more than a vexing eye condition, ocular surface disease (OSD) is now being viewed as a differentiating factor between sight and no sight. In the setting of glaucoma, OSD can interfere with treatment success,[1] potentially allowing the visually devastating pathology of glaucoma to plow onward with little restraint. Compounding the clinical challenge is the growing awareness that glaucoma-associated OSD appears to be iatrogenically induced by topical ophthalmic medications.[2-6] Daily, topical instillation of preserved prostaglandin analogs (PGAs), the most common first-line treatment for glaucoma, has been linked to a variety of OSD subtypes, including meibomian gland dysfunction (MGD).[7,8] With the goal of better understanding the development of MGD in this cohort of patients, this dissertation project first refines and then applies a preclinical experimental model to gain knowledge in how meibocytes, the lipid-producing cells of the meibomian gland, respond to prostaglandins, to a representative PGA, and to its associated preservative system. The results provide evidence toward the mechanism of glaucoma-associated MGD, shed light on how the human tear film may be altered with the topical application of PGAs, and may inform the development or modification of drug formulations to optimize treatment outcomes in patients suffering from these two common comorbidities.

GLAUCOMA

Glaucoma as a Public Health Concern

The global prevalence of glaucoma has been estimated to be 3.54%, a value corresponding to 64.3 million people in 2013 but expected to rise to 111.8 million in 2040.[9] No age, geographic region, sex, habitation, or ethnicity is spared, though being an older male in an urban area who either resides in Africa or is of African ancestry confers a greater risk of primary open angle glaucoma.[9] Asian populations also manifest high prevalence rates of glaucoma, though primarily through an angle closure mechanism.[9] In 2010, Quigley et al. estimated that 8.4 million people worldwide were bilaterally blind from glaucoma,[10] a conservative estimate of glaucoma's impact. This estimate fails to account for unilateral blindness, which represents approximately 55% of all glaucoma cases in Asia,[11] as well as other degrees of visual impairment short of blindness. Simply, glaucoma is the leading cause of irreversible blindness in the world.[12]

Glaucoma Pathophysiology

Glaucoma is a progressive optic neuropathy characterized by the death of retinal ganglion cells (RGCs), a cell type whose body resides in the inner retina yet whose axons project to the lateral geniculate nucleus of the thalamus.[12] Along their course from the retina to the brain, RGC axons within the optic nerve traverse through the lamina cribrosa, a porous meshwork continuous with the sclera. A highly compliant tissue that can succumb to elevations in intraocular pressure (IOP), the laminar pores become misshapen in glaucoma, which impinges upon the RGC axons.[12] This compression

obstructs both orthograde and retrograde axoplasmic flow which culminates into death signals that trigger RGC apoptosis.[13-15] Clinically, RGC apoptosis manifests as a progressive loss of neuroretinal rim tissue (often referred to clinically as increased cupping) that can be detected during fundoscopic evaluation, during imaging with optical coherence tomography, and—functionally—during threshold visual field assessment.[12]

With the awareness that glaucoma is an IOP-sensitive optic neuropathy, all treatment modalities are aimed to lower the IOP.[12] Early to moderate stages of glaucoma are often treated medically from six classes of ocular hypotensives: PGAs, carbonic anhydrase inhibitors, alpha-2 agonists, beta blockers, cholinergic agonists, and rho-kinase inhibitors. When cases become more severe or when topical treatment is poorly maintained, laser trabeculoplasty, laser cyclophotocoagulation, surgical trabeculectomy, or surgical filtration (by minimally invasive techniques or by external shunt insertions) may be employed.[12]

OSD as a Potential Risk Factor for Glaucoma Progression

Nearly every patient with medically treated glaucoma, stated to be about 70 to 82%, has concurrent MGD, a value that is somewhere between 33 and 52.5% for corresponding control groups.[2,3] Importantly, the surgical management of glaucoma has been associated with improvement in meibomian gland health, suggesting that any potential risk is mediated through daily dosing of topical pharmacotherapies rather than glaucoma itself.[16] Among clinical signs, Kim et al. found that glaucoma patients with MGD had a significantly reduced TBUT, even more so than a control group with MGD, and anterior migration of the line of Marx.[3] Lee and colleagues evaluated the lipid-layer

thickness (LLT), the tear film component primarily produced by the meibomian glands, and found that it was significantly thinner in the glaucomatous eye relative to the normal eye in patients with unilateral glaucoma.[4] The LLT was also significantly negatively correlated with the total number of glaucoma medications, total number of daily drops, and duration of treatment. In the study by Ghosh et al., the authors reported that although 70% of glaucoma patients had signs of MGD, only 30% reported symptoms, which failed to reach significance compared to the 24% with symptoms among controls.[2] This relationship is critically important in the care of glaucoma patients: clinicians who use a symptom-based threshold for initiating treatment for OSD may be risking progression of glaucoma, a topic further discussed below.

Though the frequency of OSD in glaucoma is staggering in itself, the real significance of glaucoma-associated OSD lies in its implications on clinical outcomes. OSD has been associated with poor IOP control and exacerbated glaucoma.[1] Topically treated glaucoma patients develop conjunctival inflammation, infiltration, and shrinkage—hallmark signs of a cicatricial conjunctivitis that has been termed pseudopemphigoid.[17,18] Inflammation and scarring have also been described in deeper tissues, such as the episclera, sclera, and trabecular meshwork, all tissues that can reduce outflow facility and increase IOP.[19] Further, the increased cellular infiltration and fibrosis associated with ocular hypotensive use have been linked to poor outcomes and poor IOP control following surgical intervention.[20] The only respite that exists among these relationships is that aggressive management of glaucoma-associated OSD may improve IOP control[1] by restoring ocular surface and tear film homeostasis. The impetus behind these pathologic changes is not fully known, but there appears to be at least some

component attributed to the altered function of the meibomian glands.[2-7] Additionally, the risk seems to be most significant for those treated with PGAs preserved with benzalkonium chloride (BAK),[21,22] relationships that are further explored in the sections that follow.

Altogether, it is clear that glaucoma is a prevalent and blinding eye condition.[9,10] Its medical management is associated with increased rates of MGD.[2-7] MGD and other forms of OSD can interfere with IOP control, and poor IOP control can cause progression that, in some cases, leads to blindness.[1,20] What is not known, however, is exactly how antiglaucoma pharmacotherapies induce MGD.

MEIBOMIAN GLAND DYSFUNCTION

The Tear Film and Its Contributors

The human tear film, once believed to be composed of three distinct layers,[23,24] is now regarded as a single, yet compartmentalized, functional unit (Figure 1).[25] Modern tear-film models depict the thicker, inner compartment as the muco-aqueous layer.[25] Interpolating with and including the glycocalyx of the corneal and conjunctival epithelium, mucins gradually decrease as they extend deeper into the tear film. The goblet cell, the corneal and conjunctival epithelia, and the lacrimal gland all contribute to the mucin content.[25-28] The accessory and main lacrimal glands, however, are the primary contributors of aqueous tears.[29,30] Resting atop the aqueous layer is the lipid layer, which, in itself, is another bilaminar structure. It consists of an inner, amphiphilic layer, whose hydrophilic functional groups interact with the aqueous beneath it, conferring a high degree of stability to the tear film.[25,31] Superficially, a thicker nonpolar lipid layer coats

the entire tear film, serving as a barrier to tear film evaporation. The meibomian glands located in the eyelids are largely responsible for producing the tear film lipid layer.[25]

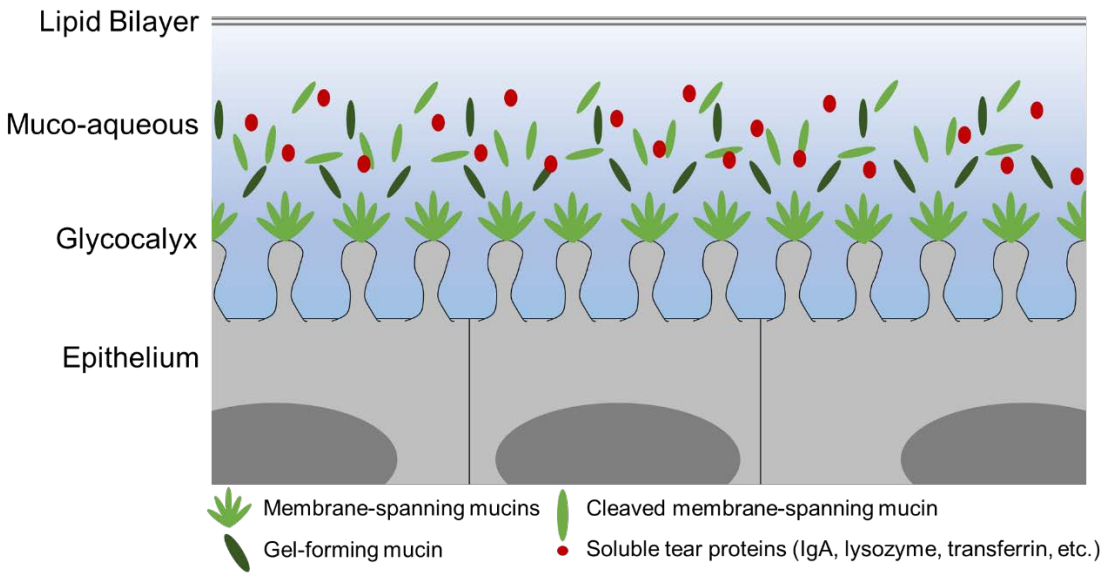

Figure 1 Modern Two-Layer Tear Film Model
Adapted from Willcox et al.[24] and Craig et al.[31]

The meibomian glands, the focal point of this dissertation, are oil-producing glands that are vertically oriented in the tarsal plates of the eyelids.[33] They have a linear structure, provided by a central duct, with grape-like outpouchings, termed acini, where the lipid content is initially synthesized. At the microanatomy level, meibomian gland stem cells are located at the periphery of these acinar units.[33,34] As the stem cells proliferate, they push older cells toward the middle of the acini. As these cells mature, they dramatically increase their lipid content until, eventually, the whole cell is lost to holocrine secretion, leaving only the predominantly lipid mixture in its wake.[35,36] The force that is generated from the peripheral, proliferating stem cells, along with the

negative pressure induced by the contraction of the muscle of Riolan during blinking, helps to propel this lipid mixture through the ductal system along its path to delivery on the eyelid margin.[33,36-38] Though yet to be experimentally confirmed, it has been hypothesized that the lipid mixture continues to be refined by the ductal epithelium, particularly by recycling phospholipids.[39,40]

Tear Film Lipid Layer Structure and Function

After the meibum is delivered to the eyelid margin, it is distributed across the ocular surface where, through a variety of intermolecular forces, it self-assembles into the bilaminar tear film lipid layer (TFLL).[33] Based on current techniques for accurate measurement, the TFLL is approximately 45 to 50 nm in thickness,[41,42] representing just 1.33% to 1.67% of the overall tear film (approximately 3 µm).[41,43,44] Despite this minimal contribution to the thickness, the TFLL confers resistance to tear evaporation and promotes stability to the tear film unit as a whole.[41]

Early attempts to measure the tear film and TFLL were met with numerous challenges and thus the reported values have shown significant variability (3 µm to 40 µm).[41] Newer, more accurate strategies have utilized interferometry techniques, a principle that measures differential coherence patterns created by the reflection of light at different interfaces, such as that between air and the TFLL, the TFLL and the muco-aqueous layer, and the muco-aqueous layer and the corneal epithelium.[41] Two interferometry methods have been successfully utilized: thickness-dependent fringes (TDF) and wavelength-dependent fringes (WDF).[41] These methods vary in their acquisition techniques. Specifically, TDF approaches require a lack of uniform tear film

thickness across a measurement area.[41] This non-uniformity is necessary to induce variations in differential interference patterns which can be extrapolated to discern thickness measurements. Alternatively, WDF uses variations in the wavelength of incident light to create differential interference patterns.[41] Both techniques have been used to measure the TFLL and have provided consistent results.[41] A more recent development has incorporated optical coherence tomography (OCT). OCT is essentially an adaptation of WDF interferometry, but it provides the added benefit of visualizing axial images of ocular structures, including the tear film.[41]

Despite the impetus for developing technologies that yield accurate tear film thickness measurements, the quality and composition of the TFLL may be more predictive of function than thickness.[41] Using WDF interferometry, King-Smith et al. found that tear film thinning rates and lipid layer thickness were poorly correlated.[45,46] Additionally, despite similar thickness values between the normal pre-corneal tear film and the pre-lens tear film during contact lens wear, the tear film thinning rate is accelerated in the presence of a contact lens.[47-49] These findings reinforce the concept that thickness alone does not confer stability. Instead, they suggest that lipid composition and structure are critical contributors to a stable tear film.[41]

Meibomian Gland Innervation and Regulation

Understanding how the meibomian glands regulate both lipid synthesis and meibum composition is still a developing area of research. At present, it is known that the meibomian glands are richly innervated by sensory, sympathetic, and parasympathetic neurons and under hormonal control of androgens, estrogens, and progestins, among

others.[33,50] Sensory neurons produce both calcitonin gene-related peptide and, to a lesser extent, substance P.[50] These afferent neurons are believed to propagate a variety of sensations, including touch, temperature changes, and dryness.[50] The sympathetic neurons, another class of neural innervation, project primarily from the superior cervical ganglion, at least in the rat, and terminate near the vasculature that perfuses the meibomian gland acinar units.[50,51] These neurons produce dopamine beta-hydroxylase, tyrosine hydroxylase, and neuropeptide Y (NPY).[50] Treatment with topical epinephrine, a sympathomimetic, induces an animal model of MGD that can lead to cyst formation and hyperkeratinization,[52] suggesting that sympathetic innervation, likely through indirect effects on nearby vasculature, can modulate meibomian gland physiology. Lastly, parasympathetic neurons project from the pterygopalatine ganglion and have been shown to express vasoactive intestinal peptide (VIP) and NPY, the latter having involvement in both the sympathetic and parasympathetic systems.[50] Localization of both neurotransmitters (VIP and NPY) is highly associated with the meibomian gland acinar units.[50] This proximity suggests that parasympathetic innervation could directly promote meibocyte proliferation and/or increased meibum production.[50]

As previously mentioned, the meibomian glands are also regulated by androgens, estrogens, and progestins.[33] These steroid hormones, particularly androgens and estrogens, can be synthesized locally by meibomian gland epithelial cells and, therefore, may represent a source of intracrine regulation.[33] In response to testosterone, meibomian gland epithelial cells in both the mouse and human upregulate genes involved in lipid metabolism, lipid transport, sterol biosynthesis, and fatty acid metabolism, among others.[33,53] Estrogens, generally, antagonize the effects of testosterone.[54] Although the

physiologic effects of estrogens on the meibomian glands are far from being resolved, it is believed that estrogen decreases lipid synthesis and promotes an MGD-like phenotype.[33] Progesterone, however, when in the presence of estrogen, may counter these adverse effects based on gene expression studies of the mouse meibomian gland and clinical trials of patients undergoing hormone replacement therapy.[55,56] Further work is needed to better elucidate the roles of sex hormones, especially the poorly understood effects of estrogens and progestins, on the physiology of the meibomian glands.

MGD Definition and Pathophysiology

Culminating in a 169-page white paper published in 2011, an international group of experts collaborated over a two-year period to provide a comprehensive review of MGD.[57] Charged with evaluating and drafting an in-depth summary of the literature, participants of this MGD Workshop synthesized an updated definition of the disease: "MGD is a chronic, diffuse abnormality of the meibomian glands, commonly characterized by terminal duct obstruction and/or qualitative/quantitative changes in the glandular secretion. This may result in alteration of the tear film, symptoms of eye irritation, clinically apparent inflammation, and ocular surface disease."[58]

Though elements of MGD's pathophysiology are embedded in its definition, further exploration and classification are necessary. MGD is associated with both molecular and physical changes within the meibomian glands.[33] Sequelae of these changes lead to physiochemical alterations of the tear film and desiccation-induced inflammation of the ocular surface.[33] Two subtypes of MGD exist: hyper- versus hyposecretory. Hypersecretory MGD is marked by seborrhea and is largely considered

the less common of the two. Hyposecretory can be further classified into obstructive and/or atrophic mechanisms.[33]

In obstructive MGD, the lipid content produced by the glands becomes altered and more viscous.[33] These molecular changes are attributed to qualitative changes in the lipid content and/or an increase in keratinization.[33,52,59,60] With time, the thicker content can block the central duct, causing stasis upstream and poor expressibility downstream onto the eyelid margin. Despite the stagnation, the stem cells continue to proliferate, maintaining a constant force pushing against the ductal obstruction. With time, intraductal hypertension develops distal to the blockage, culminating in glandular atrophy and giving rise to atrophic MGD.[33]

Lipid Classes of Human Meibum Pertinent to This Dissertation

Normal human meibum is comprised of a diverse array of mostly nonpolar lipid classes.[61] The hydrophobic wax esters (WEs) and cholesteryl esters (CEs) account for the bulk of the lipid pool, summing to approximately 90% in some reports.[62-64] Other lipid classes include diesters, free fatty acids, (O-acyl)-ω-hydroxy-fatty acids (OAHFAs), triacylglycerols (TAGs), and diacylglycerols, among others.[61] The presence of phospholipids has long been a highly debated topic, one that extends beyond the focus of this dissertation. Many groups have detected phospholipids in the meibum, as reviewed in Green-Church et al., but the relative abundance has yet to be resolved.[61] Despite this, it can largely be agreed upon that phospholipids are a minor lipid class in meibum.[61] The three classes that are most pertinent to this dissertation are CEs, WEs, and TAGs, given

their relative abundance in meibum (CEs and WEs) and their recognition as putative biomarkers of MGD (TAGs), as described below.

CEs account for approximately 40% of all lipids in meibum.[63] Structurally, CEs are a cholesterol esterified to a fatty acid (Figure 2). Based on a recent study, there have been up to 58 different CE species detected in normal human meibum, though this value varies with the analytical methods used.[62] The fatty acid chain length has been reported to span from 16 to 36, though CEs with a carbon number (n_c) 22 to 26 are the most highly expressed.[61,62,65] Meibum CEs are predominantly saturated or monounsaturated, terms that describe the extent to which carbons are hydrogenated.[62,66] Saturated fatty acyl groups are fully saturated with hydrogens and therefore lack double bonds. Monounsaturated fatty acyl groups consist of one double bond. Polyunsaturated groups, which account for the minority of the CE subtypes in meibum, possess more than one double bond. In sum, the CE profile in normal human meibum is diverse in CE chain length (spanning 16 to 36 carbons), abundant in CEs with n_c 22 to 26, and abundant in saturated and monounsaturated CEs.[61-63,65,66]

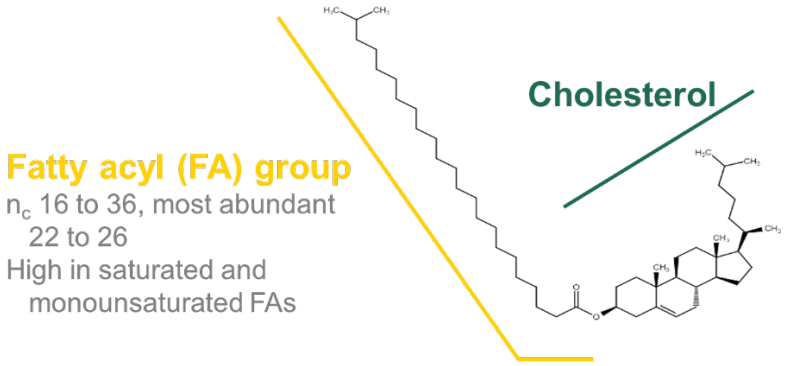

Figure 2 Structure of Cholesteryl Ester 24:0
Drawn with Marvin JS 20.14.0 (ChemAxon, Budapest, Hungary) accessible via the U.S. National Library of Medicine. n_c = carbon number

WEs are regarded as the most abundant lipid class in meibum, comprising 48% of the total lipids.[62,63] Structurally, WEs consist of a fatty alcohol (FAl) esterified to a fatty acid (FA) (Figure 3). Meibum WEs are rich in FA 18:1-, 17:0-, and 16:1-containing WEs with FAls ranging between 18 to 30 carbons.[61,62,64,67,68] WEs with FA 18:2, FA 18:3, and FA 18:4 have also been described.[69] Monounsaturated WEs are more abundant than polyunsaturated WEs.[61]

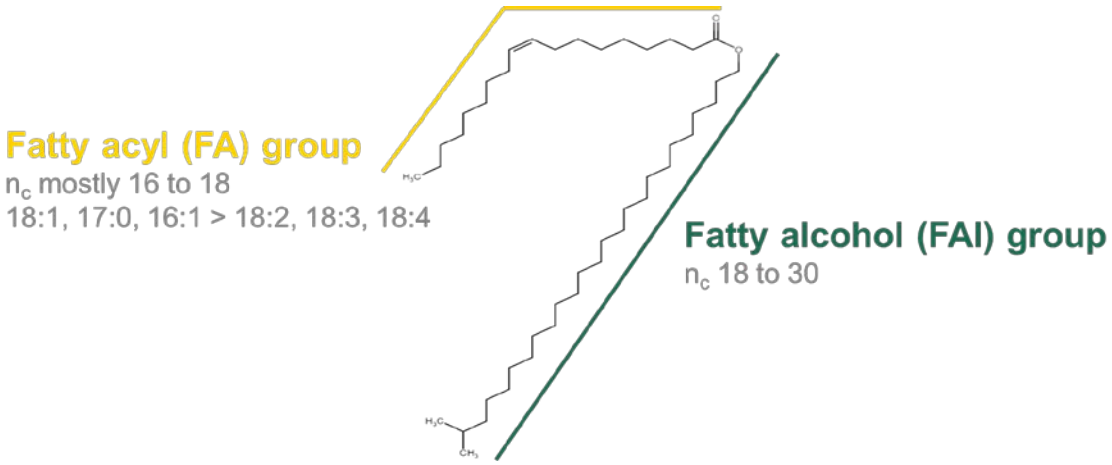

Figure 3 Structure of Wax Ester 44:1 (FA 18:1/FAl 26:0)
Drawn with Marvin JS 20.14.0 (ChemAxon, Budapest, Hungary) accessible via the U.S. National Library of Medicine. n_c = carbon number

TAGs have been cited to represent 0.05% to 6% of normal human meibum.[35,39,70-72] Structurally, TAGs consist of a glycerol backbone esterified to three fatty acyl groups (Figure 4). TAGs are an extremely diverse class of lipids, owing to their many isomeric combinations of fatty acyl groups. In meibum, FA 18:1-containing TAGs are the most abundant.[62] To date, a comprehensive evaluation of TAGs in meibum has yet to be performed, likely due to the class's inherent complexity and the overall lower abundance in meibum.

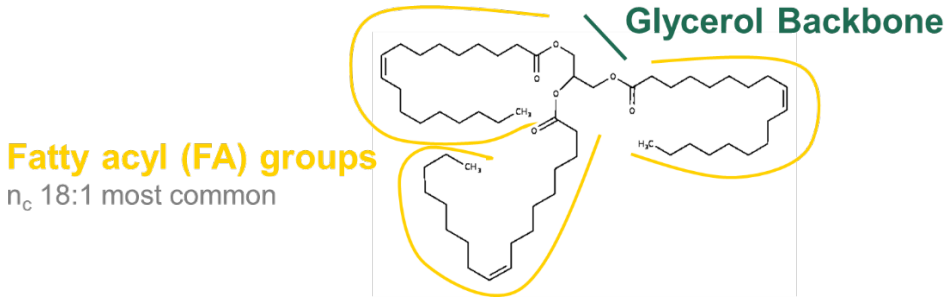

Figure 4 Structure of Triacylglycerol 54:3 (FA 18:1/FA 18:1/FA 18:1)
Courtesy of the U.S. National Library of Medicine. n_c = carbon number

Lipid Analysis by Mass Spectrometry

Developed in the early 1900s, mass spectrometry has become one of the most versatile analytical techniques in the field of biochemistry.[73] In simple terms, it converts molecules from an unknown, complex mixture of metabolites into charged ions that can be separated, detected, identified, and quantified.[73] It has been used widely in identifying the lipidomic composition of human meibum and the tear film, as previously reviewed.[25,61] A brief description specific to the mass spectrometry methods used in this dissertation is provided below.

Basic Mass Spectrometry Theory

A simplified diagram of the basic elements of a mass spectrometer are provided in Figure 5, adapted from Dass.[73] It consists of an inlet system, an ion source, a mass analyzer, and a detector. The data collected from a mass spectrometer is often graphed on a mass spectrum. The inlet is responsible for delivering the sample to the ion source, which must be undertaken without compromising the sample as it passes from atmospheric pressure in the inlet into the vacuum that exists within the ion source.[73] The

ion source then converts the neutral molecules in the sample into charged gaseous ions. The ions emerge from the source and enter the analyzer where they are subjected to electric and/or magnetic forces that manipulate the motion of the ions. The detector receives, measures, and amplifies the ion current before it is processed and displayed on a mass spectrum. The mass spectrum is simply a bar graph consisting of mass-to-charge ratios (m/z) along the x-axis and relative abundance along the y-axis. For this dissertation, an electrospray ionization source and a time-of-flight (TOF) mass spectrometer were used.

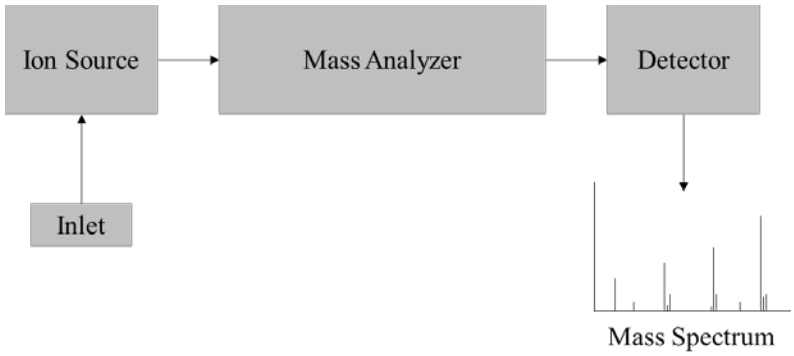

Figure 5 Simplified Schematic of Mass Spectrometer Components
Adapted from Dass 2007[73]

Electrospray ionization has become an impactful component of mass spectrometry analysis, especially in molecular biology.[73] Used on liquid-phase samples, it generates a mist of charged droplets whose solvent evaporates, converting the droplets into gaseous ions.[73] The spray itself occurs due to the electrostatic field created by the potential difference between the counter electrode and the tip of the stainless-steel tubing through which the sample travels. Solvent evaporation is facilitated by hot nitrogen. The

gas ions are then transported into the mass analyzer, sometimes with the aid of radio-frequency multipoles, as further discussed later.

The TOF mass spectrometer relies on field-free drift of the gas-phase ions at a rate that is directly proportional to their charges yet inversely proportional to their masses.[73] As the ions emerge from the ion source, especially electrospray sources, they can be multiply charged. An ion with a higher charge will accelerate more quickly through the mass analyzer, reaching the detector quicker than an ion of equivalent mass with less charge. A heavier ion, however, moves more sluggishly and will therefore reach the detector later. In essence, the TOF mass analyzer is responsible for separating the gas-phase ions based upon their masses and charges.[73]

Analysis of complex lipid samples, like tears or meibum, by mass spectrometry alone is insufficient for accurate molecular identification, however.[74] Lipids are particularly vulnerable to matrix interferences and significant isotopic overlap within and between lipid classes over a relatively small m/z range.[75] The use of tandem mass spectrometry (MS/MS), described below, is therefore necessary.

Tandem Mass Spectrometry

MS/MS involves two separate mass analyzers in one system. The first system selects for a molecule of a given mass, which is then fragmented so that the second system can perform mass analysis on these products.[73] This approach dramatically increases confidence in molecular identification as it selects for precursor (or parent) ions of a given mass and confirms its composition by evaluating its product (or daughter) ions.

The system even includes the capability of performing serial product ion scans across a range of precursor masses, permitting accurate description of the whole lipidome.

The MS/MS approach used in this dissertation pairs the TOF mass spectrometer with a triple quadrupole. The sequence of components for MS/MS herein is, therefore, inlet, ion source, quadrupole mass filter (analyzer), collision cells, TOF mass analyzer, and detector. Quadrupoles are subject to direct current and radio frequency potentials to influence how the ions move through the system.[73] The collision cell is the location for collision-induced dissociation (CID)—the term that describes how the collision between precursor ions and an inert gas generate product ion fragments.[73]

Automated Analysis

Another recent development in mass spectrometry and lipidomics is automated analysis. Previously requiring manual identification, MS/MS data can now be analyzed with software that assigns identifications based upon characteristic m/z ratios and the neutral loss of known ion fragments. With the advent of this technology, the workflow has been optimized for higher throughput analysis without compromising accuracy.[74]

Preclinical Research using HMGECs

In 2010, Liu et al. successfully immortalized a human meibomian gland epithelial cell (HMGEC) line.[53] Using donor tissue, the cells were isolated and transfected with human telomerase reverse transcriptase using a retroviral vector. Upon successful immortalization, the cells were found to increase lipid production and upregulate lipogenic genes in response to androgen exposure; both are expected behaviors for lipid-

producing meibocytes.[53] In 2018, Xie et al. reported that Lrig1 and DNase2, biomarkers of progenitor and differentiated epithelial cells, were detected from HMGECs exposed to proliferating and differentiating conditions, respectively.[76] Since the development of this cell line, the cells have been made available to numerous labs and subject to a variety of interrogations.

Most pertinent to this dissertation is the search for differentiating culture conditions. It is widely accepted that HMGECs readily proliferate when cultured in keratinocyte serum-free media (KSFM) supplemented with 5 ng/ml epidermal growth factor (EGF) and 50 µg/ml bovine pituitary extract (BPE),[53] a finding that has also been reproduced in our lab (Figure 6A and B). To promote differentiation, early reports provided evidence for switching to serum-containing media, specifically, Dulbecco's Modified Eagle's Medium (DMEM) with Ham's F-12 (1:1) containing 10 ng/ml EGF and 10% fetal bovine serum (FBS).[40,53] Under these conditions, HMGECs have been described to cease proliferation and initiate nonpolar lipid production,[40] findings that were also reproduced in our lab (Figure 6C and D). Despite this microscopic evidence of increased lipid production, the HMGEC lipidome analyzed by mass spectrometry techniques varied dramatically from normal human meibum.[40,77]

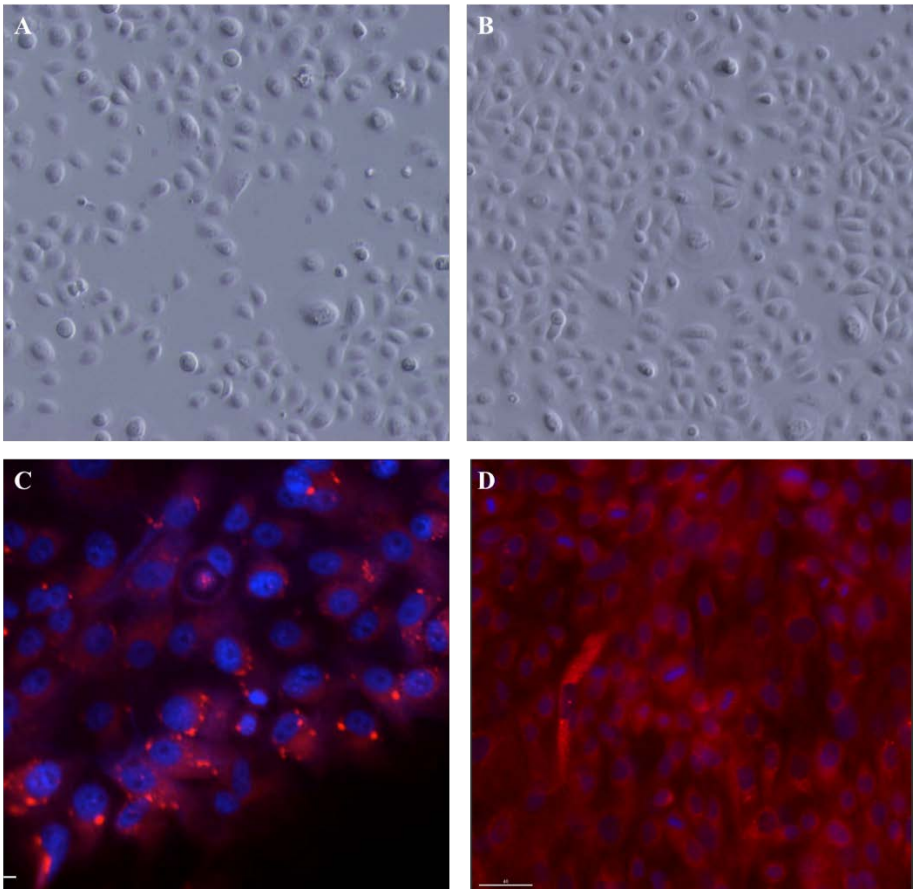

Figure 6 HMGECs Under Growth and Differentiating Conditions
(A) HMGECs are approximately 70% confluent, small, and ovoid in shape. (B) HMGECs are approximately 100% confluent, ovoid in shape, and in a cobblestone monolayer. Both A and B were taken with an Olympus IX71 Inverted Microscope (Tokyo, Japan) at 100x. (C) and (D) HMGECs stained with Nile Red (neutral lipids, pseudocolored red) and DAPI (nucleus, pseudocolored blue). HMGECs increase lipid production (A) 24 hours and (B) 48 hours after exposure to serum-containing media (10%). Both C and D were taken with a DeltaVision Deconvolution Microscope (GE Healthcare, Chicago, IL) at 100x.
Images unpublished and courtesy of Karen Dionne and Kelly Nichols.

With healthy skepticism, we sought to explore and broadly define the HMGEC lipidome. The lipidomes of serum-differentiated HMGECs after nine, 16, and 23 days failed to show any qualitative differences in the major lipid peaks or in the identified lipid classes at each time point (Figure 7A-C). From this work, it was discovered that HMGECs highly express phosphatidylcholines (PC) with n_c 30 to 38,

phosphatidylinositols (PI) with n_c 32 to 34, and phosphatidylserines (PS) with n_c 32 to 42. Free cholesterol, free fatty acids, and SMs with n_c 32-34 were also detected. Across all conditions, CEs were of very low abundance (<1%), and WEs were not detected.

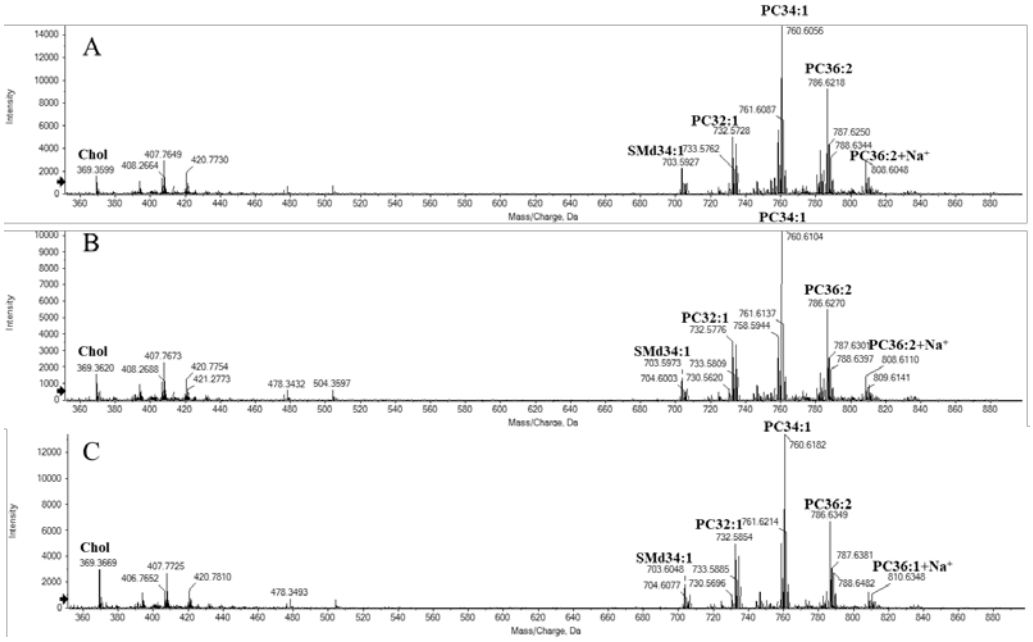

Figure 7 Major Lipid Peaks from HMGECs
Representative mass spectra from serum-differentiated HMGECs after (A) 9 days, (B) 16 days, and (C) 23 days. Unpublished data, J. Ziemanski.

Other groups had begun to question the validity of serum-induced differentiation as well, largely based on this discrepancy between the HMGEC and meibum lipidomes.[77,78] Although azithromycin supplementation has been widely used by one research group, its proposed mechanism, azithromycin-induced phospholipidosis, is inconsistent with the expected lipid expression from terminally differentiated meibocytes.[61,79,80] Beginning in 2016, several reports by Jester and colleagues began to emerge that first introduced the role of peroxisome proliferator activator receptor-γ (PPARγ) in the differentiation of mouse meibocytes.[81] Later, it was found that PPARγ

was also a critical regulator in HMGECs.[82,83] PPARγ is a nuclear receptor that, upon ligand binding, dimerizes with retinoid X receptors to regulate transcription of a variety of lipogenic genes.[84,85] There are a variety of endogenous ligands that can activate PPARγ, but experimentally, rosiglitazone has been utilized with good success.[81-85] Prior to initiating this dissertation project, however, the lipidomic response to rosiglitazone stimulation was unknown.

In 2018, a group of international researchers, inclusive of the author of this dissertation, collaborated to define the short tandem repeat (STR) profiles of commonly used cell lines in ocular surface research.[86] STR profiling is a technique widely used in forensic science and has become the mainstay for human cell line authentication by DNA identification.[87] STRs are short DNA base-pair sequences that are repeated many times in certain regions of the genome. There are typically 16 STRs that are quantified, and the number of repeats for each is defined as the STR profile, a unique and identifying attribute of each individual's genome.[86] Ideally, the STR profile would have been defined at the time of HMGEC development. Because this was not performed, several labs across the world collaborated to profile their cell stocks, compare them, and thereby establish a standard for what each cell line should be authenticated against in future research. Of the seven passages that were evaluated and compared across three labs, all STR profiles for HMGECs were found to be identical.[86]

PROSTAGLANDIN CHEMISTRY

Arachidonic Acid Pathway and Pertinent Prostaglandins

Prostaglandins are lipid autacoids, meaning they behave analogously to local hormones and regulate a wide array of cellular functions.[88] While hormones are produced by distal sites and distributed by the vascular system, autacoids are generated locally and elicit their function close to their site of production.[88] All 2-series prostaglandins are derived enzymatically from arachidonic acid, a twenty-carbon fatty acid ubiquitous to cell membranes (Figure 8). Arachidonic acid is first liberated from the cell membrane by phospholipase A_2 (PLA_2). Cyclooxygenase-1 and -2 (COX-1 and -2) then initiate the development of PGH_2, which is a common precursor to the remaining 2-series prostaglandins. Nonsteroidal anti-inflammatory drugs (NSAIDs), such as aspirin, are known nonspecific COX inhibitors that can reduce or even prevent the production of these prostaglandins.[88]

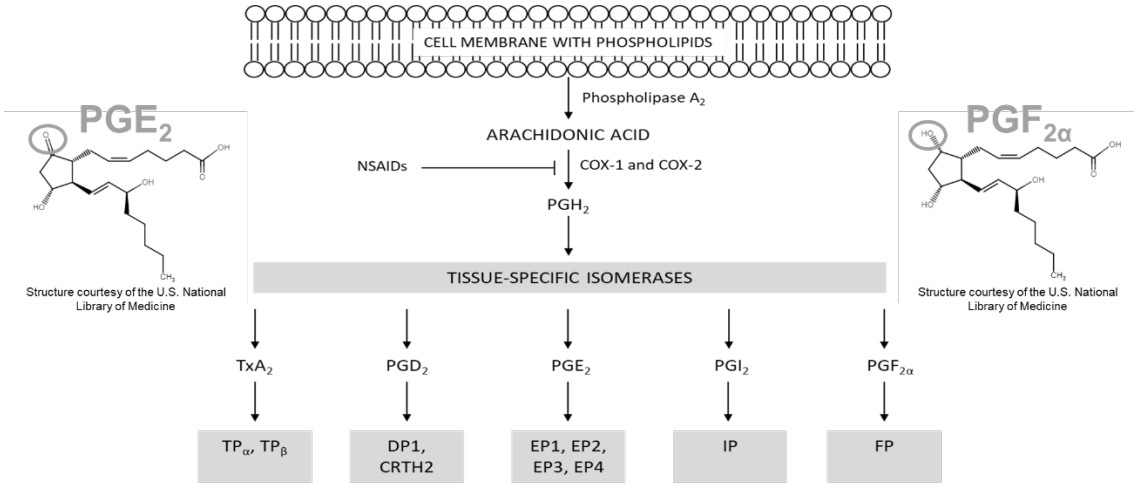

Figure 8 Arachidonic Acid Pathway
Adapted from Ricciotti and Fitzgerald 2011[88]

One notable prostaglandin, PGE_2, binds its EP-type receptors to regulate immune responses, blood pressure, and gastrointestinal health, among others.[88] Pertinent to immune regulation, PGE_2 is a common, well-characterized inflammatory mediator capable of inducing many of the cardinal signs of inflammation: pain, redness, and swelling.[89] Another relevant 2-series prostaglandin is $PGF_{2\alpha}$, whose roles are primarily described in the context of the reproductive system and in the management of intraocular pressure. Signaling through FP receptors is necessary for successful parturition,[90,91] and it also promotes upregulation of several matrix metalloproteinases capable of degrading the extracellular matrix.[92] This latter mechanism, at least in part, is credited for the FP receptor's favorable effect on IOP reduction. To date, there are no known reports that have investigated the effect of PGE_2 or $PGF_{2\alpha}$ or sought to detect their receptors on the meibomian glands or HMGECs.

Expression of Prostaglandin Receptors Around the Eye and Beyond

The ocular distribution of FP- and EP-type receptors has been explored by several groups.[93-95] All five receptors have been detected, though the receptors are differentially expressed throughout the various tissues (Table 1). The majority of the ocular surface structures, specifically the cornea and conjunctiva, express EP2, EP3, EP4, and FP receptors.[94,95] The meibomian gland and HMGECs, however, have yet to be a known target of investigation. Chen et al. discovered that a human sebocyte cell line has been shown to strongly express EP2 and EP4 receptors, weakly express EP1, and not express FP.[96] Heller et al. found that PGE_2 contributes to lipogenesis in colonic cells.[97] In summary, receptors for PGE_2 are present in sebaceous glands,[96] and at least in the colon,

PGE_2 is capable of contributing to lipogenesis.[97] It has also been shown that $PGF_{2\alpha}$ is capable of crossover binding to several EP receptors.[91,98] Therefore, regardless of whether FP receptors are present in the meibomian glands, chronic use of PGAs may elicit side effects mediated through EP receptors.

Table 1 Ocular Distribution of Receptors for PGE_2 (EP subtype) and $PGF_{2\alpha}$ (FP)

Receptor	Location
EP1	Iris vasculature, iris sphincter, iris root, ciliary body, trabecular meshwork, choroidal vessels, photoreceptors, both nuclear layers, ganglion cells
EP2	Trabecular meshwork, iris, choroid, ciliary body, retina, corneal epithelium, conjunctival epithelium
EP3	Ciliary body, trabecular meshwork, ciliary muscle, retina, choroid, corneal epithelium
EP4	Nonpigmented epithelium, ciliary muscle, choroid, iris, trabecular meshwork, cornea, conjunctival epithelium
FP	Ciliary body, choroid, iris, trabecular meshwork, cornea, lens epithelium, conjunctival stroma, optic nerve

Data compiled from Mukhopadhyay et al.,[93] Woodward et al.,[94] and Schlotzer-Schrehardt et al.[95]

Prostaglandin Analogs as Ocular Hypotensives

All of the commercially available PGAs approved for the medical management of glaucoma are $PGF_{2\alpha}$ analogs.[98] Upon FP receptor engagement by these molecules, matrix metalloproteinases are upregulated, leading to remodeling of the uveoscleral extracellular matrix.[99] This remodeling is believed to reduce outflow resistance, thereby enhancing aqueous humor egress and lowering IOP.[99] In the United States, there are currently six approved PGAs for topical use in patients with ocular hypertension or glaucoma (Table 2). All PGAs are believed to exert their therapeutic effect through the FP receptor,[98] though latanoprostene bunod (Vyzulta™, Bausch & Lomb, Bridgewater, NJ), recently approved in 2017, is also a nitric oxide-donating molecule to facilitate additional outflow

through the trabecular pathway.[100] To date, generic equivalents for Xalatan®, Lumigan®, and Travatan® Z are available in the United States, though a mild price differential still exists among these three medications. Latanoprost was the first generic to be released and is currently the most affordable (information publicly available at GoodRx.com).

Table 2 Commercially Available PGAs in the United States

Brand Name	Generic Name	Distributor
Xalatan™	Latanoprost 0.005%	Pfizer, Inc. New York, NY
Lumigan™	Bimatoprost 0.01%, 0.03%	Allergan PLC Madison, NJ
Travatan™ Z	Travoprost 0.004%	Alcon Laboratories, Inc. Fort Worth, TX
Zioptan™	Tafluprost 0.0015%	Akorn, Inc. Lake Forest, IL
Vyzulta™	Latanoprostene bunod 0.024%	Bausch & Lomb, Inc. Bridgewater, NJ
Xelpros™	Latanoprost ophthalmic emulsion 0.005%	Sun Pharmaceuticals, Inc. Cranbury, NJ

Safety Profile of Prostaglandin Analogs

One of the appeals of PGAs is its favorable systemic side effect profile.[98] There are no known adverse effects on the cardiovascular or respiratory systems, two organ systems that are vulnerable to side effects induced by beta adrenergic antagonists (beta blockers).[98,101-103] Headache has been reported as a rare event, though it seems to resolve without consequence.[98] The only two contraindications to PGA use are pregnancy and lactation due to concerns related to abortion of the fetus following high doses of prostaglandins.[98]

The ocular side effects, however, are numerous and range from minor, cosmetic issues to more severe, inflammatory conditions.[98] The most common side effects,

occurring in up to 50% of cases, are conjunctival hyperemia and eyelash growth.[98,104,105] Increased pigmentation of the iris and eyelid occur in approximately five to 10% of patients.[106-108] More severely, PGAs have been linked to rare cases of uveitis and cystoid macular edema, conditions that both appear to be reversible upon discontinuation of therapy.[109,110] Following approval of this class of medications, a new side effect was described: prostaglandin-associated periorbitopathy (PAP).[111] PAP is primarily an aesthetic concern for an acquired sunken-eyed appearance. Its onset has been attributed to inhibition of adipogenesis reducing the intraorbital fat contents that, in health, bolster the globe in place.[111] This inhibition of adipogenesis may have implications on meibomian gland vitality and function, a topic discussed at length in subsequent chapters. Beyond these side effects, as already mentioned, PGAs have been heavily associated with the development of OSD, including MGD.[7,8]

Link to MGD

To date, only speculations about the mechanism of PGA-induced OSD have been presented. In one study by Mocan et al., the obstructive subtype of MGD was detected in 95% of PGA-treated patients.[7] The presence of gland obstruction suggests that meibum becomes hyperviscous and ducts hyperkeratinized with chronic PGA instillation.[33] This theory was supported by Cunniffe et al., who described a case series of 43 consecutive patients presenting for surgical intervention of chalazia.[8] Approximately one in five patients was taking a PGA, a proportion greater than expected.[8] The authors hypothesized that PGAs may act directly on the meibomian glands to alter their secretion. Kam et al. partly addressed this hypothesis in a cell culture model using HMGECs but reported that

bimatoprost induced no change in intracellular nonpolar lipid accumulation over five days, though it did decrease phosphorylation of AKT (a kinase marker of survivability).[112] The authors, however, did not assess individual nonpolar lipid species and used a bimatoprost concentration that was up to almost two orders of magnitude less than what is available in commercial preparations. A comprehensive evaluation of the lipidome in response to PGAs, including its preservative system, has not been adequately performed.

BENZALKONIUM CHLORIDE AND PRESERVATIVE SYSTEMS

Ophthalmic Preservatives

Multidose bottles of ophthalmic medications typically require preservation to prevent microbial contamination. A favorable preservative system balances efficacy against microbial growth in the bottle with safety and physiologic compatibility when applied to the eye.[113] Common preservatives used in eye care include benzalkonium chloride (BAK), polyquaternium-1 (PQ-1, Polyquad™, Alcon Laboratories, Inc., Fort Worth, TX), stabilized oxychloro complex (SOC, Purite™, Bio-Cide International, Inc., Norman, OK), sodium perborate (GenAqua™, Novartis Ophthalmics, East Hanover, NJ), and sofZia™ (Alcon Laboratories, Inc., Fort Worth, TX).[114] BAK is the most widely used, preserving about 70% of all topical ophthalmic drops.[20,115] It, along with PQ-1, works through a detergent mechanism to disrupt lipid cell membranes of microorganisms.[114] Sodium perborate, SOC, and sofZia are considered vanishing preservatives, meaning they exert their antimicrobial effects in the bottle but rapidly dissolve when outside of the bottle. Sodium perborate degrades when exposed to water in

the tears, SOC when exposed to light, and sofZia when exposed to naturally occurring cations in the tears.[113] All three exert their preservative activity through oxidizing mechanisms.[113,114]

BAK Structure

BAK, more aptly referred to as BAK*s*, is actually a class of antiseptics, rather than a single compound, that fall under the category of quaternary ammonium compounds.[116] Structurally, BAK consists of a benzene ring and a quaternized ammonium with a hydrocarbon chain of varying lengths (8, 10, 12, 14, 16, or 18 carbons) (Figure 9). The 14- and 16-carbon structures have been described as the most bactericidal.[116]

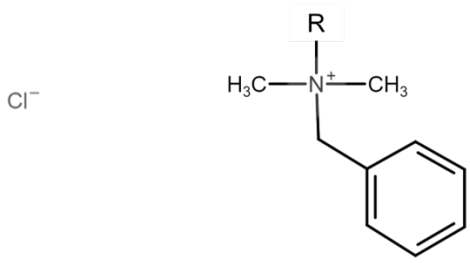

Figure 9 Benzalkonium Chloride
R = hydrocarbon chain of 8, 10, 12, 14, 16, or 18 carbons
Courtesy of the U.S. National Library of Medicine

BAK Adverse Effects and Link to MGD

BAK is used in ophthalmic formulations ranging from 0.004% to 0.02%.[117] BAK breaks cell-cell junctions in the corneal epithelium at concentrations within this range, which is simultaneously advantageous yet also destructive.[118] Degrading the corneal

barrier permits more rapid penetration of the active medication into the anterior chamber at the cost of impairing the corneal surface integrity.[119] Similar to its effect on bacterial cells, BAK can also disrupt host cell membranes leading to cell death. These effects on the corneal and conjunctival epithelium are well-documented.[117,120-124] Using confocal microscopy, Liang et al. found increased corneal infiltration from BAK-preserved glaucoma medications in an animal model.[125] From a functional perspective, BAK can reduce tear break-up time, a tear parameter of stability that is often attributed to lipid layer integrity, an unsurprising finding, given the known effects that detergents exert on lipids.[126] At the time of initiating this dissertation project, there were no known reports describing BAK's effects on HMGECs. Since then, however, two publications have emerged addressing a variety of outcome parameters from BAK-challenged HMGECs.[127,128] These papers are reviewed in context with the results from this dissertation project in the Discussion.

PRELIMINARY STUDIES

To guide the design of this dissertation project, several preliminary experiments were performed to optimize the lipid extraction protocol, identify potential biomarkers, validate assay systems, and assess safety of the drug vehicle. These experiments and their associated data, important to the subsequent papers, are presented here.

Additive Concentration

In light of the discrepancy between the nonpolar lipidomic profiles of human meibum and HMGECs, it was considered that HMGECs may be producing nonpolar

lipids, yet the extraction protocol was failing to recover them. Therefore, an early troubleshooting step evaluated several concentrations of a weak salt (ammonium acetate) as an additive to the Folch technique in an attempt to improve lipid recovery.[129] Despite higher signals being obtained for some major lipid peaks, there appeared to be no appreciable difference in the classes of lipids detected (Figure 10). Subsequent trials explored the use of higher concentrations, up to 50 mM ammonium acetate, with some further improvement in signal yet with no clear advantage in nonpolar lipid diversity (data not shown). The use of 50 mM ammonium acetate was maintained throughout all future experiments.

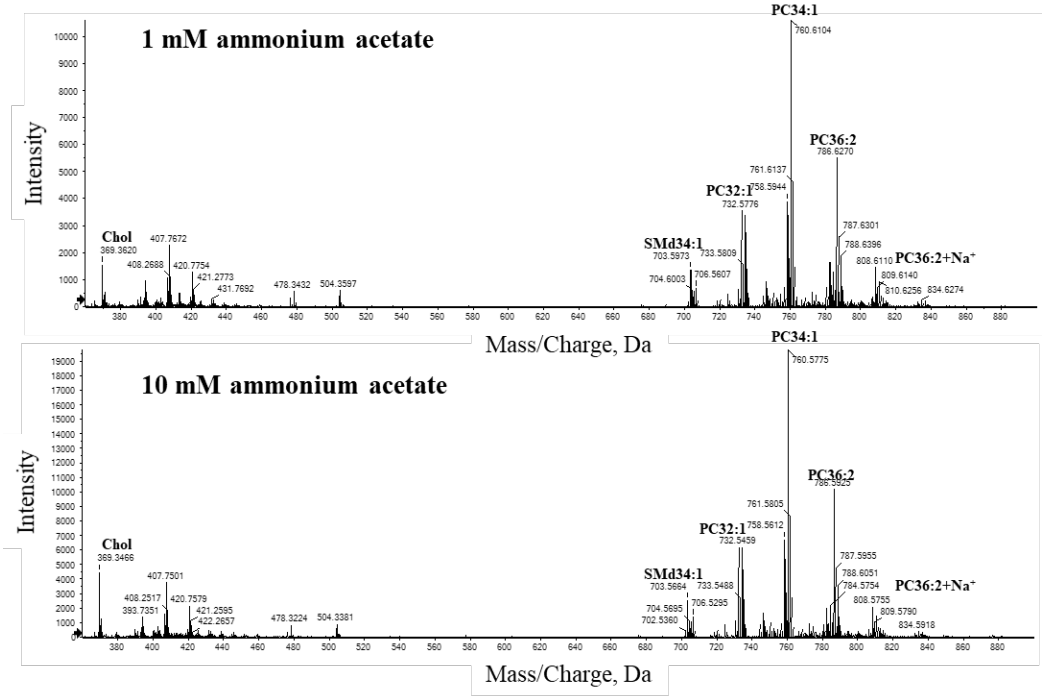

Figure 10 Major Lipid Peaks Associated with Each Additive
Representative mass spectra acquired in positive ion mode from HMGEC lipids extracted with two concentrations of ammonium acetate as an additive to the Folch technique.[115] Unpublished data, J. Ziemanski

Harvesting and Extraction Methods

Continuing with the theory that nonpolar lipids were being poorly recovered, a new hypothesis was developed: trypsin dissociation from the growth surface may be damaging the HMGEC membrane, making it vulnerable to loss of intracellular vesicles containing stores of nonpolar lipids.[130,131] Three harvesting methods were evaluated. The first was the conventional method of 0.25% trypsin-EDTA which was compared to two trypsin-free methods: 10 mM EDTA and direct application of 2:1 chloroform-methanol (v/v) to HMGECs in culture. This work has since been published[132] and is reprinted in this dissertation as Chapter Two. In summary, it was found that all three harvesting techniques were compatible with lipid extraction and that all three techniques led to relatively equivalent lipidomic profiles. The hypothesis was not supported, however, as the trypsin-free approaches failed to produce a robust increase in nonpolar lipids. Despite these null findings, it was discovered that the use of 2:1 chloroform-methanol (v/v) was a much more efficient technique and was therefore much more amenable to high-throughput analyses. This combined harvesting and extracting method was utilized in all subsequent experiments.

Following these two failed attempts to yield a more robust nonpolar lipidome, the hypothesis of poor recovery was abandoned, and an exploration of meaningful lipidomic parameters was initiated. The decision was made to focus on quantifying meibum-relevant lipids—the nonpolar lipids that are reproducibly detected in meibum. These were initially defined to be CEs and WEs, the two most abundant meibum lipid classes.[61,62] Curiosity existed, however, about whether HMGECs produce an MGD biomarker.

Biomarker of MGD in Preclinical Research

To determine whether a given lipid class or species was responsive to a known MGD-inducing compound, HMGECs were treated with 13-cis retinoic acid (isotretinoin), which is a commonly used acne medication that is highly associated with MGD development.[33] The data were analyzed by volcano plots using MetaboAnalyst[133] with threshold values of 2.0 for the fold change (FC) and 0.05 for the p-value. There were no downregulated meibum-relevant peaks following treatment with 0.5 µM 13-cis retinoic acid, but there was one CE and ten TAGs that were upregulated relative to the vehicle control (Figure 11). These results suggested that TAG synthesis is altered in this model of MGD; therefore, TAGs were included among the list of potentially meaningful lipid parameters to quantify. Guided by this experiment, the final list of meibum-relevant lipids that were targeted in this dissertation were CEs, WEs, and TAGs.

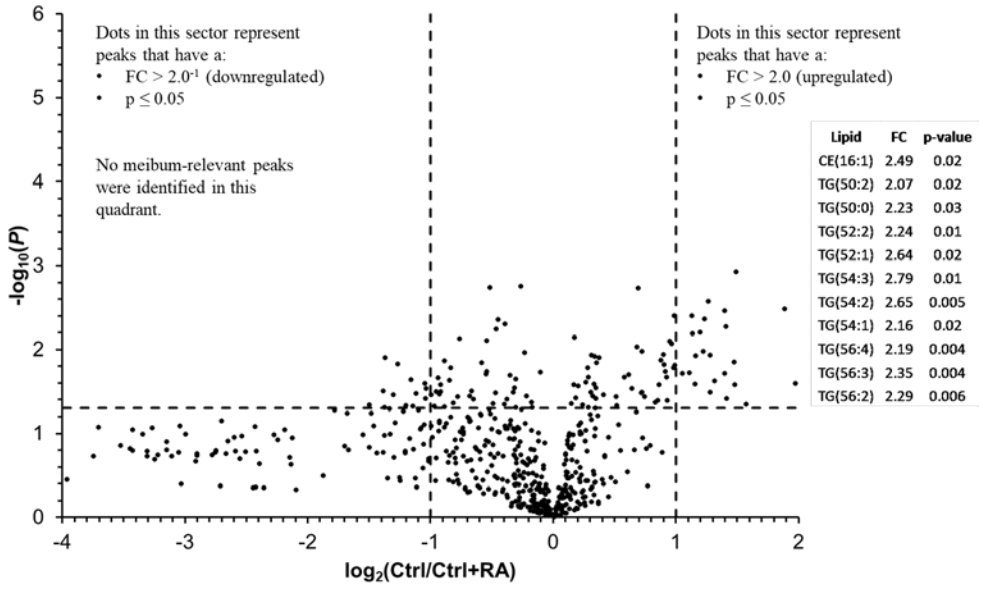

Figure 11 Differential Lipid Expression Following 13-cis Retinoic Acid
Volcano plot depicting differential expression of lipids extracted from HMGECs treated with and without 13-cis retinoic acid (isotretinoin). Unpublished data, J. Ziemanski

Validation of Cell Viability Using ATP Quantitation

The cell viability assay chosen for this dissertation was the CellTiter Glo Luminescent Cell Viability Assay (Promega, Madison, WI). This assay takes advantage of the ATP-dependent reaction of luciferin with luciferase which produces a luminescent signal that can be read with a standard plate reader.[134] Viable cells donate the ATP, emitting light that is proportional to the number of cells in the reaction. This assay was chosen due to its sensitivity to cell number, its relative resistance to artifacts, and its high efficiency.[134] To ensure that these strengths could be reproduced internally, two independent experiments were performed to assess sensitivity to cell number and to cell death. First, three wells of a 96-well plate were seeded with 0, 10, 20, 30, 40, or 50 thousand cells each and incubated at 37°C overnight. Cell viability was assessed with the CellTiter Glo Luminescent Cell Viability Assay (Promega, Madison, WI). Excellent linearity ($R^2 = 0.995$) was achieved, validating that ATP varies linearly with cell count (Figure 12A). Next, HMGECs were challenged with Triton-X 100 at 0.05%, 0.25%, 0.50%, 1.0%, and 2.0% for one hour. A dramatic decrease in luminescent signal was detected for all concentrations, suggesting that all concentrations were lethal to HMGECs (Figure 12B). The 1.0% concentration was chosen as the positive control in all future experiments.

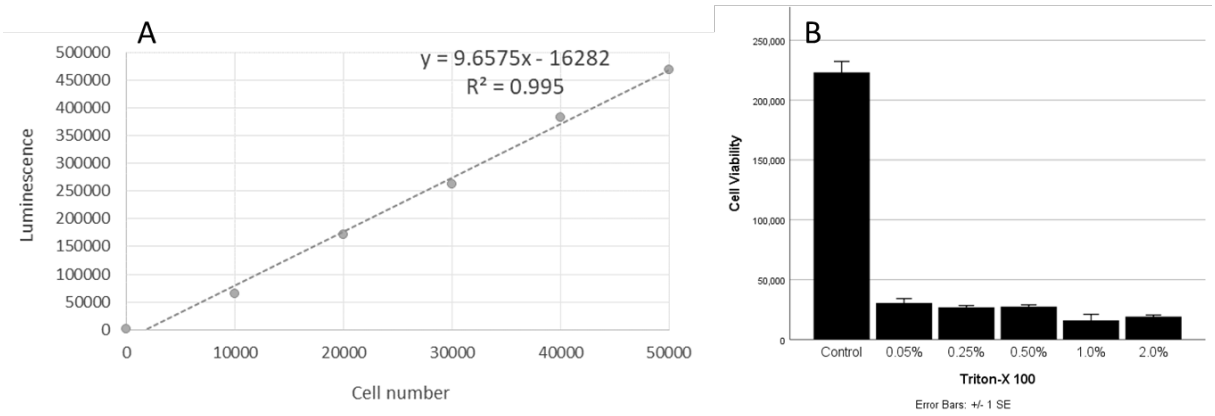

Figure 12 Validation of ATP-Based Cell Viability Assay
(A) Quantitation of ATP (luminescence) is linearly related to HMGEC number. (B) Quantitation of ATP (cell viability) is capable of detecting death induced by a known toxic compound, Triton-X 100. Unpublished data, J. Ziemanski

Safety Evaluation of Dimethylsulfoxide (DMSO) Vehicle

In preparation for the inhibition experiments performed in Aim 2 (Chapter Six), a higher concentration of the DMSO vehicle was needed to facilitate delivery of all the reagents to the culture media: rosiglitazone, latanoprost, and each of the five receptor antagonists. Experiments up to this juncture had successfully used a DMSO concentration of 0.5%, but increasing this value to 0.8% was necessary. To ensure that 0.8% DMSO yielded a similar safety profile as 0.5%, differentiated HMGECs were exposed to 0.5%, 0.6%, 0.7%, and 0.8% DMSO for 3.5 hours. Cell viability was assessed using the CellTiter Glo Luminescent Cell Viability Assay (Promega, Madison, WI). There were no differences in cell viability between any of the DMSO concentrations (Figure 13). All concentrations varied significantly relative to the positive control, 1.0% Triton-X 100 ($p < 0.001$ for each). Therefore, for the inhibition experiments described in Chapter Six, a DMSO concentration of 0.8% was used.

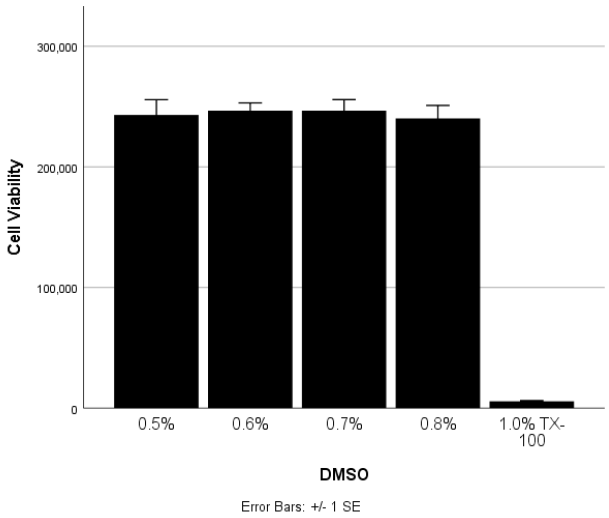

Figure 13 Safety Evaluation of DMSO
Higher concentrations of dimethylsulfoxide (DMSO) up to 0.8% show no adverse effect on cell viability with respect to 0.5%. Unpublished data, J. Ziemanski

PURPOSE, SPECIFIC AIMS, AND HYPOTHESIS

Purpose

This dissertation project aims to develop a model experimental platform for the preclinical study of MGD using HMGECs (Optimization Aim) and to elucidate the effects of prostaglandins, a representative prostaglandin analog (latanoprost), and BAK on HMGEC viability and lipidomic expression (Aims 1 and 2). The results provide evidence toward the mechanism of glaucoma-associated MGD and may inform the development of new or modified drugs or preservative systems to optimize treatment outcomes in patients suffering from these two common comorbidities.

Specific Aims

Optimization Aim: Assess the lipidomic profile produced from HMGECs after treatment with rosiglitazone, a PPARγ agonist involved in lipid metabolism.

Prior to addressing the crux of this dissertation project, the culture conditions that encourage maturation and differentiation of HMGECs needed to be refined. In this aim, the lipidomic profile, specifically CEs, WEs, and TAGs, from HMGECs were assessed in a multifactorial analysis that evaluated rosiglitazone, fetal bovine serum, and culture duration. The results of these experiments, combined with preliminary data described in this chapter and in Chapter Two, guided culture conditions and extraction methodology that were used in all subsequent experiments. The work from this Aim is presented in Chapters Three and Four.

Aim 1: Assess the roles of and mechanisms for PGE_2 and $PGF_{2\alpha}$ on differential lipid expression and cell death in HMGECs.

A paucity of evidence exists regarding the physiologic roles of endogenous prostaglandins on HMGECs. Before tackling the clinically relevant question of how latanoprost and BAK exert their pathophysiologic effects on the meibomian glands, a better understanding of how prostaglandins influence their normal physiology was needed. In this aim, HMGECs were immunostained with antibodies against FP, EP1, EP2, EP3, and EP4 to detect the presence of $PGF_{2\alpha}$ and PGE_2 receptors. Subsequently, HMGECs were treated with physiologic concentrations of $PGF_{2\alpha}$ and PGE_2. Cell viability was assayed by ATP quantitation, and lipid extracts were analyzed for CE, WEs, and TAGs by mass spectrometry. The work from this Aim is presented in Chapter Five.

Aim 2: Evaluate the pathophysiologic effects of latanoprost and BAK on HMGECs.

In this aim, HMGECs were treated with various concentrations of latanoprost, BAK, and the combination of the two. Cell viability and lipid analysis were performed identically to Aim 1. Prostanoid receptor inhibitors were also used to determine which, if any, prostanoid receptors mediated the observed changes in HMGEC viability relative to control. The work from this Aim is presented in Chapter Six.

Overarching Hypothesis

Prior to embarking on this dissertation project, it was hypothesized that HMGECs would most strongly express the EP2 and EP4 receptors. Both latanoprost and BAK were expected to modulate the lipid profile produced by HMGECs at concentrations equivalent to commercially available ophthalmic preparations. The chapters that follow describe the development of the methodology used in this project (Chapters Two, Three, and Four), the physiologic effects of endogenous prostaglandins on HMGECs (Chapter Five), and the pathophysiologic effects of latanoprost and BAK on HMGECs (Chapter Six).

CHAPTER TWO: EVALUATION OF CELL HARVESTING TECHNIQUES TO OPTIMIZE LIPIDOMIC ANALYSIS FROM HUMAN MEIBOMIAN GLAND EPITHELIAL CELLS IN CULTURE

by

JILLIAN F. ZIEMANSKI, JIANZHONG CHEN, KELLY K. NICHOLS

International Journal of Molecular Sciences 2020: 21(9)

Abstract

The lipidomic analysis of immortalized human meibomian gland epithelial cells (HMGECs) has been proposed as a preclinical model to study meibomian gland dysfunction. An in vitro study was conducted to evaluate neutral lipid recovery following three harvesting techniques and to identify candidate lipid biomarkers of HMGECs. HMGECs were cultured in serum-containing media for two days to promote lipid production. Cells were either harvested by 0.25% trypsin–ethylenediaminetetraacetic acid (EDTA), harvested by 10 mM EDTA, or simultaneously harvested and extracted by 2:1 chloroform–methanol (CM). After extraction by a modified Folch technique, the nonpolar phase was processed and infused into a TripleTOF 5600 mass spectrometer (Sciex, Framingham, MA, USA) with electrospray ionization. MS and MS/MS^{all} spectra were acquired. Nonpolar cholesteryl esters (CEs) were consistently detected in all samples, while wax esters were not. Only small differences in two out of twenty CEs were detected between harvesting methods. CM yielded less CE18:1 than the other methods but greater CE20:4 than the trypsin–EDTA method ($p < 0.05$ for all). Similar to human meibum, very long-chain CEs with carbon number (n_c) ≥ 24 were detected in all samples and may serve as HMGEC lipid biomarkers. Further work is needed to address the absence of wax esters. Overall, the three harvesting methods are reasonably equivalent, though CM promotes much better efficiency and is recommended for higher throughput.

Introduction

Human meibomian gland epithelial cells (HMGECs) have been shown to accumulate lipids, respond to androgens, and express genes involved in lipogenesis and keratinization.[1] To date, however, there have been reports of the lipidome recovered from HMGECs differing from the typical lipid profile of normal human meibum.[2,3] Specifically, human meibum is low in phospholipids but high in long-chain wax and cholesteryl esters, while the HMGEC lipidome is the opposite.[2-6]

One possible explanation for the inverse profiles between HMGECs and human meibum could be the use of an abrasive harvesting reagent that can cause increased cell permeability and the loss of intracellular contents. The combination of trypsin with ethylenediaminetetraacetic acid (EDTA) is a widely used harvesting technique in cell culture to promote the detachment of adherent cells from a growth surface. However, in metabolomic analyses, trypsin–EDTA treatment has been found to be too abrasive to the cell membrane, causing significant leakage of intracellular metabolites.[7,8] Neutral lipids produced by HMGECs are contained within intracellular vesicles[2] and therefore may be vulnerable to loss following trypsin–EDTA treatment.

Mass spectrometry is an analytical method that can be used to determine the composition of a complex fluid mixture, such as human tears, meibum, or HMGEC lysate. Mass spectrometry has been widely used in human tear and meibum analyses[4] but only in a minority of reports involving HMGECs.[2,3] The process of extracting lipids and injecting each sample into the instrument, however, is time consuming and costly. Therefore, an efficient harvesting method that limits the steps to extract lipids would expend less time and utilize fewer consumables, thereby enhancing research efficiency.

The primary objective of this pilot study was to assess trypsin-free harvesting techniques to optimize both the neutral lipid recovery from and analytical efficiency of HMGECs. In addition, considering that lipid production is the primary physiologic function of the meibomian gland, the identification of candidate lipid biomarkers that can be utilized to assess HMGEC function is paramount. Therefore, as a secondary objective, differences in nonpolar lipids between HMGECs and serum-containing media were evaluated and compared to the literature to determine their potential as HMGEC lipid biomarkers.

Results

The genotype of the HMGECs was confirmed by short-tandem repeat analyses. Our sample profile provided a 100 percent match to the reference profile at all sixteen loci.[9] Ultra-long chain cholesteryl esters (CEs) were detectable in all samples, thereby manifesting the expected phenotype of the glandular epithelial cells of the meibomian glands, as presented later. From all three techniques tested, successful harvesting and extraction were achieved (Figure 1) and, across techniques, the most abundant species were phosphatidylcholines (PC) and sphingomyelins (SM). In contrast, the peaks of wax esters and cholesteryl esters, common in human meibum, were limited in these MS spectra of HMGECs.

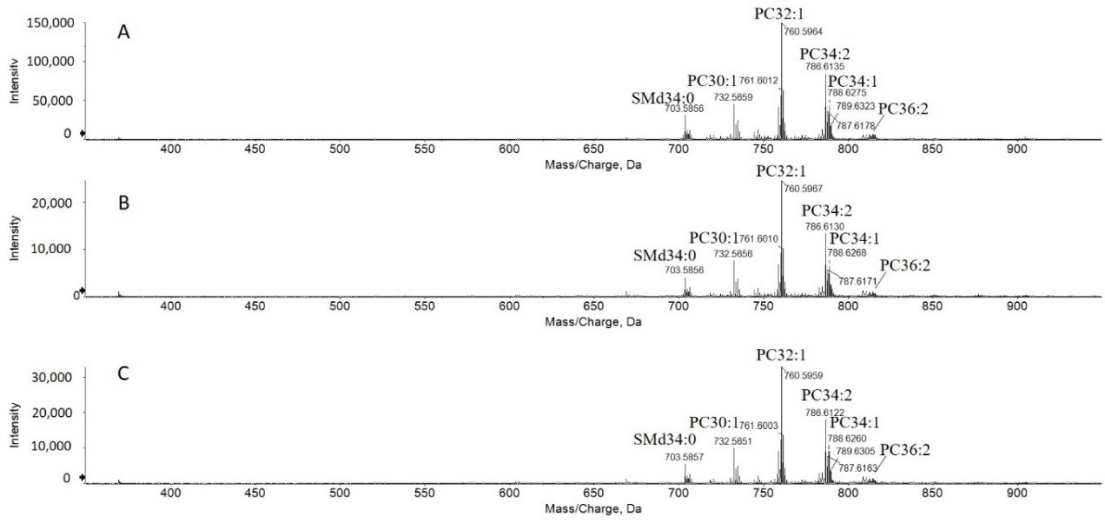

Figure 1 Representative Mass Spectra of HMGEC Lipids
Representative mass spectra of lipids from human meibomian gland epithelial cells (HMGECs) acquired in positive ion mode. HMGECs were harvested by (**A**) 2:1 chloroform–methanol, (**B**) 10 mM ethylenediaminetetraacetic acid (EDTA), and (**C**) 0.25% trypsin–EDTA. Major peaks are identified. Labeling convention is carbon number in the acyl chains: double bond. Sphingomyelin with dihydroxy base (SMd), Phosphatidylcholine (PC).

Considering that polar lipids, including phospholipids, are only a minor contributor to the lipid pool in human meibum,[10-12] specific attention was given to the two most abundant classes: CEs and wax esters (WEs). Compared to MS analysis (Figure 1), the pseudo precursor ion scanning mass spectra extracted from MS/MS^{all} data are more sensitive to the detection of these nonpolar lipids.[13] Prior to lipid extraction, all media were aspirated, and the adhered HMGECs were washed twice to remove trace amounts of lipids remaining from the serum-containing culture media. Following analysis, CEs were consistently detected in all samples (Figure 2A). Similar CE diversity was present in cells and culture media when the carbon number (n_c) was less than 24 (Figure 2A and 2B). However, very long- and ultra long-chain CEs with $n_c \geq 24$ were

only detected from cell samples and were absent from culture media (Figure 2A and 2B). WEs were not detected in any of the samples.

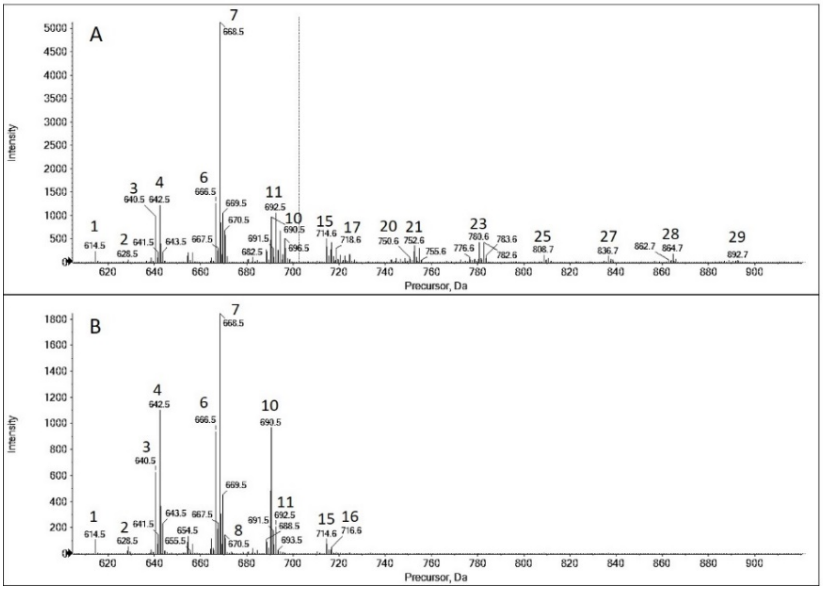

Label	*m/z*	CE (n_C : dbl bond)	Label	*m/z*	CE (n_C : dbl bond)
1	614.5	14:0	**16**	716.6	22:5
2	628.5	15:0	**17**	718.6	22:4
3	640.5	16:1	**18**	722.6	22:2
4	642.5	16:0	**19**	724.6	22:1
5	656.5	17:0	**20**	750.6	24:2
6	666.5	18:2	**21**	752.6	24:1
7	668.5	18:1	**22**	754.6	24:0
8	670.5	18:0	**23**	780.6	26:1
9	684.5	19:0	**24**	782.6	26:0
10	690.5	20:4	**25**	808.7	28:1
11	692.5	20:3	**26**	810.7	28:0
12	694.5	20:2	**27**	836.7	30:1
13	696.5	20:1	**28**	864.7	32:1
14	698.5	20:0	**29**	892.7	34:1
15	714.6	22:6			

Figure 2 Representative Pseudo Precursor Ion Scan of CEs
Representative pseudo precursor ion scanning mass spectra of cholesteryl esters (CEs, carbon number: double bond) extracted from MS/MS^{all} data for (**A**) HMGECs and (**B**) culture media. Only those CEs present in all samples are included in the legend. Only the most abundant peaks are labeled in the figures to aid readability. CEs with carbon number ($n_C < 24$) are present in both HMGECs and culture media, while CEs with $n_C \geq 24$ are only present in HMGECs.

The relative abundance of each CE was compared between the three harvesting techniques, labeled as trypsin-containing (TC, 0.25% trypsin–EDTA), EDTA (10 mM EDTA), and chloroform–methanol (CM, 2:1 chloroform–methanol). No statistical differences were found between ten of the twelve CEs (Figure 3). The CM technique, however, yielded less CE18:1 (mean = 40.37) compared to EDTA (mean = 43.51, p = 0.02) and TC (mean = 43.14, p = 0.03) and greater CE20:4 (mean = 7.17) compared to

TC (mean = 4.56, $p = 0.02$). There were no statistical differences between any of the longer-chain CEs ($n_c \geq 24$) among the three different harvesting techniques (Figure 4).

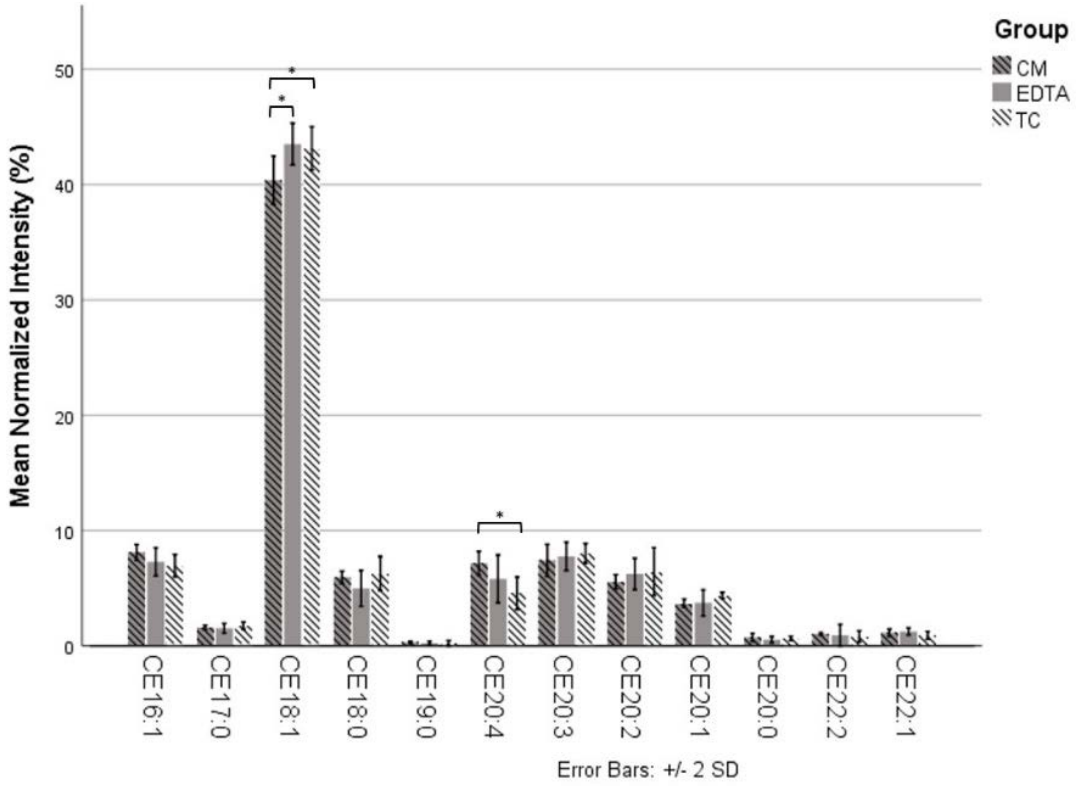

Figure 3 Comparison of Harvesting Techniques

Comparison between the three harvesting techniques for the relative abundance of the cholesteryl esters (CEs) that were common ($n_c < 24$) to both cell and media samples. There were no differences between the three techniques for 10 of the 12 CEs. The chloroform–methanol (CM) method yielded less CE18:1 than the EDTA and trypsin-containing (TC) methods but greater CE20:4 than the TC method. * $p < 0.05$, chloroform–methanol (CM), ethylenediaminetetraacetic acid (EDTA), trypsin-containing (TC) (trypsin–EDTA).

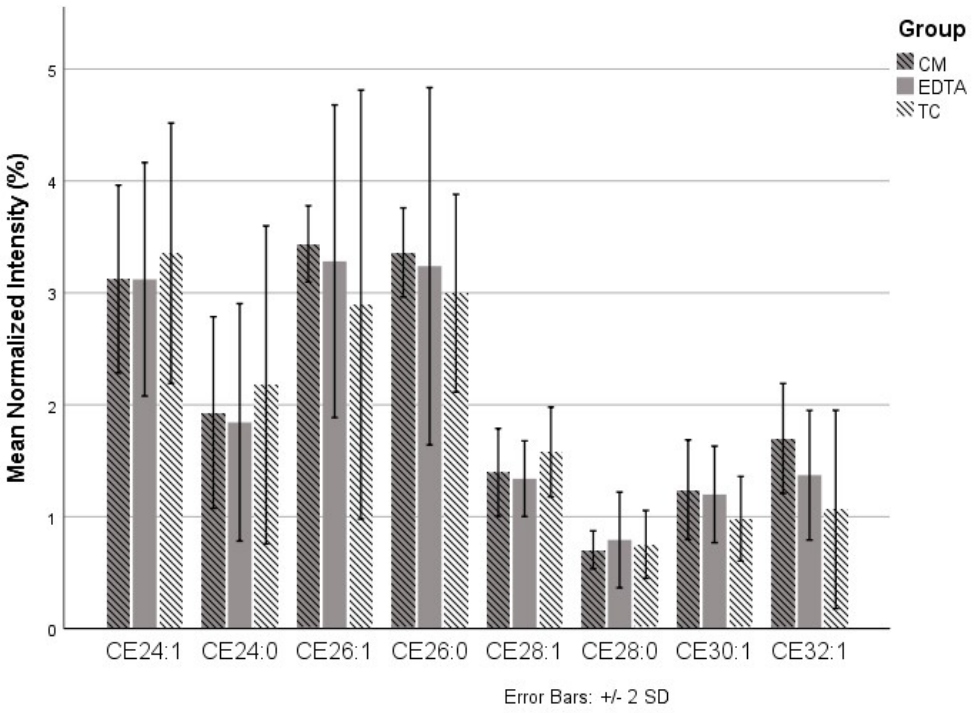

Figure 4 Comparison of CEs from HMGECs
Comparison of the three techniques for the cholesteryl esters (CEs) that were only detected in HMGECs. Chloroform–methanol (CM), ethylenediaminetetraacetic acid (EDTA), trypsin-containing (TC) (trypsin–EDTA).

Discussion

We sought to optimize neutral lipid recovery and analytical efficiency from HMGECs in culture, while simultaneously attempting to identify candidate lipid biomarkers. This pilot study suggests that CEs with $n_c \geq 24$ may be biomarkers of serum-differentiated HMGECs. Previous reports have shown that ultra-long-chain CEs ($n_c \geq 26$) are not detected in other epithelial cells[14] or in serum.[15] While the CE class, as a whole, is not specific to any particular tissue, CEs with ultra-long-chain fatty acids are very specific to meibomian and sebaceous glands.[16] CEs with $n_c \geq 24$ are attractive candidates as lipid biomarkers, considering that very long-chain (n_c = 20 to 25) and ultra-long-chain

CEs make up the most abundant CEs in normal human meibum.[11] Additionally, recent work by Borchman et al.[17] and Shrestha et al.[18] show that CEs (exact species not specified) are decreased in adults with meibomian gland dysfunction. Therefore, CEs with $n_c \geq 24$—not found in culture media, serum, other epithelial cells, or other tissues (except sebaceous glands)—may have differentiating capacity among disease states, making them promising candidate biomarkers. Further validation of these CEs to assess for change in response to challenge and intervention is needed.

We also tested the hypothesis that trypsin-free harvesting techniques promote better neutral lipid recovery, presumably by maintaining the integrity of the cell membrane until the desired extraction step. All three methods used in this study are compatible with lipid extraction. Despite using the highly sensitive MS/MS^{all} technique, we were unable to detect WEs in any of the samples in this study, a surprising finding considering that WEs are a predominant component of the lipid pool in normal human meibum.[11,19] These results suggest that serum-differentiated HMGECs fail to produce measurable levels of WEs under our experimental conditions. Hampel et al**.** used similar conditions—serum-induced differentiation for a culture duration of one day or three days.[3] Although they were able to detect WEs, they reported that it was only 0.35 to 0.46 percent of the overall lipid pool. Sullivan et al**.** also reported a presence of WEs after serum-induced differentiation, and they maintained differentiating conditions for up to two weeks.[2] They, too, acknowledged the low detection of WEs, accounting for < 1 percent of the total lipid pool. Differences in experimental conditions and/or analytical strategies could account for the discrepancy in WEs between our study (not detected) and theirs (present but at low quantities). The decision to differentiate for two days in our

experiments was based on several factors. Our main objective was to evaluate three different harvesting and extraction techniques, an objective that is largely independent of culture duration. Our second objective was to evaluate our data to identify potential candidate biomarkers of lipid-producing HMGECs. Hampel et al. reported that the nonpolar lipid content recovered from serum-differentiated HMGECs was greatest at one day and then was reduced over the following thirteen days.[3] Our pilot studies suggested that there were no qualitative differences in the overall lipid profile, including the classes of lipids produced, between 2, 9, 16, and 23 days of culture in serum-containing media.[20] Therefore, the decision to maintain differentiating conditions for two days was made in conjunction with both the literature and pilot studies, and the duration was sufficient to successfully address our aims.

Unlike WEs, very long-chain and ultra-long-chain CEs were consistently detected. There were only small differences in specific CE species between the different harvesting techniques. The CM method yielded less CE18:1 than both EDTA and TC and greater CE20:4 than TC. There were no differences in the remaining 18 CEs detected. The likelihood that these differences are attributable to the abrasive nature of trypsin, as originally hypothesized, is low, given that there were no differences between the milder EDTA technique and the more aggressive TC technique. CE18:1 is highly abundant in plasma (and presumably serum),[15] and both TC and EDTA methods require a second application of serum-containing media to prevent further protease and/or chelating activity. The chloroform–methanol in the CM method, however, is directly applied to the cells and simultaneously initiates the extraction process, thereby avoiding the second introduction of the serum lipidome. Therefore, the CM technique is not only more

efficient, but it also reduces the opportunity for serum and media contamination. The difference in CE20:4 expression levels between the CM and TC techniques is potentially of interest, considering that it is present, albeit in low quantities, in normal meibum.[13] Further investigation is warranted.

In a similar manner to our previously stated rationale for maintaining differentiating conditions for two days, we chose to differentiate by serum alone because the differentiating agent had little influence on our primary objective (comparing harvesting and extraction techniques). However, the presence of serum, a rich lipid source, is capable of influencing the recovered lipidome either through contamination or through the induction of metabolic processes that can modify lipid production.[21] As already mentioned, the importance of careful washing to remove all traces of the serum lipidome cannot be understated. Furthermore, the CM technique helps to minimize opportunities for contamination by the serum lipidome. From a meibogenesis perspective, it is not possible to state to what extent serum lipids could have been internalized, processed, and ultimately expressed by the HMGECs in this study. The involved metabolic pathways are extremely diverse, highly complex, and still in the early stages of research.[21] In general, fatty acids—the building blocks of complex lipids—are believed to derive from intracellular acetyl CoA or from circulating fatty acids in the blood. The most abundant fatty acid in plasma is C18:1 (oleic acid).[15] In this study, CE 18:1 was the most prominent CE, accounting for approximately 40 percent of all CEs. The source of oleic acid in CE 18:1 is purely speculative, but its high expression from HMGECs in this study, especially compared to its low expression in human meibum (approximately five percent[13]), could be a reflection of its uptake from serum. A similar pattern was observed

for the cholesteryl ester of arachidonic acid (CE 20:4). Further research involving a serum-free environment is needed to better understand exactly how the meibomian gland synthesizes the different types of lipids and to what extent fatty acids are produced de novo versus taken up from the blood. Most importantly, CEs with $n_c \geq 24$ are not present in serum-containing media. Therefore, these particular CEs are confidently derived from, or at least modified by, cultured HMGECs.

Importantly, across all of the different harvesting and extraction techniques, the lipidome from HMGECs still shows significant differences relative to the lipidome from normal human meibum. One possibility to explain these discrepant findings is that immortalized HMGECs may fail to fully differentiate in culture, as previously hypothesized by other groups,[3,22,23] though the methodology of Schroder et al.[23] has recently been challenged.[24] Hampel et al. stated that HMGECs that are differentiated by serum reach only an early stage of differentiation.[25] Other groups, however, have reported successful differentiation through several mechanisms beyond serum.[26-31] These disagreements in the literature are likely the result of an ill-defined biomarker that is sensitive to the early, middle, and late stages of differentiation. Until comprehensive work can be done to define the stages of meibocyte differentiation on the molecular level, this issue will continue to be unresolved. In the meantime, the molecular analysis of meibum by mass spectrometry appears to be a specific approach for the quantitation of targeted meibum-relevant lipids. Our data suggest that cholesteryl esters, particularly those with $n_c \geq 24$, are viable outcome measures for future experiments using HMGECs.

Another hypothesis to explain the discrepancies in the lipidomes is that HMGECs may be dependent on other glandular tissue or biochemical reactions in vivo to finalize

meibum composition, an idea previously suggested by Chen et al**.** in 2010.[19] It has been proposed, in dermal sebaceous glands, that phospholipid recycling occurs across the ductal epithelium.[32] This process may dramatically reduce phospholipid content in the final excreta. Therefore, it is possible that the HMGEC lipidome should not be identical to human meibum. Despite these differences, experimentation using HMGECs continues to be a powerful tool in dry-eye and meibomian gland dysfunction research. In vitro experimentation can answer research questions that are either poorly controlled or unethical to perform in human patients. To appropriately use preclinical models—such as HMGECs or another recently described mouse meibocyte cell line[33]—in experimental manipulations, researchers should use carefully optimized methodology and target parameters that have been validated as similar to human meibum, such as CEs with $n_c \geq 24$. Further experimentation is needed to address the differences between HMGECs and human meibum, as well as to further validate responsive and physiologically meaningful outcome parameters.

In conclusion, we have demonstrated that CEs with $n_c \geq 24$ are candidate lipid biomarkers of HMGECs. Further research is needed to validate these markers in other culture conditions that may influence HMGEC differentiation. The lipidome as determined by mass spectrometry, however, shows minimal variation when using trypsin-containing versus trypsin-free harvesting methods, particularly for these very long-chain and ultra-long-chain CEs. The CM technique, though, has the added advantage of improved efficiency as it reduces the need for reagent incubation times and several time-consuming washing steps. Reducing the duration of sample preparation makes the use of mass spectrometry, an already time-consuming method, more feasible and more

accessible. When high output is needed, the direct application of chloroform–methanol to cells in culture serves as the preferred harvesting method, thereby improving research efficiency.

Materials and Methods

Cell Culture

Immortalized HMGECs were maintained in keratinocyte serum-free media (KSFM) supplemented with 5 ng/mL epidermal growth factor (EGF) and 50 μg/mL bovine pituitary extract (BPE) until 80% confluence.[1] To promote differentiation and lipid synthesis, the culture medium was changed to Dulbecco's modified Eagle's medium (DMEM) and Ham's F12 (1:1) containing 10 ng/mL EGF and 10% fetal bovine serum (FBS).[2]

Harvesting and Lipid Extraction

After two days of culture, the culture medium was withdrawn and retained for lipidomic analysis. Three different harvesting techniques were evaluated. The first technique was the standard 0.25% trypsin–EDTA for 5 min at 37 °C. Following incubation, all cells were confirmed to have visibly detached from the growth surface. The second technique was 10 mM EDTA at 37 °C for a total of 10 min. Cells were monitored for complete detachment after 5 min, but complete detachment was not achieved until 10 min. The third technique represents a newer adaptation of the Folch extraction[34] that simultaneously harvests and extracts lipids from cells in culture. To avoid the common issue of plastic additives overshadowing the

detection of neutral lipids by mass spectrometry, HMGECs were cultured in 6-cm glass petri dishes. At the time of extraction, the culture media was withdrawn and retained, and the cells were washed twice with ice-cold HPLC-grade water. A phosphate buffer was avoided to ensure compatibility with mass spectrometric analysis. Pre-mixed chloroform–methanol (2:1 *v*/*v*, 3 mL), prechilled to −20 °C, was directly applied to the glass petri dish surface with adhered HMGECs. The growth surfaces were then scraped with a stainless steel scraper, and the sample was transferred to a glass vial for the remainder of the extraction steps. All experiments were completed in triplicate.

Both cell lysates and culture media were analyzed. Lipids were extracted from all samples by a modified Folch technique.[34] Pre-mixed 2:1 chloroform–methanol (*v*/*v*) was added directly to each sample, followed by 50 mM ammonium acetate in HPLC-grade water for cells or 67 mM ammonium acetate for culture media. Consistent with the Folch technique, the final ratio of chloroform–methanol–water for all samples, both cells and media, was 8:4:3. The resulting emulsion was agitated at 350 rpm for 20 min on ice on an orbital shaker and then centrifuged at 1600× *g* for 5 min to promote stratification. The lower, nonpolar phase was withdrawn for subsequent mass spectrometric analysis. All steps involving organic solvents were performed with glass, stainless steel, or polytetrafluoroethylene (PTFE) and in the absence of any other plastics to minimize the interference of plasticizers.

Mass Spectrometric Analysis

All samples were then diluted tenfold with methanol and ammonium acetate (final concentration = 2 mM). The sample was directly infused into a Triple TOF 5600 mass

spectrometer (SCIEX, Framingham, MA, USA) with electrospray ionization at a flow rate of 7 µL/min, as previously described[13.] MS and MS/MS^{ALL} spectra were acquired in both positive and negative ion modes. MS/MS^{ALL} analysis was performed with the SWATH technology (Sequential Window Acquisition of All Theoretical mass spectra, SCIEX), where product ion MS/MS spectra for all precursor ions were acquired in the *m*/*z* range of interest (200 to 1200) at every one Dalton step with 6 min for each detection mode. The collision energy was 40 eV for positive ion mode and −54 eV for negative ion mode. The collision energy spread was 40 eV for both modes. At least four rinses were performed between sample runs, and results were monitored by mass spectrometry to ensure that carryover was negligible.

Data Analysis

Up to 90 percent of normal human meibum is comprised of wax esters (WEs) and cholesteryl esters (CEs);[11,19] therefore, these lipid classes were the primary focus of this pilot study. Only the lipid species that were present in all samples were included in the analysis. Signal intensity for each identified peak was normalized to sum intensity per class and was therefore reported as percent per class. Differences between harvesting methods were assessed by one-way ANOVA with Tukey post-hoc testing (SPSS v26, Armonk, NY, USA), when tests of normality (Shapiro–Wilk) and homogeneity of variance (Levene's Test) were satisfied. In the few instances where these assumptions were violated, the nonparametric Kruskal–Wallis test was performed.

Acknowledgments: The authors would like to thank David Sullivan for providing the human meibomian gland epithelial cells.

Funding: This research was funded by the American Optometric Foundation Beta Sigma Kappa Research Fellowship with additional support by the National Eye Institute under P30 EY003039 and the Office of Research Infrastructure Programs of the National Institutes of Health under S10 RR027822-01.

References

1. Liu, S.; Hatton, M.P.; Khandelwal, P.; Sullivan, D.A. Culture, immortalization, and characterization of human meibomian gland epithelial cells. Invest. Ophthalmol. Vis. Sci. 2010, 51, 3993–4005, doi:10.1167/iovs.09-5108.

2. Sullivan, D.A.; Liu, Y.; Kam, W.R.; Ding, J.; Green, K.M.; Shaffer, S.A.; Hatton, M.P.; Liu, S. Serum-induced differentiation of human meibomian gland epithelial cells. Invest. Ophthalmol. Vis. Sci. 2014, 55, 3866–3877, doi:10.1167/iovs.13-13407.

3. Hampel, U.; Schroder, A.; Mitchell, T.; Brown, S.; Snikeris, P.; Garreis, F.; Kunnen, C.; Willcox, M.; Paulsen, F. Serum-induced keratinization processes in an immortalized human meibomian gland epithelial cell line. PLoS ONE 2015, 10, e0128096, doi:10.1371/journal.pone.0128096.

4. Green-Church, K.B.; Butovich, I.; Willcox, M.; Borchman, D.; Paulsen, F.; Barabino, S.; Glasgow, B.J. The international workshop on meibomian gland dysfunction: Report of the subcommittee on tear film lipids and lipid-protein interactions in health and disease. Invest. Ophthalmol. Vis. Sci. 2011, 52, 1979–1993, doi:10.1167/iovs.10-6997d.

5. Saville, J.T.; Zhao, Z.; Willcox, M.D.; Ariyavidana, M.A.; Blanksby, S.J.; Mitchell, T.W. Identification of phospholipids in human meibum by nano-electrospray ionisation tandem mass spectrometry. Exp. Eye Res. 2011, 92, 238–240, doi:10.1016/j.exer.2010.12.012.

6. Butovich, I.A.; Uchiyama, E.; McCulley, J.P. Lipids of human meibum: Mass-spectrometric analysis and structural elucidation. J. Lipid. Res. 2007, 48, 2220–2235, doi:10.1194/jlr.M700237-JLR200.

7. Bi, H.; Krausz, K.W.; Manna, S.K.; Li, F.; Johnson, C.H.; Gonzalez, F.J. Optimization of harvesting, extraction, and analytical protocols for UPLC-ESI-MS-based metabolomic analysis of adherent mammalian cancer cells. Anal. Bioanal. Chem. 2013, 405, 5279–5289, doi:10.1007/s00216-013-6927-9.

8. Dettmer, K.; Nurnberger, N.; Kaspar, H.; Gruber, M.A.; Almstetter, M.F.; Oefner, P.J. Metabolite extraction from adherently growing mammalian cells for metabolomics studies: Optimization of harvesting and extraction protocols. Anal. Bioanal. Chem. 2011, 399, 1127–1139, doi:10.1007/s00216-010-4425-x.

9. McDermott, A.M.; Baidouri, H.; Woodward, A.M.; Kam, W.R.; Liu, Y.; Chen, X.; Ziemanski, J.F.; Vistisen, K.; Hazlett, L.D.; Nichols, K.K.; et al. Short Tandem Repeat (STR) Profiles of Commonly Used Human Ocular Surface Cell Lines. Curr. Eye Res. 2018, 43, 1097–1101, doi:10.1080/02713683.2018.1480043.

10. Brown, S.H.; Kunnen, C.M.; Duchoslav, E.; Dolla, N.K.; Kelso, M.J.; Papas, E.B.; Lazon de la Jara, P.; Willcox, M.D.; Blanksby, S.J.; Mitchell, T.W. A comparison of patient matched meibum and tear lipidomes. Invest. Ophthalmol. Vis. Sci. 2013, 54, 7417–7424, doi:10.1167/iovs.13-12916.

11. Chen, J.; Green, K.B.; Nichols, K.K. Quantitative profiling of major neutral lipid classes in human meibum by direct infusion electrospray ionization mass spectrometry. Invest. Ophthalmol. Vis. Sci. 2013, 54, 5730–5753, doi:10.1167/iovs.12-10317.

12. Lam, S.M.; Tong, L.; Duan, X.; Petznick, A.; Wenk, M.R.; Shui, G. Extensive characterization of human tear fluid collected using different techniques unravels the presence of novel lipid amphiphiles. J. Lipid Res. 2014, 55, 289–298, doi:10.1194/jlr.M044826.

13. Chen, J.; Nichols, K.K. Comprehensive shotgun lipidomics of human meibomian gland secretions using MS/MS (all) with successive switching between acquisition polarity modes. J. Lipid. Res. 2018, 59, 2223–2236, doi:10.1194/jlr.D088138.

14. Sampaio, J.L.; Gerl, M.J.; Klose, C.; Ejsing, C.S.; Beug, H.; Simons, K.; Shevchenko, A. Membrane lipidome of an epithelial cell line. Proc. Natl. Acad. Sci. USA 2011, 108, 1903–1907, doi:10.1073/pnas.1019267108.

15. Quehenberger, O.; Armando, A.M.; Brown, A.H.; Milne, S.B.; Myers, D.S.; Merrill, A.H.; Bandyopadhyay, S.; Jones, K.N.; Kelly, S.; Shaner, R.L., et al. Lipidomics reveals a remarkable diversity of lipids in human plasma. J. Lipid Res. 2010, 51, 3299–3305, doi:10.1194/jlr.M009449.

16. Sassa, T.; Kihara, A. Metabolism of very long-chain Fatty acids: Genes and pathophysiology. Biomol. Ther. 2014, 22, 83–92, doi:10.4062/biomolther.2014.017.

17. Borchman, D.; Ramasubramanian, A.; Foulks, G.N. Human Meibum Cholesteryl and Wax Ester Variability With Age, Sex, and Meibomian Gland Dysfunction. Invest. Ophthalmol. Vis. Sci. 2019, 60, 2286–2293, doi:10.1167/iovs.19-26812.

18. Shrestha, R.K.; Borchman, D.; Foulks, G.N.; Yappert, M.C.; Milliner, S.E. Analysis of the composition of lipid in human meibum from normal infants, children, adolescents, adults, and adults with meibomian gland dysfunction using (1)H-NMR spectroscopy. Invest. Ophthalmol. Vis. Sci. 2011, 52, 7350–7358, doi:10.1167/iovs.11-7391.

19. Chen, J.; Green-Church, K.B.; Nichols, K.K. Shotgun lipidomic analysis of human meibomian gland secretions with electrospray ionization tandem mass spectrometry. Invest. Ophthalmol. Vis. Sci. 2010, 51, 6220–6231, doi:10.1167/iovs.10-5687.

20. Material not intended for publication: Ziemanski, JF; Chen, J; Nichols, KK. University of Alabama at Birmingham, Birmingham, AL. Effect of culture duration on the lipid profile produced from human meibomian gland epithelial cells, 2016.

21. Butovich, I.A.; McMahon, A.; Wojtowicz, J.C.; Lin, F.; Mancini, R.; Itani, K. Dissecting lipid metabolism in meibomian glands of humans and mice: An integrative study reveals a network of metabolic reactions not duplicated in other tissues. Biochim. Biophys. Acta 2016, 1861, 538–553, doi:10.1016/j.bbalip.2016.03.024.

22. Asano, N.; Hampel, U.; Garreis, F.; Schroder, A.; Schicht, M.; Hammer, C.M.; Paulsen, F. Differentiation Patterns of Immortalized Human Meibomian Gland Epithelial Cells in Three-Dimensional Culture. Invest. Ophthalmol. Vis. Sci. 2018, 59, 1343–1353, doi:10.1167/iovs.17-23266.

23. Schroder, A.; Abrar, D.B.; Hampel, U.; Schicht, M.; Paulsen, F.; Garreis, F. In vitro effects of sex hormones in human meibomian gland epithelial cells. Exp. Eye Res. 2016, 151, 190–202, doi:10.1016/j.exer.2016.08.009.

24. Sahin, A.; Liu, Y.; Kam, W.R.; Darabad, R.R.; Sullivan, D.A. Dihydrotestosterone suppression of proinflammatory gene expression in human meibomian gland epithelial cells. Ocul. Surf. 2020, 18, 199–205, doi:10.1016/j.jtos.2020.02.006.

25. Hampel, U.; Garreis, F. The human meibomian gland epithelial cell line as a model to study meibomian gland dysfunction. Exp. Eye Res. 2017, 163, 46–52, doi:10.1016/j.exer.2017.03.011.

26. Liu, Y.; Kam, W.R.; Ding, J.; Sullivan, D.A. Effect of azithromycin on lipid accumulation in immortalized human meibomian gland epithelial cells. JAMA Ophthalmol. 2013, doi:10.1001/jamaophthalmol.2013.6030.

27. Liu, Y.; Kam, W.R.; Ding, J.; Sullivan, D.A. One man’s poison is another man’s meat: Using azithromycin-induced phospholipidosis to promote ocular surface health. Toxicology 2014, 320, 1–5, doi:10.1016/j.tox.2014.02.014.

28. Ding, J.; Sullivan, D.A. The effects of insulin-like growth factor 1 and growth hormone on human meibomian gland epithelial cells. JAMA Ophthalmol. 2014, 132, 593–599, doi:10.1001/jamaophthalmol.2013.8295.

29. Liu, Y.; Kam, W.R.; Ding, J.; Sullivan, D.A. Can tetracycline antibiotics duplicate the ability of azithromycin to stimulate human meibomian gland epithelial cell differentiation? Cornea 2015, 34, 342–346, doi:10.1097/ICO.0000000000000351.

30. Kim, S.W.; Xie, Y.; Nguyen, P.Q.; Bui, V.T.; Huynh, K.; Kang, J.S.; Brown, D.J.; Jester, J.V. PPARgamma regulates meibocyte differentiation and lipid synthesis of

cultured human meibomian gland epithelial cells (hMGEC). Ocul. Surf. 2018, 16, 463–469, doi:10.1016/j.jtos.2018.07.004.

31. Kim, S.W.; Brown, D.J.; Jester, J.V. Transcriptome analysis after PPARgamma activation in human meibomian gland epithelial cells (hMGEC). Ocul. Surf. 2019, 17, 809–816, doi:10.1016/j.jtos.2019.02.003.

32. Thiboutot, D. Regulation of human sebaceous glands. J. Invest. Dermatol. 2004, 123, 1–12, doi:10.1111/j.1523-1747.2004.t01-2-.x.

33. Jester, J.V.; Potma, E.; Brown, D.J. PPARgamma Regulates Mouse Meibocyte Differentiation and Lipid Synthesis. Ocul. Surf. 2016, 14, 484–494, doi:10.1016/j.jtos.2016.08.001.

34. Folch, J.; Lees, M.; Sloane Stanley, G.H. A simple method for the isolation and purification of total lipides from animal tissues. J. Biol. Chem. 1957, 226, 497–509.

CHAPTER THREE: SATURATION OF CHOLESTERYL ESTERS PRODUCED BY HUMAN MEIBOMIAN GLAND EPITHELIAL CELLS AFTER TREATMENT WITH ROSIGLITAZONE

JILLIAN F. ZIEMANSKI, LANDON WILSON, STEPHEN BARNES, KELLY K. NICHOLS

In preparation for *The Ocular Surface*

Format adapted for dissertation

Abstract

Purpose: The purpose of this study was to compare the cholesteryl ester (CE) profiles expressed from human meibomian gland epithelial cells (HMGECs) in response to rosiglitazone-induced differentiation to that of normal human meibum.

Methods: HMGECs were cultured with rosiglitazone (vehicle control, 20 μM, or 50 μM) and fetal bovine serum (FBS, 2% or 10%) for 2 days or 5 days. Following culture, lipid extracts were processed and analyzed by ESI-$MSMS^{ALL}$ in positive ion mode. CEs were identified using both LipidView 1.2 and PeakView 2.2 (SCIEX, Framingham, MA) and compared to literature reports of CEs in normal human meibum.

Results: There were 34 CEs with carbon number ranging from 14 to 34 detected from HMGECs. Across all conditions, HMGECs provided a CE profile that was 14.0% saturated, 60.6% monounsaturated, and 25.4% polyunsaturated. Culturing with 50 μM rosiglitazone and 2% FBS for 2 days resulted in the greatest number of upregulated saturated and monounsaturated CEs and downregulated polyunsaturated CEs. Five CEs were identified as being the most responsive to 50 μM rosiglitazone: CE 24:1, CE 28:1, CE 26:1, CE 18:1, and CE 22:1.

Conclusion: Although differences in the CE profile exist between meibum and HMGECs, rosiglitazone promotes upregulation of highly expressed meibum-relevant CEs and shifts the saturation level toward a more meibum-like profile. The use of rosiglitazone as a differentiating agent is recommended in HMGEC research, and analysis by ESI-

$MSMS^{ALL}$ is encouraged to differentiate meibum-relevant CEs from other nonpolar distractors detected by vital stains.

Introduction

Human meibomian gland epithelial cells (HMGECs) were first isolated, immortalized, and described in 2010.[1] HMGECs have been shown to accumulate lipids, express genes for enzymes involved in lipogenesis, and respond to androgen exposure.[1] Despite these similarities to the meibomian gland's function in vivo, there have also been reports of scarce lipid production or aberrant lipid profiles that have prompted additional investigation into differentiating conditions.[2] Serum, azithromycin, omega-3 and -6 fatty acids, and brimonidine have all demonstrated the ability to promote differentiation and lipid production from HMGECs.[3-8] More recently, though, rosiglitazone, a peroxisome proliferator activator receptor-γ (PPARγ) agonist, has also been proposed as a differentiating agent.[9,10]

PPARγ is a nuclear receptor that has been shown to regulate differentiation and lipid production in both adipocytes and sebocytes.[11,12] In 2016, Jester et al. reported that it also regulates differentiation and lipid synthesis in primary and immortalized mouse meibocytes.[9] Later, Kim et al. found that rosiglitazone, via its agonistic effects on PPARγ, also increases lipogenic gene expression and lipogenesis in HMGECs.[10] In the latter paper, lipid production was quantified by LipidTox staining—an efficient method for visualizing nonpolar lipid production when only a gestalt measure is necessary. While LipidTox does show specificity for nonpolar lipids, it lacks discrimination among

different nonpolar lipid classes and species.[2] For this level of resolution, mass spectrometry can be used to more fully interrogate aspects of the HMGEC lipidome.

The lipidome of normal human meibum, however, has already been well characterized. Comprised of >90% nonpolar lipids, human meibum consists primarily of wax esters (WEs, 48 ± 4% of total lipid pool) and cholesteryl esters (CEs, 40 ± 2% of total lipid pool) with smaller contributions by triacylglycerols, diacylglycerols, and others.[13] For CEs specifically, there have been 28 to 58 different species detected in meibum (depending on analytical methods) with hydrocarbon chain lengths varying from 16 to 36.[13,14] Of note, very long-chain CEs (carbon number [n_c] 20 to 25) and ultra long-chain CEs ($n_c \geq 26$) are characteristic of meibum and sebum.[15] However, those CEs with $n_c \geq 26$ are absent from other lipid sources, such as plasma and epithelial cells.[16,17] Previous reports have been in agreement that polyunsaturated CEs are of low abundance in meibum, while saturated and monounsaturated CEs are of high abundance.[13,14,18,19] Taken together, the signature lipid profile of normal human meibum is predominantly nonpolar, high in CEs (and WEs), diverse in CE chain length (16 to 36), highly abundant in saturated and monounsaturated CEs, and highly abundant in CEs with n_c 22 to 26.[14]

In this study, the effects of serum, rosiglitazone, and culture duration were evaluated on the lipidomic profile produced by HMGECs. We hypothesized that increased concentrations of rosiglitazone would positively influence HMGEC differentiation as determined by the upregulation of meibum-relevant CEs (saturated and monounsaturated CEs with carbon number 16 to 32).

Materials and Methods

Cell culture and lipid extraction

Immortalized HMGECs were maintained until 80% confluence in keratinocyte serum-free media (KSFM) with 5 ng/ml epidermal growth factor (EGF) and 50 µg/ml bovine pituitary extract (BPE). HMGECs were differentiated at a density of one million cells per 6-cm glass petri dish in Dulbecco's modified Eagle's medium (DMEM) and Ham's F12 (1:1) containing 10 ng/ml EGF, fetal bovine serum (FBS, 2% or 10%), and rosiglitazone (20 µM or 50 µM, Cayman Chemical, Ann Arbor, MI). Rosiglitazone was dissolved in sterile-filtered dimethyl sulfoxide (DMSO, Hybri-Max^{TM}, Sigma-Aldrich, St. Louis, MO) as a vehicle and was added to the culture media as the last step before exposure to HMGECs. The concentration of DMSO was maintained at 0.5% across all conditions. All experiments consisted of two experimental replicates and two technical replicates.

After two days or five days, the culture media was withdrawn, and the cells were washed twice with molecular biology-grade water. A modified Folch technique was used for lipid extraction.[20,21] Specifically, 3 mL of pre-mixed and pre-chilled chloroform-methanol (2:1 v/v at -20°C) was added directly to the adhered cells. The growth surface was scraped with a sterile stainless-steel scraper, and the resulting solution was transferred to a glass vial. Ammonium acetate in molecular biology-grade water (50 mM, 0.75 mL) was added to the samples, creating a final ratio of chloroform-methanol-water of 8:4:3, consistent with the Folch technique. The emulsion was agitated on ice at 350 rpm for 20 minutes then centrifuged at 1600 x g for 5 minutes to promote phase separation. The lower, nonpolar phase was withdrawn and kept for mass spectrometric

analysis. All steps involving organic solvents were performed with glass, polytetrafluoroethylene (PTFE), or stainless steel.

Analysis by mass spectrometry

All samples were directly infused into a Triple TOF 5600 mass spectrometer (SCIEX, Framingham, MA) with electrospray ionization by isocratic flow at 7 µl/min. MS and MS/MS^{ALL} spectra were acquired in positive ion mode. MS/MS^{ALL} analysis was performed with the SWATH technology. Product ion MS/MS spectra for all precursor ions were acquired between 200 m/z and 1,200 m/z at every one Dalton step over six minutes. Collision energy per step was 35 eV, and collision energy spread was 15 eV. The acquired MS and MS/MS^{ALL} data were processed and lipid species identified using LipidView 1.2 (SCIEX, Framingham, MA). Spectra were viewed and interpreted using PeakView 2.2 (SCIEX, Framingham, MA).

Data analysis

CEs were the predominant focus of this study. The labeling convention for CEs is n_c:db, where n_c and db are the number of carbons and double bonds, respectively, in the fatty acyl chain. To be included in the analysis, a given CE species had to be present in all replicates of at least one condition. Each analyzed CE was normalized to the sum intensity and reported as percent of the overall CE pool. One-way ANOVA with Tukey post-hoc testing (SPSS v26, Armonk, NY) was used to compare means between conditions when tests of normality (Kolmogorov-Smirnov) and homogeneity of variance (Levene's Test) were satisfied. If Levene's Test was violated, then Games-Howell post-

hoc testing was used. If Kolmogorov-Smirnov testing was violated, then the non-parametric Kruskal Wallis test was used. A significance threshold was set at 0.05.

Results

Description of the CE profile

There were 68 CEs detected across all samples; however, only 34 met the criteria for inclusion in the analysis. Across all conditions, the chain length varied from 14 to 34, and the most abundant CE was CE 18:1 (Figure 1). Very long-chain ($20 \leq n_c \leq 25$) and ultra long-chain CEs ($n_c \geq 26$) were detected from all conditions and comprised 30.6% (SD = 1.6) of the overall CE pool. Of the 34 included CEs, seven were saturated, 12 were monounsaturated, and 15 were polyunsaturated. Monounsaturated CEs were the most abundant (60.6%, SD = 10.6%), followed by polyunsaturated (25.4%, SD = 2.2%) and saturated (14.0%, SD = 3.1%).

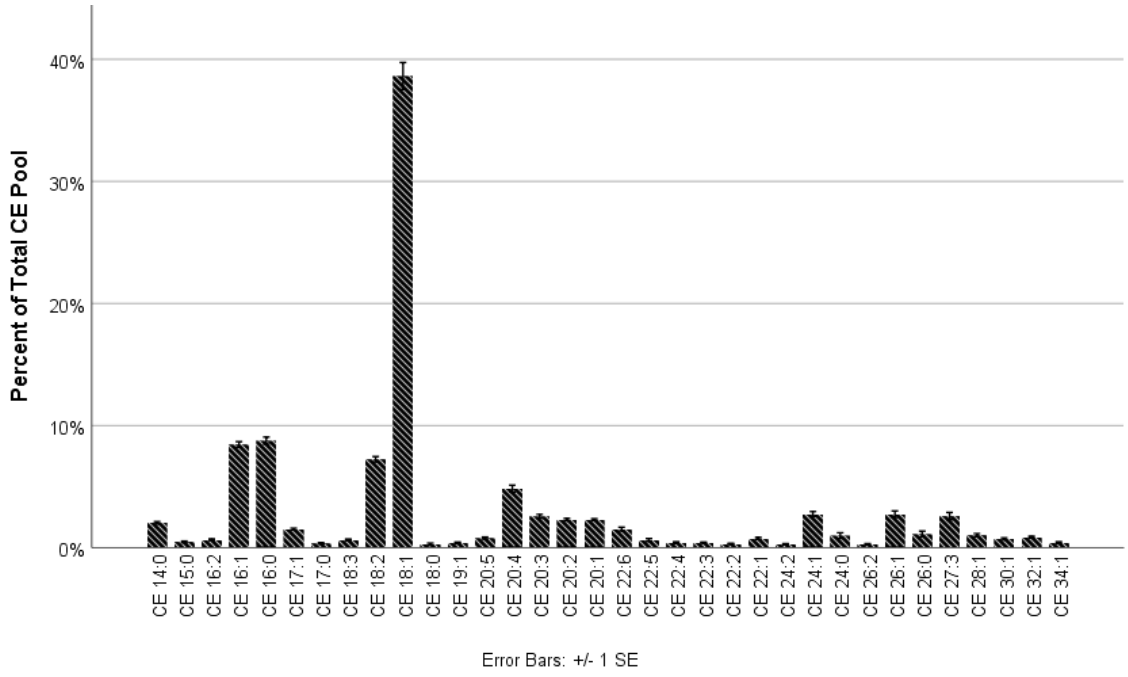

Figure 1 Description of HMGEC CE Lipidome
A diverse CE profile, rich in monounsaturated CEs, was quantified across all conditions in this study. CE 18:1 dominated the CE pool.

Comparison of the CE profile across culture conditions

HMGECs were differentiated in culture conditions containing FBS (2% or 10%) and rosiglitazone (vehicle control, 20 µM, or 50 µM) for two days or five days. Culturing with the three concentrations of rosiglitazone and 10% FBS for two days yielded significant differences among seven of the 34 CEs (Table 1). The remaining 27 CEs showed no differences (Figure 2). Of the seven that were significantly different, one was saturated (CE 18:0), three were monounsaturated (CE 26:1, CE 24:1, and CE 28:1), and three were polyunsaturated (CE 22:6, CE 16:2, and CE 22:4). For all seven CEs, culturing with 50 µM rosiglitazone increased expression of the saturated and monounsaturated CEs but decreased expression of the polyunsaturated CEs. Extending

the culture duration from two days to five days did not alter expression of any CEs (Figure 3).

Table 1 Effect of Rosiglitazone

Cholesteryl Esters (CEs)	10-DMSO-2d (vehicle control)		10-20-2d		10-50-2d	
	Abundance (%)	SEM	Abundance (%)	SEM	Abundance (%)	SEM
CE 18:0	0.28	0.16	0.30	0.22	1.76	0.48
			p = 0.037			
CE 24:1	2.16	0.18	1.96	0.22	3.91	0.36
	p = 0.009					
			p = 0.002			
CE 26:1	2.08	0.47	2.05	0.26	4.20	0.56
	p = 0.004					
			p = 0.003			
CE 28:1	0.52	0.30	0.67	0.24	1.93	0.13
	p = 0.003					
			p = 0.012			
CE 16:2	0.97	0.22	0.81	0.17	0.13	0.08
	p = 0.043					
CE 22:6	3.03	0.19	3.77	0.22	1.57	0.29
	p = 0.001					
			p < 0.001			
CE 22:4	0.95	0.25	1.41	0.21	0.19	0.22
	p = 0.048					
			p < 0.001			

HMGECs were cultured with a vehicle control (DMSO) or rosiglitazone (20 µM or 50 µM) and 10% FBS for two days. Culture conditions are abbreviated as FBS % – Rosiglitazone (µM) – Duration. Only the cholesteryl esters (CEs) that reached statistical significance are displayed in the table. CEs are listed with two numbers. The two numbers denote the number of carbons and double bonds in the acyl chains, respectively.
SEM = standard error of the mean

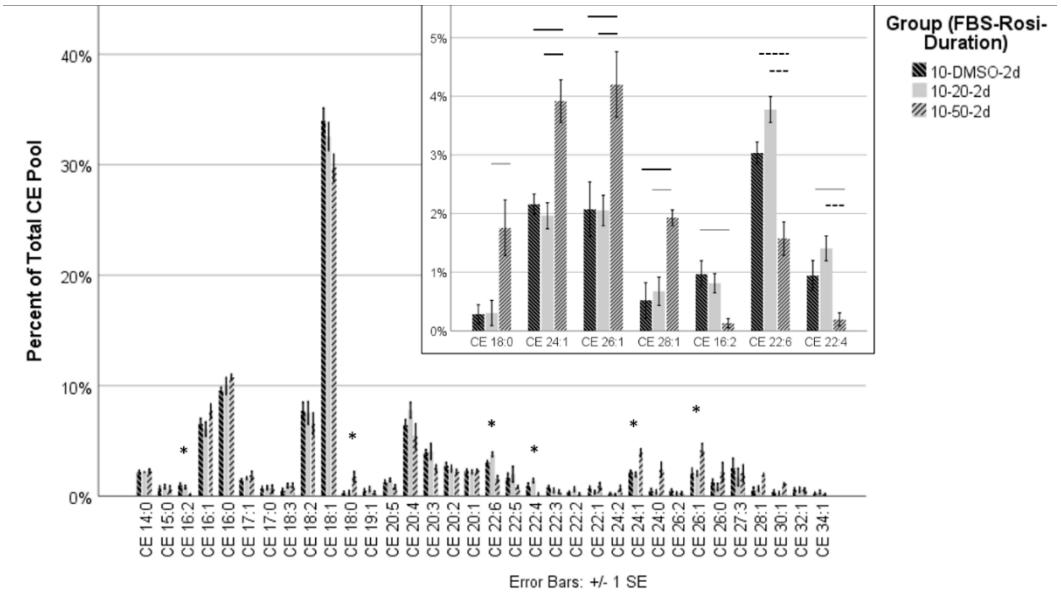

Figure 2 Effect of Rosiglitazone

HMGECs were cultured with a vehicle control (DMSO) or rosiglitazone (20 µM or 50 µM) and 10% FBS for two days. There was a significant change in seven CEs following culture with 50 µM rosiglitazone (inset). The order of the CEs in the inset has been rearranged to separate saturated, monounsaturated, and polyunsaturated CEs. One saturated and three monounsaturated CEs were upregulated with 50 µM rosiglitazone, and two polyunsaturated CEs were downregulated—a pattern consistent with the CE profile in normal human meibum. * denotes statistical significance. Gray bar denotes significance at $p \leq 0.05$. Black bar denotes significance at $p \leq 0.01$. Dashed line denotes significance at $p \leq 0.001$.

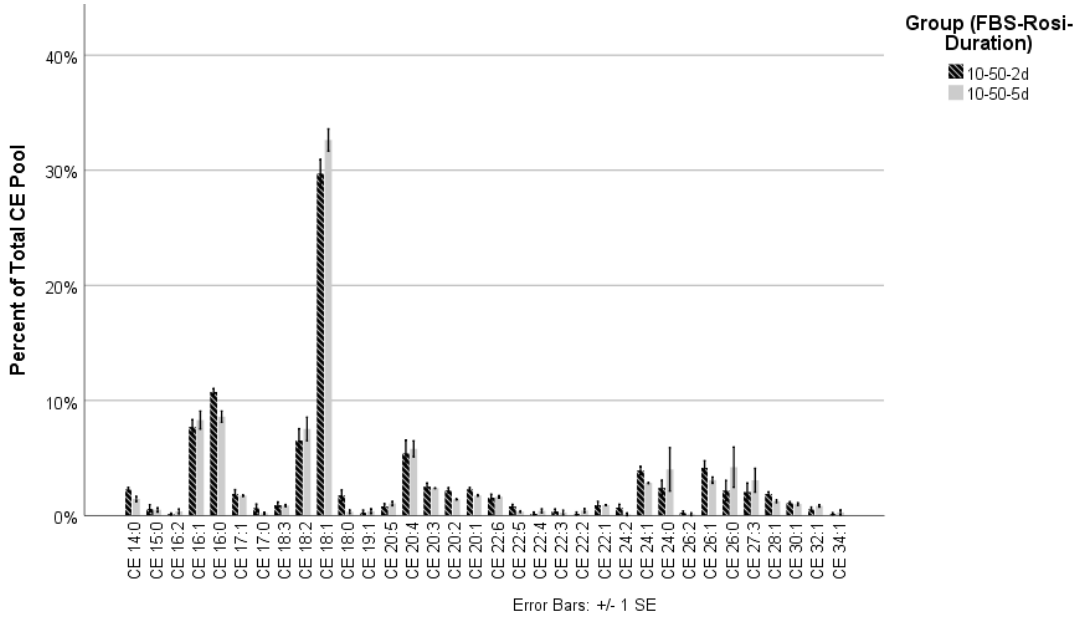

Figure 3 Effect of Culture Duration
Extending the culture duration of HMGECs in 10% FBS and 50 µM rosiglitazone from two days to five days revealed no changes in relative CE expression.

Reducing the serum concentration from 10% to 2% in the presence of 50 µM rosiglitazone for two days yielded significant differences among six of the 34 CEs (Table 2, Figure 4). The remaining 28 were unchanged. Of the six that were significantly different, one was saturated (CE 26:0), two were monounsaturated (CE 16:1 and CE 26:1), and three were polyunsaturated (CE 18:3, CE 22:6, and CE 22:5). Culturing with 2% FBS yielded higher abundance of monounsaturated CEs and lower abundance of polyunsaturated CEs. Culturing with 10% FBS, however, yielded a higher abundance of the saturated CE 26:0.

Table 2 Effect of Serum Concentration

	10-50-2d		2-50-2d	
	Mean (%)	SEM	Mean (%)	SEM
CE 26:0	2.17	0.89	0.28	0.28
	p = 0.023			
CE 16:1	7.70	0.64	10.70	0.22
	p = 0.004			
CE 26:1	4.20	0.56	7.60	0.58
	p < 0.001			
CE 18:3	0.95	0.23	0.00	0.00
	p = 0.025			
CE 22:6	1.57	0.29	0.42	0.42
	p = 0.02			
CE 22:5	0.83	0.14	0.14	0.14
	p = 0.033			

The decrease of 10% FBS to 2% FBS in the presence of 50 µM rosiglitazone after two days of culture resulted in a significant change in six cholesteryl esters (CEs). Only the CEs that reached statistical significance are displayed in the table. Culture conditions are abbreviated as FBS % – Rosiglitazone (µM) – Duration. CEs are listed with two numbers. The two numbers denote the number of carbons and double bonds in the acyl chains, respectively.

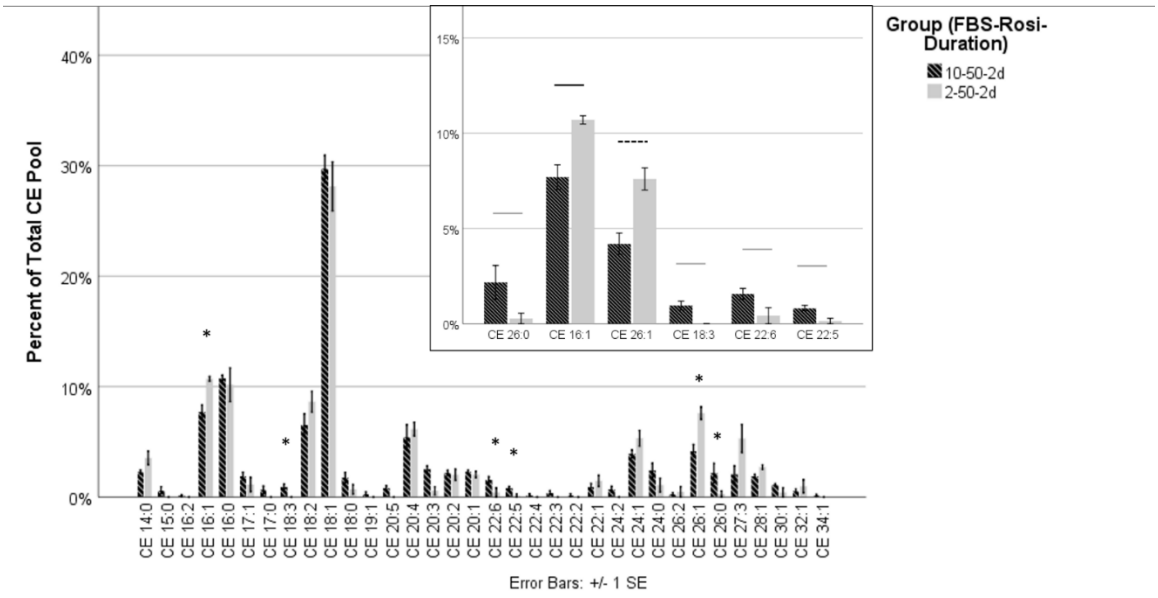

Figure 4 Effect of FBS

The decrease of 10% FBS to 2% FBS in the presence of 50 µM rosiglitazone after two days of culture resulted in a significant change in six CEs (inset). The order of the CEs has been rearranged in the inset to separate saturated, monounsaturated, and polyunsaturated CEs.

Two monounsaturated CEs were upregulated with 2% FBS, while one saturated and three monounsaturated CEs were downregulated. The CE profile of normal human meibum is high in saturated and monounsaturated CEs and low in polyunsaturated CEs. * denotes statistical significance. Gray bar denotes significance at $p \leq 0.05$. Black bar denotes significance at $p \leq 0.01$. Dashed line denotes significance at $p \leq 0.001$.

Comparison of optimized culture conditions to normal human meibum

To evaluate the performance of each condition, the number of CEs that favor each condition was summed and compared (Table 3). Of the 34 total CEs that met the criteria for analysis, 10 had no significant differences between any of the conditions. Of the remaining 24, 10 CEs favored 50 μM rosiglitazone with 2% FBS for 2 days (denoted as 2-50-2d [FBS-rosiglitazone-duration]), meaning that saturated and monosaturated CEs were maximized while polyunsaturated CEs were minimized. The remaining 14 CEs favored a mix of seven different conditions, with no other condition being favored by more than three CEs. Culturing with 2-50-2d ultimately yielded the most favorable profile—as defined by the patterns observed in normal human meibum—for 82.4% of the CEs. All other conditions varied between 55.9% to 79.4%.

Table 3 Summary Table

Condition (FBS % - Rosi µM – Duration)	Number of CEs with no significant difference across all conditions	Number of CEs where given condition is superior to all other conditions	Number of CEs where given condition is equivalent to the superior condition ($p > 0.05$)	Number of CEs where given condition is inferior to the superior condition ($p \leq 0.05$)	Total Number of CEs	Percentage of CEs that responded optimally to each condition
	A	B	C	D	E	([A+B+C]/E)*100
2-DMSO-2d	10	2	14	8	34	76.5%
2-DMSO-5d	10	2	11	11	34	67.7%
2-20-2d	10	0	16	8	34	76.5%
2-20-5d	10	0	14	10	34	70.6%
2-50-2d	**10**	**10**	**8**	**6**	**34**	**82.4%**
2-50-5d	10	3	14	7	34	79.4%
10-DMSO-2d	10	0	9	15	34	55.9%
10-DMSO-5d	10	1	8	15	34	55.9%
10-20-2d	10	0	11	13	34	61.8%
10-20-5d	10	1	8	15	34	55.9%
10-50-2d	10	2	14	8	34	76.5%
10-50-5d	10	3	11	10	34	70.6%

Each culture condition was evaluated to determine the number of cholesteryl esters (CEs) that responded optimally. Culture conditions are abbreviated as FBS % – Rosiglitazone (µM) – Duration. CEs are listed with two numbers. The two numbers denote the number of carbons and double bonds in the acyl chains, respectively. n = 4 for each culture condition.

A total of 34 CEs, as shown in Column E, met the criteria for analysis in this study. Column A shows that 10 CEs did not vary across all twelve culture conditions. The definition of a "superior" condition in Column B is dependent on a given CE's saturation level. For saturated and monounsaturated CEs, a condition was deemed superior if it yielded the highest expression relative to the other conditions. For polyunsaturated CEs, a condition was considered superior if it yielded the lowest expression relative to the other conditions. If a given condition was not the "superior" condition, then one of two other outcomes were possible: it could either have been statistically equivalent to the superior condition (Column C) or statistically inferior to the superior condition (Column D). The final column represents the percentage of CEs that responded optimally to each condition. Culturing with 50 uM rosiglitazone and 2% FBS for two days optimized 82.4% of CEs and was considered superior for 10 of 34 (29.4%) of CEs.

Most responsive CEs to rosiglitazone supplementation

To determine which CEs were most responsive to rosiglitazone treatment, correlation coefficients were calculated (Table 4). Thirteen CEs showed a significant correlation with respect to rosiglitazone. Three of the thirteen were saturated, six were monounsaturated, and four were polyunsaturated. The following CEs all had statistically significant correlation coefficients at or above 0.50, which is considered the minimum for a moderately high correlation:[22] CE 24:1 (ρ = +0.70), CE 28:1 (ρ = +0.69), CE 26:1 (ρ = +0.66), CE 18:1 (ρ = -0.59), and CE 22:1 (ρ = +0.50).

Table 4 Correlation Coefficients Between Cholesteryl Esters and Rosiglitazone

Cholesteryl Ester (CE)	Correlation Coefficient (ρ)	Significance (p-value)	Cholesteryl Ester (CE)	Correlation Coefficient (ρ)	Significance (p-value)
CE 14:0	0.127	0.389	CE 22:6	-0.094	0.525
CE 15:0	-0.230	0.116	CE 22:5	-0.089	0.549
CE 16:2	**-0.469**	**0.001**	CE 22:4	-0.209	0.154
CE 16:1	0.273	0.061	CE 22:3	-0.077	0.602
CE 16:0	**0.337**	**0.019**	CE 22:2	-0.086	0.561
CE 17:1	-0.011	0.941	**CE 22:1**	**0.500**	**<0.001**
CE 17:0	-0.063	0.670	CE 24:2	0.227	0.122
CE 18:3	-0.011	0.940	**CE 24:1**	**0.698**	**<0.001**
CE 18:2	-0.041	0.785	**CE 24:0**	**0.453**	**0.001**
CE 18:1	**-0.589**	**<0.001**	CE 26:2	0.168	0.253
CE 18:0	**0.426**	**0.003**	**CE 26:1**	**0.656**	**<0.001**
CE 19:1	-0.187	0.203	CE 26:0	0.130	0.378
CE 20:5	**-0.295**	**0.042**	CE 27:3	0.026	0.862
CE 20:4	0.133	0.369	**CE 28:1**	**0.694**	**<0.001**
CE 20:3	**-0.300**	**0.038**	CE 30:1	0.245	0.093
CE 20:2	**-0.346**	**0.016**	CE 32:1	-0.085	0.566
CE 20:1	-0.022	0.881	**CE 34:1**	**-0.384**	**0.007**

Spearman's correlation coefficients were calculated between each cholesteryl ester (CE) and rosiglitazone. CEs are listed with two numbers. The two numbers denote the number of carbons and double bonds in the acyl chains, respectively. All correlations are positive unless otherwise denoted. Thirteen CEs (bolded) reached statistical

significance. Five of these CEs had moderate to high correlations: CE 24:1, CE 28:1, CE 26:1, CE 18:1, and CE 22:1. n = 48 for each CE.

Discussion

This report demonstrates that HMGECs readily express cholesteryl esters, including very long-chain and ultra long-chain CEs that are characteristic of human meibum. It also establishes culture conditions that promote a better preclinical model of meibomian gland physiology relative to serum-induced differentiation alone.[3] When supplemented with rosiglitazone, a PPARγ agonist, HMGECs modulate their CE expression profile to better mirror the saturation profile of normal human meibum: upregulation of select saturated and monounsaturated CEs and downregulation of select polyunsaturated CEs. The duration of culture provides little influence on the CE profile; however, reducing the serum concentration to 2% further refines CE expression toward that which is observed in vivo. Together, these findings suggest that rosiglitazone imparts significant effects on the differentiation of and lipid expression by HMGECs, which carries implications for future culturing conditions and potentially therapeutic benefits.

Cholesteryl esters, particularly with respect to saturation level, are attractive targets in HMGEC research. At the ocular surface, CEs are less abundant than WEs with a molar ratio recently reported as 0.49:1 (CE:WE) in normals.[23] In MGD, however, CE expression decreases and the molar ratio drops to 0.33:1.[23,24] Functionally, it is still unknown what precise roles CEs play in the tear film. Large differences in CE expression have been observed in subsets of normal meibum donors who have stable tear films, suggesting that large variations can be tolerated without an impact on tear dynamics.[23,25] CEs, therefore, are unlikely to confer stability to tears at the ocular surface. Instead, tear

film CEs have unique properties that allow them to be powerful modulators of phase transition temperatures and, thus, meibum viscosity.[26] Partly owing to its five-fold increase in saturation relative to wax esters,[13] reductions in CEs may inversely affect the melting point of meibum, thereby increasing its viscosity—findings that have been reported clinically, biochemically, and biophysically in patients with MGD.[27,28] The observation that CEs of all saturation levels are responsive to the agonistic effects on PPARγ by rosiglitazone reinforces their adequacy as a meaningful outcome parameter in HMGEC research.

Although all CE saturation levels varied with rosiglitazone, five specific monounsaturated CEs emerged as being the most responsive: CE 24:1, CE 28:1, CE 26:1, CE 18:1, and CE 22:1. The expression of all five of these CEs stratified with respect to rosiglitazone concentration. The longer-chain CEs (24:1, 28:1, 26:1, and 22:1) were all positively correlated, demonstrating higher expression in response to the highest concentration of rosiglitazone. Conversely, CE 18:1 demonstrated a negative correlation and therefore showed lower expression in response to the highest concentration of rosiglitazone. In general, these patterns are mostly consistent with the work of Jester et al. and Kim et al.[9,10] Using LipidTox staining of all nonpolar lipids, Jester et al. found that nonpolar lipid production in mouse meibocytes increased in a dose-dependent manner from 0 to 50 μM rosiglitazone.[9] In HMGECs, again stained with LipidTox, Kim et al. found a linear, dose-dependent increase in nonpolar lipid production from 0 to 30 μM; however, beyond this concentration, lipid production began to decrease.[10] Neither of these studies sought to describe the relationship between rosiglitazone and the production of specific nonpolar lipid classes, nonetheless specific CE species. Our work shows that

although all CEs are nonpolar, differential expression is observed among specific CEs in response to rosiglitazone (Table 2). The use of a vital stain like LipidTox can mask some of these effects; therefore, the use of analytical methods that can provide molecular data is recommended for greatest resolution.

Of further interest, the four CEs with the strongest positive correlation to rosiglitazone (CE 24:1, CE 28:1, CE 26:1, and CE 22:1) are among the 10 most highly expressed CEs in normal human meibum, comprising up to 24.5% of the overall CE pool.[14] Further, CE 24:1, the CE manifesting the highest responsivity to rosiglitazone, is also the most highly abundant in meibum. In our study, as well as others,[29] CE 18:1 is expressed disproportionately high in HMGECs relative to meibum. Expression approaching 40% was detected across all conditions in this study, but this value decreased to 28.1% under optimized conditions: 50 μM rosiglitazone and 2% serum for two days. Thus, a negative correlation between CE 18:1 and rosiglitazone is consistent with a shift toward a more meibum-like profile, considering that CE 18:1 was reported to be 5.5% of all CEs in a recent study of meibum.[14] These findings are also consistent with other reports.[13,18] Rosiglitazone's role in promoting production of meibum-relevant lipids from HMGECs further supports its use as a differentiating agent and builds upon the strong foundational work by Jester et al. and Kim et al.[9,10,30]

Beyond rosiglitazone, the effects of serum concentration were also investigated in this study. Early reports described serum as a powerful differentiating agent on HMGECs.[1,3] In 2014, Sullivan and colleagues cultured HMGECs in serum-free media (SFM) or serum-containing media (SCM, 10%) for fourteen days and detected altered expression of 2,789 genes, many involved in cell differentiation and lipid metabolism.[3]

Separated and analyzed by liquid chromatography-mass spectrometry (LC-MS), lipid extracts from HMGECs exposed to SCM showed high levels of phospholipid production, which represented 58.7% of the total lipid pool. Forty-seven species of WEs (0.92% of total lipid pool) and fourteen species of CEs (1.97% of total lipid pool) were also identified; however, for CEs, the acyl chain length only varied from 14 to 24, and the CEs that were reported to be most responsive to serum supplementation were highly polyunsaturated (CE 20:3, CE 20:4, CE 22:4). This described lipidome—high expression of phospholipids, upregulation of polyunsaturated CEs, and expression of shorter-chain CEs—bears little resemblance to human meibum, which is believed to have a very low pool of phospholipids (0.006%).[31] Further skepticism of serum-induced differentiation was reported in 2015 when Hampel and colleagues discovered a significant increase in cytokeratins after serum supplementation.[29] Hyperkeratinization is thought to be a core mechanism in MGD[27] and thus may be a better indicator of pathology, rather than a sign of differentiation. Recently, Kim et al. found that HMGECs treated with 10% SCM showed little nonpolar lipid production by LipidTox staining and appeared to be equivalent to the production observed by SFM.[10] Our results seem to be in agreement with the latter two reports and suggest that a lower concentration of serum—or perhaps none at all—may be more favorable when part of differentiating conditions.

Culture duration was the third factor that was varied in our study. Most reports that have investigated HMGEC lipid production have ranged in culture duration from between one and fourteen days. One study found that in serum-treated HMGECs, lipid production was greatest at the one-day time point when monitored at intervals up to 14 days.[29] For the rosiglitazone studies on meibocytes, differentiating conditions were

maintained from one to seven days.[9,10] In mouse meibocytes, a time-dependent increase in lipid production was observed with rosiglitazone-induced differentiation. The greatest increase was detected between three (about two-fold increase versus control) and five days (about five-fold increase versus control).[9] In HMGECs, there was a gradual increase in lipid droplet formation visualized between two days and six days.[10] In our studies, a significant effect due to culture duration was not found. Extending differentiating conditions from two days to five days provided no effect on CE expression. One reason that we may not have detected a time-dependent effect associated with rosiglitazone is that we quantified relative expression, rather than absolute expression, of each CE. Therefore, if there was a uniform increase in CE production between two and five days, this effect would have been masked by our normalization methods. Similarly, Hampel et al. reported little change in relative expression of meibum-relevant lipids, such as WEs, CEs, and TAGs, between one day and three days.[2,29] For future HMGEC research, the decision to pursue a given culture duration should be determined by analytical methods. If vital stains and fluorescent microscopy will be used, then absolute expression may be needed for optimal thresholding procedures, and a longer duration should be considered. If greater resolution is needed to identify specific lipid subclasses or species, then a sensitive technique like mass spectrometry may be needed, and a shorter culture duration would provide greater efficiency and reduce use of consumables.

Previous reports have raised concern about the adequacy of the HMGEC line's ability to replicate the lipid profile of normal human meibum, primarily due to very abundant expression of the polar phospholipids.[2] Having focused our analyses on cholesteryl esters, our experiments were designed and our methods optimized to identify

this specific subclass, rather than the lipidome as a whole. Despite this, our observations support that phospholipids, at least with our mass spectrometry acquisition parameters, continue to be the highest lipid class produced by HMGECs (data not shown). Further comparison of any classes other than CEs is outside of the scope of this study. However, our CE profile from HMGECs can be compared with and contrasted against literature reports of the CE pool in normal human meibum.

A recent report by Chen and Nichols comprehensively defined the meibum lipidome, including CEs.[14] Depending on the mass spectrometry methodology, normal human meibum has been reported to express between 28 and 58 different CEs, ranging in chain length from 16 to 36 carbons.[14] By comparison, we identified 34 unique CEs that met our criteria for inclusion. The carbon numbers ranged from 14 to 34, aligning well with the diversity and chain lengths observed in meibum. The contribution of saturated, monounsaturated, and polyunsaturated CEs to the overall CE pool in meibum is 48.8%, 44.8%, and 6.3%, respectively.[14] In our study of HMGECs, when cultured with 2% FBS and 50 μM rosiglitazone for two days, we found 15.8%, 60.5%, and 23.7%. While our monounsaturated CE content was relatively similar, we found more polyunsaturated CEs, at the expense of saturated CEs, from HMGECs. There were further differences in the top five most abundant CEs. Meibum shows high levels of CE 24:1, CE 25:0, CE 24:0, CE 26:0, and CE 22:1 (in descending order, ranging from 9.6% to 6.0% of the total CE pool).[14] From our studies of HMGECs, high expression was detected for CE 18:1, CE 16:1, CE 16:0, CE 18:2, and CE 26:1 (ranging from 28.1% to 7.6% of the total CE pool). The four most abundant CEs from HMGECs all have shorter acyl chains, a finding that is poorly aligned with meibum CEs. These discrepancies in the CE lipidome between

normal human meibum and HMGECs emphasizes the importance of using rosiglitazone as a differentiating agent. As previously stated, CE 24:1, CE 28:1, CE 26:1, and CE 22:1 were the CEs that demonstrated the greatest increase with rosiglitazone supplementation. All four of these are among the ten most prominent CEs in meibum, accounting for 24.5% of the total CE pool. This comparison further highlights the importance of using mass spectrometry to analyze lipid production, as vital stains, such as LipidTox, cannot differentiate the relevant CEs from the less relevant ones. Taken together, variations do indeed exist in the CE lipidomes between meibum and HMGECs, but differentiation by rosiglitazone increases the most meibum-relevant CEs toward a more meibum-like profile.

Conclusion

This study reveals that cholesteryl esters are responsive to PPARγ agonism by rosiglitazone and that they are attractive outcome parameters in HMGEC research. Rosiglitazone positively influences HMGEC differentiation as detected by the upregulation of select saturated and monounsaturated cholesteryl esters and the downregulation of select polyunsaturated cholesteryl esters. Culturing HMGECs with 50 μM rosiglitazone and 2% serum for two days yields a CE profile that is more similar to that of human meibum than when culturing with serum alone. We further report that four CEs that are among the highest expressed in human meibum are also the most sensitive to rosiglitazone supplementation: CE 24:1, CE 28:1, CE 26:1, and CE 22:1. In conclusion, we concur with previous researchers who have proposed rosiglitazone as a differentiating

agent for HMGECs[9,10,30] and advocate for the use of mass spectrometry to focus on specific CE species that are the most relevant to human meibum.

Acknowledgments: The authors would like to thank Dr. David Sullivan (Schepens Eye Research Institute) for providing the human meibomian gland epithelial cells.

Funding: This work was supported by the Office of Research Infrastructure Programs of the National Institutes of Health under S10 RR027822-01 and the National Eye Institute under K23 EY028629-01.

References

1. Liu S, Hatton MP, Khandelwal P, Sullivan DA. Culture, immortalization, and characterization of human meibomian gland epithelial cells. Invest Ophthalmol Vis Sci. 2010;51(8):3993-4005.

2. Hampel U, Garreis F. The human meibomian gland epithelial cell line as a model to study meibomian gland dysfunction. Exp Eye Res. 2017;163:46-52.

3. Sullivan DA, Liu Y, Kam WR, et al. Serum-induced differentiation of human meibomian gland epithelial cells. Invest Ophthalmol Vis Sci. 2014;55(6):3866-3877.

4. Liu Y, Kam WR, Ding J, Sullivan DA. Effect of azithromycin on lipid accumulation in immortalized human meibomian gland epithelial cells. JAMA Ophthalmology. 2013.

5. Liu Y, Kam WR, Ding J, Sullivan DA. One man's poison is another man's meat: using azithromycin-induced phospholipidosis to promote ocular surface health. Toxicology. 2014;320:1-5.

6. Liu Y, Kam WR, Sullivan DA. Influence of Omega 3 and 6 Fatty Acids on Human Meibomian Gland Epithelial Cells. Cornea. 2016;35(8):1122-1126.

7. Hampel U, Kruger M, Kunnen C, Garreis F, Willcox M, Paulsen F. In vitro effects of docosahexaenoic and eicosapentaenoic acid on human meibomian gland epithelial cells. Exp Eye Res. 2015;140:139-148.

8. Han X, Liu Y, Kam WR, Sullivan DA. Effect of brimonidine, an alpha2 adrenergic agonist, on human meibomian gland epithelial cells. Exp Eye Res. 2018;170:20-28.

9. Jester JV, Potma E, Brown DJ. PPARgamma Regulates Mouse Meibocyte Differentiation and Lipid Synthesis. Ocul Surf. 2016;14(4):484-494.

10. Kim SW, Xie Y, Nguyen PQ, et al. PPARgamma regulates meibocyte differentiation and lipid synthesis of cultured human meibomian gland epithelial cells (hMGEC). Ocul Surf. 2018;16(4):463-469.

11. Janani C, Ranjitha Kumari BD. PPAR gamma gene--a review. Diabetes Metab Syndr. 2015;9(1):46-50.

12. Dozsa A, Dezso B, Toth BI, et al. PPARgamma-mediated and arachidonic acid-dependent signaling is involved in differentiation and lipid production of human sebocytes. J Invest Dermatol. 2014;134(4):910-920.

13. Chen J, Green KB, Nichols KK. Quantitative profiling of major neutral lipid classes in human meibum by direct infusion electrospray ionization mass spectrometry. Invest Ophthalmol Vis Sci. 2013;54(8):5730-5753.

14. Chen J, Nichols KK. Comprehensive shotgun lipidomics of human meibomian gland secretions using MS/MS(all) with successive switching between acquisition polarity modes. J Lipid Res. 2018;59(11):2223-2236.

15. Sassa T, Kihara A. Metabolism of very long-chain Fatty acids: genes and pathophysiology. Biomolecules & therapeutics. 2014;22(2):83-92.

16. Sampaio JL, Gerl MJ, Klose C, et al. Membrane lipidome of an epithelial cell line. Proceedings of the National Academy of Sciences of the United States of America. 2011;108(5):1903-1907.

17. Quehenberger O, Armando AM, Brown AH, et al. Lipidomics reveals a remarkable diversity of lipids in human plasma. J Lipid Res. 2010;51(11):3299-3305.

18. Butovich IA. Cholesteryl esters as a depot for very long chain fatty acids in human meibum. J Lipid Res. 2009;50(3):501-513.

19. Butovich IA. Fatty acid composition of cholesteryl esters of human meibomian gland secretions. Steroids. 2010;75(10):726-733.

20. Folch J, Lees M, Sloane Stanley GH. A simple method for the isolation and purification of total lipides from animal tissues. J Biol Chem. 1957;226(1):497-509.

21. Ziemanski JF, Chen J, Nichols KK. Evaluation of Cell Harvesting Techniques to Optimize Lipidomic Analysis from Human Meibomian Gland Epithelial Cells in Culture. Int J Mol Sci. 2020;21(9).

22. Mukaka MM. Statistics corner: A guide to appropriate use of correlation coefficient in medical research. Malawi Med J. 2012;24(3):69-71.

23. Borchman D, Ramasubramanian A, Foulks GN. Human Meibum Cholesteryl and Wax Ester Variability With Age, Sex, and Meibomian Gland Dysfunction. Invest Ophthalmol Vis Sci. 2019;60(6):2286-2293.

24. Shrestha RK, Borchman D, Foulks GN, Yappert MC, Milliner SE. Analysis of the composition of lipid in human meibum from normal infants, children, adolescents, adults, and adults with meibomian gland dysfunction using (1)H-NMR spectroscopy. Invest Ophthalmol Vis Sci. 2011;52(10):7350-7358.

25. Eftimov P, Yokoi N, Tonchev V, Nencheva Y, Georgiev GA. Surface properties and exponential stress relaxations of mammalian meibum films. Eur Biophys J. 2017;46(2):129-140.

26. Borchman D, Yappert MC, Milliner SE, et al. 13C and 1H NMR ester region resonance assignments and the composition of human infant and child meibum. Exp Eye Res. 2013;112:151-159.

27. Knop E, Knop N, Millar T, Obata H, Sullivan DA. The international workshop on meibomian gland dysfunction: report of the subcommittee on anatomy, physiology, and pathophysiology of the meibomian gland. Invest Ophthalmol Vis Sci. 2011;52(4):1938-1978.

28. Green-Church KB, Butovich I, Willcox M, et al. The international workshop on meibomian gland dysfunction: report of the subcommittee on tear film lipids and lipid-protein interactions in health and disease. Invest Ophthalmol Vis Sci. 2011;52(4):1979-1993.

29. Hampel U, Schroder A, Mitchell T, et al. Serum-induced keratinization processes in an immortalized human meibomian gland epithelial cell line. PLoS One. 2015;10(6):e0128096.

30. Kim SW, Brown DJ, Jester JV. Transcriptome analysis after PPARgamma activation in human meibomian gland epithelial cells (hMGEC). Ocul Surf. 2019;17(4):809-816.

31. Brown SH, Kunnen CM, Duchoslav E, et al. A comparison of patient matched meibum and tear lipidomes. Invest Ophthalmol Vis Sci. 2013;54(12):7417-7424.

CHAPTER FOUR: TRIACYLGLYCEROL LIPIDOME FROM HUMAN MEIBOMIAN GLAND EPITHELIAL CELLS: DESCRIPTION, RESPONSE TO CULTURE CONDITIONS, AND PERSPECTIVE ON FUNCTION

by

JILLIAN F. ZIEMANSKI, LANDON WILSON, STEPHEN BARNES, KELLY K. NICHOLS

In preparation for *Experimental Eye Research*

Format adapted for dissertation

Abstract

Preliminary work has shown that select triacylglycerols (TAGs) are upregulated in a preclinical model of MGD, suggesting that TAGs may be an important outcome variable in research involving human meibomian gland epithelial cells (HMGECs). The purpose of this study was to explore the HMGEC TAG lipidome in culture conditions known to influence differentiation. HMGECs were differentiated in DMEM/F12 with 10 ng/ml EGF, FBS (2% or 10%), and rosiglitazone (0, 20, or 50 µM) for two or five days. Following culture, lipids were extracted, processed, and directly infused into a Triple TOF 5600 mass spectrometer (SCIEX, Framingham, MA) with electrospray ionization. MS and MS/MS^{ALL} spectra were acquired in the positive ion mode and performed with the SWATH technology. Only the TAGs that were present in all 48 samples were included in the analysis. Multiple regression techniques were utilized to assess the effects of each factor (FBS, rosiglitazone, and culture duration) on each expressed TAG. The HMGEC TAG lipidome consisted of 115 TAGs with 42 to 62 carbons and zero to 10 double bonds. Fatty acyl chains had 14 to 26 carbons and zero to five double bonds. C18:1 (oleic acid, 25/115, 21.7%) and C16:0 (palmitic acid, 16/115, 13.9%) were the most common fatty acids. FBS, rosiglitazone, and culture duration were significant predictors for 93 TAGs (80.9%) with R^2 values ranging from 0.20 to 0.77 ($p < 0.05$). FBS and rosiglitazone achieved significance ($p < 0.05$) for 80 (69.6%) and 67 TAGs (58.3%), respectively. Rosiglitazone demonstrated a selective upregulation of TAGs containing 16

or 18 carbons. Culture duration reached significance ($p < 0.05$) for only 36 TAGs (31.3%). When comparing the 10 most abundant C18:1-containing TAGs in meibum, FBS was a negative predictor for five TAGs (mean standardized coefficient [SC] = -0.58, $p < 0.001$), rosiglitazone was a positive predictor for six TAGs (mean SC = 0.41, $p \leq 0.03$), and culture duration weakly influenced one TAG (SC = 0.27, $p = 0.008$). FBS and rosiglitazone, unlike culture duration, are powerful modulators of the TAG profile. Rosiglitazone induces changes that could be consistent with fatty acid synthesis, suggesting that quantifying the TAG lipidome could be an indirect measure of lipogenesis. Though both have been described as differentiating agents, FBS and rosiglitazone induce opposing effects on meibum-relevant TAGs. Culturing with rosiglitazone is associated with a TAG profile that is more consistent with the expected outcome of lipogenesis and with the profile observed in normal human meibum.

Introduction

Immortalized human meibomian gland epithelial cells (HMGECs) have immense potential in meibomian gland dysfunction (MGD) research. The use of preclinical models permits better assessment of cause-and-effect relationships but only to the extent that they replicate normal physiology. Early reports of HMGECs revealed increased gene expression for lipogenic enzymes in response to androgen exposure[1,2]—an expected behavior of lipid-producing meibocytes. Manifesting the expected phenotype, HMGECs have also been shown to increase nonpolar lipid production following exposure to a variety of differentiating agents, a finding that is often assessed by vital dyes and fluorescent microscopy.[1,3-10] This method provides strong visual evidence of nonpolar

lipid upregulation, but it lacks differentiation among the various lipid classes (nonetheless, species), complicating our understanding of whether the produced lipidome truly mirrors that from the meibomian gland in vivo.

Meibomian gland secretion, termed meibum, is a complex mixture of primarily nonpolar lipids. The composition of this mixture has been extensively analyzed by mass spectrometry, a tool that permits the identification and quantification of specific lipid species.[11] Previous reports have shown that the nonpolar wax and cholesteryl esters dominate the lipid pool, accounting for nearly 90% of all lipids.[12] Triacylglycerols (TAGs), another nonpolar lipid family, have been cited to represent between 0.05% to 6%.[13-17] Although TAGs do not represent a major lipid class in meibum, our preliminary studies have suggested that select TAGs are upregulated in a preclinical disease model of MGD,[18] suggesting that they may be an important indicator of pathology. To date, however, a description of the TAG lipidome produced by HMGECs has not been published, nor is it known how it responds to culture conditions known to influence HMGEC differentiation.

Although several differentiating agents for HMGECs have been described, the original mechanism for inducing differentiation utilized 10% serum in culture media.[1,3] This method has since been challenged, however, in more recent reports that failed to detect a significant increase in lipid production.[9,19] More recently, the use of rosiglitazone, a peroxisome proliferator activator receptor-γ (PPARγ) agonist, was introduced in a compelling series of experiments that has recently been expanded to include whole transcriptome analysis.[9,20] PPARγ, a key player in both sebocyte and adipocyte differentiation, is a nuclear receptor that upon binding to one of its many

ligands, such as rosiglitazone, associates with other nuclear receptors and cofactors to ultimately regulate transcription of a variety of genes involved in cellular differentiation and lipid metabolism.[21,22] We previously evaluated the effects of rosiglitazone on the expression of cholesteryl esters by HMGECs and found that the lower serum concentration (2%) and the highest rosiglitazone concentration (50 µM) after two days of culture yielded a more meibum-like profile.[23]

In this study, we sought to define the TAG lipidome, specifically related to its fatty acid (FA) composition and assess its viability as an outcome measure in HMGEC lipidomic research. To this end, the effects of serum, rosiglitazone, and culture duration were evaluated in a 2 x 3 x 2 experimental design using multiple regression techniques to explore the collective and individual effects of each factor on each expressed TAG.

Material and methods

Cell culture

Immortalized HMGECs were maintained in proliferating conditions in keratinocyte serum-free media (KSFM), 5 ng/ml epidermal growth factor (EGF), and 50 µg/ml bovine pituitary extract (BPE) until 80% confluence.[1] HMGECs were split into 6-cm glass petri dishes at a density of one million cells per dish and exposed to various differentiating conditions, all of which included Dulbecco's modified Eagle's medium (DMEM) and Ham's F12 (1:1) with 10 ng/ml EGF. All differentiation media also consisted of fetal bovine serum (FBS, 2% or 10%) and rosiglitazone (0 µM, 20 µM, or 50 µM, Cayman Chemical, Ann Arbor, MI). Stock solutions (4 mM or 10 mM) were made by dissolving rosiglitazone into sterile-filtered dimethyl sulfoxide (DMSO, Hybri-Max™,

Sigma-Aldrich, St. Louis, MO) and stored under nitrogen at -20°C. Rosiglitazone was added to each media immediately prior to introducing it to the cells. The concentration of DMSO was held constant at 0.5% across all samples. Differentiating conditions were maintained for either two days or five days; media changes were performed every other day. All experiments consisted of two technical replicates and two experimental replicates.

Lipid extraction

After incubation for two days or five days, HMGECs were washed twice and then simultaneously harvested and extracted by the direct application of 3 ml chloroform-methanol (2:1, v/v), an adaptation of the Folch technique,[24] to increase extraction efficiency from cultured cells.[25] The surface of the glass dish was scraped with a sterile stainless-steel scraper, and the sample was transferred to a glass vial. Ammonium acetate (0.75 ml, 50 mM) in molecular biology-grade water was added to each sample, and the resulting emulsion was agitated on ice at 350 rpm for 20 minutes. To facilitate phase separation, the samples were centrifuged at 1600 x g for five minutes. The lower, nonpolar phase was withdrawn by glass pipet and stored at -80°C until analysis. All materials that contacted organic solvents were made of glass, polytetrafluoroethylene (PTFE), or stainless steel.

Analysis by mass spectrometry (MS)

Samples were analyzed by mass spectrometry using methods previously described.[23] Briefly, dried lipids were reconstituted in 2:1 methanol/chloroform (v/v) with

5 mM ammonium acetate, and the solution was directly infused into a Triple TOF 5600 mass spectrometer (SCIEX, Framingham, MA) with electrospray ionization at a flow rate of 7 µl/min. The direct infusing syringe was cleaned before and after each sample run with two flushes of 100% methanol, 100% acetonitrile, 100% isopropyl alcohol, and 2:1 methanol-chloroform. MS and MS/MS^{ALL} spectra were acquired in the positive ion mode and performed with the SWATH technology (Sequential Window Acquisition of all THeoretical mass spectra, SCIEX, Framingham, MA). Product ion MS/MS spectra for all parent ions were acquired between 200 to 1200 m/z at every one Dalton step. Collision energy was fixed at 35 eV. The acquisition time was six minutes per sample.

Data analysis

All acquired MS data were processed using LipidView 1.2 (SCIEX, Framingham, MA), which assigns lipid identities based upon known ion fragmentations. The mass tolerance window was set to 5 mDa. Only the TAG peaks with a signal-to-noise ratio greater than three that were present in all samples were included in the analysis. Each analyzed TAG was normalized to the sum intensity and is therefore reported as percent of the overall TAG pool. The labeling convention for TAGs is TAG n_c:db (FA or TAG n_c:db), where n_c is the total carbon count of the fatty acyl chain(s) and db is the number of double bonds. The parent ion is provided first, and the product ion (either a FA or a TAG) is provided second. For example, TAG 54:3 (FA 18:1) denotes that a fatty acid with 18 carbons and one double bond was detected in the product ion scan from the parent TAG of 54 carbons and three double bonds.

To determine the response of the TAG lipidome to each of the three variables—FBS, rosiglitazone, and duration of culture—all data were analyzed by multiple regression techniques using SPSS v26 (Armonk, NY). Rosiglitazone was analyzed in two concentrations (20 μM and 50 μM), rather than as a continuous variable. This technique is valuable in multiple regression when data are not assumed to be linear, an important consideration since Kim et al. observed a non-linear relationship between lipid production and rosiglitazone between 0 and 50 μM.[9] When the assumptions of normality (Kolmogorov-Smirnov) and equal variance (Levene's test) were violated, the data were transformed by ranking prior to performing the multiple regression analysis. A p-value of 0.05 was considered statistically significant.

Results

Description of the TAG lipidome

Across all samples, 2,131 unique TAGs were identified; however, only 115 met the inclusion criterion of being present in all 48 samples. The total carbon count from the three acyl chains, excluding the glycerol backbone, ranged from 42 to 62 with the majority (83/115, 72.2%) falling within the range of 48 to 54 (Figure 1A). An even carbon count was significantly more common (90/115, 78.3%) than an odd carbon count (25/115, 21.7%).

The number of double bonds in the acyl chains of the TAGs varied from zero to 10. Very few TAGs were fully saturated (4/115, 3.5%). The degree of unsaturation followed a bimodal distribution (Figure 1B). TAGs were primarily of low unsaturation (49/115, 42.6%, one to three double bonds) or of high unsaturation (61/115, 53.0%, six to

10 double bonds). Only five of 115 (4.4%) had a moderate degree of unsaturation (four to five double bonds).

The LipidView 1.2 software identified the neutral loss of 17 unique fatty acyl chains from the 115 TAGs (Figure 1C). Their individual carbon counts varied from 14 to 26 with double bonds ranging from zero to five. Similar to the parent TAG molecules, an even carbon count (84/115, 80.0%) was much more common than an odd carbon count (15/115, 15.2%). The most frequently observed fatty acyl group was oleic acid (FA 18:1), which was present in 25 of 115 TAGs (21.7%). The second most common was palmitic acid (FA 16:0), which was present in 16 (12.8%) TAGs. Very few TAGs, only seven of 115 (6.1%), consisted of very long-chain fatty acids (at least 20 carbons).

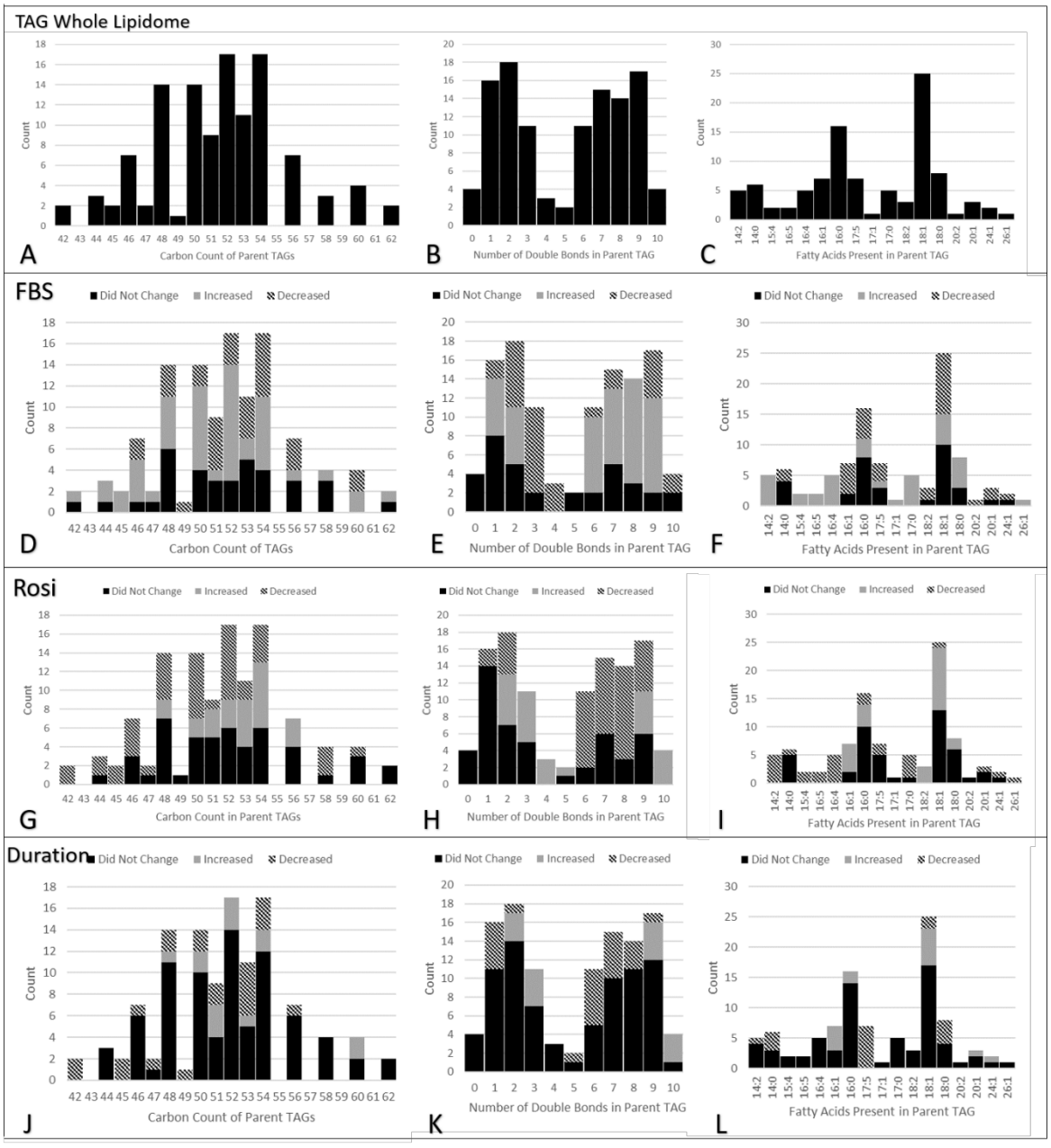

Figure 1 Description of HMGEC TAG Lipidome

HMGECs were treated with varying concentrations of FBS and rosiglitazone for 2 days or 5 days. Lipid extracts (n = 48) were analyzed by tandem mass spectrometry in the positive ion mode to identify triacylglycerols (TAGs). (A-C) There were 115 identified TAGs present in all 48 samples with carbon counts varying from 42 to 62 and double bonds varying from zero to 10. LipidView 1.2 detected the neutral loss of seventeen unique fatty acyl chains. FA 18:1 and FA 16:0 were the most frequently observed. (D-L) Multiple regression analyses were performed to assess the individual contribution of each factor (FBS in Panels D-F, rosiglitazone in Panels G-I, and culture duration in Panels J-L) to the

variance observed in each TAG. Notable observations include a narrow range of carbon counts (48 to 56, Panel G) and FA-containing TAGs (16 or 18 carbons, Panel I) that increase with rosiglitazone. Further description of the distributions is detailed in the text. The carbon count includes the total number of carbons present in the three acyl chains. Fatty acids are labeled as two numbers separated by a colon, where the first number is the number of carbons and the second number is the number of double bonds.
HMGEC = human meibomian gland epithelial cell
TAG = triacylglycerol
FBS = fetal bovine serum
Rosi = rosiglitazone
FA = fatty acid

FBS, rosiglitazone, and culture duration—collectively—on the TAG profile

Multiple regression was performed for each of the 115 TAGs to determine the predictive capacity—or contribution of effect—of each of our factors (FBS, rosiglitazone, and culture duration). Of the 115 TAGs analyzed, the factors significantly predicted 93 (80.9%) TAGs. Of these 93, zero were saturated, eight (8.6%) were monounsaturated, and the remaining 85 (91.4%) were polyunsaturated. The eight that were monounsaturated represented 50% of the overall monounsaturated TAGs produced by HMGECs. Statistically significant R^2 values ranged from relatively weak (0.20) to strong (0.77) (Figure 2).

Only 22 (19.1%) of 115 TAGs showed no association with the statistical model. Of these 22, their profile was largely consistent with the overall TAG profile, possessing similarities in both carbon counts and double-bond counts. Among these TAGs, the range of their carbon numbers varied from 44 to 62, and the double-bond count varied from zero to eight. Of note, all four (100%) of the saturated TAGs detected from our samples were not predicted by the factors in the model: TAG 46:0 (FA 16:0), TAG 48:0 (FA 16:0), TAG 48:0 (FA 14:0), and TAG 52:0 (FA 16:0).

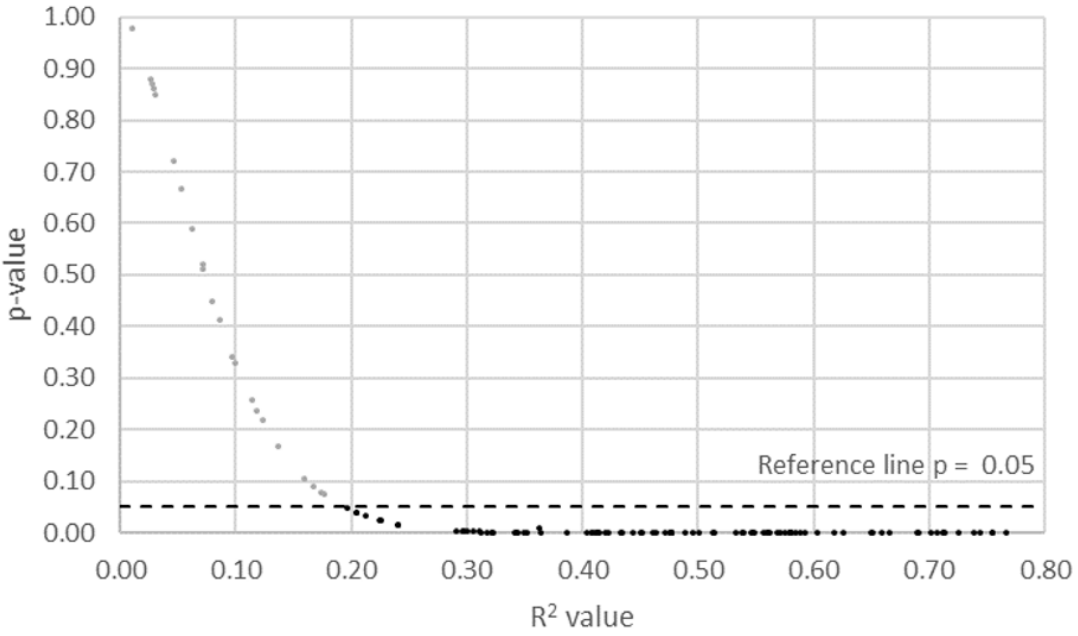

Figure 2 Statistical Significance and R2 for Expressed TAGs
Each dot represents one of 115 identified TAGs that were present in all 48 samples of HMGECs treated with varying concentrations of FBS and rosiglitazone for two days or five days. Multiple regression was performed to determine the predictive potential of all three factors—FBS, rosiglitazone, and culture duration—on the variance observed for each TAG. The model was able to significantly predict 93 of 115 TAGs, as denoted by the black dots that fall beneath the p = 0.05 reference line. Significant R^2 values ranged from 0.20 to 0.77, and p-values ranged from < 0.001 to 0.978.
TAG = triacylglycerol
HMGEC = human meibomian gland epithelial cell
FBS = fetal bovine serum

Influence of FBS on TAG profile

To determine the individual contribution of FBS on each of the 115 TAGs analyzed, the standardized coefficients (SC) from the multiple regression analysis were evaluated. Standardized coefficients are a ratio of the amount of change in standard-deviation units for the outcome variable (here, each TAG) per corresponding change in the predictor variable (here, FBS). Controlling for both rosiglitazone and culture duration,

FBS was a significant predictor for 80 of 115 TAGs (69.6%), where 49 TAGs (61.3%) were positively associated and 31 TAGs (38.7%) were negatively associated. In general, TAGs with nearly all carbon counts and double-bond counts were affected, ranging from 42 to 62 and one to 10, respectively (Figure 1D-E). Of the 25 TAGs containing FA 18:1, 10 (40.0%) were not associated with FBS, five (20.0%) were positively associated, and 10 (40.0%) were negatively associated (Figure 1F). Of the 10 that were inversely associated, six of them (60%) were among the most responsive to changes in FBS (Table 1).

Table 1 Most Responsive TAGs (90th Percentile) Per Factor

	Most Positively Associated			Most Negatively Associated		
	TAG	Std Coeff	p-value	TAG	Std Coeff	p-value
FBS	TAG 48:7 (TAG 36:1)	0.75	<0.001	TAG 56:3 (FA 20:1)	-0.78	<0.001
	TAG 54:8 (FA 16:4)	0.73	<0.001	TAG 48:2 (FA 18:1)	-0.74	<0.001
	TAG 54:9 (FA 17:0)	0.72	<0.001	TAG 56:3 (FA 18:1)	-0.71	<0.001
	TAG 54:1 (FA 18:0)	0.72	<0.001	TAG 50:3 (FA 18:1)	-0.65	<0.001
	TAG 44:6 (TAG 32:0)	0.72	<0.001	TAG 50:2 (FA 18:1)	-0.64	<0.001
	TAG 52:6 (FA 14:2)	0.70	<0.001	TAG 51:10 (FA 16:1)	-0.64	<0.001
	TAG 52:8 (FA 17:0)	0.68	<0.001	TAG 48:2 (FA 16:1)	-0.64	<0.001
	TAG 54:9 (FA 18:1)	0.67	<0.001	TAG 54:3 (FA 18:1)	-0.62	<0.001
	TAG 58:1 (FA 16:0)	0.66	<0.001	TAG 53:10 (FA 18:1)	-0.61	<0.001
	TAG 53:8 (FA 18:0)	0.65	<0.001	TAG 52:3 (FA 16:1)	-0.60	<0.001
	TAG 48:9 (TAG 36:3)	0.65	<0.001	TAG 46:1 (FA 16:0)	-0.55	<0.001
Rosiglitazone (50 µM)	TAG 56:5 (FA 18:1)	0.81	<0.001	TAG 42:6 (TAG 30:0)	-0.71	<0.001
	TAG 53:10 (FA 16:0)	0.71	<0.001	TAG 48:6 (FA 14:2)	-0.64	<0.001
	TAG 52:3 (FA 18:2)	0.63	<0.001	TAG 50:6 (FA 14:2)	-0.63	<0.001
	TAG 54:4 (FA 18:1)	0.62	<0.001	TAG 42:7 (TAG 30:1)	-0.62	<0.001
	TAG 54:3 (FA 18:2)	0.61	<0.001	TAG 50:6 (FA 16:5)	-0.61	<0.001
	TAG 53:9 (FA 16:1)	0.60	<0.001	TAG 50:7 (FA 14:2)	-0.58	<0.001
	TAG 54:2 (FA 18:0)	0.59	<0.001	TAG 44:7 (TAG 32:1)	-0.58	<0.001
	TAG 53:9 (FA 18:0)	0.59	<0.001	TAG 52:9 (FA 16:4)	-0.56	<0.001
	TAG 54:4 (FA 18:2)	0.59	<0.001	TAG 50:8 (FA 17:0)	-0.56	<0.001
	TAG 56:4 (FA 18:1)	0.56	<0.001	TAG 53:6 (FA 17:5)	-0.55	<0.001
	TAG 51:9 (FA 16:0)	0.55	<0.001	TAG 52:8 (FA 16:4)	-0.55	<0.001

Culture Duration	TAG 52:9 (FA 16:0)	0.49	<0.001	TAG 53:8 (FA 17:5)	-0.70	<0.001
	TAG 60:3 (FA 24:1)	0.48	<0.001	TAG 50:1 (FA 14:0)	-0.61	<0.001
	TAG 54:10 (FA 18:1)	0.45	<0.001	TAG 49:6 (FA 17:5)	-0.53	<0.001
	TAG 52:9 (FA 18:1)	0.44	0.001	TAG 45:8 (TAG 33:2)	-0.52	<0.001
	TAG 60:3 (FA 18:1)	0.39	0.004	TAG 53:9 (FA 17:5)	-0.50	<0.001
	TAG 51:9 (FA 16:1)	0.38	<0.001	TAG 51:6 (FA 17:5)	-0.49	<0.001
	TAG 51:10 (FA 16:1)	0.35	<0.001	TAG 51:7 (FA 17:5)	-0.49	<0.001
	TAG 52:3 (FA 16:1)	0.29	0.001	TAG 53:7 (FA 17:5)	-0.48	<0.001
	TAG 50:2 (FA 18:1)	0.27	0.008	TAG 45:7 (TAG 33:1)	-0.46	<0.001
	TAG 51:9 (FA 16:0)	0.27	0.014	TAG 47:7 (FA 14:0)	-0.40	0.006
	TAG 54:2 (FA 20:1)	0.27	0.04	TAG 48:6 (TAG 36:1)	-0.36	0.004

The TAG labeling convention is described under Data Analysis in the Material and Methods section.

Influence of rosiglitazone on TAG profile

Although the statistical model does not assume linearity, tests of linearity were performed to determine the relationship between rosiglitazone and each of the TAGs. Only nine of 115 (7.8%) deviated from linearity: TAG 46:6 (TAG 34:0), TAG 48:8 (TAG 36:2), TAG 53:10 (FA 16:0), TAG 54:4 (FA 18:1), TAG 54:4 (FA 18:2), TAG 54:3 (FA 18:2), TAG 54:2 (FA 18:0), TAG 56:4 (FA 18:1), and TAG 58:2 (FA 24:1). There was no individual effect due to the intermediate concentration of rosiglitazone on any of the expressed TAGs, as all p-values were greater than 0.05. When controlling for both FBS and culture duration, however, the highest concentration of rosiglitazone (50 μM) was a significant predictor for 67 of 115 TAGs (58.3%). Of these, 25 TAGs (37.3%) were positively associated and 42 (62.7%) were negatively associated. Of the 25 TAGs that were positively associated, only a narrow range of carbon counts (48 to 56) varied with rosiglitazone; the large majority (20/25, 80.0%) of these were between 50 and 54 (Figure 1G). All 25 were polyunsaturated, primarily bearing two to four double bonds or nine to 10 double bonds (Figure 1H). None of the saturated or monounsaturated TAGs

were positively associated with rosiglitazone. Of particular interest, TAGs with only a small subset of FAs (carbon number 16 or 18) were positively associated with rosiglitazone (Figure 1I): FA 18:1 (11/25, 44.0%), FA 16:1 (5/25, 20.0%), FA 16:0 (4/25, 16.0%), FA 18:2 (3/25, 12.0%), and FA 18:0 (2/25, 8.0%). The most responsive TAGs to rosiglitazone supplementation are provided in Table 1.

Of the 42 TAGs that were negatively associated with rosiglitazone, the profile showed less selectivity and was more similar to the overall TAG profile for HMGECs. The carbon count ranged from 42 to 60, and the double-bond distribution was bimodal with peaks at one to two double bonds and six to nine double bonds (Figure 1G-H). TAGs with 12 different fatty acids consisting of individual carbon counts varying from 14 to 26 inversely varied with rosiglitazone (Figure 1I). Of note, only one FA 18:1-containing TAG decreased (TAG 58:2).

Influence of culture duration on TAG profile

Controlling for both FBS and rosiglitazone, culture duration was a significant predictor for 36 (31.3%) of 115 TAGs, where 14 (38.9%) were positively associated and 22 (61.1%) were negatively associated. Of the 14 TAGs that were positively associated, their carbon counts ranged from 48 to 60, and their double-bond counts were bimodally distributed with peaks at two to three and nine to 10 (Figure 1J-K). Only select FA-containing TAGs were positively associated with culture duration (Figure 1L): FA 18:1 (6/14, 42.9%), FA 16:1 (4/14, 28.6%), FA 16:0 (2/14, 14.3%), FA 20:1 (1/14, 7.1%), and FA 24:1 (1/14, 7.1%).

Of the 22 TAGs that were negatively associated with culture duration, their carbon counts ranged from 42 to 56, and their double-bond counts ranged from one to two and five to nine (Figure 1J-K). A similar pattern of selectivity for certain fatty acids was seen among the negatively associated TAGs, though the selectivity was different. TAGs containing FA 17:5 (7/17, 41.2%), FA 18:0 (4/17, 23.5%), FA 14:0 (3/17, 17.7%), FA 18:1 (2/14, 11.8%), and FA 14:2 (1/17, 5.9%) were negatively associated with culture duration. All seven of the FA 17:5-containing TAGs that were present in the overall TAG lipidome were inversely associated with culture duration (Figure 1L). The most responsive TAGs to culture duration are provided in Table 1.

Opposing effects of FBS and rosiglitazone on meibum-relevant TAGs

The collective and individual contributions of FBS, rosiglitazone, and culture duration were evaluated on the 10 most abundant TAGs containing FA 18:1 in meibum (Table 2).[46] The model statistically significantly predicted six of the 10 TAGs with R^2 values ranging from 0.32 to 0.58 ($p < 0.01$ for all). All three variables added significantly to the prediction for TAG 50:2 ($p < 0.01$). FBS and rosiglitazone—but not culture duration—added significantly to the prediction for four TAGs: TAG 54:3, TAG 52:2, TAG 54:4, and TAG 56:3 ($p < 0.05$ for all). Rosiglitazone was the only significant predictor in the model for TAG 54:2 ($p = 0.001$). Of note, FBS and rosiglitazone had opposing effects on the meibum-relevant TAGs that were statistically significant (Figure 3). FBS was always negatively associated, while rosiglitazone was always positively associated.

Table 2 Predictive Capacity of Each Factor for Common Meibum-Relevant TAGs

Meibum-Relevant TAG (All FA 18:1-containing TAGs)	Overall Model		FBS		Rosiglitazone (50 μM)		Culture Duration	
	R^2	p-value	Std. Coeff.	p-value	Std. Coeff.	p-value	Std. Coeff.	p-value
TAG 54:3	0.58	<0.001	-0.62	<0.001	0.43	0.001	0.14	0.18
TAG 52:2	0.39	<0.001	-0.53	<0.001	0.31	0.03	0.15	0.21
TAG 54:2	0.32	0.002	-0.20	0.13	0.53	0.001	0.02	0.90
TAG 52:3	Not detected							
TAG 53:2	Not detected							
TAG 52:1	0.11	0.26	0.26	0.08	-0.07	0.67	-0.21	0.16
TAG 50:2	0.58	<0.001	-0.64	<0.001	0.34	0.004	0.27	0.008
TAG 54:4	0.56	<0.001	-0.41	<0.001	0.62	<0.001	0.006	0.95
TAG 56:3	0.58	<0.001	-0.71	<0.001	0.25	0.03	0.16	0.115
TAG 50:1	0.01	0.98	0.08	0.61	-0.01	0.96	-0.06	0.68

The standardized coefficients for FBS, rosiglitazone, and culture duration for each of the 10 most abundant FA 18:1-containing TAGs from Chen et al.[46] were evaluated to determine the predictive capacity of each factor on meibum-relevant TAGs. Standardized coefficients are a ratio of the amount of change in standard-deviation units for the outcome variable (here, each TAG) per corresponding change in the predictor variable (here, either FBS, rosiglitazone, or culture duration). Graphical data are provided in Figure 3. Bolded values denote statistical significance. The TAG labeling convention is described under Data Analysis in the Material and Methods section.

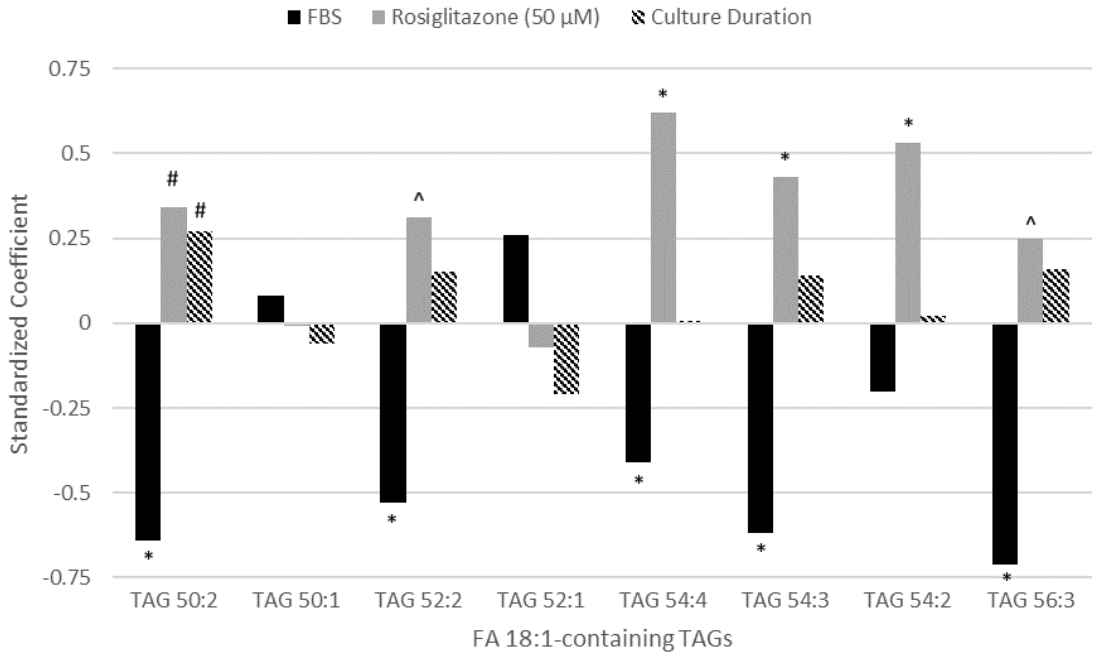

Figure 3 Standardized Coefficients for Each Factor

The standardized coefficients for FBS, rosiglitazone, and culture duration for each of the 10 most abundant FA 18:1-containing TAGs from Chen et al.[46] were evaluated to determine the predictive capacity of each factor on meibum-relevant TAGs. Standardized coefficients are a ratio of the amount of change in standard-deviation units for the outcome variable (here, each TAG) per corresponding change in the predictor variable (here, either FBS, rosiglitazone, or culture duration). Numeric data are provided in Table 2. Two of the 10 TAGs did not meet the inclusion criteria for analysis. Rosiglitazone, FBS, and culture duration were significant predictors for six, five, and one TAG(s), respectively. Rosiglitazone was always positively associated with meibum-relevant TAG expression, while FBS was always negatively associated. TAGs are labeled by two numbers separated by a colon, where the first number is the total number of carbons in the three acyl chains and the second number is the number of double bonds.

FBS = fetal bovine serum

TAG = triacylglycerol

FA 18:1 = oleic acid

* $p \leq 0.001$

$p \leq 0.01$

^ $p \leq 0.05$

Discussion

This report describes the TAG lipidome produced by HMGECs and explores its response to common differentiating conditions. The TAG lipidome from HMGECs is robust, diverse, dynamic, and responsive to culture conditions. Multiple regression techniques were used to assess both the combined and individual effects of serum, rosiglitazone, and culture duration on TAG expression. Serum and rosiglitazone, both purported as HMGEC differentiating agents, were shown to strongly modulate the TAG profile, yet they elicited opposing effects on many meibum-relevant TAGs. The highest concentration of rosiglitazone (50 μM) and the lower concentration of serum (2%) promoted a more meibum-like TAG profile. Culture duration, however, had minimal effect. Together, these findings suggest that culture conditions affect lipid metabolism and that supplementation with the ideal concentrations of serum and rosiglitazone should be carefully considered in preclinical models involving HMGECs. Our results further support previous assertions that rosiglitazone could have a therapeutic role in meibomian gland dysfunction and should be further investigated.[9,27]

Effects of serum on the HMGEC TAG lipidome

The effects of serum on HMGEC differentiation have been a source of debate in recent literature. It has been stated that serum is a strong inducer of HMGEC differentiation;[3] however, serum's effects have been poorly replicated among different research groups.[3,9,19] Some reports describe a significant upregulation of lipid production;[1,3] other reports describe minimal change in lipid production yet an increase in keratinization.[9,19] This keratin upregulation implies that serum-treated HMGECs may be

a better disease model of the hyperkeratinization that occurs in MGD pathophysiology.[28] Using mass spectrometry, we—and others—have reported production of meibum-relevant cholesteryl esters following 10% serum supplementation, albeit in low relative abundance.[3,19,25] We later found that reducing the serum content to 2% resulted in a more optimized and more similar CE profile to that present in normal human meibum.[23] The exact mechanism for how HMGECs modulate TAG expression in response to serum supplementation, however, remains largely unknown. In our present study, FBS induced significant changes to the TAG profile produced by HMGECs where nearly 70% of all detected TAGs varied in some way. The characteristics of the TAGs that increased and those that decreased were similar to the TAG profile as a whole, complicating the ability to draw any conclusions regarding how serum affects TAG production. Because of this overlap, it is likely that there are several pathways involved in lipid metabolism, both lipogenesis and lipolysis, occurring simultaneously that are influenced by serum.

One intriguing observation is the negative association between serum and many of the FA 18:1-containing TAGs. Specifically, 2% serum, when compared to 10% serum, yielded higher production of 10 TAGs bearing oleic acid (FA 18:1), the most predominant fatty acid in meibum-relevant TAGs.[26] Further, six of these 10 TAGs were among those that showed the highest response to serum (Table 1). HMGECs exposed to low-serum environments have less access to serum-borne lipids, proteins, and growth factors that are abundant in high-serum environments. Serum-free or low-serum environments may, therefore, be analogous to a relative state of exogenous lipid starvation. It has been shown that culture media supplemented with lipid-deficient FBS halts cell growth and promotes lipogenesis,[29] both of which are believed to be hallmarks

of HMGEC differentiation.[30] In culture conditions completely devoid of serum altogether, a similar increase in lipid production has also been observed.[31,32] Lipogenesis, or fatty acid synthesis, yields the production of palmitic acid (FA 16:0), which can be further elongated and desaturated to produce oleic acid.[33] Indeed, both palmitic acid and palmitoleic acid (FA 16:1), additional signs of fatty acid synthesis, were also strongly upregulated with the lower serum concentration. Lastly, the observation that intracellular oleic acid is higher in a low-serum environment argues against oleic-acid uptake or contamination from the serum-containing media, further supporting the conjecture of increased fatty acid synthesis in low-serum (and likely serum-free) environments. Considering that oleic acid is present in approximately 60% to 75% of all wax esters,[15,34,35] a class that in itself represents 40% to 50% of all meibum lipids,[12,17,34] the production and storage of oleic acid in TAG depots would be of physiologic relevance. Additional work is needed to evaluate the mechanism of serum deficiency on fatty acid synthesis.

The possibility that residual lipids from the serum lipidome could have contributed to our extracted TAG profile from HMGECs, despite careful washing steps, was considered. Had this occurred, HMGECs cultured in 10% serum would have had higher levels of serum-relevant TAGs relative to those cultured in 2% serum. Our results reveal the opposite: the higher serum concentration was typically associated with a decrease in serum-relevant TAGs. Thirty variations (based on the fatty acid composition) were detected of the 16 TAGs reported to be abundant in FBS (Table 3).[29] Of these, 11 had no significant associations with FBS, 14 were negatively associated, and only five were positively associated. This pattern—or lack thereof—rules out the possibility of

trace amounts of the serum lipidome contaminating our HMGEC lipid extracts and reinforces the complex influence that serum has on lipid metabolism.

Table 3 Standardized Coefficients for FBS and TAGs Reported in Serum

TAG	Standardized Coefficients							
	FA 14:0	FA 16:1	FA 16:0	FA 18:2	FA 18:1	FA 18:0	FA 20:2	FA 20:1
48:3	nd							
48:2	nd	-0.64 p < 0.001	-0.48 p < 0.001	nd	-0.74 p < 0.001	nd	nd	nd
48:1	-0.18 p = 0.21	-0.15 p = 0.30	-0.28 p = 0.06	nd	-0.21 p = 0.15	nd	nd	nd
50:3	nd	nd	nd	nd	-0.65 p < 0.001	nd	nd	nd
50:2	nd	nd	nd	nd	-0.64 p < 0.001	nd	nd	nd
50:1	0.00 p = 1.00	0.02 p = 0.92	0.34 p = 0.02	nd	0.08 p = 0.61	0.49 p < 0.001	nd	nd
52:4	nd							
52:3	nd	-0.60 p < 0.001	nd	-0.23 p = 0.05	nd	nd	nd	nd
52:2	nd	nd	nd	nd	-0.53 p < 0.001	nd	nd	nd
52:1	nd	nd	0.60 p < 0.001	nd	0.26 p =0.08	nd	nd	nd
54:4	nd	nd	nd	-0.44 p < 0.001	-0.41 p < 0.001	nd	nd	nd
54:2	nd	nd	-0.40 p < 0.01	nd	-0.20 p = 0.13	0.24 p = 0.05	nd	-0.31 p = 0.02
56:4	nd	nd	nd	nd	-0.40 p < 0.01	nd	nd	nd
56:3	nd	nd	nd	nd	-0.71 p < 0.001	nd	nd	-0.78 p < 0.001
56:2	nd	nd	nd	nd	-0.05 p = 0.76	0.41 p < 0.01	nd	-0.07 p = 0.63
56:1	nd							

The standardized coefficients for FBS with respect to each serum-relevant TAG[140] were evaluated. Multiple isomers were detected for each TAG provided in Brovkovych et al.[140] Standardized coefficients are a ratio of the amount of change in standard-deviation units for the outcome variable (here, each TAG) per corresponding change in the predictor variable (here, FBS). Positive values describe a positive association, while negative values describe a negative association. Fourteen of 19 isomers that reached significance were negatively associated with FBS, ruling out the possibility for FBS contamination or spillover into our extracted HMGEC lipidome. Bolded values denote significance.

FBS = fetal bovine serum

TAG = triacylglycerol

HMGEC = human meibomian gland epithelial cell

Effects of rosiglitazone on the HMGEC TAG lipidome

The effects of rosiglitazone and the downstream events of PPARγ activation have been well-studied in many different cell types, including HMGECs.[9,20,23] Upon PPARγ activation, transcriptional activity is upregulated for many genes involved in lipid metabolism.[21] Specifically, lipoprotein lipase, an enzyme that catalyzes the release and facilitates the internalization of fatty acids from extracellular TAGs, is increased.[36] Fatty acids are then shuttled through the hydrophilic cytosol via fatty acid transport proteins to areas where they can undergo oxidation to harness their energy or be converted into other long-chain fatty acids through enzyme systems.[36,37] Additionally, new fatty acids are synthesized de novo from acetyl coA in the cytosol.[38] Ultimately, the end product of this process is lipid assembly, often taking the form of bundling fatty acids into TAGs for storage in lipid droplets.[38] Importantly, gene targets of PPARγ are integrally involved in every step of this process.[39]

Although our study was not designed to interrogate the mechanisms of PPARγ activation and sequelae, our findings provide a remarkably consistent snapshot of how these concerted actions manifest in the TAG lipidome. We found that 25 TAGs, all possessing 48 to 56 carbons, were increased with 50 μM rosiglitazone. All 25 of these TAGs consisted of a 16- or 18-carbon fatty acid, which likely represents the product of increased fatty acid synthesis, as discussed in the preceding section. While the possibility of selective internalization of 16- and 18-carbon fatty acids from the media cannot be ruled out, past experiments assessing the substrate specificity of lipoprotein lipase have concluded that there is no fatty acid specificity.[40] All fatty acids are capable of being cleaved from TAGs by lipoprotein lipase and internalized, albeit at different rates.[40] We

propose that after the fatty acids were non-discriminately absorbed and shuttled through the cell, they likely proceeded toward one of three fates, depending on which would have been the most energetically favorable. They would either be unprocessed and rapidly sequestered into TAGs (in the case of 16- and 18-carbon fatty acids), modified by simple enzymatic steps into 16- or 18-carbon FAs, or—especially if several steps would have been necessary—degraded into their components via beta oxidation. The fragments could subsequently be assembled into palmitic acid (FA 16:0) via fatty acid synthase, which is highly expressed in HMGECs and the human meibomian gland,[1,30,41] followed by elongation and/or desaturation to convert into a combination of 16- to 18-carbon fatty acids that are either fully saturated or bearing just one or two double bonds.[33] Additional pathways are likely, if not probable, as comprehensively described in a recent review article on TAG metabolism.[42] These three pathways, however, may represent the most common pathways and would explain the accumulation of the 16- and 18-carbon fatty acids in response to rosiglitazone. Of note, these fatty acids (FA 18:1, FA 16:0, FA 16:1, and FA 18:2) are among the primary fatty acids found in TAGs in human meibum.[13] The preference for differentiated HMGECs to accumulate 16- or 18-carbon fatty acids could be a sign of increased demand, particularly by wax esters in need of FA 18:1,[15,34,35] which was found to be present in nearly half of the elevated TAGs associated with rosiglitazone in our study. Taken together, as in other cell types, TAGs likely serve as a depot of fatty acids in HMGECs to support production of other lipid classes, and evaluating the TAG lipidome may serve as an indirect assessment of lipid metabolism.[42]

The highest concentration of rosiglitazone had a negative association with 42 TAGs. Less selectivity was observed among this cohort compared to those that were

positively associated, suggesting that, generally, rosiglitazone stimulates the cell to use any fatty acid sources available without much discrimination. There did appear to be a minor preference to decrease the TAGs that included 14- and 15-carbon fatty acids, as well as highly polyunsaturated 16-carbon fatty acids with four or five double bonds. This same pattern was reflected among the parent TAGs also. Those with a high number of double bonds (six to nine) were much more likely to decrease in response to rosiglitazone treatment. The significance of this observation is unknown, but it may represent an attempt by the differentiated cell to tighten its spectrum of fatty acid-containing TAGs (stated differently, to decrease fatty-acid diversity) toward a profile that contains the building blocks that are in greatest demand for ongoing lipogenesis in the meibomian gland.

Effects of culture duration on the HMGEC TAG lipidome

The last variable that was assessed was culture duration. Compared to serum and rosiglitazone, culture duration demonstrated an overall weaker effect. Fewer TAG molecules varied with respect to culture duration, and the magnitude of change, when change was observed, was also comparatively smaller (Table 1). Approximately 70% of TAGs were unchanged between two days and five days of culture. Of the 30% that did change, the slightly shorter-chain fatty acids (14 to 18 carbons) decreased over time, while slightly longer-chain fatty acids (16 to 24) increased over time. The peaks in the bimodal distribution of unsaturation level also shifted slightly. Those TAGs bearing just one to two or six to nine double bonds decreased, while those with two to three or nine to 10 increased. These observations may provide hints to the kinetics of the enzymes

involved in elongation and desaturation within the differentiated HMGEC. Perhaps these enzyme systems experience a greater degree of upregulation between two and five days of culture. Ultimately, however, the overall weaker effect of culture duration is worthy of re-emphasis. Despite the observation of some mild trends in the TAG lipidome, the vast majority of TAGs did not vary with time.

In the literature, across a wide variety of differentiating approaches, HMGECs have been exposed to differentiating conditions for as little as one day and for up to 28 days.[3,10,19] Lipid production by HMGECs is a frequent outcome variable; however, its response to serum differentiation is poorly replicated among different laboratories. An early report stated that serum-differentiated HMGECs dramatically increase lipid production over time up to 13 days.[3] Another report stated that lipid production was maximized after one day and waned thereafter.[19] A third report failed to find a significant increase in lipid production following serum differentiation through a period of two to six days.[9] Using mass spectrometry, our previous work has shown that meibum-relevant cholesteryl esters are detected after just two days of culture in serum-containing media [25] and that extending culture duration to five days had a negligible effect on these CEs.[23] Our present work focuses on TAGs and is consistent with our previous results: duration of culture has less of an impact on the TAG lipidome compared to other differentiating factors.

Rosiglitazone-induced differentiation, however, has indeed shown a time-dependent increase in lipid production over two to six days of culture using vital dye and fluorescent microscopy.[9] The authors of this same paper also performed transcriptome analysis on rosiglitazone-differentiated HMGECs and found that genes involved in

cellular differentiation and lipid metabolism were already upregulated after just 24 hours and likely sustained for up to six days.[20] Our decision, therefore, to assess the lipidome at two days and five days is supported by the kinetics of PPARγ activation by rosiglitazone: the necessary genes are upregulated during this interval. One important distinction worth mentioning between our methodology and that of these other reports is that our methods allow us to evaluate changes in the relative abundance of specific lipid species but do not allow us to detect absolute changes in overall lipid production as a whole. A direct comparison of lipid production, therefore, would not be appropriate. A strength of our approach, however, is the ability to identify and quantify the exact lipids that are being produced to ensure consistency with the human meibum profile obtained in vivo. Based on our work, the duration of culture has a relatively weak effect on the TAG lipidome (and the CE lipidome[23]). The decision to use a certain culture duration should be guided by research objectives, methodology, and outcome variables.

Comparison of the TAG lipidomes between HMGECs and human meibum

A common criticism of the HMGEC line is the discrepancy between its lipidome and that of meibum's, a topic we have previously discussed.[3,25,43] It is therefore of utmost importance to evaluate and establish culture conditions that yield a lipidomic profile that is as close to human meibum as possible. We previously reported that 2% FBS and 50 µM rosiglitazone in DMEM/F12 supplemented with EGF optimized the cholesteryl ester profile of HMGECs.[23] In our present paper, we have focused not only on the TAG lipidome, but also on defining what contribution each factor (FBS, rosiglitazone, and culture duration) has on each TAG. To do this, each factor's contribution to the 10 most

abundant 18:1-containing TAGs reported in human meibum by Chen et al. was evaluated.[26] Two of the 10 did not meet our inclusion criteria and were therefore not included in our analysis. Six of the remaining eight varied significantly with serum, rosiglitazone, and/or culture duration (Table 2, Figure 3). Consistent with our discussion above, culture duration provided little contribution to the observed changes and only reached significance with a low magnitude of effect for one meibum-relevant TAG. FBS and rosiglitazone, however, were significant predictors for five and six meibum-relevant TAGs, respectively. Interestingly, though, their effects were in opposite directions. Across all significant meibum-relevant TAGs, the highest concentration of rosiglitazone and the lower concentration of serum yielded a more meibum-like profile. Although both substances have been purported to be differentiating agents, their divergent effects suggest otherwise. Our findings support the growing body of literature that serum alone is a poor differentiating agent for HMGECs, at least when evaluating variables related to lipid production and/or expression.[19,27,43] Conversely, rosiglitazone appears to induce a transcriptome and lipid-producing phenotype that are more consistent with what would be expected from differentiated HMGECs.[9,20,23]

Perspective on the role of TAGs in meibum and the human tear film

Likely owing to their structural complexity and lower abundance relative to some of the major lipid classes (e.g., wax esters and cholesteryl esters), TAGs, as a meibum lipid class, are largely understudied. Systemically, TAGs are known to be dense energy stores, vehicles for fatty acid mobilization through the vasculature, depots of fatty acids for intracellular lipid metabolism, and scavengers of free fatty acids to reduce oxidative

stress.[42] In the human tear film, however, little is known about their function. TAGs have been stated to comprise about 0.05% to 6% of the entire lipid pool in human meibum,[13-17] which begs the question of whether a minor lipid class with such low abundance could confer a structural role to the tear film lipid layer (TFLL). Granted, (O-acyl)-ω-hydroxy fatty acids (OAHFAs), accounting for just 0.69% to 3.1% of lipids in human meibum, are thought to be responsible for TFLL stability;[44-46] however, their amphipathic properties allow them the unique capacity to help form a monolayer at the aqueous-lipid interface to facilitate nonpolar lipid spreading.[47-49] Despite having some degree of polarity due to its glycerol backbone,[50] TAGs, overall, are regarded as nonpolar lipids and lack this amphipathic property. Indeed, they are capable of interacting with this polar lipid monolayer by intercalating two of their fatty acid chains with those of the polar layer, leaving its third chain embedded within the thicker, nonpolar lipid layer. Whether this preferential organization confers any structural effect, as previously proposed by McCulley and Shine, remains to be seen.[50] It could just be the natural positioning of a nonpolar lipid bearing very weak polar activity seeking to minimize a variety of intermolecular forces.

Another hypothesis could link the unique structure of triacylglycerols (a glycerol backbone esterified to three fatty acids) with TFLL fluidity. Indeed, the structure of TAGs could interfere with ordered packing of other major lipid species, possibly decreasing TFLL viscosity. A greater proportion of TAGs relative to wax esters and cholesteryl esters would likely be needed to elicit such an important physiological role. Notably, cholesteryl esters have a five-fold increase in saturation compared to wax esters, conferring the ability to influence phase transition temperatures and meibum

viscosity.[12,51] This degree of saturation likely positions cholesteryl esters as a primary modulator of lipid layer viscosity in the tear film.[51]

It is possible that the presence of TAGs in the TFLL is a result of passive release rather than intentional secretion. Perhaps TAGs in the tear film represent spilled contents from the intracellular compartment of meibocytes during holocrine secretion. Our findings support that under circumstances of induced differentiation due to PPARγ activation by rosiglitazone, the fatty-acid profile of TAGs in HMGECs shifts toward the common end products of fatty acid synthesis (palmitic acid, FA 16:0) elongated and/or desaturated into oleic acid (FA 18:1), stearic acid (FA 18:0), linoleic acid (FA 18:2), and palmitoleic acid (FA 16:1). In vivo, we suggest that these fatty acids, which are in high demand in the lipid-producing meibocyte,[12,15] are bundled into TAGs and stored in lipid droplets until ultimately needed for processing (e.g., further elongation and/or desaturation) and assembly into other lipid molecules. While waiting in queue, the stimulus for holocrine secretion may be received, and the cell may dump these fatty acid depots into meibum, effectively serving as a timestamp of lipid metabolism at the point of holocrine secretion. Once secreted in the tear film, the TAGs likely have biological activity, but the activity conferred by each individual TAG species may be secondary to its primary role of serving as a fatty acid reservoir intracellularly. As such, the parent TAG molecule may have less relevance than its fatty-acid constituents. As the field continues to pivot toward a better understanding of the role of individual lipid classes in the tear film, attention should be given to not just the TAG parent identities (i.e., the sums of carbons and double bonds in the three fatty acyl chains) but also to their specific fatty acids.

Conclusions

In conclusion, this study reveals that the triacylglycerol lipidome produced by HMGECs is affected by culture conditions. Both serum and rosiglitazone are strong, yet opposing, modulators of TAG expression. Rosiglitazone tends to positively influence meibum-relevant, oleic acid-bearing TAGs; serum tends to negatively influence them. Culture duration, however, elicits a minor effect on a minority of TAGs and is deemed a low contributor, at least when evaluating relative TAG expression. To optimize HMGEC's ability to serve as a preclinical model, culturing with 50 μM rosiglitazone and 2% serum appears to promote a more meibum-like TAG (and cholesteryl ester[23]) profile. Additional work is needed to evaluate serum-free conditions on HMGEC differentiation. Lastly, we proposed the hypothesis that any function associated with TAGs in the TFLL may be incidental or perhaps secondary to its primary role, which may be to serve as a fatty acid depot in meibocytes. TAGs present in the TFLL may represent a snapshot of intracellular lipid metabolism and lipid storage at the time of holocrine secretion. This conjecture was reported as a perspective, rather than a research conclusion, and is an area ripe for further scientific inquiry.

Acknowledgments: The authors would like to acknowledge Dr. David Redden (University of Alabama at Birmingham) for lending his biostatistical expertise to this project and to Dr. David Sullivan (Schepens Eye Research Institute) for generously gifting the immortalized human meibomian gland epithelial cells.

Funding: This work was supported by the Office of Research Infrastructure Programs of the National Institutes of Health under S10 RR027822-01 and the National Eye Institute under K23 EY028629-01.

References

1. Liu S, Hatton MP, Khandelwal P, Sullivan DA. Culture, immortalization, and characterization of human meibomian gland epithelial cells. Invest Ophthalmol Vis Sci. 2010;51(8):3993-4005.

2. Khandelwal P, Liu S, Sullivan DA. Androgen regulation of gene expression in human meibomian gland and conjunctival epithelial cells. Mol Vis. 2012;18:1055-1067.

3. Sullivan DA, Liu Y, Kam WR, et al. Serum-induced differentiation of human meibomian gland epithelial cells. Invest Ophthalmol Vis Sci. 2014;55(6):3866-3877.

4. Liu Y, Kam WR, Ding J, Sullivan DA. Effect of azithromycin on lipid accumulation in immortalized human meibomian gland epithelial cells. JAMA Ophthalmol. 2014;132(2):226-228.

5. Liu Y, Ding J. The combined effect of azithromycin and insulin-like growth factor-1 on cultured human meibomian gland epithelial cells. Invest Ophthalmol Vis Sci. 2014;55(9):5596-5601.

6. Liu Y, Kam WR, Ding J, Sullivan DA. One man's poison is another man's meat: using azithromycin-induced phospholipidosis to promote ocular surface health. Toxicology. 2014;320:1-5.

7. Hampel U, Kruger M, Kunnen C, Garreis F, Willcox M, Paulsen F. In vitro effects of docosahexaenoic and eicosapentaenoic acid on human meibomian gland epithelial cells. Exp Eye Res. 2015;140:139-148.

8. Liu Y, Kam WR, Sullivan DA. Influence of Omega 3 and 6 Fatty Acids on Human Meibomian Gland Epithelial Cells. Cornea. 2016;35(8):1122-1126.

9. Kim SW, Xie Y, Nguyen PQ, et al. PPARgamma regulates meibocyte differentiation and lipid synthesis of cultured human meibomian gland epithelial cells (hMGEC). Ocul Surf. 2018;16(4):463-469.

10. Asano N, Hampel U, Garreis F, et al. Differentiation Patterns of Immortalized Human Meibomian Gland Epithelial Cells in Three-Dimensional Culture. Invest Ophthalmol Vis Sci. 2018;59(3):1343-1353.

11. Green-Church KB, Butovich I, Willcox M, et al. The international workshop on meibomian gland dysfunction: report of the subcommittee on tear film lipids and lipid-protein interactions in health and disease. Invest Ophthalmol Vis Sci. 2011;52(4):1979-1993.

12. Chen J, Green KB, Nichols KK. Quantitative profiling of major neutral lipid classes in human meibum by direct infusion electrospray ionization mass spectrometry. Invest Ophthalmol Vis Sci. 2013;54(8):5730-5753.

13. Chen J, Green-Church KB, Nichols KK. Shotgun lipidomic analysis of human meibomian gland secretions with electrospray ionization tandem mass spectrometry. Invest Ophthalmol Vis Sci. 2010;51(12):6220-6231.

14. Cory CC, Hinks W, Burton JL, Shuster S. Meibomian gland secretion in the red eyes of rosacea. Br J Dermatol. 1973;89(1):25-27.

15. Nicolaides N, Kaitaranta JK, Rawdah TN, Macy JI, Boswell FM, 3rd, Smith RE. Meibomian gland studies: comparison of steer and human lipids. Invest Ophthalmol Vis Sci. 1981;20(4):522-536.

16. McCulley JP, Shine W. A compositional based model for the tear film lipid layer. Trans Am Ophthalmol Soc. 1997;95:79-88; discussion 88-93.

17. Mathers WD, Lane JA. Meibomian gland lipids, evaporation, and tear film stability. Adv Exp Med Biol. 1998;438:349-360.

18. Ziemanski J, Chen J, Nichols KK. The effects of omega-6:omega-3 fatty acid ratios on the lipidome from human meibomian gland epithelial cells treated with and without 13-cis retinoic acid. ARVO; 2018; Honolulu, HI.

19. Hampel U, Schroder A, Mitchell T, et al. Serum-induced keratinization processes in an immortalized human meibomian gland epithelial cell line. PLoS One. 2015;10(6):e0128096.

20. Kim SW, Brown DJ, Jester JV. Transcriptome analysis after PPARgamma activation in human meibomian gland epithelial cells (hMGEC). Ocul Surf. 2019;17(4):809-816.

21. Janani C, Ranjitha Kumari BD. PPAR gamma gene--a review. Diabetes Metab Syndr. 2015;9(1):46-50.

22. Dozsa A, Dezso B, Toth BI, et al. PPARgamma-mediated and arachidonic acid-dependent signaling is involved in differentiation and lipid production of human sebocytes. J Invest Dermatol. 2014;134(4):910-920.

23. Material intended for publication: Ziemanski JF, Wilson L, Barnes S, Nichols KK. Saturation of cholesteryl esters produced by human meibomian gland epithelial cells after treatment with rosiglitazone. 2020.

24. Folch J, Lees M, Sloane Stanley GH. A simple method for the isolation and purification of total lipides from animal tissues. J Biol Chem. 1957;226(1):497-509.

25. Ziemanski J, Chen J, Nichols K. Evaluation of cell harvesting techniques to optimize lipidomic analysis from human meibomian gland epithelial cells in culture. International Journal of Molecular Sciences. 2020;21(3277):1-10.

26. Chen J, Nichols KK. Comprehensive shotgun lipidomics of human meibomian gland secretions using MS/MS(all) with successive switching between acquisition polarity modes. J Lipid Res. 2018;59(11):2223-2236.

27. Jester JV, Potma E, Brown DJ. PPARgamma Regulates Mouse Meibocyte Differentiation and Lipid Synthesis. Ocul Surf. 2016;14(4):484-494.

28. Knop E, Knop N, Millar T, Obata H, Sullivan DA. The international workshop on meibomian gland dysfunction: report of the subcommittee on anatomy, physiology, and pathophysiology of the meibomian gland. Invest Ophthalmol Vis Sci. 2011;52(4):1938-1978.

29. Brovkovych V, Aldrich A, Li N, Atilla-Gokcumen GE, Frasor J. Removal of Serum Lipids and Lipid-Derived Metabolites to Investigate Breast Cancer Cell Biology. Proteomics. 2019;19(18):e1800370.

30. Liu S, Kam WR, Ding J, Hatton MP, Sullivan DA. Effect of growth factors on the proliferation and gene expression of human meibomian gland epithelial cells. Invest Ophthalmol Vis Sci. 2013;54(4):2541-2550.

31. Ho ST, Tanavde VM, Hui JH, Lee EH. Upregulation of Adipogenesis and Chondrogenesis in MSC Serum-Free Culture. Cell Med. 2011;2(1):27-41.

32. Ichikawa J. Serum-free medium with osteogenic supplements induces adipogenesis in rat bone marrow stromal cells. Cell Biol Int. 2010;34(6):615-620.

33. Stetten D, Schoenheimer R. The Conversion of Palmitic Acid into Stearic and Palmitoleic Acids in Rats. J Biol Chem. 1940;133:329-345.

34. Butovich IA, Arciniega JC, Lu H, Molai M. Evaluation and quantitation of intact wax esters of human meibum by gas-liquid chromatography-ion trap mass spectrometry. Invest Ophthalmol Vis Sci. 2012;53(7):3766-3781.

35. Chen J, Green KB, Nichols KK. Compositional Analysis of Wax Esters in Human Meibomian Gland Secretions by Direct Infusion Electrospray Ionization Mass Spectrometry. Lipids. 2016;51(11):1269-1287.

36. Mead JR, Irvine SA, Ramji DP. Lipoprotein lipase: structure, function, regulation, and role in disease. J Mol Med (Berl). 2002;80(12):753-769.

37. Weisiger RA. Mechanisms of intracellular fatty acid transport: role of cytoplasmic-binding proteins. J Mol Neurosci. 2007;33(1):42-44.

38. Liu H, Liu JY, Wu X, Zhang JT. Biochemistry, molecular biology, and pharmacology of fatty acid synthase, an emerging therapeutic target and diagnosis/prognosis marker. Int J Biochem Mol Biol. 2010;1(1):69-89.

39. Varga T, Czimmerer Z, Nagy L. PPARs are a unique set of fatty acid regulated transcription factors controlling both lipid metabolism and inflammation. Biochim Biophys Acta. 2011;1812(8):1007-1022.

40. Wang CS, Hartsuck J, McConathy WJ. Structure and functional properties of lipoprotein lipase. Biochim Biophys Acta. 1992;1123(1):1-17.

41. Butovich IA, McMahon A, Wojtowicz JC, Lin F, Mancini R, Itani K. Dissecting lipid metabolism in meibomian glands of humans and mice: An integrative study reveals a network of metabolic reactions not duplicated in other tissues. Biochim Biophys Acta. 2016;1861(6):538-553.

42. Coleman RA, Mashek DG. Mammalian triacylglycerol metabolism: synthesis, lipolysis, and signaling. Chem Rev. 2011;111(10):6359-6386.

43. Hampel U, Garreis F. The human meibomian gland epithelial cell line as a model to study meibomian gland dysfunction. Exp Eye Res. 2017;163:46-52.

44. Chen J, Nichols KK, Wilson L, Barnes S, Nichols JJ. Untargeted lipidomic analysis of human tears: A new approach for quantification of O-acyl-omega hydroxy fatty acids. Ocul Surf. 2019;17(2):347-355.

45. Brown SH, Kunnen CM, Duchoslav E, et al. A comparison of patient matched meibum and tear lipidomes. Invest Ophthalmol Vis Sci. 2013;54(12):7417-7424.

46. Lam SM, Tong L, Reux B, et al. Lipidomic analysis of human tear fluid reveals structure-specific lipid alterations in dry eye syndrome. J Lipid Res. 2014;55(2):299-306.

47. Millar TJ, Schuett BS. The real reason for having a meibomian lipid layer covering the outer surface of the tear film - A review. Exp Eye Res. 2015;137:125-138.

48. Cwiklik L. Tear film lipid layer: A molecular level view. Biochim Biophys Acta. 2016;1858(10):2421-2430.

49. Butovich IA. Lipidomics of human Meibomian gland secretions: Chemistry, biophysics, and physiological role of Meibomian lipids. Prog Lipid Res. 2011;50(3):278-301.

50. McCulley JP, Shine WE. Meibomian gland function and the tear lipid layer. Ocul Surf. 2003;1(3):97-106.

51. Borchman D, Yappert MC, Milliner SE, et al. 13C and 1H NMR ester region resonance assignments and the composition of human infant and child meibum. Exp Eye Res. 2013;112:151-159.

CHAPTER FIVE: PROSTAGLANDIN E_2 AND F_{2A} ALTER EXPRESSION OF SELECT CHOLESTERYL ESTERS AND TRIACYLGLYCEROLS PRODUCED BY HUMAN MEIBOMIAN GLAND EPITHELIAL CELLS

by

JILLIAN F. ZIEMANSKI, LANDON WILSON, STEPHEN BARNES, KELLY K. NICHOLS

In preparation for *Current Eye Research*

Format adapted for dissertation

Abstract

Purpose: $PGF_{2\alpha}$ analogs are commonly used to treat glaucoma and have been linked to higher rates of meibomian gland dysfunction (MGD) in this patient population. The purpose of this study was to evaluate the physiological effects of $PGF_{2\alpha}$ and PGE_2 on cell viability and lipidomic expression of immortalized human meibomian gland epithelial cells (HMGECs).

Methods: HMGECs were immunostained for the four PGE_2 receptors (EP1, EP2, EP3, EP4) and the one $PGF_{2\alpha}$ receptor (FP) and imaged with a fluorescent microscope. To assess cell viability and evaluate differential lipid expression, HMGECs were differentiated by rosiglitazone for two days prior to exposing HMGECs to a broad range of $PGF_{2\alpha}$ and PGE_2 concentrations (10^{-9} to 10^{-6}) for three hours. Cell viability was assessed by an ATP-based luminescent assay, and lipid extracts were analyzed for cholesteryl esters (CEs), wax esters (WEs), and triacylglycerols (TAGs) by ESI-$MSMS^{ALL}$ in positive ion mode by a Triple TOF 5600 Mass Spectrometer (SCIEX, Framingham, MA) using SCIEX LipidView 1.3.

Results: HMGECs express three of the PGE_2 receptors (EP1, EP2, EP4) and the one $PGF_{2\alpha}$ receptor (FP). Neither PGE_2 nor $PGF_{2\alpha}$ showed signs of cytotoxicity at any of the physiologic concentrations tested. WEs were not detected from any of the samples, but CEs and TAGs both exhibited a diverse and dynamic profile with respect to prostaglandin supplementation. PGE_2 suppressed select meibum-relevant CEs (CE 22:1,

CE 26:0, CE 28:1, CE 30:1). $PGF_{2\alpha}$ dose dependently increased several meibum-relevant CEs (CE 20:2, CE 20:1, CE 22:1, CE 24:0) yet decreased others. Both prostaglandins led to nonspecific TAG remodeling.

Conclusion: PGE_2 and $PGF_{2\alpha}$ do not affect HMGEC viability at physiologic concentrations. $PGF_{2\alpha}$ influences lipid expression greater than PGE_2 and may do so by interfering with meibocyte differentiation. This work may provide insight into the mechanism of meibomian gland dysfunction development in glaucoma patients treated with $PGF_{2\alpha}$ analogs.

Introduction

There are greater than 64.3 million people between the ages of 40 and 80 who suffer from glaucoma worldwide.[1] Up to 80 percent, more than 50 million of these patients, may also have concurrent meibomian gland dysfunction (MGD).[2] This number is even more alarming when considering that ocular surface diseases, such as MGD, may exacerbate glaucoma by interfering with intraocular pressure (IOP) reduction and/or surgical outcomes.[3,4] Aggressive management of glaucoma-associated MGD with both oral and topical medications has shown to improve not only the signs and symptoms of MGD, but also IOP management.[3] The mechanism that underlies the onset of MGD in glaucoma patients is not fully understood, but there is strong evidence that the medical management of glaucoma is culpable.[2,3,5-13]

Prostaglandin analogs (PGAs), which are primarily $PGF_{2\alpha}$ analogs, are a common first-line treatment in glaucoma patients, owing to their efficacy, affordability, convenient dosing schedule, and favorable systemic side effect profile.[14] Their therapeutic benefits

are thought to be mediated through the $PGF_{2\alpha}$ FP receptor, a seven transmembrane G-protein coupled receptor.[15,16] Upon ligand binding, the FP receptor induces a calcium-dependent chloride current, as well as accumulation of inositol triphosphate.[17,18] Signaling through FP receptors promotes upregulation of several matrix metalloproteinases capable of degrading the extracellular matrix.[19] This mechanism is largely credited for the FP receptor's favorable effect on IOP: a degraded extracellular matrix of the ciliary body reduces aqueous humor outflow resistance, permits increased outflow, and ultimately lowers the IOP.[15,19]

Unlike the minimal adverse effects observed systemically, the ocular side effects of PGAs are numerous and may be partly mediated through crossover binding to other prostaglandin receptors, such as those for PGE_2 (EP1, EP2, EP3, and EP4).[14] The PGA side effects consist of redness, burning, itching, pigmentation changes, and eyelash growth, among several others.[14] More recently, development and/or progression of MGD has also been associated with chronic PGA use.[12] The mechanism, though currently unknown, is likely related to pathologic changes induced by the topical application of both the PGA and its preservative system. One hypothesis is that the increase in MGD may be due to an alteration in the secretions from the meibomian gland secondary to stimulation by PGAs.[20]

The meibomian glands produce a lipid-rich fluid, termed meibum, that spreads across the ocular surface to form the tear film lipid layer.[21] Meibum is comprised mostly of nonpolar lipids with significant contributions provided by the hydrophobic wax esters (WEs, 48 percent) and cholesteryl esters (CEs, 40 percent).[22,23] Another nonpolar lipid class, triacylglycerols (TAGs), is of less abundance, ranging between 0.05 to 6 percent,[24-

[28] but preliminary work has suggested that several TAGs are upregulated in a preclinical model of MGD[29] that uses the same human meibomian gland epithelial cell line (HMGEC) as in this study. We have previously described the CE and TAG profiles from differentiated HMGECs;[30,31] WE expression from these cells, however, appears to be minimal or undetectable.[32-35] As the only human meibocyte cell line available, this HMGEC model was used to better understand the outcomes provoked by PGE_2 and $PGF_{2\alpha}$ on the differential expression of CEs, WEs, and TAGs. We hypothesize that HMGECs undergo a shift in their lipid expression following supplementation with PGE_2 and $PGF_{2\alpha}$ and that these lipidomic alterations are likely mediated through prostaglandin receptors found on HMGECs.

Methods

Reagents and Materials

Rosiglitazone, PGE_2, and $PGF_{2\alpha}$ were purchased from Cayman Chemical (Ann Arbor, MI). Stock solutions were made by dissolving each compound in sterile-filtered dimethyl sulfoxide (DMSO, Hybri-Max™, Sigma-Aldrich, St. Louis, MO) and stored under nitrogen at -20°C. Rosiglitazone, PGE_2, and $PGF_{2\alpha}$ were added fresh to media preparations just prior to each experiment. DMSO concentration was maintained at 0.5% in all samples. Falcon 8-well chambered cell culture slides were used for immunocytochemistry and purchased from ThermoFisher (Waltham, MA). Clear-bottom, white-walled 96-well plates were used for luminescent cell viability assays and were also purchased from ThermoFisher (Waltham, MA). Glass petri dishes were used for lipidomics experiments and were purchased from Sigma Aldrich (St. Louis, MO).

Immunocytochemistry

HMGECs were cultured on 8-well chambered slides and maintained in proliferating conditions consisting of KSFM with 5 ng/ml epidermal growth factor (EGF) and 50 µg/ml bovine pituitary extract. Media changes were performed every other day until 80 to 90% confluence when the culture media was changed to DMEM/F12 with 10 ng/ml EGF, 2% fetal bovine serum (FBS), and 50 µM rosiglitazone. After 24 hours, HMGECs were fixed in freshly prepared PBS containing 4% paraformaldehyde for 10 mins at room temperature, followed by four consecutive wash cycles. Fixed HMGECs were blocked with PBS containing 10% goat serum (ThermoFisher, Waltham, MA), 1% bovine serum albumin (BSA), and 0.3% Triton-X 100 for 30 mins on ice, then washed four times. Blocked HMGECs were incubated at room temperature for one hour in a humidified chamber with a rabbit polyclonal antibody against one of the following receptors: EP1, EP2, EP3, EP4, or FP. All primary antibodies were purchased from Thermo-Fisher and diluted 1:50 in PBS with 1% BSA and 0.3% Triton-X 100. Following four wash cycles, HMGECs were incubated with goat anti-rabbit IgG (ThermoFisher, Waltham, MA) conjugated to Alexa Fluor Plus 555 for one hour in the dark (1:500 dilution in PBS with 1% BSA and 0.3% Triton-X 100). Each slide was mounted with mounting media consisting of DAPI counterstain, 70% glycerol, 10% n-propyl gallate, and 20% PBS. Slides were imaged with a Zeiss Axioplan 2 Fluorescent Microscope (Jena, Germany). Images were captured with a 40x objective at a z-step of 0.4 µm. To optimize signal-to-noise ratios, laser intensities were set at 25% and 75% and exposure times at 250 ms and 1500 ms for the channels exciting DAPI and Alexa Fluor Plus 555, respectively. Image stacks were corrected for chromatic aberration and crosstalk and

deconvolved with Huygens Professional Software v19.10 (Scientific Volume Imaging, Hilversum, North Holland, Netherlands). All wash cycles consisted of a five-minute period on a shaker at 50 rpm. All experiments consisted of two experimental replicates and two technical replicates.

Cell viability

HMGECs were grown to 80 to 90% confluence and then split at a density of 30,000 cells per well in 96-well plates. All cells were differentiated for 48 hours in DMEM/F12 with 10 ng/ml EGF, 2% FBS, and 50 µM rosiglitazone. PGE_2- or $PGF_{2\alpha}$-containing media (10^{-9}, 10^{-8}, 10^{-7}, and 10^{-6} M) were added to HMGECs and allowed to incubate for three hours. Following incubation, cell viability was assessed using the Cell Titer-Glo Luminescent Cell Viability Assay (Promega, Madison, WI) according to the manufacturer's instructions. Luminescence was quantified using the Wallac Perkin-Elmer 1420-041 Victor2 Multiplate Multifluorescence Reader (Mt. Waverly, Victoria, Australia) over an acquisition time of one second. All experiments were performed with two experimental replicates and three technical replicates.

Lipid extraction and analysis by mass spectrometry

HMGECs were seeded at one million cells per 6-cm glass petri dish in differentiation media consisting of DMEM/F12 with 10 ng/ml EGF, 2% FBS, and 50 µM rosiglitazone for two days. Following incubation, HMGECs were exposed to PGE_2 or $PGF_{2\alpha}$ (10^{-8}, 10^{-7}, or 10^{-6} M) for three hours. Lipids were extracted using a recently described modification of the Folch technique optimized to efficiently extract lipids from

cultured HMGECs.[32,36] Briefly, 3 ml of pre-chilled chloroform-methanol (2:1 v/v, -20°C) were added directly to the HMGECs, which were then scraped with a sterile stainless steel scraper. The suspension was then transferred to a glass vial where 0.75 ml of molecular biology-grade water containing ammonium acetate (50 mM) was added. The emulsion was shaken at 350 rpm for 20 mins on ice and centrifuged at 1600 xg for five mins to promote stratification. The lower nonpolar phase was withdrawn and stored at -80°C until analysis. All steps involving organic solvents were performed with glass, stainless steel, or polytetrafluoroethylene (PTFE). All experiments were performed with two experimental replicates and two technical replicates.

Untargeted lipidomics was performed on dried lipids using a SCIEX Triple TOF 5600 Mass Spectrometer (SCIEX, Framingham, MA) in positive ion mode via direct infusion. The direct infusion solvent was methanol-chloroform (2:1) with 5 mM ammonium acetate. Each sample was delivered to the source by isocratic flow at 7 µl/min using a 500 µl Hamilton Gas Tight Syringe (Reno, NV). Prior to and after each sample, the syringe was cleaned with two flushes each of 100% methanol, 100% acetonitrile, 100% isopropyl alcohol, and 100% direct infusion solvent. Calibration runs were performed in positive mode with the APCI Positive Calibration Solution (SCIEX, Framingham, MA). The analyte mass evaluation range was 200 to 1200 *m/z*. A high-resolution time-of-flight (TOF) scan was acquired initially for 250 ms, then a series of high-sensitivity product ion scans were acquired per one Dalton (1 *m/z*) mass starting at 200 *m/z* through 1200 *m/z*. The collision energy was fixed at 35 eV, curtain gas to 20.00, GS1 to 20.00, GS2 to 15.00, spray voltage to 5000 volts, and interface temperature to 400°C. The acquisition time per sample was six minutes.

The acquired mass spectrometry data were processed with SCIEX LipidView 1.3 software (Framingham, MA). Lipid identities were assigned by LipidView, which utilizes a database of known ion fragmentations. To confirm selected lipid identities, SCIEX PeakView 2.2 was used to further investigate fragments. The mass tolerance window was set to 5 mDa, and the peaks greater than a signal-to-noise ratio of three were considered for analysis. Identification of individual lipid species from LipidView assignments was based on mass accuracy (<5 ppm) and MS/MS spectra obtained from PeakView.

Data analysis

For mass spectrometry data, CEs, WEs, and TAGs were the predominant focus of this study. To be included in the analysis, a given lipid species had to be present in all replicates of all conditions. Each lipid was normalized to the sum intensity per class and reported as percent of the overall class. For TAGs, only those that were present at a threshold concentration of 0.1% were included. All data for both cell viability and lipidomics were analyzed by one-way ANOVA with Tukey post-hoc testing (SPSS v26, Armonk, NY) when tests of normality (Kolmogorov-Smirnov) and homogeneity of variance (Levene's Test) were satisfied. If the assumption of equal variance was violated, then Games-Howell post-hoc testing was used. If the assumption of normality was violated, then the non-parametric Kruskal Wallis test was used. A p-value of 0.05 was considered significant.

The labeling convention for CEs consists of two numbers, separated by a colon. The two numbers represent the numbers of carbons and double bonds, respectively, in the fatty acyl chain. For some species, a third number is present, which denotes that the CE

has been oxidized with the specified number of oxygenations. Each parent TAG is identified similarly by the total numbers of carbons and double bonds in the three fatty acyl chains. Following each TAG, however, is a product ion, either a fatty acid (FA) or another TAG, which is labeled similarly. This notation represents that the LipidView software identified a neutral loss corresponding to that specific fatty acid or TAG. As an example, TAG 54:3 (FA 18:1) is a TAG that has 54 total carbons and three total double bonds among its fatty acyl chains, where one of those chains consists of 18 carbons and one double bond.

Results

Expression of FP- and EP-type receptors

HMGECs were immunostained against the four PGE_2 receptors (EP1, EP2, EP3, and EP4) and the one $PGF_{2\alpha}$ receptor (FP) and imaged by fluorescent microscopy. Positive signal (pseudocolored red) was observed for EP1, EP2, EP4, and FP receptors (Figure 1). There was no appreciable EP3 signal above background.

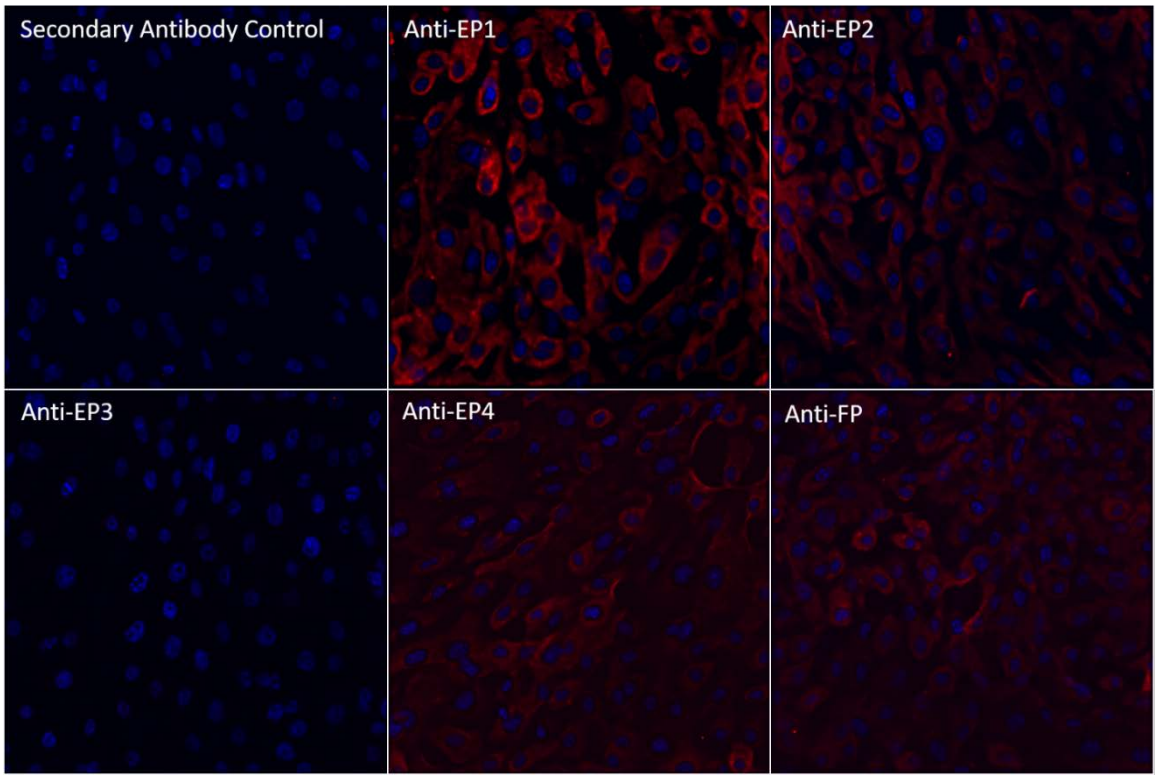

Figure 1 EP- and FP-type Receptor Expression on HMGECs
Fluorescent microscopy images (40x) of HMGECs stained with primary antibodies against PGE_2 (EP1, EP2, EP3, or EP4) or $PGF_{2\alpha}$ (FP) receptors and counterstained with DAPI (blue) after 24 hours of culture in differentiation media containing DMEM/F12, 10 ng/ml EGF, 2% FBS, and 50 µM rosiglitazone. Positive signal for each primary antibody (pseudocolored red) was detected for EP1, EP2, EP4, and FP receptors.
PGE_2: prostaglandin E_2
$PGF_{2\alpha}$: prostaglandin $F_{2\alpha}$

Influence of prostaglandins on cell viability

To determine whether PGE_2 or $PGF_{2\alpha}$ affects cell viability of differentiated HMGECs, ATP was quantitated from HMGECs exposed to 10^{-9}, 10^{-8}, 10^{-7}, and 10^{-6} M PGE_2 or $PGF_{2\alpha}$ for three hours. As shown in Figure 2, none of the PGE_2 concentrations ($p = 0.20$) or $PGF_{2\alpha}$ concentrations ($p = 0.82$) reduced viability compared to the vehicle control. Further, there were no differences in viability between any of the PGE_2 and

$PGF_{2\alpha}$ concentrations (p = 0.32). The cytotoxic detergent Triton-X 100 (1%) served as a positive control and strongly reduced viability.

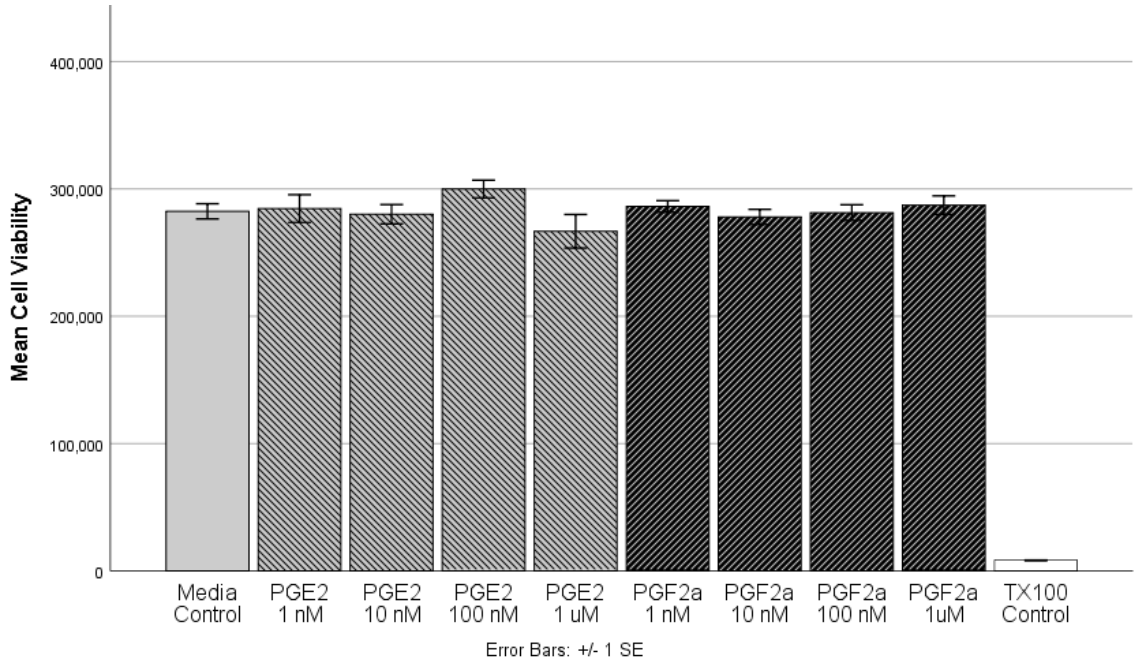

Figure 2 Effects of Prostaglandins on HMGEC Viability
HMGECs were differentiated for two days (see Methods) prior to exposure to PGE_2 or $PGF_{2\alpha}$ for three hours. After incubation, cell viability was assessed with a luminescent ATP-based assay. There were no significant differences between the vehicle control and any of the PGE_2 or $PGF_{2\alpha}$ concentrations. Further there were no differences between PGE_2 or $PGF_{2\alpha}$. Triton-X 100 (1%) was used as a positive control, which differed significantly from all other concentrations ($p < 0.001$). n = 6 per condition
HMGEC: human meibomian gland epithelial cell
PGE_2: prostaglandin E_2
$PGF_{2\alpha}$: prostaglandin $F_{2\alpha}$

Description of the CE and TAG profiles across all samples

This study focused on the expression of CEs, WEs, and TAGs. Although WEs were not detected among any of the samples in this study, CEs and TAGs were. There were 107 CEs detected across all samples; however, only 39 met the criteria for inclusion

in the analysis (Figure 3). The chain length varied from 11 carbons to 32 carbons, and the double-bond count varied from zero to five. Six CEs were found to be oxidized. The most abundant CE was CE 18:1. Very long-chain ($20 \leq$ carbon number $[n_c] \leq 25$) and ultra long-chain CEs ($n_c \geq 26$) were present from all conditions and comprised 26.2% and 6.9% of the overall CE pool, respectively. Of the 39 CEs, nine were saturated, 15 were monounsaturated, and 15 were polyunsaturated. Monounsaturated CEs were the most abundant (51.1%), followed by polyunsaturated (28.4%) and saturated (20.5%).

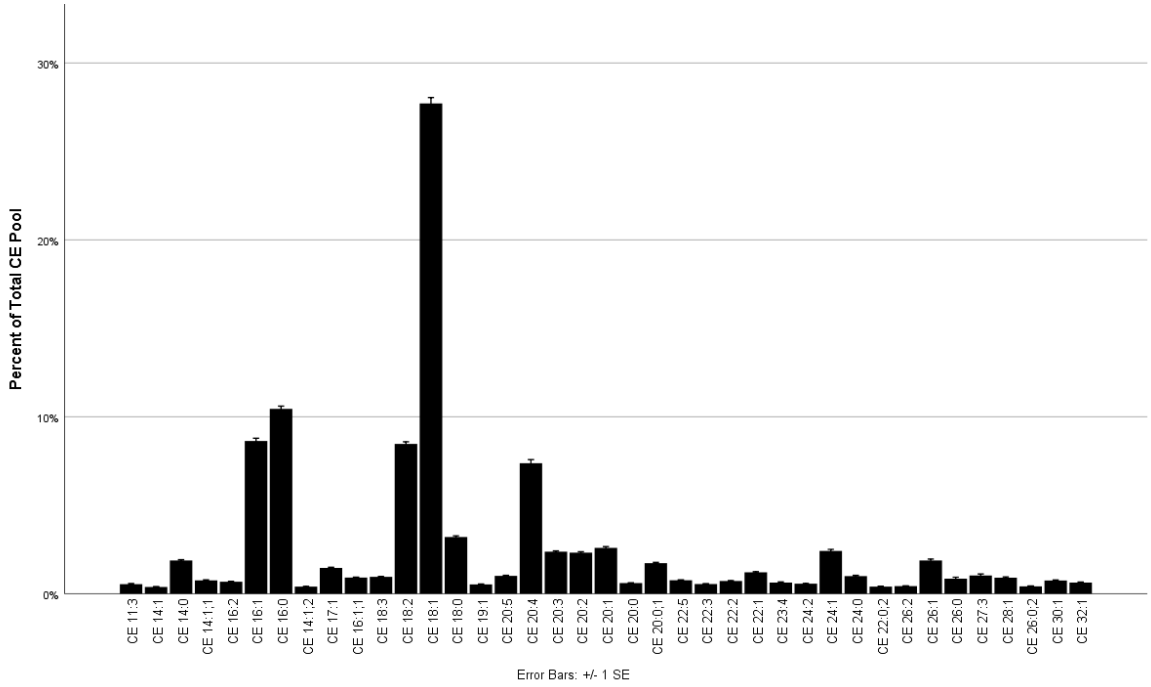

Figure 3 Description of HMGEC CE Lipidome
HMGECs expressed 39 unique CEs, including 6 oxidized CEs (oxCEs). CE 18:1 was the most abundant, followed by CE 16:0. The chain length varied from 11 carbons to 32 carbons. The double-bond count ranged from zero to five. CEs are labeled by carbon number and double-bond count, respectively. When a third number is present, it denotes an oxCE with the corresponding number of oxygenations. n = 28
HMGEC: human meibomian gland epithelial cell
CE: cholesteryl ester

There were 3,706 TAGs detected across all samples; however, only 145 met the criteria for inclusion in the analysis. The total carbon count from the three acyl chains, excluding the glycerol backbone, ranged from 44 to 72 with the majority (137/145, 94.5%) falling within the range of 46 to 56 (Figure 4A). All expressed TAGs consisted of an even carbon count (145/145, 100%). The number of double bonds in the acyl chains of the TAGs varied from zero to 12. Very few TAGs were fully saturated (7/145, 4.8%). The degree of unsaturation followed a bimodal distribution (Figure 4B) that was heavily weighted toward a lower degree of unsaturation. TAGs were primarily of lower unsaturation (106/145, 73.1%, one to five double bonds) or of higher unsaturation (22/145, 15.2%, eight to ten double bonds). Only five of 145 (3.4%) had a moderate degree of unsaturation (six or seven double bonds) or a very high degree of unsaturation (11 or 12 double bonds). The LipidView 1.3 software identified the neutral loss of 16 unique fatty acyl chains from the 145 TAGs (Figure 4C). Their individual carbon counts varied from 12 to 26 with double bonds ranging from zero to 4. Similar to the parent TAG molecules, all fatty acyl chains consisted exclusively of even numbers of carbons. The most frequently observed fatty acyl group was oleic acid (FA 18:1), which was present in 23 of 145 TAGs (15.9%). The second most common was palmitic acid (FA 16:0) and palmitoleic acid (FA 16:1), which were each present in 15 (10.3%) TAGs. Several TAGs (18/145, 12.4%) consisted of very long-chain fatty acids (at least 20 carbons).

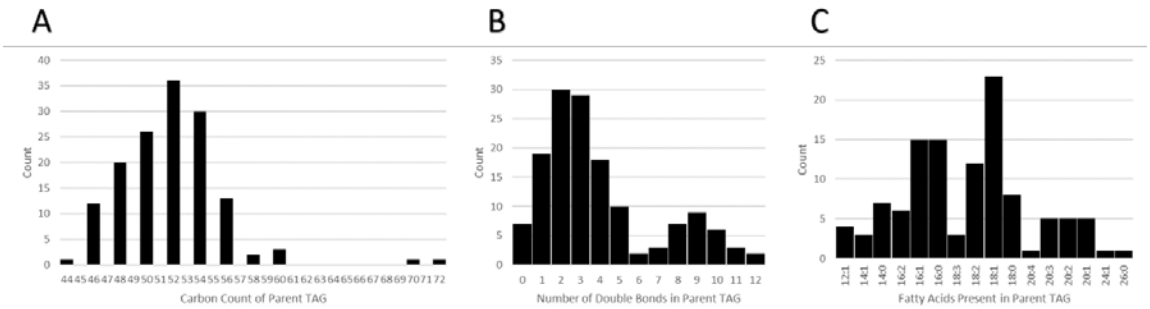

Figure 4 Description of the HMGEC TAG Lipidome
HMGECs expressed 145 TAGs that met the criteria for analysis (see Methods). The carbon count varied from 44 to 72 (A), and the double-bond count varied from zero to 12 (B). LipidView 1.3 detected the neutral loss of 16 unique fatty acyl chains from the parent TAGs. FA 18:1 was the most frequently observed. n = 28
HMGEC: human meibomian gland epithelial cell
TAG: triacylglycerol
FA: fatty acid

Influence of $PGF_{2\alpha}$ on CE and TAG expression

To determine the effects of $PGF_{2\alpha}$ on CE expression, lipid extracts from differentiated HMGECs were exposed to 10^{-8}, 10^{-7}, and 10^{-6} M $PGF_{2\alpha}$ for three hours. Of the 39 CEs analyzed, expression of seven CEs was significantly different among the concentrations (Figure 5). CE 14:1 and CE 26:0 were suppressed relative to control at all tested concentrations of $PGF_{2\alpha}$, though the 10^{-6} M concentration failed to reach significance for both CEs. One oxidized CE (CE 26:0;2) reached significance, showing a decrease in expression at higher $PGF_{2\alpha}$ concentrations. The remaining 4 CEs (CE 20:2, CE 20:1, CE 22:1, and CE 24:0) demonstrated a dose-dependent increase in expression among the three $PGF_{2\alpha}$ concentrations; however, the low-dose $PGF_{2\alpha}$ suppressed expression relative to the vehicle control.

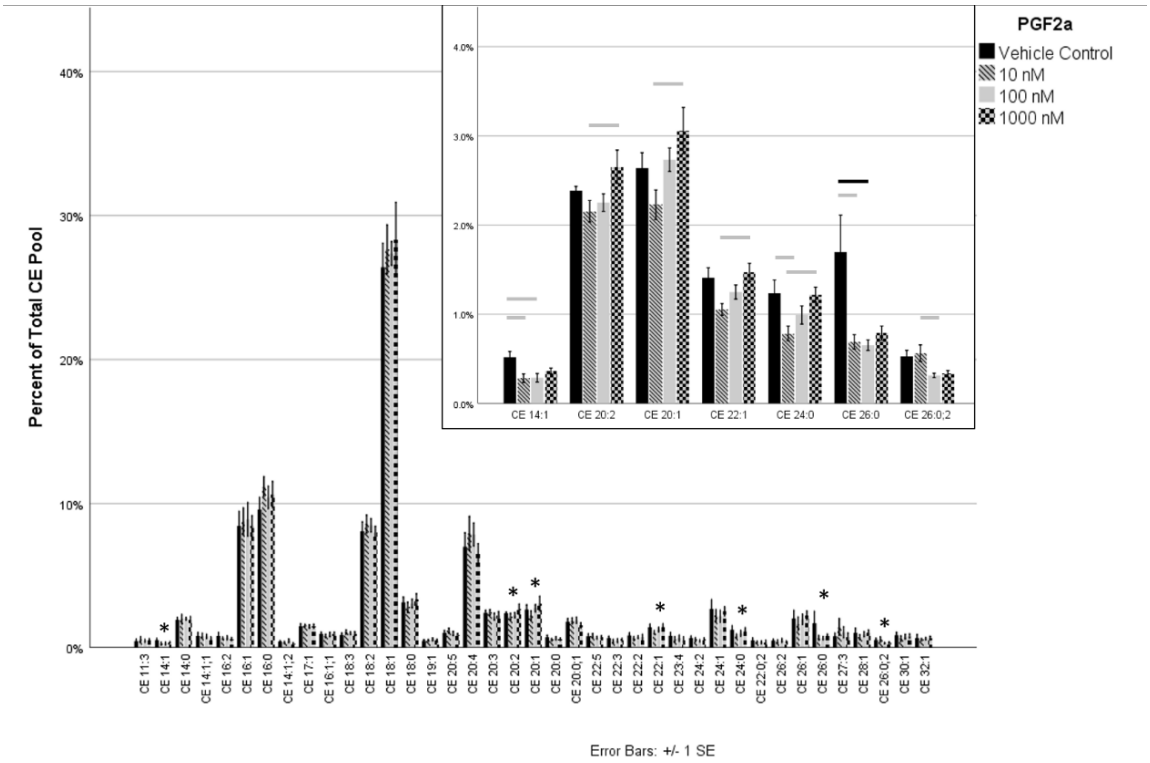

Figure 5 Effect of $PGF_{2\alpha}$ on the CE Lipidome
HMGECs were differentiated for two days (see Methods) prior to exposure to $PGF_{2\alpha}$ for three hours. Lipid extracts were analyzed by mass spectrometry, and 39 CEs met the criteria for analysis. Seven of the 39 varied significantly with $PGF_{2\alpha}$ supplementation (inset). All significant CEs were reduced with low-dose $PGF_{2\alpha}$; however, four of these CEs demonstrated a dose-dependent relationship with $PGF_{2\alpha}$. CEs are labeled by carbon number and double-bond count, respectively. When a third number is present, it denotes an oxCE with the corresponding number of oxygenations. n = 4 per condition
* denotes significance
gray bar $p \leq 0.05$, black bar $p \leq 0.01$
HMGEC: human meibomian gland epithelial cell
CE: cholesteryl ester
oxCE: oxidized cholesteryl ester

Twenty-three of 145 TAGs showed statistically significant differences in expression among the different $PGF_{2\alpha}$ concentrations (Figure 6). Four of the 23, however, failed to reach significance in pairwise comparisons: TAG 48:1 (FA 16:1), TAG 50:2 (FA 16:1), TAG 52:9 (TAG 35:2), and TAG 56:2 (FA 18:1). Six of the 23 were

upregulated across all concentrations: TAG 48:2 (FA 18:1), TAG 54:2 (FA 18:2), TAG 54:3 (FA 20:2), TAG 56:4 (FA 20:2), TAG 48:2 (FA 14:0), and TAG 52:3 (FA 20:2). Two were decreased across all concentrations: TAG 50:9 (TAG 33:1) and TAG 54:10 (TAG 35:2). Seven were upregulated at low-dose $PGF_{2\alpha}$ but reduced at higher doses, including all of the FA 12:1-containing TAGs: TAG 46:2 (FA 12:1), TAG 46:3 (FA 12:1), TAG 48:2 (FA 12:1), TAG 48:3 (FA 12:1), TAG 48:6 (TAG 36:1), TAG 48:7 (TAG 36:1), and TAG 48:11 (TAG 36:2). The remaining four TAGs were reduced at low-dose $PGF_{2\alpha}$ but upregulated at higher doses: TAG 48:1 (FA 14:0), TAG 48:1 (FA 16:0), TAG 48:1 (FA 18:1), and TAG 50:0 (FA 18:0).

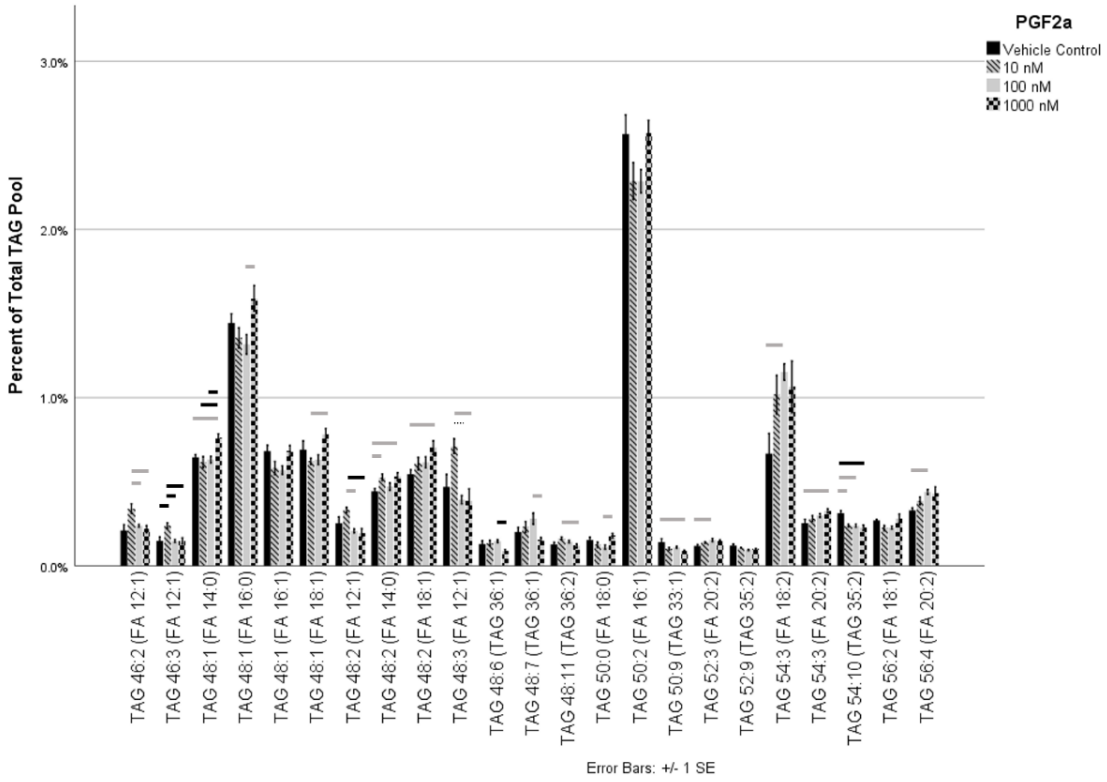

Figure 6 Effect of $PGF_{2\alpha}$ on HMGEC TAG Lipidome
HMGECs were differentiated for two days (see Methods) prior to exposure to $PGF_{2\alpha}$ for three hours. Lipid extracts were analyzed by mass spectrometry, and 145 TAGs met the criteria for analysis. To aid legibility, only the 23 that varied significantly with $PGF_{2\alpha}$ are displayed. Four of the 23 failed to reach significance in pairwise comparisons. $PGF_{2\alpha}$

promoted generalized TAG remodeling, affecting 15.9% of all analyzed TAGs. TAGs are labeled by two numbers corresponding to the total number of carbons and the total number of double bonds, respectively. The fatty acid in parentheses represents one of the three fatty acids of the parent TAG molecule. n = 4 per condition
gray bar $p \leq 0.05$, black bar $p \leq 0.01$, dashed bar $p \leq 0.001$
HMGEC: human meibomian gland epithelial cell
TAG: triacylglycerol
FA: fatty acid

Influence of PGE_2 on CE and TAG expression

To determine the effects of PGE_2 on CE expression, lipid extracts from differentiated HMGECs exposed to 10^{-8}, 10^{-7}, or 10^{-6} M PGE_2 for three hours were analyzed by mass spectrometry. Of the 39 CEs that met the inclusion criteria, four showed a statistically significant change in expression (Figure 7). A dose-dependent decrease was observed in CE 22:1 and CE 26:0. For CE 22:1, significance was achieved between the media control lacking PGE_2 and the 10^{-6} M concentration ($p = 0.01$). For CE 26:0, significance was achieved between the media control and both the 10^{-7} M and 10^{-6} M concentrations ($p = 0.01$ for both). CE 28:1 and CE 30:1 also reached significance, where the 10^{-6} M ($p = 0.02$) and 10^{-7} M ($p = 0.04$) concentrations, respectively, were decreased relative to 10^{-8} M PGE_2.

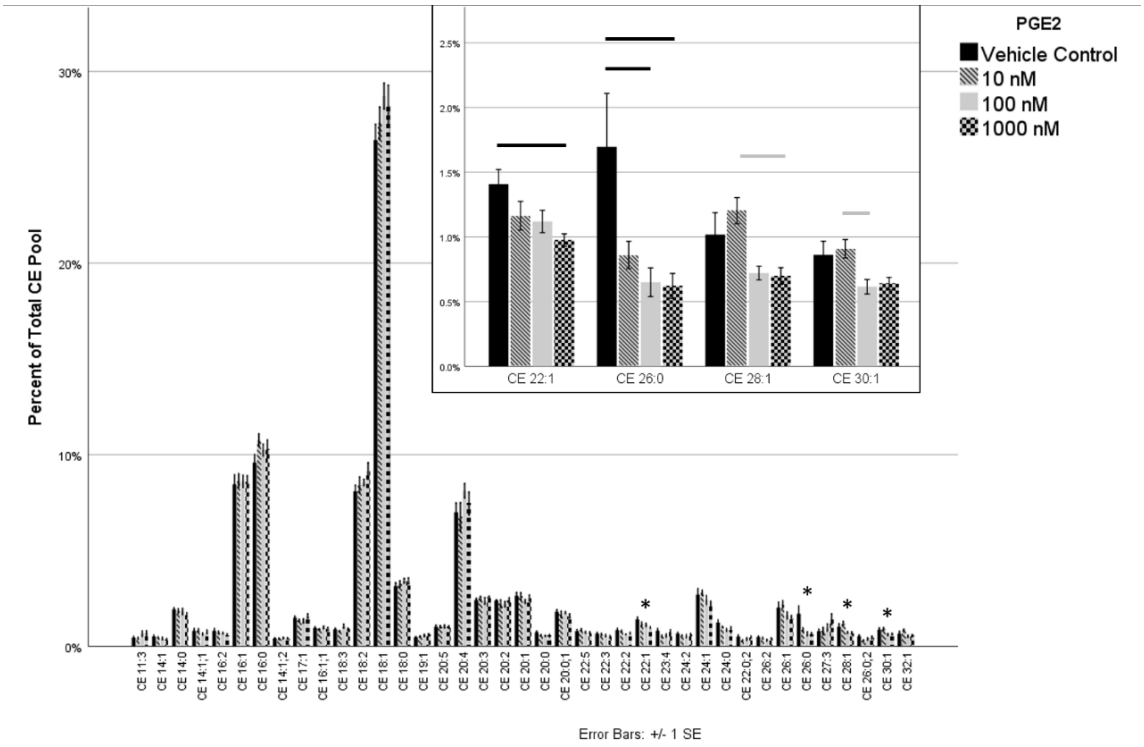

Figure 7 Effect of PGE_2 on HMGEC CE Lipidome
HMGECs were differentiated for two days (see Methods) prior to exposure to PGE_2 for three hours. Lipid extracts were analyzed by mass spectrometry, and 39 CEs met the criteria for analysis. Four of the 39 varied significantly with PGE_2 supplementation (inset), and all were reduced with increased PGE_2 concentrations. CEs are labeled by carbon number and double-bond count, respectively. When a third number is present, it denotes an oxCE with the corresponding number of oxygenations. n = 4 per condition
* denotes significance
gray bar $p \leq 0.05$, black bar $p \leq 0.01$, dashed bar $p \leq 0.001$
HMGEC: human meibomian gland epithelial cell
CE: cholesteryl ester
oxCE: oxidized cholesteryl ester

Only nine of 145 analyzed TAGs (6.2%) showed statistically significant differences in expression among the different PGE_2 concentrations (Figure 8). The remaining 136 (93.8%) did not vary significantly with respect to PGE_2. Two of the nine that were statistically significant, however, failed to reach significance in pairwise comparisons: TAG 48:3 (FA 12:1) and TAG 60:3 (FA 24:1). Two of the remaining seven

TAGs showed a dose-dependent increase in response to PGE_2: TAG 52:12 (TAG 34:0) and TAG 54:10 (TAG 35:2). TAG 54:10 (FA 16:1) and TAG 50:3 (FA 18:1) were elevated across all PGE_2 concentrations. TAG 54:5 (FA 18:1) appeared to have reduced expression across all PGE_2 concentrations. The remaining two TAGs that reached significance had varying degrees of expression among the different concentrations of PGE_2: TAG 48:0 (FA 16:0) and TAG 54:10 (TAG 38:3).

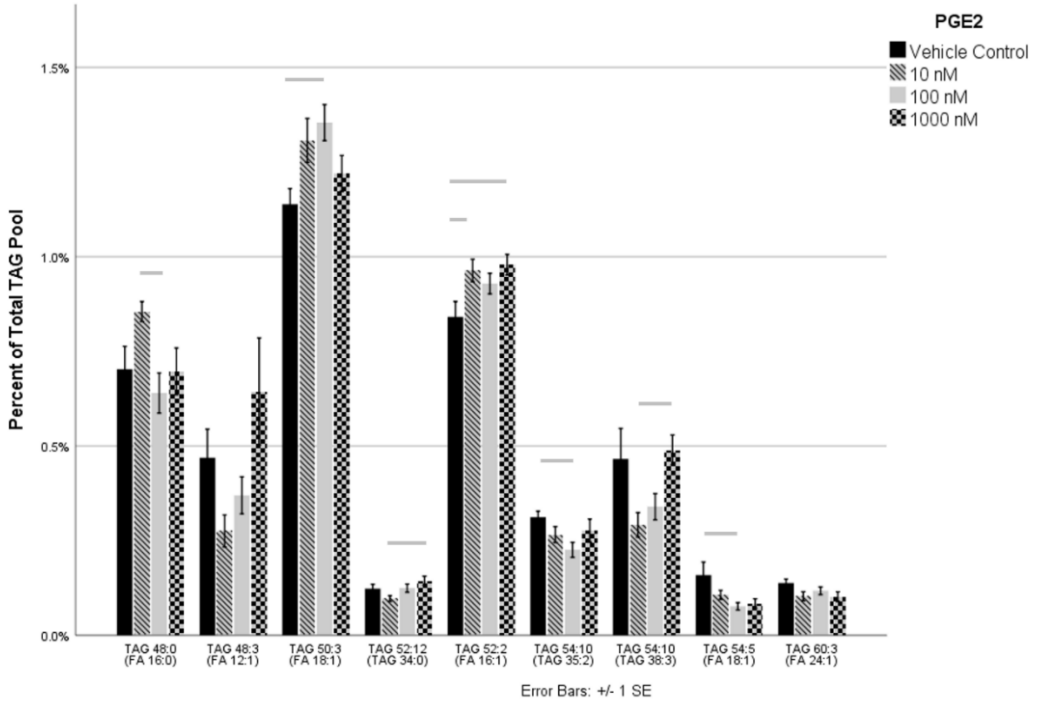

Figure 8 Effect of PGE_2 on HMGEC TAG Lipidome
HMGECs were differentiated for two days (see Methods) prior to exposure to PGE_2 for three hours. Lipid extracts were analyzed by mass spectrometry, and 145 TAGs met the criteria for analysis. To aid legibility, only the nine that varied significantly with PGE_2 are displayed. Two of the 9 failed to reach significance in pairwise comparisons. PGE_2 promoted generalized TAG remodeling. TAGs are labeled by two numbers corresponding to the total number of carbons and the total number of double bonds, respectively. The fatty acid in parentheses represents one of the three fatty acids of the parent TAG molecule. n = 4 per condition
gray bar $p \leq 0.05$
HMGEC: human meibomian gland epithelial cell
TAG: triacylglycerol
FA: fatty acid

Discussion

In light of growing awareness of the association between chronic PGA use in glaucoma and development of MGD,[2,12,20] the physiologic effects of PGE_2 and $PGF_{2\alpha}$ on HMGECs in culture were investigated. We report, for the first time, that HMGECs express three of the four PGE_2 receptors (EP1, EP2, and EP4) and the one $PGF_{2\alpha}$ receptor (FP). Across a broad range of physiologic concentrations (10^{-9} to 10^{-6} M), neither PGE_2 nor $PGF_{2\alpha}$ altered cell viability. Though their effects were not cytotoxic, the observed changes in the HMGEC lipidome suggest that prostaglandins, particularly $PGF_{2\alpha}$, affect lipid expression and/or metabolism. Much of this variation is consistent with general lipidomic remodeling, though specific patterns following $PGF_{2\alpha}$ exposure support the presence of multiple, competing pathways that appear to be concentration dependent. Taken together, these findings suggest that the meibomian glands express FP- and EP-type receptors, making them vulnerable to unwanted side effects associated with commercially available PGAs. Just one "dose" administered in this study, which was orders of magnitude less than commercially available formulations, modulated the lipid profile after only three hours. In vivo, lipidomic remodeling may translate into altered tear film lipid layer quality, accelerated tear evaporation, and/or poor tear film stability.

Expression of FP- and EP-type receptors

A notable advancement from this work is the discovery that HMGECs express FP receptors. This finding suggests that the meibomian gland could be added to the long list of other ocular and adnexal tissues known to express FP receptors: conjunctiva, cornea, sclera, iris, ciliary body, lens, retina, and optic nerve.[37-39] The FP receptor's role in

meibomian gland physiology is largely unknown, but in adipocytes and sebocytes, other cells optimized for high lipid turnover, signal transduction cascades that are initiated by FP binding ultimately inactivate PPARγ,[40] a known inducer of differentiation.[41,42] Recently, Kim et al. have shown that PPARγ regulates differentiation in HMGECs,[43,44] and we have found that most of the CEs and TAGs produced by HMGECs are highly modulated in response to PPARγ agonism.[30,31] Therefore, FP expression in the meibomian gland may have a direct yet adverse influence on cellular differentiation and nonpolar lipid production. Because $PGF_{2\alpha}$ is capable of binding EP receptors at 10^{-8} to 10^{-6} M affinities,[17] we were also interested in PGE_2 and the EP-type receptors. We found that HMGECs express EP1, EP2, and EP4 but not EP3 receptors, similar to the expression pattern reported in human sebocytes.[45] The effect of EP receptor engagement depends upon its exact EP subtype, the specific G protein it is coupled to, and its downstream signal transduction pathways,[46] a topic further discussed below.

Influence of prostaglandins on cell viability

Across all the concentrations tested in this study, neither PGE_2 nor $PGF_{2\alpha}$ affected HMGEC viability. Although some reports have linked PGE_2 to apoptosis by promoting calcium influx, these responses are typically at much higher PGE_2 concentrations—approximately 50 times greater than the highest concentration used in this study.[47,48] At physiologic concentrations, PGE_2 and $PGF_{2\alpha}$ have been shown to promote cell survival and/or inhibit apoptosis,[49-51] supporting our observation of sustained viability during the three-hour incubation with either prostaglandin. Although the exact concentrations of PGE_2 and $PGF_{2\alpha}$ are unknown in or near the meibomian glands, their concentrations have

been measured in the tear film. PGE_2 varies between 0.4 to 2.5 nM in normal patients and 0.5 to 7.7 nM in those with dry eye or MGD.[52-54] $PGF_{2\alpha}$ shows less disparity, averaging 1.0 nM in normals and 1.4 nM in MGD.[52] To account for potential differences in fluid concentrations versus tissue concentrations,[55] PGE_2 and $PGF_{2\alpha}$ concentrations were investigated in 10x increments from 1 nM to 1 μM. Even after incubating with the upper limit of physiologic concentrations of either prostaglandin, cell viability was not affected.

Influence of prostaglandins on lipid expression

Our results support that $PGF_{2\alpha}$ influences lipid expression, an outcome strongly influenced in HMGECs by cellular differentiation.[56,57] Nearly 18% of all expressed CEs and 16% of all expressed TAGs varied in response to $PGF_{2\alpha}$ supplementation. $PGF_{2\alpha}$ was associated with nonspecific changes in several TAG species, suggesting that it induces generalized TAG remodeling. Regarding CEs, however, more consistent patterns emerged. Low-dose $PGF_{2\alpha}$ (10^{-8} M) decreased expression of six of the seven statistically significant CEs compared to control. Despite this low-dose suppression, four of these six CEs (CE 20:2, CE 20:1, CE 22:1, and CE 24:0) increased thereafter in a dose-dependent fashion with $PGF_{2\alpha}$ (Figure 5). For this pattern to consistently emerge, we hypothesize that multiple, competing pathways that influence cellular differentiation and/or lipid synthesis are concurrently activated.

First, we believe that $PGF_{2\alpha}$ may be inducing a relative suppression of differentiation and thus reducing meibum-relevant lipid expression. Previous reports have not only shown that $PGF_{2\alpha}$ suppresses adipocyte differentiation but that it does so via the FP receptor.[58] The exact mechanism was later identified: FP binding activates MAP

kinase, which phosphorylates and inactivates PPARγ, preventing differentiation.[40] In our experimental model, HMGECs were differentiated with rosiglitazone, a PPARγ agonist, for two days prior to introducing $PGF_{2\alpha}$ for three hours. During that three-hour incubation, we believe that $PGF_{2\alpha}$ led to a heterogeneous mixture of both phosphorylated (inactive) and unphosphorylated (active) forms of PPARγ. $PGF_{2\alpha}$, therefore, would have effectively decreased the relative concentration of active PPARγ compared to rosiglitazone alone (control), leading to less transcription of lipogenic genes and less expression of lipids mediated by these gene products. If this were the only pathway at play, however, a dose-dependent decrease would have been observed across the remaining $PGF_{2\alpha}$ concentrations.

Instead, we observed an increase in four specific CEs and believe this effect may be related to the known opposing effects that different prostaglandins have on adipogenesis, all converging on PPARγ.[40] It is possible that the higher concentrations of $PGF_{2\alpha}$ may be stimulating a positive feedback loop, attempting to generate more prostaglandins by increasing expression of cyclooxygenases (COX). This autoregulatory loop has been described in other cell types.[59,60] COX catalyzes an early step in the prostaglandin production pathway, permitting the synthesis of the four main 2-series prostaglandins (and thromboxane), including PGD_2 that leads to PGJ_2.[40,61] PGD_2 and PGJ_2 have both been shown to potently activate PPARγ at a rate of approximately 80-fold and 20-fold, respectively.[62] This exact pathway ($PGF_{2\alpha}$-induced upregulation of PGD_2) has been described by Yousufzai and colleagues in iris and ciliary muscle.[63]

If these two pathways are occurring simultaneously, as hypothesized, a portion of PPARγ protein would be inactivated by $PGF_{2\alpha}$ and another portion activated by PGD_2

and PGJ_2. For this latter mechanism to explain the dose-dependent increase observed in our study, then PPARγ activation by PGD_2 and PGJ_2 must dominate over the relative PPARγ inhibition by $PGF_{2\alpha}$. To better interrogate these pathways, additional work is needed to isolate these mechanisms using receptor antagonists, COX inhibitors, and quantitative methods for other prostaglandins, PPARγ, and associated gene products.

The effects of PGE_2 on lipid expression were also assessed. PGE_2 led to a significant decrease in 10% of meibum-relevant CEs (CE 22:1, CE 26:0, CE 28:1, and CE 30:1) and significant remodeling of just 6% of TAGs. The role of PGE_2 on lipid synthesis is complex, yet its seemingly dichotomous effects may be explained by its diverse array of receptors. Some sources cite PGE_2 as an inhibitor of lipogenesis, which is mediated through the EP3 receptor.[64,65] Other sources credit PGE_2 for promoting lipogenesis and fat accumulation, an outcome attributed to EP2 and EP4 signaling.[66] Here, we did not detect EP3 expression on HMGECs, so the inhibitory effect of PGE_2 on lipogenesis may not exist in these cells. In the absence of this mechanism, it is currently unknown how PGE_2 induced the suppression of several meibum-relevant CEs in this study. Additional work is needed with receptor antagonists to determine which EPs are mediating this observation.

We detected the presence of six unique oxidized CEs (oxCEs) from our samples, only one of which (CE 26:0;2) varied significantly between low-dose and higher-dose $PGF_{2\alpha}$. None of the six oxCEs varied with respect to PGE_2. Lipid oxidation of the tears has been previously investigated by Borchman et al., who found that the degree of lipid oxidation is greater in normal subjects compared to those with MGD.[67] They further described these oxide moieties to be hydrophilic groups among hydrophobic regions,

interfering with lipid-lipid interactions and conferring increased fluidity to the overall lipid compartment. In simpler terms, a greater degree of oxidation decreases lipid order and promotes a more fluid secretion. In MGD, a lesser degree of oxidation increases lipid order and, thus, increases viscosity. The origin, mechanism of production, and significance of the oxCEs that were discovered from HMGECs remains to be explored.

Potential for $PGF_{2\alpha}$'s effects to translate to the ocular surface with dosing of anti-glaucoma PGAs

Our experiments were designed to identify changes in the lipidome and cell viability due to PGE_2 and $PGF_{2\alpha}$ after one exposure for three hours. It is currently unknown whether these changes in lipid expression are also produced by anti-glaucoma PGAs, but other researchers have begun investigating similar outcomes. Kam et al. first reported that bimatoprost adversely influences a marker of HMGEC survivability but that it has no effect on lipid production assessed by LipidTOX, a nonpolar lipid stain.[68] Unfortunately, the use of bimatoprost in this study complicates generalizability to other PGAs, as bimatoprost is technically a prostamide analog whose functions may or may not be mediated through the FP receptor.[14,69,70] More recently, Rath and colleagues evaluated several preserved and non-preserved formulations of PGAs on HMGECs.[71] They found that only latanoprost affected cell viability and that bimatoprost upregulated cornulin and involucrin mRNA, two keratins that may be upregulated in MGD.[71] This study reportedly used commercially available formulations of PGAs, though it was unclear how these eye drops were added to the cell culture media without affecting the original concentration of the PGAs and without diluting the components of the culture media itself. Regardless, it

is important to note that antiglaucoma PGAs are significantly more concentrated than the physiologic concentrations of $PGF_{2\alpha}$ that were used in this study. Specifically, commercially available latanoprost is approximately 100 times more concentrated than our highest dose of $PGF_{2\alpha}$; bimatoprost is about 240 to 720 times more concentrated. Ultimately, it remains unknown whether anti-glaucoma PGAs mimic the effects of $PGF_{2\alpha}$ observed here, what concentrations of PGAs reach the meibomian glands, or whether there are cumulative effects with daily instillation.

Conclusions

A perceived weakness of our study may be our decision to differentiate with rosiglitazone, a PPARγ agonist, considering that $PGF_{2\alpha}$ is known to influence PPARγ function. Previous research has shown that $PGF_{2\alpha}$ can block differentiation of adipocytes by inhibiting PPARγ if introduced in the first two days of treatment.[58] We, however, did not introduce the prostaglandins until two days after the initial exposure to differentiating conditions, allowing the cells to reach a more mature, differentiated state. Further, the decision to utilize rosiglitazone-induced differentiation is well-supported by literature that has more comprehensively defined and characterized its mechanism[30,31,43,44,72] compared to other differentiating agents,[33,73,74] reinforcing its use as a preferred method for HMGEC differentiation. Lastly, terminally differentiated meibocytes *in vivo* are believed to be under the influence of PPARγ regulation, so any interference by prostaglandins would likely translate into a similar interference that would occur at the ocular surface.[75]

In conclusion, we have reported that HMGECs express FP receptors and three EP receptors (EP1, EP2, and EP4), potentially making them vulnerable to undesirable side effects caused by the $PGF_{2\alpha}$ analogs used in clinical practice to treat glaucoma. Just one exposure to $PGF_{2\alpha}$, to an extent greater than PGE_2, led to lipidomic remodeling of HMGECs with significant changes observed in the expression of both CEs and TAGs. Alterations to the lipid chemistry of the meibomian gland secretions could affect the biochemical and biophysical interactions of the tear film lipid layer, potentially altering tear film viscosity and tear film stability. Further work is needed to determine how these observations translate to commercially available PGAs on the ocular surface.

Acknowledgments: The authors would like to thank Drs. Jose Luis Roig-Lopez and Steven Pittler for their assistance with immunocytochemistry, fluorescent microscopy, and image deconvolution.

Funding: This work was supported by the Office of Research Infrastructure Programs of the National Institutes of Health under S10 RR027822-01 and the National Eye Institute under P30 EY003039 and K23 EY028629-01.

References

1. Tham YC, Li X, Wong TY, Quigley HA, Aung T, Cheng CY. Global prevalence of glaucoma and projections of glaucoma burden through 2040: a systematic review and meta-analysis. Ophthalmology. 2014;121(11):2081-2090.

2. Uzunosmanoglu E, Mocan MC, Kocabeyoglu S, Karakaya J, Irkec M. Meibomian Gland Dysfunction in Patients Receiving Long-Term Glaucoma Medications. Cornea. 2016;35(8):1112-1116.

3. Batra R, Tailor R, Mohamed S. Ocular surface disease exacerbated glaucoma: optimizing the ocular surface improves intraocular pressure control. J Glaucoma. 2014;23(1):56-60.

4. Broadway DC, Grierson I, O'Brien C, Hitchings RA. Adverse effects of topical antiglaucoma medication. II. The outcome of filtration surgery. Arch Ophthalmol. 1994;112(11):1446-1454.

5. Ghosh S, O'Hare F, Lamoureux E, Vajpayee RB, Crowston JG. Prevalence of signs and symptoms of ocular surface disease in individuals treated and not treated with glaucoma medication. Clin Exp Ophthalmol. 2012;40(7):675-681.

6. Kim JH, Shin YU, Seong M, Cho HY, Kang MH. Eyelid Changes Related to Meibomian Gland Dysfunction in Early Middle-Aged Patients Using Topical Glaucoma Medications. Cornea. 2018;37(4):421-425.

7. Agnifili L, Brescia L, Oddone F, et al. The ocular surface after successful glaucoma filtration surgery: a clinical, in vivo confocal microscopy, and immune-cytology study. Sci Rep. 2019;9(1):11299.

8. Lee SM, Lee JE, Kim SI, Jung JH, Shin J. Effect of topical glaucoma medication on tear lipid layer thickness in patients with unilateral glaucoma. Indian J Ophthalmol. 2019;67(8):1297-1302.

9. Schwab IR, Linberg JV, Gioia VM, Benson WH, Chao GM. Foreshortening of the inferior conjunctival fornix associated with chronic glaucoma medications. Ophthalmology. 1992;99(2):197-202.

10. Liesegang TJ. Conjunctival changes associated with glaucoma therapy: implications for the external disease consultant and the treatment of glaucoma. Cornea. 1998;17(6):574-583.

11. Tauber J, Melamed S, Foster CS. Glaucoma in patients with ocular cicatricial pemphigoid. Ophthalmology. 1989;96(1):33-37.

12. Mocan MC, Uzunosmanoglu E, Kocabeyoglu S, Karakaya J, Irkec M. The Association of Chronic Topical Prostaglandin Analog Use With Meibomian Gland Dysfunction. J Glaucoma. 2016;25(9):770-774.

13. Cho WH, Lai IC, Fang PC, et al. Meibomian Gland Performance in Glaucomatous Patients With Long-term Instillation of IOP-lowering Medications. J Glaucoma. 2018;27(2):176-183.

14. Hollo G. The side effects of the prostaglandin analogues. Expert Opin Drug Saf. 2007;6(1):45-52.

15. Lindsey JD, Kashiwagi K, Boyle D, Kashiwagi F, Firestein GS, Weinreb RN. Prostaglandins increase proMMP-1 and proMMP-3 secretion by human ciliary smooth muscle cells. Curr Eye Res. 1996;15(8):869-875.

16. Breyer MD, Breyer RM. G protein-coupled prostanoid receptors and the kidney. Annu Rev Physiol. 2001;63:579-605.

17. Breyer RM, Bagdassarian CK, Myers SA, Breyer MD. Prostanoid receptors: subtypes and signaling. Annu Rev Pharmacol Toxicol. 2001;41:661-690.

18. Abramovitz M, Boie Y, Nguyen T, et al. Cloning and expression of a cDNA for the human prostanoid FP receptor. J Biol Chem. 1994;269(4):2632-2636.

19. Schachtschabel U, Lindsey JD, Weinreb RN. The mechanism of action of prostaglandins on uveoscleral outflow. Curr Opin Ophthalmol. 2000;11(2):112-115.

20. Cunniffe MG, Medel-Jimenez R, Gonzalez-Candial M. Topical antiglaucoma treatment with prostaglandin analogues may precipitate meibomian gland disease. Ophthalmic Plast Reconstr Surg. 2011;27(5):e128-129.

21. Green-Church KB, Butovich I, Willcox M, et al. The international workshop on meibomian gland dysfunction: report of the subcommittee on tear film lipids and lipid-protein interactions in health and disease. Invest Ophthalmol Vis Sci. 2011;52(4):1979-1993.

22. Chen J, Green KB, Nichols KK. Quantitative profiling of major neutral lipid classes in human meibum by direct infusion electrospray ionization mass spectrometry. Invest Ophthalmol Vis Sci. 2013;54(8):5730-5753.

23. Chen J, Nichols KK. Comprehensive shotgun lipidomics of human meibomian gland secretions using MS/MS(all) with successive switching between acquisition polarity modes. J Lipid Res. 2018;59(11):2223-2236.

24. Chen J, Green-Church KB, Nichols KK. Shotgun lipidomic analysis of human meibomian gland secretions with electrospray ionization tandem mass spectrometry. Invest Ophthalmol Vis Sci. 2010;51(12):6220-6231.

25. Nicolaides N, Kaitaranta JK, Rawdah TN, Macy JI, Boswell FM, 3rd, Smith RE. Meibomian gland studies: comparison of steer and human lipids. Invest Ophthalmol Vis Sci. 1981;20(4):522-536.

26. McCulley JP, Shine W. A compositional based model for the tear film lipid layer. Trans Am Ophthalmol Soc. 1997;95:79-88; discussion 88-93.

27. Cory CC, Hinks W, Burton JL, Shuster S. Meibomian gland secretion in the red eyes of rosacea. Br J Dermatol. 1973;89(1):25-27.

28. Mathers WD, Lane JA. Meibomian gland lipids, evaporation, and tear film stability. Adv Exp Med Biol. 1998;438:349-360.

29. Ziemanski J, Chen J, Nichols KK. The effects of omega-6:omega-3 fatty acid ratios on the lipidome from human meibomian gland epithelial cells treated with and without 13-cis retinoic acid. ARVO; 2018; Honolulu, HI.

30. Material intended for publication: Ziemanski JF, Wilson L, Barnes S, Nichols KK. Saturation of cholesteryl esters produced by human meibomian gland epithelial cells after treatment with rosiglitazone. 2020.

31. Material intended for publication: Ziemanski JF, Wilson L, Barnes S, Nichols KK. Triacylglycerol lipidome from human meibomian gland epithelial cells: description, response to culture conditions, and perspective on function. 2020.

32. Ziemanski JF, Chen J, Nichols KK. Evaluation of Cell Harvesting Techniques to Optimize Lipidomic Analysis from Human Meibomian Gland Epithelial Cells in Culture. Int J Mol Sci. 2020;21(9).

33. Sullivan DA, Liu Y, Kam WR, et al. Serum-induced differentiation of human meibomian gland epithelial cells. Invest Ophthalmol Vis Sci. 2014;55(6):3866-3877.

34. Liu S, Hatton MP, Khandelwal P, Sullivan DA. Culture, immortalization, and characterization of human meibomian gland epithelial cells. Invest Ophthalmol Vis Sci. 2010;51(8):3993-4005.

35. Hampel U, Schroder A, Mitchell T, et al. Serum-induced keratinization processes in an immortalized human meibomian gland epithelial cell line. PLoS One. 2015;10(6):e0128096.

36. Folch J, Lees M, Sloane Stanley GH. A simple method for the isolation and purification of total lipides from animal tissues. J Biol Chem. 1957;226(1):497-509.

37. Woodward DF, Regan JW, Lake S, Ocklind A. The molecular biology and ocular distribution of prostanoid receptors. Surv Ophthalmol. 1997;41 Suppl 2:S15-21.

38. Mukhopadhyay P, Bian L, Yin H, Bhattacherjee P, Paterson C. Localization of EP(1) and FP receptors in human ocular tissues by in situ hybridization. Invest Ophthalmol Vis Sci. 2001;42(2):424-428.

39. Schlotzer-Schrehardt U, Zenkel M, Nusing RM. Expression and localization of FP and EP prostanoid receptor subtypes in human ocular tissues. Invest Ophthalmol Vis Sci. 2002;43(5):1475-1487.

40. Reginato MJ, Krakow SL, Bailey ST, Lazar MA. Prostaglandins promote and block adipogenesis through opposing effects on peroxisome proliferator-activated receptor gamma. J Biol Chem. 1998;273(4):1855-1858.

41. Rosen ED, Spiegelman BM. PPARgamma : a nuclear regulator of metabolism, differentiation, and cell growth. J Biol Chem. 2001;276(41):37731-37734.

42. Hammarstedt A, Andersson CX, Rotter Sopasakis V, Smith U. The effect of PPARgamma ligands on the adipose tissue in insulin resistance. Prostaglandins Leukot Essent Fatty Acids. 2005;73(1):65-75.

43. Kim SW, Xie Y, Nguyen PQ, et al. PPARgamma regulates meibocyte differentiation and lipid synthesis of cultured human meibomian gland epithelial cells (hMGEC). Ocul Surf. 2018;16(4):463-469.

44. Kim SW, Brown DJ, Jester JV. Transcriptome analysis after PPARgamma activation in human meibomian gland epithelial cells (hMGEC). Ocul Surf. 2019;17(4):809-816.

45. Chen W, Tsai SJ, Wang CA, Tsai JC, Zouboulis CC. Human sebocytes express prostaglandin E2 receptors EP2 and EP4 but treatment with prostaglandin E2 does not affect testosterone production. Br J Dermatol. 2009;161(3):674-677.

46. Markovic T, Jakopin Z, Dolenc MS, Mlinaric-Rascan I. Structural features of subtype-selective EP receptor modulators. Drug Discov Today. 2017;22(1):57-71.

47. Foller M, Kasinathan RS, Duranton C, Wieder T, Huber SM, Lang F. PGE2-induced apoptotic cell death in K562 human leukaemia cells. Cell Physiol Biochem. 2006;17(5-6):201-210.

48. Lang PA, Kempe DS, Myssina S, et al. PGE(2) in the regulation of programmed erythrocyte death. Cell Death Differ. 2005;12(5):415-428.

49. Turini ME, DuBois RN. Cyclooxygenase-2: a therapeutic target. Annu Rev Med. 2002;53:35-57.

50. Tsujii M, DuBois RN. Alterations in cellular adhesion and apoptosis in epithelial cells overexpressing prostaglandin endoperoxide synthase 2. Cell. 1995;83(3):493-501.

51. Jansen KM, Pavlath GK. Prostaglandin F2alpha promotes muscle cell survival and growth through upregulation of the inhibitor of apoptosis protein BRUCE. Cell Death Differ. 2008;15(10):1619-1628.

52. Ambaw YA, Chao C, Ji S, et al. Tear eicosanoids in healthy people and ocular surface disease. Sci Rep. 2018;8(1):11296.

53. Lekhanont K, Sathianvichitr K, Pisitpayat P, Anothaisintawee T, Soontrapa K, Udomsubpayakul U. Association between the levels of prostaglandin E2 in tears and severity of dry eye. Int J Ophthalmol. 2019;12(7):1127-1133.

54. Shim J, Park C, Lee HS, et al. Change in prostaglandin expression levels and synthesizing activities in dry eye disease. Ophthalmology. 2012;119(11):2211-2219.

55. Kroin JS, Buvanendran A, Watts DE, Saha C, Tuman KJ. Upregulation of cerebrospinal fluid and peripheral prostaglandin E2 in a rat postoperative pain model. Anesth Analg. 2006;103(2):334-343, table of contents.

56. Liu S, Kam WR, Ding J, Hatton MP, Sullivan DA. Effect of growth factors on the proliferation and gene expression of human meibomian gland epithelial cells. Invest Ophthalmol Vis Sci. 2013;54(4):2541-2550.

57. Knop E, Knop N, Millar T, Obata H, Sullivan DA. The international workshop on meibomian gland dysfunction: report of the subcommittee on anatomy, physiology, and pathophysiology of the meibomian gland. Invest Ophthalmol Vis Sci. 2011;52(4):1938-1978.

58. Casimir DA, Miller CW, Ntambi JM. Preadipocyte differentiation blocked by prostaglandin stimulation of prostanoid FP2 receptor in murine 3T3-L1 cells. Differentiation. 1996;60(4):203-210.

59. Maldve RE, Kim Y, Muga SJ, Fischer SM. Prostaglandin E(2) regulation of cyclooxygenase expression in keratinocytes is mediated via cyclic nucleotide-linked prostaglandin receptors. J Lipid Res. 2000;41(6):873-881.

60. Ueno T, Fujimori K. Novel suppression mechanism operating in early phase of adipogenesis by positive feedback loop for enhancement of cyclooxygenase-2 expression through prostaglandin F2alpha receptor mediated activation of MEK/ERK-CREB cascade. FEBS J. 2011;278(16):2901-2912.

61. Ricciotti E, FitzGerald GA. Prostaglandins and inflammation. Arterioscler Thromb Vasc Biol. 2011;31(5):986-1000.

62. Yu K, Bayona W, Kallen CB, et al. Differential activation of peroxisome proliferator-activated receptors by eicosanoids. J Biol Chem. 1995;270(41):23975-23983.

63. Yousufzai SY, Ye Z, Abdel-Latif AA. Prostaglandin F2 alpha and its analogs induce release of endogenous prostaglandins in iris and ciliary muscles isolated from cat and other mammalian species. Exp Eye Res. 1996;63(3):305-310.

64. Neyrinck AM, Margagliotti S, Gomez C, Delzenne NM. Kupffer cell-derived prostaglandin E2 is involved in regulation of lipid synthesis in rat liver tissue. Cell Biochem Funct. 2004;22(5):327-332.

65. Mater MK, Thelen AP, Jump DB. Arachidonic acid and PGE2 regulation of hepatic lipogenic gene expression. J Lipid Res. 1999;40(6):1045-1052.

66. Enomoto N, Ikejima K, Yamashina S, et al. Kupffer cell-derived prostaglandin E(2) is involved in alcohol-induced fat accumulation in rat liver. Am J Physiol Gastrointest Liver Physiol. 2000;279(1):G100-106.

67. Borchman D, Foulks GN, Yappert MC, Milliner SE. Differences in human meibum lipid composition with meibomian gland dysfunction using NMR and principal component analysis. Invest Ophthalmol Vis Sci. 2012;53(1):337-347.

68. Kam WR, Liu Y, Ding J, Sullivan DA. Do Cyclosporine A, an IL-1 Receptor Antagonist, Uridine Triphosphate, Rebamipide, and/or Bimatoprost Regulate Human Meibomian Gland Epithelial Cells? Invest Ophthalmol Vis Sci. 2016;57(10):4287-4294.

69. Woodward DF, Liang Y, Krauss AH. Prostamides (prostaglandin-ethanolamides) and their pharmacology. Br J Pharmacol. 2008;153(3):410-419.

70. Camras CB, Toris CB, Sjoquist B, et al. Detection of the free acid of bimatoprost in aqueous humor samples from human eyes treated with bimatoprost before cataract surgery. Ophthalmology. 2004;111(12):2193-2198.

71. Rath A, Eichhorn M, Trager K, Paulsen F, Hampel U. In vitro effects of benzalkonium chloride and prostaglandins on human meibomian gland epithelial cells. Ann Anat. 2019;222:129-138.

72. Jester JV, Potma E, Brown DJ. PPARgamma Regulates Mouse Meibocyte Differentiation and Lipid Synthesis. Ocul Surf. 2016;14(4):484-494.

73. Liu Y, Kam WR, Ding J, Sullivan DA. One man's poison is another man's meat: using azithromycin-induced phospholipidosis to promote ocular surface health. Toxicology. 2014;320:1-5.

74. Liu Y, Kam WR, Ding J, Sullivan DA. Effect of azithromycin on lipid accumulation in immortalized human meibomian gland epithelial cells. JAMA Ophthalmol. 2014;132(2):226-228.

75. Hwang HS, Parfitt GJ, Brown DJ, Jester JV. Meibocyte differentiation and renewal: Insights into novel mechanisms of meibomian gland dysfunction (MGD). Exp Eye Res. 2017;163:37-45.

CHAPTER SIX: LATANOPROST AND BENZALKONIUM CHLORIDE ALTER CELL VIABILITY AND THE NONPOLAR LIPID PROFILE PRODUCED BY HUMAN MEIBOMIAN GLAND EPITHELIAL CELLS IN CULTURE

by

JILLIAN F. ZIEMANSKI, LANDON WILSON, STEPHEN BARNES, KELLY K. NICHOLS

In preparation for *Cornea*

Format adapted for dissertation

Abstract

Purpose: The purpose of this study was to explore the effects of a common anti-glaucoma $PGF_{2\alpha}$ analog, latanoprost, and its preservative system, benzalkonium chloride (BAK), on the cell viability and lipidomic expression of immortalized human meibomian gland epithelial cells (HMGECs).

Methods: HMGECs were differentiated for two days prior to introducing latanoprost (0.05, 0.5, 5, or 50 µg/ml), BAK (0.2, 2, 20, or 200 µg/ml), or combined latanoprost-BAK (0.05-0.2, 0.5-2, 5-20, or 50-200 µg/ml) for three hours. To determine receptor involvement, EP- and FP-type receptors, the cognate receptors of PGE_2 and $PGF_{2\alpha}$, were inhibited, thereby sparing and isolating the function of one receptor per condition. Cell viability was assessed by ATP quantitation, and lipid extracts were analyzed by ESI-$MSMS^{ALL}$ in positive ion mode by a Triple TOF 5600 Mass Spectrometer (SCIEX, Framingham, MA) using SCIEX LipidView 1.3.

Results: Both latanoprost and BAK were lethal to HMGECs at concentrations equivalent to commercially available eye drops ($p < 0.001$ for both). The cytotoxicity of latanoprost was mediated through an FP- and EP-independent mechanism. Both latanoprost and BAK significantly modulated the lipidomic expression of several cholesteryl esters (8% and 30%, respectively) and triacylglycerols (10% and 12%, respectively). The combination of latanoprost and BAK appeared to be no more toxic and to only negligibly alter the lipid profile relative to its individual components.

Conclusion: The use of latanoprost and BAK in glaucoma may alter the viability of and lipid expression from the meibomian glands in vivo. Non-preserved latanoprost has less cytotoxicity at lower doses and fewer lipidomic effects compared to BAK, further strengthening the argument for the use of BAK-free pharmaceutical preparations.

Introduction

Worldwide, glaucoma is a leading cause of irreversible blindness.[1] Though incurable, glaucoma can be managed medically or surgically by lowering the intraocular pressure, the disease's only modifiable risk factor.[2] There are currently five available classes of anti-glaucoma eye drops, but prostaglandin $F_{2\alpha}$ analogs (PGAs) are the most common first-line agent owing to their convenient dosing schedule, favorable systemic side effect profile, and overall efficacy.[3] Chronic, daily use of this medication class, however, can lead to alterations of the ocular surface, including meibomian gland dysfunction (MGD).[4] Associated with ocular burning, redness, dryness, and fluctuating vision, among others, ocular surface disease has the potential to limit treatment success in glaucoma patients by interfering with drop adherence, with reliable data acquisition (routine imaging and threshold visual field assessment), and arguably treatment efficacy.[4-7]

MGD is a diffuse alteration to the structure and/or function of the lipid-producing meibomian glands.[8] It can be classified as obstructive or hypersecretory. In obstructive MGD, the lipid secretion, termed meibum, becomes altered, often resulting in increased meibum viscosity, stagnation, and ultimately ductal obstruction. Over time, obstructed glands lead to intraglandular hypertension and eventually meibomian gland atrophy.[8]

Mocan et al. found a high propensity for patients with PGA-treated glaucoma to develop obstructive MGD.[9] The exact mechanism for how PGAs promote this pathway remains unknown, though some have hypothesized that PGAs may alter the lipid secretion from meibomian glands.[10] We support this assertion, considering our recent discovery that a human meibomian gland epithelial cell (HMGEC) line expresses the $PGF_{2\alpha}$ FP receptor and that treatment with $PGF_{2\alpha}$ modifies the lipidomic profile produced by HMGECs.[11]

The role of the preservative system, particularly benzalkonium chloride (BAK), in the development of ocular surface disease must also be acknowledged. BAK is a cationic surfactant, exhibiting its antimicrobial properties through a detergent mechanism that disrupts lipid cell membranes.[12] As collateral damage, BAK also perturbs host cell membranes of the cornea and conjunctiva[13] and, functionally, reduces tear stability.[14] Several authors have found that preservative-free PGAs lead to less inflammatory cell infiltration[15-19] and less apoptosis of corneal epithelium[19] compared to BAK-preserved PGAs. The exact contribution of PGAs and BAK to the underlying pathophysiology of MGD remains to be fully elucidated.

To approach this question, we sought to explore the individual and combined effects of latanoprost (a common PGA) and BAK on cell viability and nonpolar lipid expression in an immortalized human meibomian gland epithelial cell (HMGEC) line. We hypothesized that BAK exposure would decimate HMGECs at concentrations found in commercially available eye drops. We further hypothesized that treatment with latanoprost and BAK, both in isolation and in combination, would significantly alter the HMGEC lipidomic profile.

Methods

Reagents and Materials

Latanoprost and benzalkonium chloride were purchased from Sigma Aldrich (St. Louis, MO). Rosiglitazone was purchased from Cayman Chemical (Ann Arbor, MI). All receptor antagonists were also purchased from Cayman Chemical: SC-51322 (EP1 inhibitor), PF-04418948 (EP2 inhibitor), L-798,106 (EP3 inhibitor), ONO-AE3-208 (EP4 inhibitor), and AL 8810 (FP inhibitor). Stock solutions of latanoprost, rosiglitazone, and all receptor antagonists were made by dissolving each in dimethyl sulfoxide (DMSO, Hybri-Max^{TM}, Sigma Aldrich). All stock solutions were purged with nitrogen, stored at -20°C, and freshly added to the media just prior to experimentation. The DMSO concentration was maintained at 0.5% in all experiments, except cell viability experiments that utilized receptor antagonists, where the concentration was maintained at 0.8%. Clear-bottom, white-walled 96-well plates (ThermoFisher, Waltham, MA) were used for luminescent cell viability assays. Glass petri dishes (Sigma Aldrich, St. Louis, MO) were used for cell culture during lipidomics experiments. All experiments consisted of two or three independent experimental replicates and two or three technical replicates.

Cell viability

HMGECs were seeded at 30,000 cells per well in 96-well plates and differentiated in DMEM/F12 with 10 ng/ml EGF, 2% fetal bovine serum (FBS), and 50 µM rosiglitazone.[67,68,138,163] After 48 hours of differentiation, HMGECs were exposed to this same differentiation media containing latanoprost (0.05, 0.5, 5, or 50 µg/ml), BAK (0.2, 2, 20, or 200 µg/ml), or combined latanoprost-BAK (0.05-0.2, 0.5-2, 5-20, or 50-200

µg/ml) for three hours. Following incubation, the CellTiter Glo Luminescent Cell Viability Assay (Promega, Madison, WI) was used to quantify ATP as a measure of cell viability according to the manufacturer's instructions. Luminescence was quantified by the Wallac Perkin-Elmer 1420-041 Victor2 Multiplate Multifluorescent Reader (Mt. Waverly, Victoria, Australia) over an acquisition time of one second.

For inhibition experiments, HMGECs were seeded in 96-well plates and differentiated with identical methodology as just described. After 48 hours of differentiation, HMGECs were pre-treated with an antagonist cocktail for 30 minutes prior to incubating with latanoprost 50 µg/ml for 3 hours. The antagonist cocktail inhibited all EP and FP receptors except one for each condition (Figure 1) and was maintained during the three-hour challenge with latanoprost. Cell viability was assessed with the same CellTiter Glo assay.

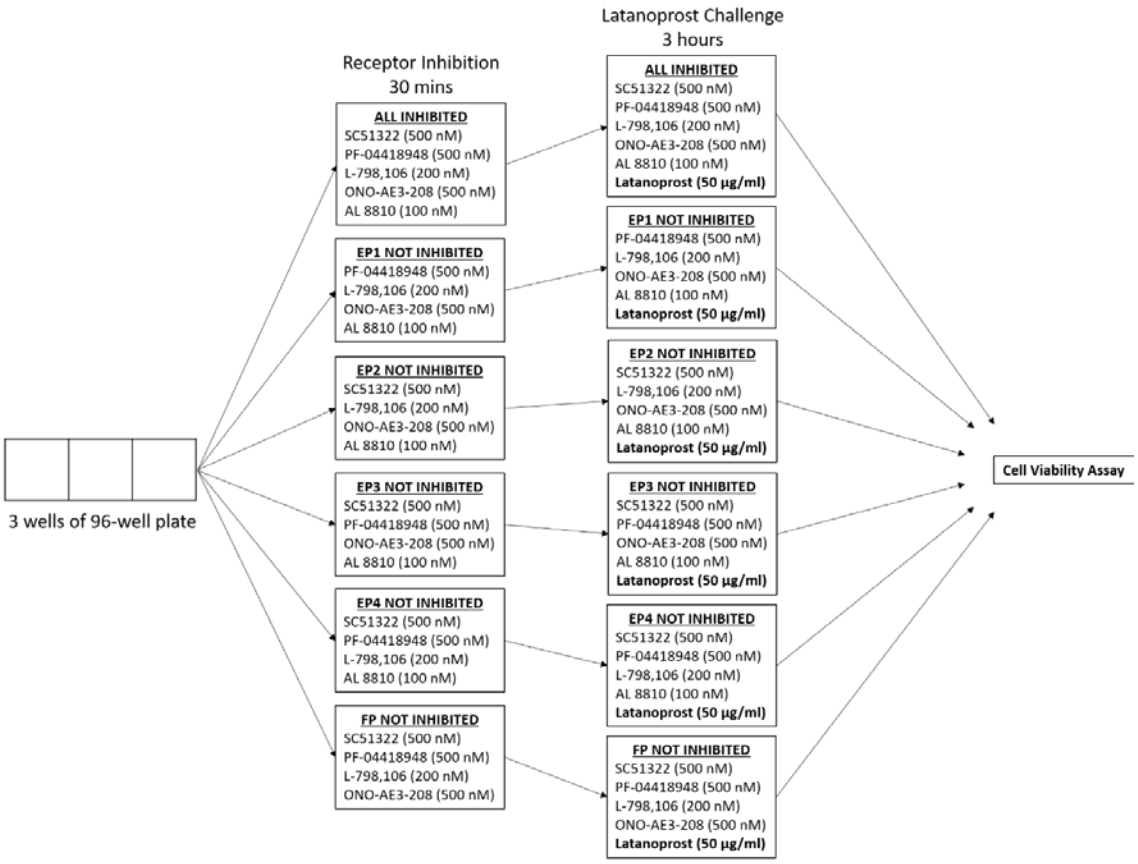

Figure 1 Study Design for Inhibition Experiments
Each well was seeded with 30,000 HMGECs and allowed to differentiate for 48 hours (see Methods). HMGECs were pre-treated with receptor inhibitors for 30 minutes prior to introduction of latanoprost 50 µg/ml for three hours. Following incubation, cell viability was assayed with the Cell Titer-Glo Luminescent Cell Viability Assay (see Methods). n = 9 per condition (3 experimental replicates and 3 technical replicates)
SC51322 (EP1 inhibitor), PF-04418948 (EP2 inhibitor), L-798,106 (EP3 inhibitor), ONO-AE3-208 (EP4 inhibitor), AL 8810 (FP inhibitor)

Lipid extraction and analysis by mass spectrometry

HMGECs were seeded at one million cells per 6-cm glass petri dish and differentiated for 48 hours as described above. Following incubation, HMGECs were exposed to latanoprost (0.05, 0.5, or 5 µg/ml), BAK (0.2 or 2 µg/ml), or combined latanoprost-BAK (0.05-0.2 or 0.5-2 µg/ml). Lipids were extracted as previously

described.[24] Samples were stored at -80°C until analysis. Glass, stainless steel, or polytetrafluoroethylene were used for all steps that involved organic solvents.

Lipid extracts were analyzed by direct infusion ESI-MSMS^{ALL} in positive mode ionization with a SCIEX Triple TOF 5600 Mass Spectrometer (SCIEX, Framingham, MA) as previously described.[11,20,21] All data were processed with SCIEX LipidView 1.3 software. Lipid identities were assigned by LipidView utilizing a database of known ion fragments and confirmed by SCIEX PeakView 2.2 if further investigation was warranted. The mass tolerance window was set to 5 mDa, and only peaks with a signal-to-noise ratio greater than or equal to three were analyzed.

Data analysis and labeling convention

For all lipidomics experiments, cholesteryl esters (CEs), wax esters (WEs), and triacylglycerols (TAGs) were the primary focus of this study. To be included in the data analysis, each lipid species had to be detectable in all replicates from all samples. For TAGs, an additional criterion was used, which required a threshold abundance of 0.1%. All data for both cell viability and lipidomics were analyzed by one-way ANOVA with Tukey post-hoc testing (SPSS v26, Armonk, NY) when tests of normality (Kolmogorov-Smirnov) and homogeneity of variance (Levene's Test) were satisfied. If variance was not equal, then Games-Howell post-hoc testing was used. If distributions deviated from normal, then the non-parametric Kruskal Wallis test was used. A p-value of 0.05 was considered significant.

All CEs are labeled as n_c:db, where n_c and db represent the number of carbons and double bonds, respectively, in the fatty acyl chain. If a third number is present, then it

represents the number of oxygenations present on an oxidized CE (oxCE). TAGs follow a similar convention (n_c:db) to denote the total number of carbons (n_c) and double bonds (db) present in all three fatty acyl groups. TAGs are further labeled in parentheses with a product ion, either a fatty acid (FA) or another TAG, which also follows the same two-number labeling convention. This TAG notation represents that the LipidView software identified a neutral loss corresponding to the FA or TAG in parentheses. For example, TAG 54:3 (FA 18:1) describes a TAG with 54 total carbons and three total double bonds among its three fatty acyl chains, where one of those chains consists of 18 carbons and one double bond.

Results

Influence of latanoprost and BAK on cell viability

To determine whether latanoprost affects HMGEC viability, ATP was quantitated from differentiated HMGECs exposed to latanoprost (0.05, 0.5, 5, or 50 µg/ml) for three hours. There was a statistically significant difference among group means ($p < 0.001$) driven by latanoprost 50 µg/ml, which varied significantly from vehicle control (95.8% reduction, $p < 0.001$) and all other latanoprost concentrations (mean 95.4% reduction, $p < 0.01$ for all, Figure 2).

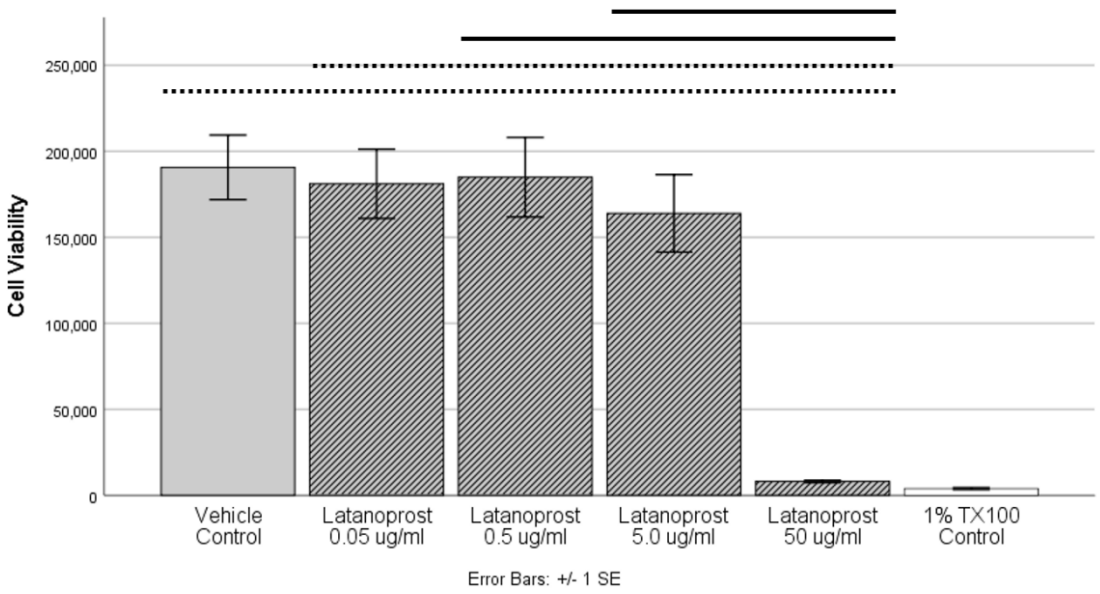

Figure 2 Effect of Latanoprost on HMGEC Viability
HMGECs were differentiated for 48 hours prior to exposure to latanoprost for three hours. At 50 µg/ml, latanoprost was lethal to HMGECs.
TX100: Triton-X 100 positive control
Black bar: $p \leq 0.01$
Dashed bar: $p \leq 0.001$

In an attempt to determine whether an FP- or EP-type prostaglandin receptor mediated this latanoprost-induced cell death, HMGECs were pre-treated with a cocktail of receptor antagonists for 30 minutes (Figure 1), leaving one receptor uninhibited per condition, before challenging with latanoprost 50 µg/ml. Receptor inhibition was maintained during the three-hour challenge. As already shown, latanoprost 50 µg/ml significantly reduced viability relative to the vehicle control by 93.1% ($p = 0.007$). However, inhibiting all EP and FP receptors failed to prevent latanoprost-induced cell death (Figure 3). There were no significant differences between the samples treated only with latanoprost 50 µg/ml and any of the samples pre-treated with receptor antagonists.

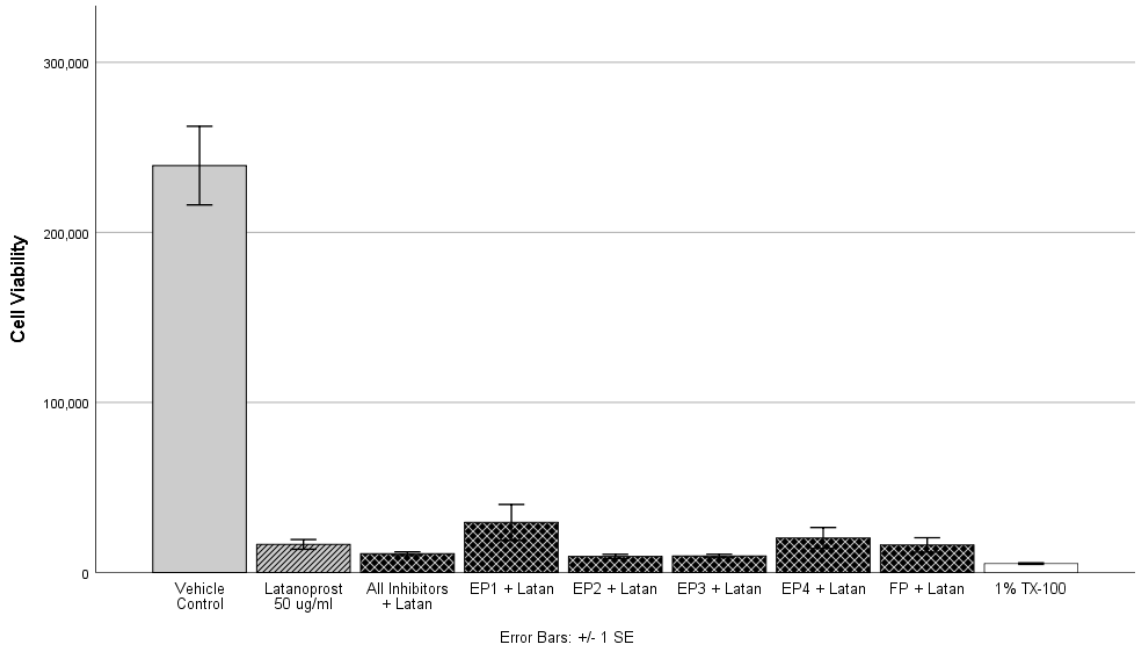

Figure 3 Effect of EP- and FP-type Receptors on Latanoprost-Induced Cell Death
HMGECs were differentiated for 48 hours, pre-treated with receptor inhibitors for 30 minutes, and exposed to latanoprost 50 µg/ml for three hours, as depicted in Figure 2. Treatment with receptor inhibitors did not prevent latanoprost-induced cell death.
TX100: Triton-X 100 positive control
Latan: latanoprost

To determine the extent of toxicity of BAK, ATP was quantitated from differentiated HMGECs exposed to BAK (0.2, 2, 20, or 200 µg/ml) for three hours. A dose-dependent effect was observed, where BAK reduced viability relative to control by 17.9% (not significant), 77.6% ($p = 0.003$), and 95.6% ($p = 0.001$) for the 2, 20, and 200 µg/ml concentrations, respectively (Figure 4).

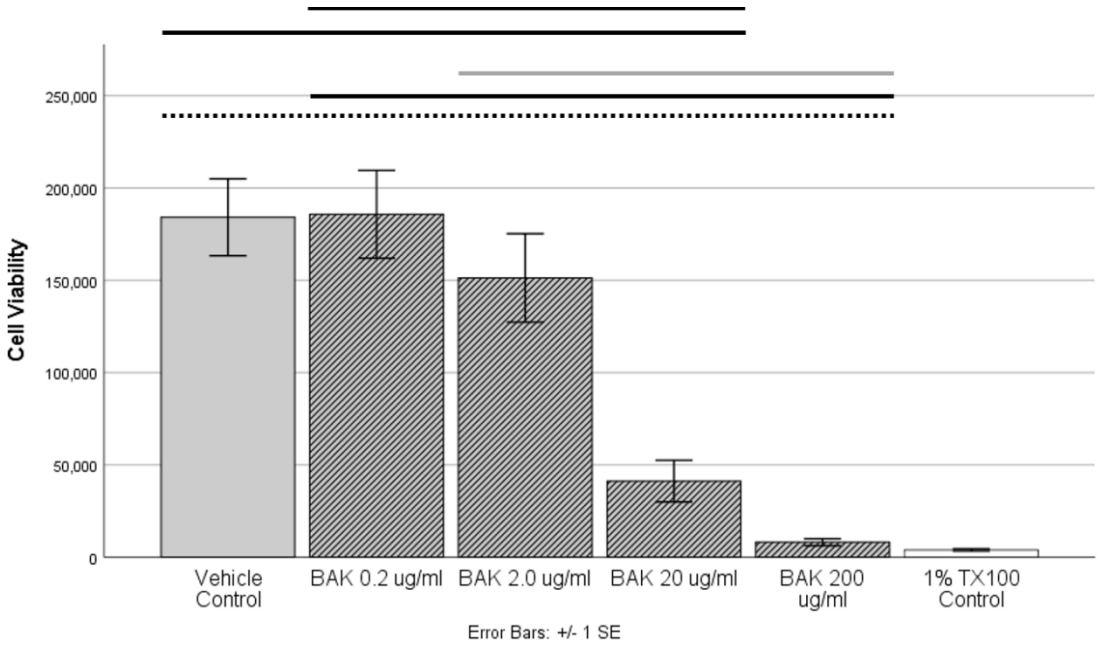

Figure 4 Effect of BAK on HMGEC Viability
HMGECs were differentiated for 48 hours prior to exposure to BAK for three hours. At 20 and 200 µg/ml, BAK was lethal to HMGECs.
BAK: benzalkonium chloride
TX100: Triton-X 100 positive control
Gray bar: $p \leq 0.05$
Black bar: $p \leq 0.01$
Dashed bar: $p \leq 0.001$

To assess whether the combination of latanoprost and BAK was more lethal than its components, differentiated HMGECs were exposed to both compounds for three hours prior to quantitating ATP as a measure of cell viability. The toxicity of the combinations was equivalent to its most lethal component(s) across all concentrations tested (Figure 5).

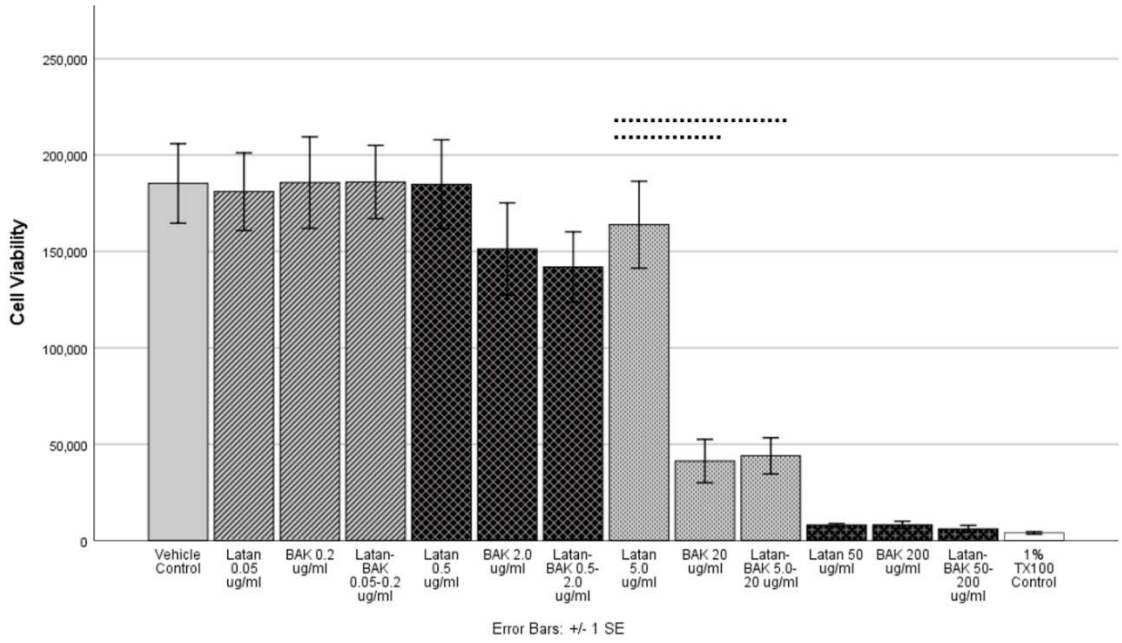

Figure 5 Effect of Combined Latanoprost and BAK on HMGEC Viability
HMGECs were differentiated for 48 hours prior to exposure to latanoprost-BAK for three hours. The effect of combined latanoprost-BAK was equivalent to its most toxic component at all concentrations, indicating no additive effect in toxicity. Significance markers are only shown within each triad of concentrations.
Latan: latanoprost
BAK: benzalkonium chloride
TX100: Triton-X 100 positive control
Dashed bar: $p \leq 0.001$

Description of the CE and TAG profiles across all samples

WEs were not detectable across all HMGEC samples, but CE and TAGs were. There were 50 unique CEs detected across all samples that met the criteria for inclusion in the analysis (Figure 6). The chain length varied from 11 to 34, and the double-bond count varied from zero to five. Nine CEs were found to be oxidized. The most abundant CE was CE 18:1. Very long-chain ($20 \leq$ carbon number $[n_c] \leq 25$) and ultra long-chain CEs ($n_c \geq 26$) were present from all conditions and comprised 22.9% and 10.5% of the overall CE pool, respectively. Of the 50 CEs, nine were saturated, 22 were

monounsaturated, and 19 were polyunsaturated. Monounsaturated CEs were the most abundant (50.9%), followed by polyunsaturated (27.9%) and saturated (21.2%).

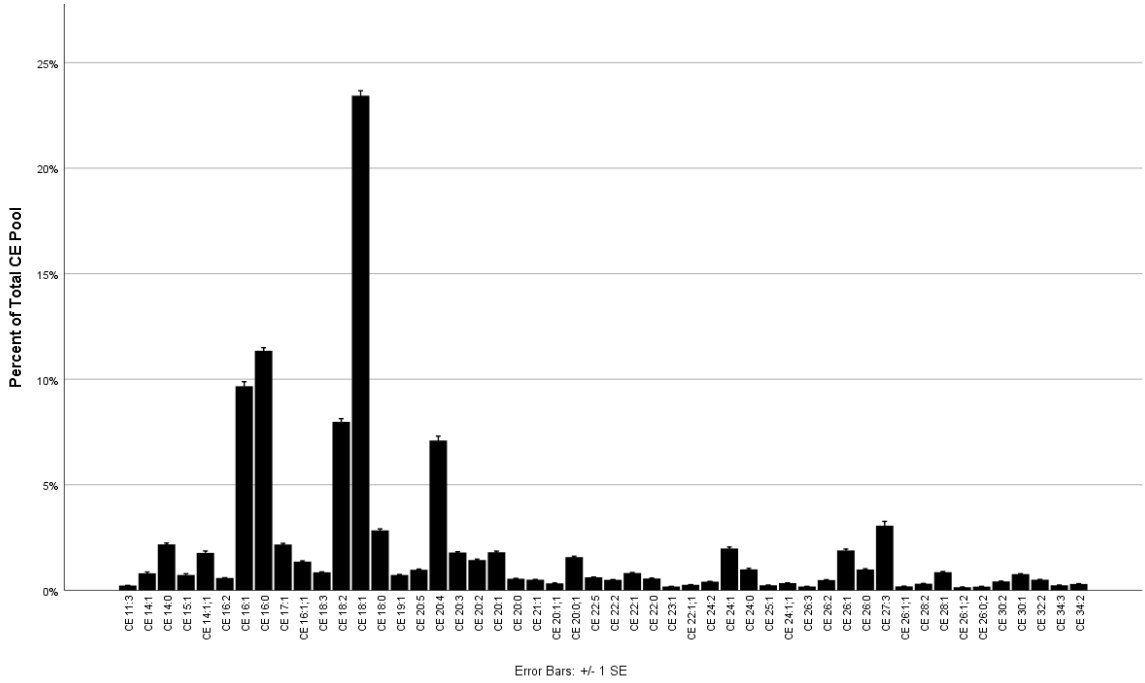

Figure 6 Description of HMGEC CE Profile
HMGECs express a diverse profile of cholesteryl esters (CEs) across all conditions. CE 18:1 was the most abundant. CEs are labeled by carbon number and double-bond count, respectively. When a third number is present, it denotes an oxCE with the corresponding number of oxygenations. n = 4 per condition
oxCE: oxidized cholesteryl ester

There were 5,155 TAGs detected across all samples; however, only 121 met the criteria for inclusion in the analysis. The total carbon count from the three acyl chains, excluding the glycerol backbone, ranged from 46 to 60 with the majority (113/121, 93.4%) falling within the range of 46 to 56 (Figure 7A). All TAGs except one consisted of an even carbon count (120/121, 99.2%). The number of double bonds in the acyl chains of the TAGs varied from zero to 10. Very few TAGs were fully saturated (5/121, 4.1%). The degree of unsaturation followed a bimodal distribution (Figure 7B) that was

heavily weighted toward a lower degree of unsaturation. TAGs were primarily of lower unsaturation (77/121, 63.6%, one to three double bonds) or of higher unsaturation (39/121, 32.2%, seven to 10 double bonds). There were zero TAGs with a moderate degree of unsaturation (four to six double bonds). The LipidView 1.3 software identified the neutral loss of 24 unique fatty acyl chains from the 121 TAGs (Figure 7C). Their individual carbon counts varied from 10 to 20 with double bonds ranging from zero to three. Although nearly all of the parent TAGs consisted of an even carbon count, many of the fatty acyl chains consisted of an odd number of carbons (27/121, 22.3%). The most frequently observed fatty acyl groups were oleic acid (FA 18:1) and palmitoleic acid (FA 16:1), which were both present in 18 of 121 TAGs (14.9%). The next most common was palmitic acid (FA 16:0), which was present in 16 (13.2%) TAGs. Relatively few TAGs (8/121, 6.6%) consisted of very long-chain fatty acids (at least 20 carbons).

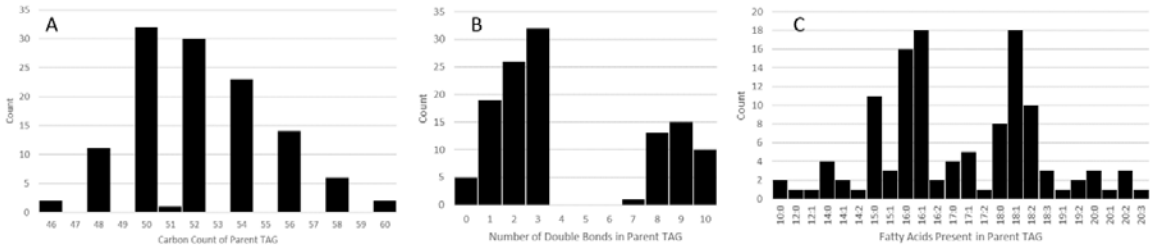

Figure 7 Description of HMGEC TAG Lipidome
HMGECs express a diverse TAG lipidome with carbon counts ranging from 46 to 60 (A) and double-bond counts ranging from zero to 10 (B). There were 24 unique fatty acyl chains identified from parent TAGs.
TAG: triacylglycerol

Influence of latanoprost on CE and TAG expression

To determine the effects of latanoprost on CE and TAG expression, lipid extracts from differentiated HMGECs exposed to 0.05, 0.5, or 5 µg/ml latanoprost were analyzed.

Of the 50 analyzed CEs, only 4 (8.0%) showed a statistically significant change in expression: CE 24:1, CE 25:1, CE 26:1, and CE 28:1 (Figure 8). All four CEs demonstrated higher expression with higher concentrations of latanoprost, but only one concentration (0.5 µg/ml) for one CE (CE 25:1) reached significance against the vehicle control in pairwise comparisons (0.29 ± 0.02% vs 0.20 ± 0.06%, p = 0.04).

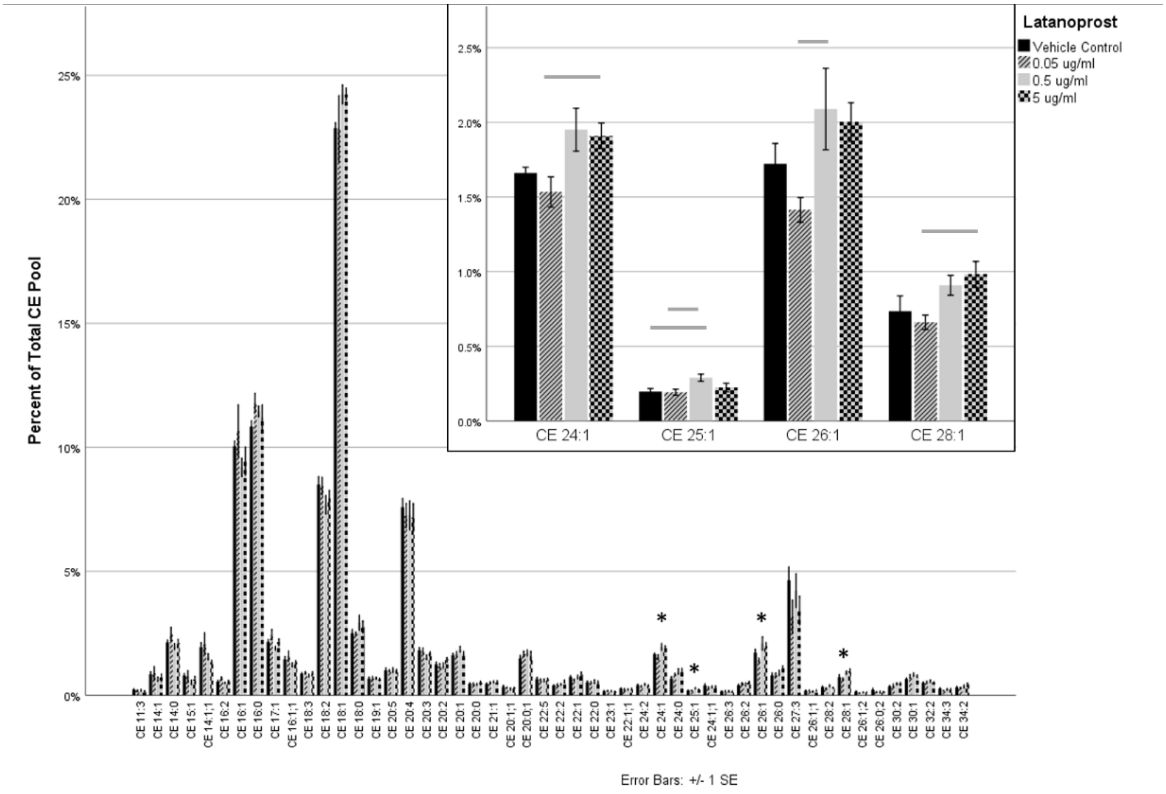

Figure 8 Effect of Latanoprost on CE Lipidome
HMGECs were differentiated for 48 hours prior to exposure to latanoprost for three hours. Lipid extracts were analyzed by ESI-MSMS^{ALL} (see Methods). The inset depicts only the CEs that reached significance. Only four of 50 CEs (8.0%) were significantly altered with latanoprost supplementation. CEs are labeled by carbon number and double-bond count, respectively. When a third number is present, it denotes an oxCE with the corresponding number of oxygenations. n = 4 per condition
CE: cholesteryl ester
oxCE: oxidized cholesteryl ester
Gray bar: $p \leq 0.05$
Black bar: $p \leq 0.01$
Dashed bar: $p \leq 0.001$

A similar portion of TAGs significantly varied in response to latanoprost supplementation (Figure 9): 12/121 (9.9%). Most of the significant TAGs consisted of 50 (3/12, 25.0%), 52 (5/12, 41.7%), or 54 (2/12, 16.7%) carbons and one (4/12, 33.3%), two (5/12, 41.7%), or three (2/12, 16.7%) double bonds. TAGs with the following fatty acids increased with latanoprost supplementation: FA 16:1 (3/9, 33.3%), FA 18:1 (2/9, 22.2%), FA 18:2 (3/9, 33.3%), and FA 20:0 (1/9, 11.1%). Those with the following fatty acids decreased with latanoprost supplementation: FA 10:0 (1/2, 50.0%) and FA 15:0 (1/2, 50.0%).

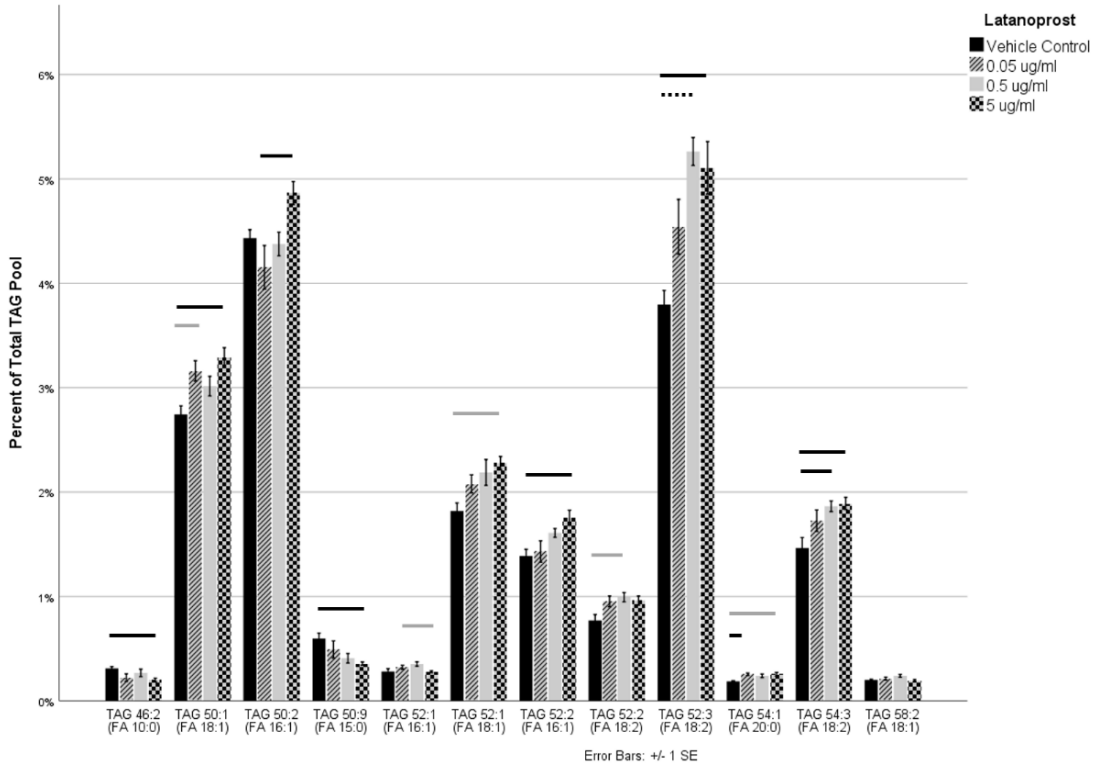

Figure 9 Effect of Latanoprost on HMGEC TAG Lipidome
HMGECs were differentiated for 48 hours prior to exposure to latanoprost for three hours. Lipid extracts were analyzed by ESI-MSMS^{ALL} (see Methods). Only the TAGs that reached significance are shown. Only 12 of 121 TAGs (9.9%) were significantly altered with latanoprost supplementation. TAG 58:2 (FA 18:1) failed to reach significance in pairwise comparisons. TAGs are labeled by two numbers corresponding to the total number

of carbons and the total number of double bonds, respectively. The fatty acid in parentheses represents one of the three fatty acids of the parent TAG molecule. n = 4 per condition
HMGEC: human meibomian gland epithelial cell
TAG: triacylglycerol
FA: fatty acid
Gray bar: $p \leq 0.05$
Black bar: $p \leq 0.01$
Dashed bar: $p \leq 0.001$

Influence of BAK on CE and TAG expression

To determine the effects of BAK on CE and TAG expression, lipid extracts from differentiated HMGECs treated with 0.2 or 2 µg/ml BAK were analyzed. Of the 50 detected CEs, 15 (30.0%) showed a statistically significant difference among the group means (Figure 10). Five CEs were downregulated with both concentrations of BAK: CE 16:0, CE 18:3, CE 18:2, CE 20:4, and CE 20:0;1. Nine CEs were upregulated with both concentrations of BAK: CE 18:0, CE 20:0, CE 21:1, CE 20:1;1, CE 24:0, CE 25:1, CE 24:1;1, CE 26:0, and CE 26:1;1. One CE (CE 28:2) failed to reach significance in pairwise comparisons.

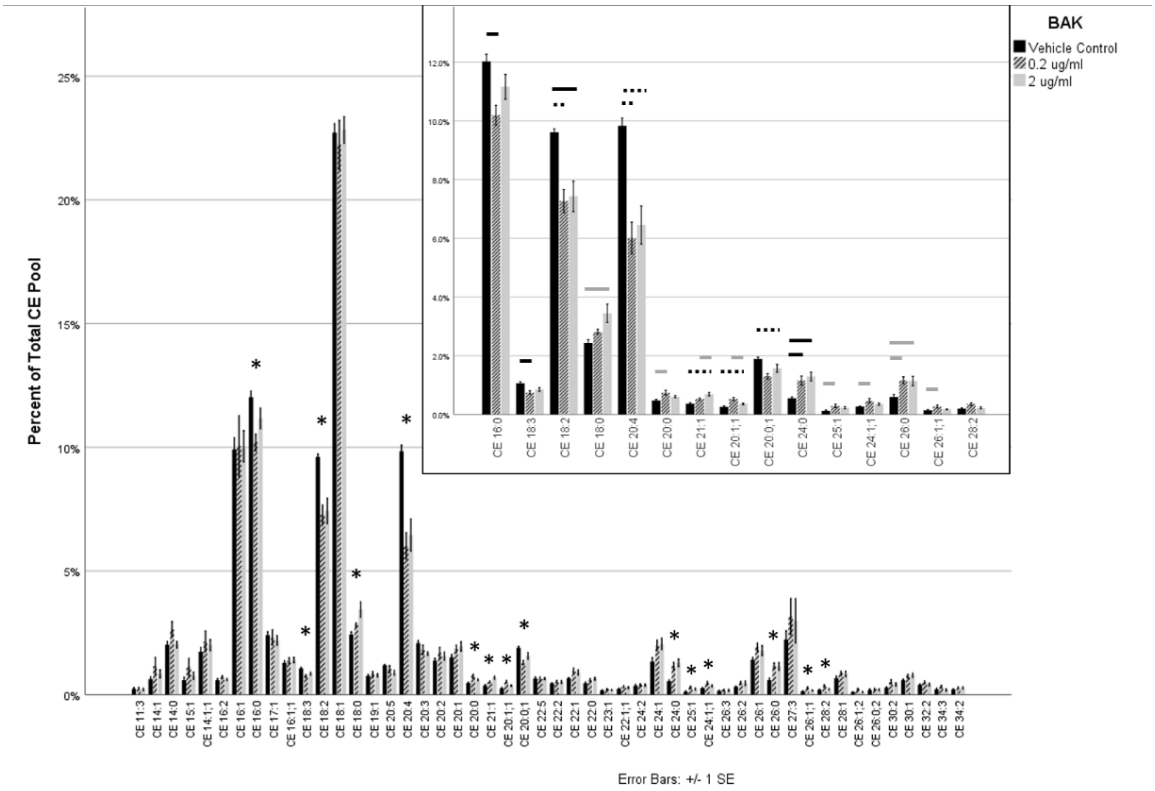

Figure 10 Effect of BAK on HMGEC CE Lipidome
HMGECs were differentiated for 48 hours prior to exposure to BAK for three hours. Lipid extracts were analyzed by ESI-MSMS^{ALL} (see Methods). The inset depicts only the CEs that reached significance. Fifteen of 50 CEs (30.0%) were significantly altered with BAK supplementation. CE 28:2 failed to reach significance in pairwise comparisons. CEs are labeled by carbon number and double-bond count, respectively. When a third number is present, it denotes an oxCE with the corresponding number of oxygenations. n = 4 per condition
BAK: benzalkonium chloride
CE: cholesteryl ester
oxCE: oxidized cholesteryl ester
Gray bar: $p \leq 0.05$
Black bar: $p \leq 0.01$
Dashed bar: $p \leq 0.001$

Of the 121 detected TAGs, 15 (12.4%) varied significantly with BAK supplementation. Most of the significant TAGs consisted of 50 (6/15, 40.0%) or 52 (3/15, 20.0%) carbons. Its preference for saturation level was less specific compared to

latanoprost, as TAGs with zero, one, two, three, nine, or 10 double bonds were all affected, though a slight preference may have been observed for one (3/15, 20.0%) or two (4/15, 26.7%) double bonds. TAGs with 10 unique fatty acyl groups also varied significantly (Figure 11). The significant TAGs with 16- or 18-carbon fatty acids more commonly increased rather than decreased.

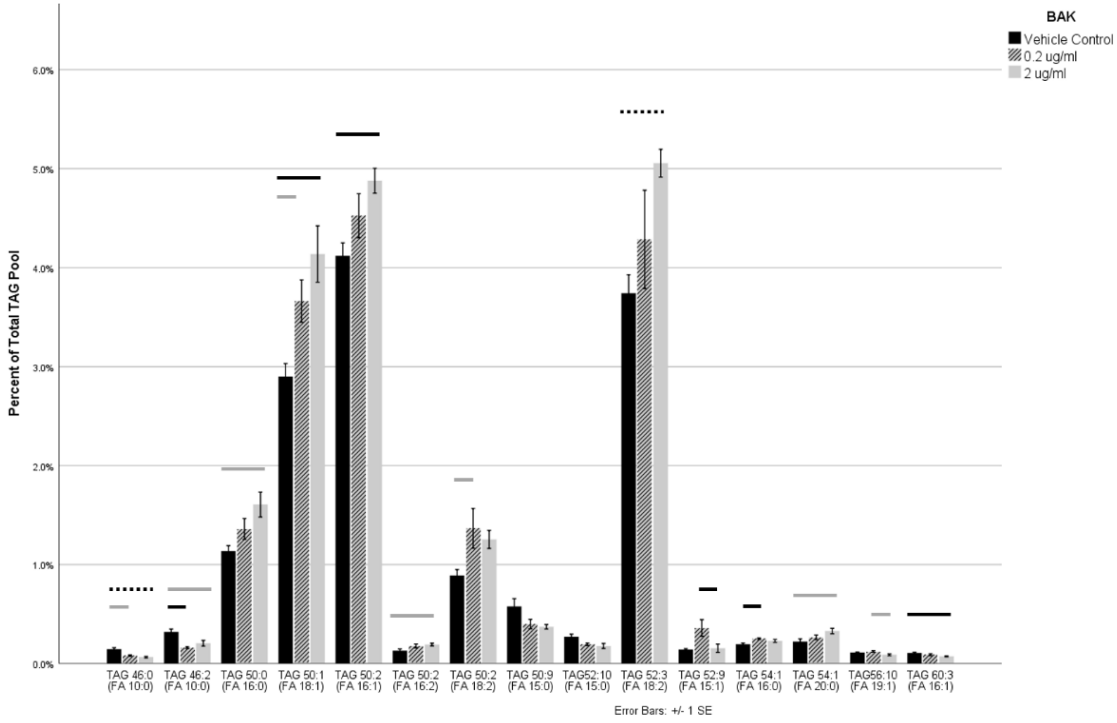

Figure 11 Effect of BAK on HMGEC TAG Lipidome
HMGECs were differentiated for 48 hours prior to exposure to BAK for three hours. Lipid extracts were analyzed by ESI-MSMS^{ALL} (see Methods). Only the TAGs that reached significance are shown. Only 15 of 121 TAGs (12.4%) were significantly altered with latanoprost supplementation. TAG 50:9 (FA 15:0) and TAG 52:10 (FA 15:0) failed to reach significance in pairwise comparisons. TAGs are labeled by two numbers corresponding to the total number of carbons and the total number of double bonds, respectively. The fatty acid in parentheses represents one of the three fatty acids of the parent TAG molecule. n = 4 per condition
HMGEC: human meibomian gland epithelial cell
TAG: triacylglycerol
FA: fatty acid
Gray bar: $p \leq 0.05$
Black bar: $p \leq 0.01$

Dashed bar: $p \leq 0.001$

Influence of combined latanoprost and BAK on CE and TAG expression

To determine whether the combination of latanoprost and BAK elicited changes that differed from its components, lipid extracts from differentiated HMGECs exposed to latanoprost-BAK 0.05-0.2 µg/ml and 0.5-2 µg/ml were analyzed. At the 0.05-0.2 µg/ml concentration, the effect of the combination mirrored its components for all CEs and TAGs except CE 18:2, CE 18:0, CE 24:1, CE 26:2, and CE 26:1 (Figures 12 and 13). At the 0.5-2 µg/ml concentration, the effect of the combination mirrored its components for all CEs and TAGs except TAG 50:2 (FA 18:1), TAG 52:0 (FA 16:0), and TAG 52:1 (FA 16:1) (Figures 14 and 15).

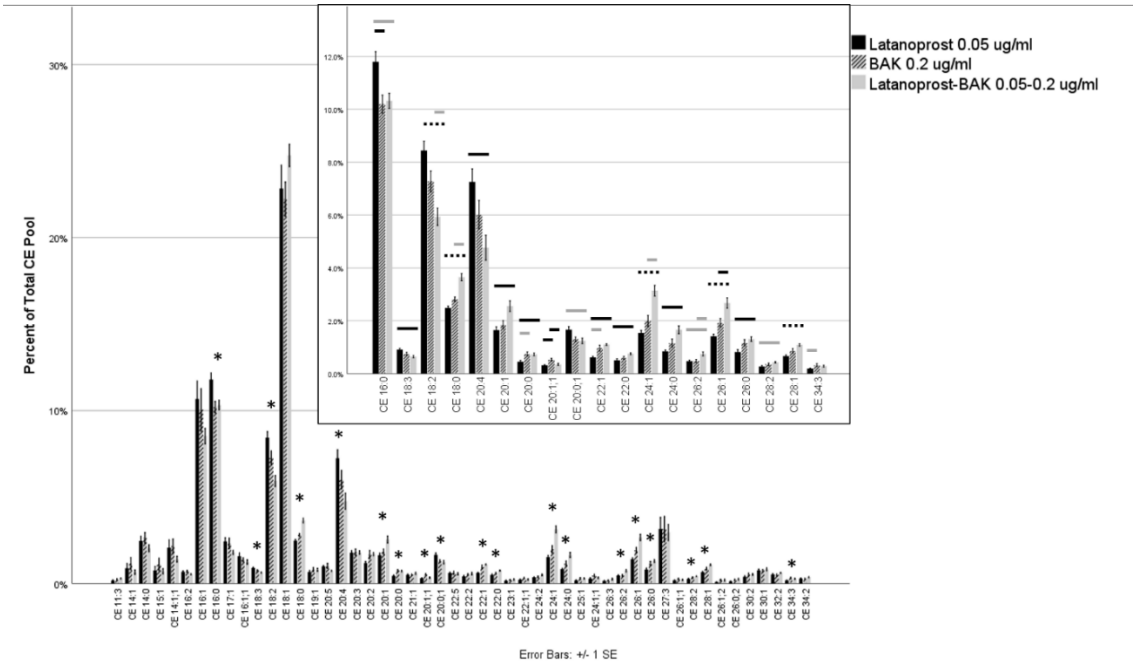

Figure 12 Effect of Latanoprost-BAK 0.05-0.2 µg/ml on the HMGEC CE Lipidome
HMGECs were differentiated for 48 hours prior to exposure to combined latanoprost-BAK for three hours. Lipid extracts were analyzed by ESI-MSMS^{ALL} (see Methods). The inset depicts only the CEs that reached significance. Nineteen of 50 CEs (38.0%) were significantly different between latanoprost alone, BAK alone, or combined latanoprost-

BAK. However, only a few CEs (CE 18:2, CE 18:0, CE 24:1, CE 26:2, and CE 26:1) showed significant differences between combined latanoprost-BAK and each component in isolation. CEs are labeled by carbon number and double-bond count, respectively. When a third number is present, it denotes an oxCE with the corresponding number of oxygenations. n = 4 per condition
BAK: benzalkonium chloride
CE: cholesteryl ester
oxCE: oxidized cholesteryl ester
Gray bar: $p \leq 0.05$
Black bar: $p \leq 0.01$
Dashed bar: $p \leq 0.001$

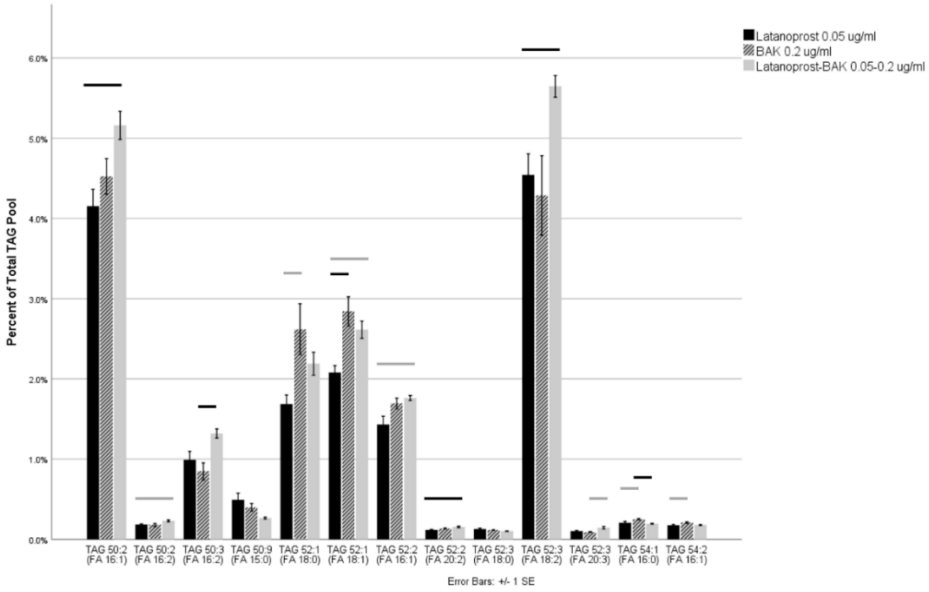

Figure 13 Effect of Latanoprost-BAK 0.05-0.2 µg/ml on the HMGEC TAG Lipidome
HMGECs were differentiated for 48 hours prior to exposure to combined latanoprost-BAK for three hours. Lipid extracts were analyzed by ESI-MSMS^{ALL} (see Methods). Only the TAGs that reached significance are shown. Thirteen of 121 TAGs (10.7%) were significantly different between latanoprost alone, BAK alone, or combined latanoprost-BAK. However, there were no TAGs that showed significant differences between combined latanoprost-BAK and each component in isolation. TAGs are labeled by two numbers corresponding to the total number of carbons and the total number of double bonds, respectively. The fatty acid in parentheses represents one of the three fatty acids of the parent TAG molecule. n = 4 per condition
BAK: benzalkonium chloride
CE: cholesteryl esters
Gray bar: $p \leq 0.05$
Black bar: $p \leq 0.01$
Dashed bar: $p \leq 0.001$

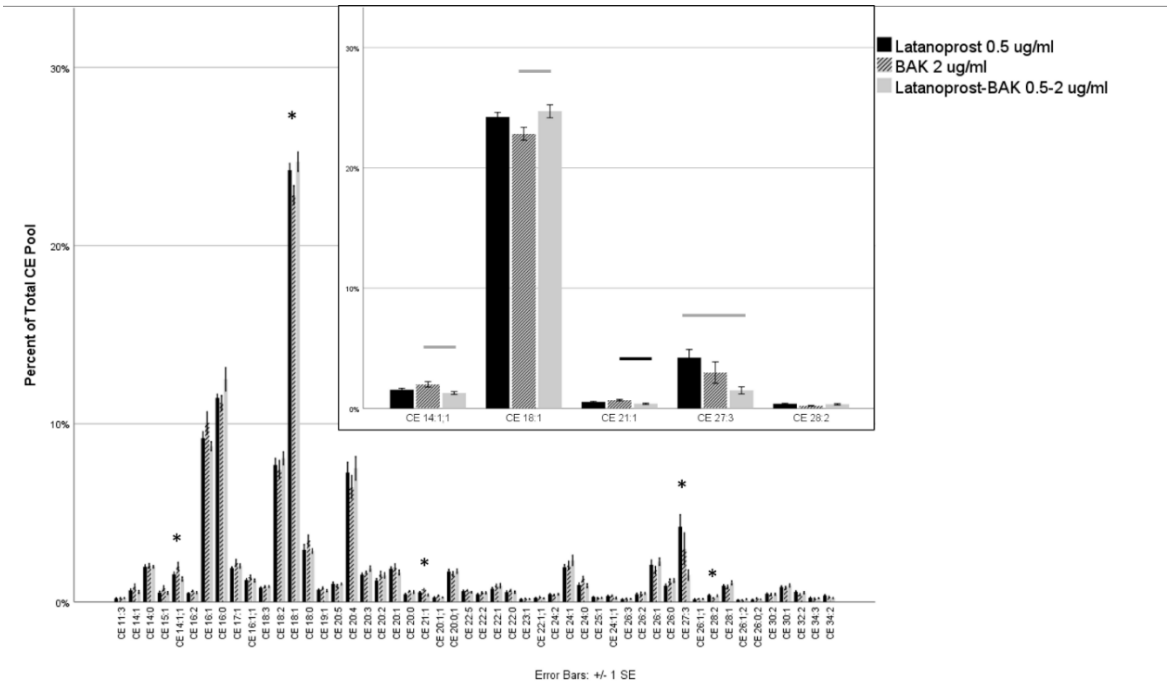

Figure 14 Effect of Latanoprost-BAK 0.5-2 µg/ml on the HMGEC CE Lipidome
HMGECs were differentiated for 48 hours prior to exposure to combined latanoprost-BAK for three hours. Lipid extracts were analyzed by ESI-MSMS^{ALL} (see Methods). The inset depicts only the CEs that reached significance. Five of 50 CEs (10.0%) were significantly different between latanoprost alone, BAK alone, or combined latanoprost-BAK. CE 28:2 failed to reach significance in pairwise comparisons. There were no CEs that showed significant differences between combined latanoprost-BAK and each component in isolation. CEs are labeled by carbon number and double-bond count, respectively. When a third number is present, it denotes an oxCE with the corresponding number of oxygenations. n = 4 per condition
BAK: benzalkonium chloride
CE: cholesteryl ester
oxCE: oxidized cholesteryl ester
Gray bar: $p \leq 0.05$
Black bar: $p \leq 0.01$

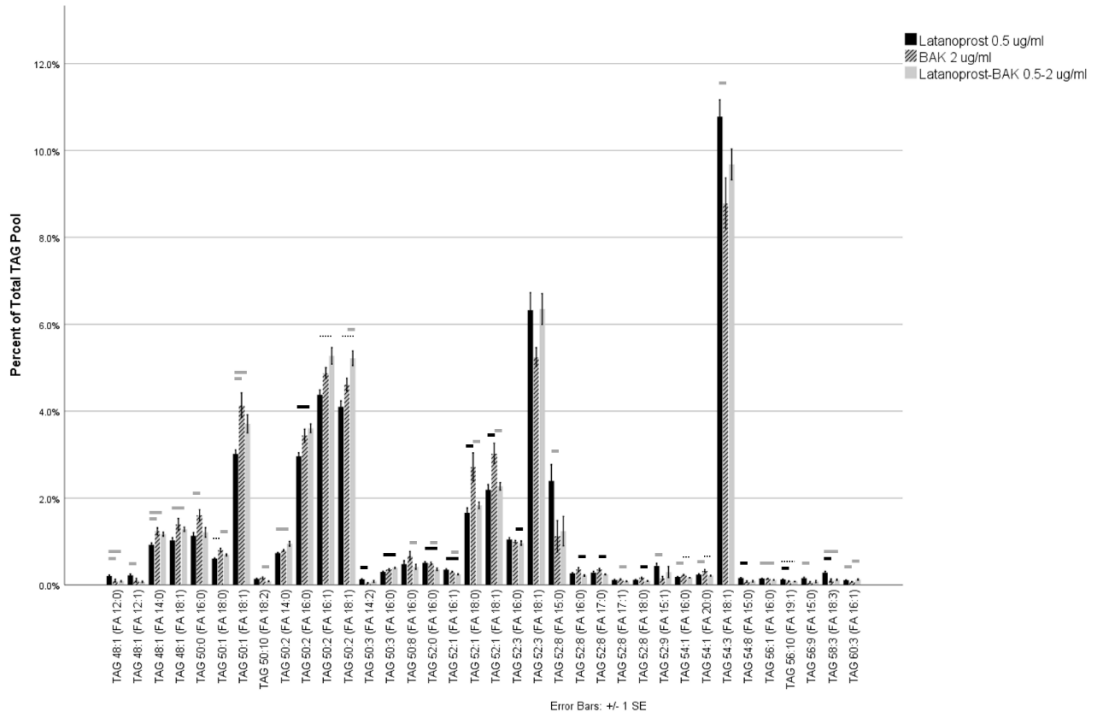

Figure 15 Effect of Latanoprost-BAK 0.5-2 µg/ml on the HMGEC TAG Lipidome
HMGECs were differentiated for 48 hours prior to exposure to combined latanoprost-BAK for three hours. Lipid extracts were analyzed by ESI-MSMS^{ALL} (see Methods). Only the TAGs that reached significance are shown. Thirty-six of 121 TAGs (29.8%) were significantly different between latanoprost alone, BAK alone, or combined latanoprost-BAK. However, only three TAGs (TAG 50:2 [FA 18:1], TAG 52:0 [FA 16:0], and TAG 52:1 [FA 16:1]) showed significant differences between combined latanoprost-BAK and each component in isolation. TAGs are labeled by two numbers corresponding to the total number of carbons and the total number of double bonds, respectively. The fatty acid in parentheses represents one of the three fatty acids of the parent TAG molecule. n = 4 per condition
BAK: benzalkonium chloride
CE: cholesteryl esters
Gray bar: $p \leq 0.05$
Black bar: $p \leq 0.01$
Dashed bar: $p \leq 0.001$

Discussion

A growing body of evidence supports the association between MGD and the use of $PGF_{2\alpha}$ analogs to treat glaucoma.[5,10] We previously found that HMGECs do indeed

express FP, the receptor for $PGF_{2\alpha}$, and when exposed to $PGF_{2\alpha}$, HMGECs modify their lipidomic profile.[11] Therefore, the effects of latanoprost and its preservative BAK were explored on cell viability and lipidomic expression in HMGECs. We report that both latanoprost and BAK are lethal to HMGECs at concentrations found in commercially available eye drops. At sublethal concentrations, both compounds are capable of significantly shifting the lipidomic profile of cholesteryl esters and triacylglycerols. When assessing the combination of latanoprost and BAK, there was no additional toxicity and only negligible changes in the lipidome relative to the individual components alone. These results suggest that, at the ocular surface, instillation of latanoprost and BAK has the potential to change the chemical composition of the tear film lipid layer, likely altering tear film dynamics and ocular surface lubrication.

Both latanoprost and BAK were toxic at the concentrations of 50 and 200 μg/ml, respectively, the same concentrations found in commercially available latanoprost. These results are unsurprising and consistent with our hypothesis for BAK, whose cytotoxic effects have been well-documented in the literature.[13,14,25-28] The absolute lethality associated with latanoprost, however, was greater than expected, though having some degree of toxicity is consistent with other literature reports. Others have also detected decreased viability following latanoprost stimulation in HMGECs[25] and other cell types.[26,29,30] Kam et al. assessed a prostamide (a PGA-like compound), bimatoprost, and found that it significantly reduced phosphorylation of protein kinase B, a surrogate marker of decreased cell survival.[31] Whether latanoprost is toxic to the meibomian glands in vivo, though, remains unknown. The concentration that reaches the tarsal plate has yet to be elucidated. In the aqueous humor, however, peak concentration is approximately 10^{-}

$^{-7}$ M (roughly equivalent to the lowest concentration used in this study).[32] If similar tissue distribution dynamics exist through the eyelid, then latanoprost would be at a sublethal concentration in the tarsal plate.

Of particular interest, latanoprost appears to induce its toxic effects through a mechanism other than signaling through FP and EP receptors—the cognate receptors for $PGF_{2\alpha}$ and PGE_2. Even with total FP- and EP-receptor blockade, the lethality of latanoprost 50 μg/ml was unchanged (Figure 3). These findings are in agreement with the recent report by Shen et al.[30] They evaluated the mechanism of cellular death attributed to latanoprost and found that both the extrinsic and intrinsic apoptotic pathways, which are mediated by death receptors on the cell surface and the mitochondria, respectively, are activated. While death receptors were once believed to send only pro-apoptotic signals, emerging data reveals that death receptors contribute to the regulation of cell proliferation, cell differentiation, inflammation, and chemokine production, among others.[33] The results of Shen et al., combined with our findings, highlight the possibility of alternate mechanisms beyond FP- and EP-receptor engagement for the numerous local side effects observed clinically with PGA use.

Beyond their lethal effects at therapeutic doses, both latanoprost and BAK demonstrated the ability to modulate lipid expression at sublethal concentrations. These findings are consistent with our[11] and others' previous work.[34] These effects are presumed to be mediated through the FP receptor's downstream inhibition of peroxisome proliferator activator receptor γ (PPARγ),[35] as previously discussed at length,[11] and through BAK's regulation of genes involved in sterol biosynthesis and liver X receptor.[34] An unexpected finding, though, was what appeared to be a mostly positive influence on

the expression of select cholesteryl esters and triacylglycerols by both latanoprost and BAK. Latanoprost exhibited a concentration-dependent increase, albeit relatively weak, on a few monounsaturated CEs that consisted of either very long- or ultra long-chain fatty acyl groups—CEs that are considered to be "meibum-relevant"[20] and abundantly expressed in vivo.[36] BAK downregulated select polyunsaturated CEs and upregulated some saturated and monounsaturated CEs, particularly those with very or ultra long-chain fatty acyl groups, emulating a profile that is similar to normal human meibum.[20,36] Further, both latanoprost and BAK upregulated select TAGs mostly bearing 16 or 18 carbons, which may potentially serve as a surrogate marker of fatty acid synthesis.[21] If these observed trends in the lipidomic profile are translated to the ocular surface, then it appears that latanoprost and BAK, paradoxically, could promote a more normal expression profile from the meibomian glands.

One possibility to explain this phenomenon is oxidative stress-induced fatty acid synthesis. Sedlak et al. recently reported that latanoprost was associated with several elevated oxidative stress markers in human tears and that these markers were further exacerbated by BAK.[37] There is also strong evidence for a role of oxidative stress in both MGD and dry eye disease.[38-40] Despite this association with ocular surface disease, recent papers have highlighted the link between oxidative stress, fatty acid metabolism,[41] and lipid droplet accumulation.[42] Even the mouse model of MGD used by Bu et al. describes an association between oxidative stress and lipid accumulation.[40] Historically, in this line of research, authors, we included, have associated lipid accumulation as a normal marker of meibomian gland health. However, these reports are suggesting that lipid accumulation may also be associated with oxidative stress, a known contributor to ocular surface

disease. These observations emphasize the tissue-level complexity of MGD pathophysiology and highlight opportunities for further research.

Extrapolating these findings to the ocular surface in vivo should be performed with caution. Our experiments focused on lipidomic expression and cell viability in a meibomian gland epithelial cell line. Other mechanisms for MGD development in response to latanoprost and BAK could include hyperkeratinization,[43] inflammatory cell infiltration,[15-19] and physicochemical tear disruption,[44] to name a few. Future research directions include a mechanistic interrogation into oxidative stress and fatty acid synthesis in HMGECs.

In conclusion, both latanoprost and BAK are lethal at therapeutic concentrations found in commercially available eye drops, an effect that appears to be independent of FP and EP receptors. The extent to which this toxicity is observed *in vivo* remains unknown and is likely contingent upon the degree of latanoprost's and BAK's penetration into the tarsal plate. We further report that both compounds are capable of modulating the lipidomic profile of HMGECs but do so, paradoxically, by promoting increased expression of CEs and TAGs that are largely believed to be associated with normal human meibum. As a conjecture, we presented the hypothesis that oxidative stress-induced fatty acid synthesis could be mediating these observations. Moving forward, clinicians involved in the care of glaucoma patients should consider the effects of PGAs and their preservative systems on the meibomian glands, evaluate the efficacy and safety profiles of other options prior to initiating treatment, and opt for BAK-free formulations when circumstances permit.

Funding: This work was supported by the Office of Research Infrastructure Programs of the National Institutes of Health under S10 RR027822-01 and the National Eye Institute under P30 EY003039 and K23 EY028629-01.

References

1. Quigley HA, Broman AT. The number of people with glaucoma worldwide in 2010 and 2020. Br J Ophthalmol. 2006;90(3):262-267.

2. Coleman AL, Kodjebacheva G. Risk factors for glaucoma needing more attention. Open Ophthalmol J. 2009;3:38-42.

3. Hollo G. The side effects of the prostaglandin analogues. Expert Opin Drug Saf. 2007;6(1):45-52.

4. S DIS, Agnifili L, Cecannecchia S, A DIG, Ciancaglini M. In Vivo Analysis of Prostaglandins-induced Ocular Surface and Periocular Adnexa Modifications in Patients with Glaucoma. In Vivo. 2018;32(2):211-220.

5. Batra R, Tailor R, Mohamed S. Ocular surface disease exacerbated glaucoma: optimizing the ocular surface improves intraocular pressure control. J Glaucoma. 2014;23(1):56-60.

6. Broadway DC, Grierson I, O'Brien C, Hitchings RA. Adverse effects of topical antiglaucoma medication. II. The outcome of filtration surgery. Arch Ophthalmol. 1994;112(11):1446-1454.

7. Boimer C, Birt CM. Preservative exposure and surgical outcomes in glaucoma patients: The PESO study. J Glaucoma. 2013;22(9):730-735.

8. Knop E, Knop N, Millar T, Obata H, Sullivan DA. The international workshop on meibomian gland dysfunction: report of the subcommittee on anatomy, physiology, and pathophysiology of the meibomian gland. Invest Ophthalmol Vis Sci. 2011;52(4):1938-1978.

9. Mocan MC, Uzunosmanoglu E, Kocabeyoglu S, Karakaya J, Irkec M. The Association of Chronic Topical Prostaglandin Analog Use With Meibomian Gland Dysfunction. J Glaucoma. 2016;25(9):770-774.

10. Cunniffe MG, Medel-Jimenez R, Gonzalez-Candial M. Topical antiglaucoma treatment with prostaglandin analogues may precipitate meibomian gland disease. Ophthalmic Plast Reconstr Surg. 2011;27(5):e128-129.

11. Material intended for publication: Ziemanski JF, Wilson L, Barnes S, Nichols KK. Prostaglandin E2 and F2a alter expression of select cholesteryl esters and triacylglycerols produced by human meibomian gland epithelial cells. 2020.

12. Pereira B, Tagkopoulos I. Benzalkonium chloride: uses, regulatory status, and microbial resistance. Applied and Environmental Microbiology. 2019;85(13):1-13.

13. Tripathi BJ, Tripathi RC, Kolli SP. Cytotoxicity of ophthalmic preservatives on human corneal epithelium. Lens Eye Toxic Res. 1992;9(3-4):361-375.

14. Baudouin C, de Lunardo C. Short-term comparative study of topical 2% carteolol with and without benzalkonium chloride in healthy volunteers. Br J Ophthalmol. 1998;82(1):39-42.

15. Liang H, Baudouin C, Pauly A, Brignole-Baudouin F. Conjunctival and corneal reactions in rabbits following short- and repeated exposure to preservative-free tafluprost, commercially available latanoprost and 0.02% benzalkonium chloride. Br J Ophthalmol. 2008;92(9):1275-1282.

16. Liang H, Baudouin C, Faure MO, Lambert G, Brignole-Baudouin F. Comparison of the ocular tolerability of a latanoprost cationic emulsion versus conventional formulations of prostaglandins: an in vivo toxicity assay. Mol Vis. 2009;15:1690-1699.

17. Mastropasqua L, Agnifili L, Mastropasqua R, et al. In vivo laser scanning confocal microscopy of the ocular surface in glaucoma. Microsc Microanal. 2014;20(3):879-894.

18. Mastropasqua R, Agnifili L, Fasanella V, et al. The Conjunctiva-Associated Lymphoid Tissue in Chronic Ocular Surface Diseases. Microsc Microanal. 2017;23(4):697-707.

19. Pauly A, Roubeix C, Liang H, Brignole-Baudouin F, Baudouin C. In vitro and in vivo comparative toxicological study of a new preservative-free latanoprost formulation. Invest Ophthalmol Vis Sci. 2012;53(13):8172-8180.

20. Material intended for publication: Ziemanski JF, Wilson L, Barnes S, Nichols KK. Saturation of cholesteryl esters produced by human meibomian gland epithelial cells after treatment with rosiglitazone. 2020.

21. Material intended for publication: Ziemanski JF, Wilson L, Barnes S, Nichols KK. Triacylglycerol lipidome from human meibomian gland epithelial cells: description, response to culture conditions, and perspective on function. 2020.

22. Kim SW, Xie Y, Nguyen PQ, et al. PPARgamma regulates meibocyte differentiation and lipid synthesis of cultured human meibomian gland epithelial cells (hMGEC). Ocul Surf. 2018;16(4):463-469.

23. Kim SW, Brown DJ, Jester JV. Transcriptome analysis after PPARgamma activation in human meibomian gland epithelial cells (hMGEC). Ocul Surf. 2019;17(4):809-816.

24. Ziemanski JF, Chen J, Nichols KK. Evaluation of Cell Harvesting Techniques to Optimize Lipidomic Analysis from Human Meibomian Gland Epithelial Cells in Culture. Int J Mol Sci. 2020;21(9).

25. Rath A, Eichhorn M, Trager K, Paulsen F, Hampel U. In vitro effects of benzalkonium chloride and prostaglandins on human meibomian gland epithelial cells. Ann Anat. 2019;222:129-138.

26. Brasnu E, Brignole-Baudouin F, Riancho L, Guenoun JM, Warnet JM, Baudouin C. In vitro effects of preservative-free tafluprost and preserved latanoprost, travoprost, and bimatoprost in a conjunctival epithelial cell line. Curr Eye Res. 2008;33(4):303-312.

27. Chang C, Zhang AQ, Kagan DB, Liu H, Hutnik CM. Mechanisms of benzalkonium chloride toxicity in a human trabecular meshwork cell line and the protective role of preservative-free tafluprost. Clin Exp Ophthalmol. 2015;43(2):164-172.

28. Chen X, Sullivan DA, Sullivan AG, Kam WR, Liu Y. Toxicity of cosmetic preservatives on human ocular surface and adnexal cells. Exp Eye Res. 2018;170:188-197.

29. Robciuc A, Witos J, Ruokonen SK, et al. Pure Glaucoma Drugs Are Toxic to Immortalized Human Corneal Epithelial Cells, but They Do Not Destabilize Lipid Membranes. Cornea. 2017;36(10):1249-1255.

30. Shen JW, Shan M, Peng YY, Fan TJ. Cytotoxic Effect of Latanoprost on Human Corneal Stromal Cells in vitro and its Possible Mechanisms. Curr Eye Res. 2017;42(4):534-541.

31. Kam WR, Liu Y, Ding J, Sullivan DA. Do Cyclosporine A, an IL-1 Receptor Antagonist, Uridine Triphosphate, Rebamipide, and/or Bimatoprost Regulate Human Meibomian Gland Epithelial Cells? Invest Ophthalmol Vis Sci. 2016;57(10):4287-4294.

32. Sjoquist B, Stjernschantz J. Ocular and systemic pharmacokinetics of latanoprost in humans. Surv Ophthalmol. 2002;47 Suppl 1:S6-12.

33. Guicciardi ME, Gores GJ. Life and death by death receptors. FASEB J. 2009;23(6):1625-1637.

34. Herron JM, Hines KM, Tomita H, Seguin RP, Cui JY, Xu L. Multi-omics investigation reveals benzalkonium chloride disinfectants alter sterol and lipid homeostasis in the mouse neonatal brain. Toxicol Sci. 2019.

35. Reginato MJ, Krakow SL, Bailey ST, Lazar MA. Prostaglandins promote and block adipogenesis through opposing effects on peroxisome proliferator-activated receptor gamma. J Biol Chem. 1998;273(4):1855-1858.

36. Chen J, Nichols KK. Comprehensive shotgun lipidomics of human meibomian gland secretions using MS/MS(all) with successive switching between acquisition polarity modes. J Lipid Res. 2018;59(11):2223-2236.

37. Sedlak L, Zych M, Wojnar W, Wygledowska-Promienska D. Effect of Topical Prostaglandin F2alpha Analogs on Selected Oxidative Stress Parameters in the Tear Film. Medicina (Kaunas). 2019;55(7).

38. Yoon CH, Ryu JS, Hwang HS, Kim MK. Comparative Analysis of Age-Related Changes in Lacrimal Glands and Meibomian Glands of a C57BL/6 Male Mouse Model. Int J Mol Sci. 2020;21(11).

39. Seen S, Tong L. Dry eye disease and oxidative stress. Acta Ophthalmol. 2018;96(4):e412-e420.

40. Bu J, Wu Y, Cai X, et al. Hyperlipidemia induces meibomian gland dysfunction. Ocul Surf. 2019;17(4):777-786.

41. Mikalayeva V, Cesleviciene I, Sarapiniene I, et al. Fatty Acid Synthesis and Degradation Interplay to Regulate the Oxidative Stress in Cancer Cells. Int J Mol Sci. 2019;20(6).

42. Lee J, Homma T, Kurahashi T, Kang ES, Fujii J. Oxidative stress triggers lipid droplet accumulation in primary cultured hepatocytes by activating fatty acid synthesis. Biochem Biophys Res Commun. 2015;464(1):229-235.

43. Hampel U, Schroder A, Mitchell T, et al. Serum-induced keratinization processes in an immortalized human meibomian gland epithelial cell line. PLoS One. 2015;10(6):e0128096.

44. Georgiev GA, Yokoi N, Ivanova S, Krastev R, Lalchev Z. Surface chemistry study of the interactions of pharmaceutical ingredients with human meibum films. Invest Ophthalmol Vis Sci. 2012;53(8):4605-4615.

CHAPTER SEVEN: DISCUSSION

The goals of this dissertation were twofold. The first objective was to develop an experimental "prototype" for cell culture methods specific to HMGECs after which future lipidomic experiments could be modeled. The development of the prototype sought to define methods for cell harvesting and differentiating culture conditions. The second objective was to use this experimental model to better understand the physiologic effects of prostaglandins, specifically PGE_2 and $PGF_{2\alpha}$, and the pathophysiologic effects of latanoprost, a $PGF_{2\alpha}$ analog, and its preservative system, benzalkonium chloride (BAK), on HMGECs. It was hypothesized that HMGECs would express two PGE_2 receptors—EP2 and EP4—to which latanoprost would exhibit cross-over binding to alter lipid expression. From preliminary work described in the Introduction (Chapter One) and the first three papers (Chapters Two, Three, and Four), an experimental prototype for cell culture methods was successfully developed. The model was applied in the subsequent experiments using PGE_2, $PGF_{2\alpha}$, latanoprost, and BAK. The results of these experiments are summarized and placed in context with the literature below.

DEVELOPMENT OF AN EXPERIMENTAL PROTOTYPE

Methods for cell harvesting

Prior to initiating this project, there were several motivations underpinning the need for an optimized harvesting protocol. First and foremost among these motivations

was the concern for the discrepancy between the lipidomic profiles obtained from HMGECs in culture[40,77,132] and from human meibum *in vivo*.[62,63] The dissimilar profiles had been previously described,[78] raising concern for whether HMGECs were an accurate cell culture model of the meibomian glands. It was also known that trypsin—a protease widely used in cell culture for dissociating adhered cells from the growth surface during passaging or in preparation for experimental manipulations—could be overly abrasive to the cell membrane, resulting in leakage of intracellular metabolites into the extracellular environment.[130] A review of published papers at the time revealed that trypsin was the only harvesting method that had been utilized.[40,77] An additional motivating factor, though weaker in comparison to the aforementioned two, was the awareness that mass spectrometry is poorly configured for high throughput analysis, given the time-consuming nature of sample preparation and lipid analysis. A more efficient method for harvesting and extracting lipids would make mass spectrometry a more accessible tool to researchers in the field of cell-based lipidomics.

This dissertation evaluated three different cell harvesting methods in Chapter Two: 0.25% trypsin-EDTA (the classic method), 10 mM ethylenediaminetetraacetic acid (EDTA, a trypsin-free dissociation agent), and 2:1 chloroform-methanol (v/v). It was demonstrated that all three methods yielded sufficient lipid extraction and similar lipid profiles. The hypothesis that trypsin reduces membrane integrity and promotes neutral lipid loss was not supported, however, as the trypsin-free techniques did not provide a more robust nonpolar lipid profile. A key advancement from this work, though, was greater efficiency with the direct application of 2:1 chloroform-methanol (v/v) to HMGECs in culture. This method combined the steps of cell harvesting with the early

steps of lipid extraction, abrogating the need for subsequent time-consuming wash steps and a second introduction of the serum lipidome, a potential source of lipid contamination. Though progress was made in the way of improved research efficiency, optimization of an HMGEC lipid profile that bore resemblance to normal human meibum continued.

Methods for culture conditions to induce differentiation

The focus shifted toward culture conditions, specifically toward an agent that could stimulate terminal differentiation of HMGECs with the goal of promoting increased neutral lipid production. Since the HMGEC line was first developed in 2010,[53] several differentiating agents have been used. The first and most common was serum-induced differentiation;[40,53] however, this method was later questioned due to poor replication of nonpolar lipid accumulation and increased cytokeratin expression.[77,82] Azithromycin has also been proposed,[80,135,136] yet its mechanism of inducing phospholipidosis is not consistent with the lipid content from meibomian gland secretions.[62,63] As somewhat of a mechanistic breakthrough, Jester and his colleagues found that PPARγ regulated differentiation in mouse meibocytes in 2016[81] and in immortalized HMGECs in 2018.[82] Given that PPARγ agonism was the first, well-validated differentiating method for HMGECs, attention was shifted toward rosiglitazone, a PPARγ agonist, as a means to differentiate these cells.

In Chapters Three and Four, several parameters related to differentiating culture conditions were evaluated. A 3 x 2 x 2 factor design was utilized to assess rosiglitazone (0, 20, or 50 µM), FBS (2% versus 10%), and culture duration (two days versus five

days). In these experiments, optimization was guided by the expression of cholesteryl esters (CE), a nonpolar lipid class that has been comprehensively described and well-characterized in meibum.[61,62,64-66] It was found that HMGECs that were differentiated with 50 μM rosiglitazone and 2% FBS for two days yielded a CE profile that was more consistent with human meibum—specifically, a profile with higher levels of saturated and monounsaturated CEs and lower levels of polyunsaturated CEs (Chapter Three).[62,65,66]

To further delve into nonpolar lipids, particularly TAGs, an exploratory analysis on these same factors was presented in Chapter Four. TAGs are a complex lipid class, primarily owing to their isomeric variability. This complexity, paired with its overall lower abundance in human meibum, is likely why TAGs have not been characterized in meibum as comprehensively as CEs (and WEs). Optimization on a poorly characterized variable would be fraught with challenges; therefore, a factor analysis to better understand how each differentiating parameter (rosiglitazone, FBS, and culture duration) influenced TAG expression was performed. The results were particularly insightful. Both FBS and rosiglitazone were found to be powerful modulators of the majority of expressed TAGs from HMGECs (about 70% and 60%, respectively). The most striking discovery, however, was that FBS and rosiglitazone induced opposing effects on meibum-relevant TAGs. Culturing with rosiglitazone yielded a TAG profile that was more consistent with the expected outcome of lipogenesis[137] and with the profile observed in normal human meibum.[62]

These two papers (Chapters Three and Four), both evaluating different parameters and utilizing different statistical approaches, arrived at the same conclusions: more

rosiglitazone, less FBS, and a shorter duration promote a more meibum-like lipid profile from HMGECs. It remains worthy of emphasis, however, that the overall lipid profile from HMGECs, though optimized through the experiments just described, remains significantly different from normal human meibum. A perspective on these differences is presented in the Limitations section below.

The remainder of the dissertation experiments used HMGECs that had been differentiated with 50 μM rosiglitazone and 2% FBS for two days. HMGECs were harvested and lipids were extracted by directly adding 2:1 chloroform-methanol (v/v) to the cells in culture. Therefore, upon conclusion of this preliminary work, the first goal of the dissertation—to develop an experimental prototype after which future experiments could be modeled—had been achieved.

EVALUATION OF PROSTAGLANDINS ON HMGECs

With experimental methods established, focus was shifted toward the underlying clinical motivation for this dissertation: patients with glaucoma who are treated with prostaglandin analogs (PGAs) develop high rates of meibomian gland dysfunction (MGD).[7,8,138] In the planning stages of this project, however, it was realized that very little was known about prostaglandins, let alone their analogs, on the meibomian glands or in HMGECs. As an intermediate step toward addressing PGA-associated MGD, a series of experiments were added to understand the physiologic effects of $PGF_{2\alpha}$ and PGE_2 on HMGECs.

Initially, it was only known that bimatoprost (another ocular hypotensive with PGA-like qualities) decreased a marker of HMGEC survivability but induced no effect on

lipid production.[112] However, this experiment was performed on pre-differentiated HMGECs and used a low dose of bimatoprost, a prostamide that may work through an FP-independent mechanism,[139] rather than a true $PGF_{2\alpha}$ analog. This field of research, therefore, was largely nascent and untapped, requiring that hypotheses be generated from literature examples of other cell culture systems. It was hypothesized that HMGECs would most strongly express EP2 and EP4 receptors, similar to sebocytes,[96] and that treatment with PGE_2 and perhaps $PGF_{2\alpha}$ would stimulate these receptors, ultimately modifying lipid production, as observed in colonic epithelium.[97]

Upon completion of the work, it was found that HMGECs do indeed express receptors for PGE_2 (EP1, EP2, and EP4) and $PGF_{2\alpha}$ (FP) and that a broad physiologic range of concentrations for these prostaglandins had no effect on HMGEC viability. While this EP expression pattern is consistent with the documented pattern observed in sebocytes,[96] expression of the FP receptor seems to be an interesting difference between the two cells, emphasizing that meibocytes possess unique characteristics that distinguish them from sebocytes. It was learned through these experiments that $PGF_{2\alpha}$ has the capacity to modulate the CE and TAG profiles more powerfully than PGE_2, deviating from the hypothesis that lipidomic influence would be mediated through EP-type receptors. With new perspective, the updated hypothesis has been revised such that $PGF_{2\alpha}$'s effects are believed to be mediated through the FP receptor with downstream events resulting in—paradoxically—both PPARγ inhibition and activation, mechanisms previously described in both adipocytes and sebocytes (Figure 1).[140,141] If this new hypothesis is correct, then potential exists for competition between rosiglitazone and

$PGF_{2\alpha}$ in the experimental model, a topic discussed in detail in Chapter Five and touched upon again in the Limitations section below.

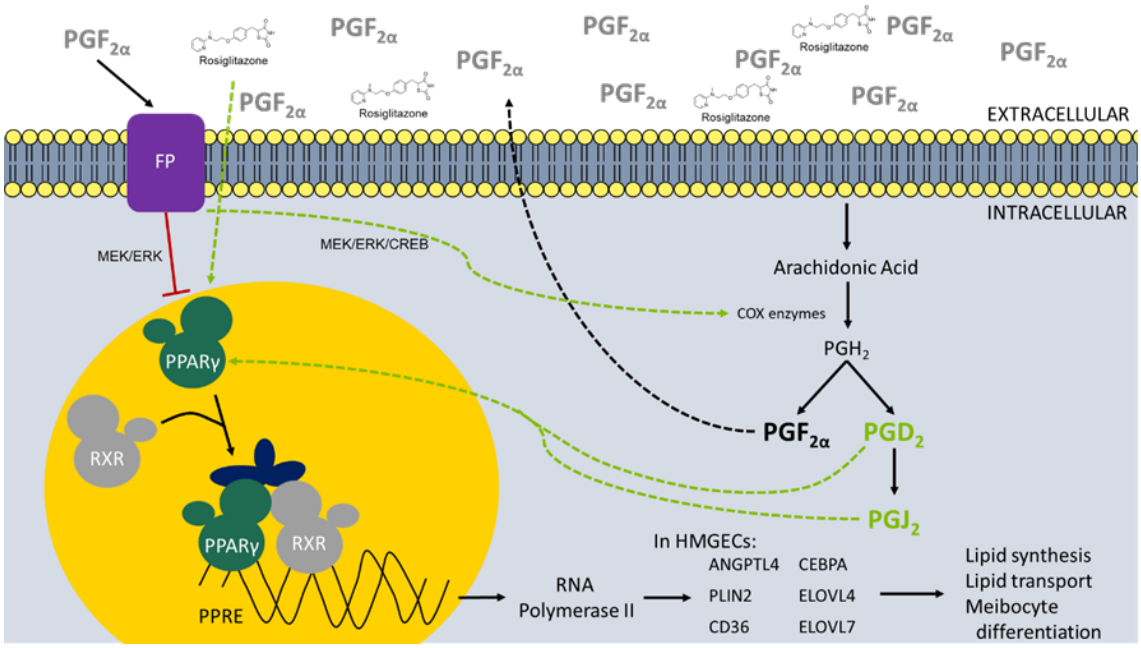

Figure 1 Theoretical Construct of Converging Pathways on PPARγ
HMGECs were differentiated with rosiglitazone, a PPARγ agonist. Upon activation, PPARγ dimerizes with RXR, associates with other co-activators, and binds to PPRE. Transcription occurs via RNA polymerase II, resulting in the upregulation of several transcripts (ANGPTL4, PLIN2, CD36, CEBPA, ELOVL4, and ELOVL7) involved in lipid synthesis, lipid transport, and meibocyte differentiation. In the experimental model described in Aim 1 (Chapter Five), multiple competing pathways, all converging on PPARγ, were likely present. $PGF_{2\alpha}$ leads to the phosphorylation and inhibition of PPARγ through FP receptor signaling. It also leads to upregulation of COX-2 synthesis via a MEK/ERK/CREB pathway. In the presence of increased COX enzymes, arachidonic acid is converted into PGH_2, a common precursor to $PGF_{2\alpha}$ and PGD_2. PGD_2 and PGJ_2 are both potent activators of PPARγ. Therefore, the FP receptor may be capable of inducing signal transduction pathways that ultimately simultaneously activate and inhibit PPARγ. Adding to the complexity, rosiglitazone was present in the culture media to maintain the HMGECs in a differentiated state, which provided an additional source of PPARγ activation. Figure was adapted from Jack Vanden Heuvel, PhD (Nuclear Receptor Resource, nrresource.org) and modified to include Kim et al. 2019,[83] Reginato et al. 1998,[141] and Ueno and Fujimori 2011.[142]
MEK = mitogen-activated protein kinase kinase
ERK = mitogen-activated protein kinase (also known as MAPK)
CREB = cyclic AMP response element-binding protein
PPARγ = peroxisome proliferator activator receptor gamma

RXR = retinoid X receptor
PPRE = peroxisome proliferator response elements
COX = cyclooxygenase
HMGEC = human meibomian gland epithelial cell

EVALUATION OF LATANOPROST AND BAK ON HMGECs

Armed with the knowledge that HMGECs express FP receptors and that $PGF_{2\alpha}$ induces lipidomic remodeling, suspicion that latanoprost would behave similarly was heightened. An early distinction in the experimental objectives for these two aims was to evaluate the *physiologic* effects of endogenous prostaglandins and the *patho*physiologic effects of synthetic prostaglandin analogs. $PGF_{2\alpha}$ and PGE_2 concentrations were chosen to vary from 10^{-9} to 10^{-6} M, while latanoprost was chosen to vary from approximately 10^{-7} to 10^{-4} M (0.05 µg/ml to 50 µg/ml). This higher range for latanoprost was chosen to span from the peak concentration detected in the aqueous humor after instillation[143] up to the full therapeutic dose delivered to the ocular surface. Upon completing the cell viability experiments, it was found that latanoprost was lethal at a therapeutic concentration (50 µg/ml). Considering that latanoprost exhibits nanomolar affinity for the FP receptor,[91] even greater than the affinity of $PGF_{2\alpha}$,[91] it was initially thought that excessive stimulation of the FP receptor at this 100x greater dose may have been mediating the observed dramatic increase in cell death. Contrary to this conjecture, however, was the outcome of subsequent experiments: when all FP and EP receptors were inhibited, latanoprost at 50 µg/ml was still just as lethal, suggesting an FP- and EP-independent mechanism for promoting cell death. As was discussed in Chapter Six, the prevailing thought is that this FP-independent mechanism includes stimulation of both the extrinsic and intrinsic apoptotic pathways.[144]

The bigger question, here, is whether latanoprost promotes cell death in vivo. The residence time of latanoprost on the ocular surface is likely rather rapid, as a certain portion of the full therapeutic dose would be quickly metabolized and absorbed by the various tissues of the ocular surface within a few minutes. The portion that is not quickly taken up by the tissues would be subject to drainage through the nasolacrimal system with each blink of the eyelids.[145] Therefore, the full therapeutic concentration of 50 µg/ml would not reach the meibomian glands, though the exact concentration that does reach them is unknown. If similar penetration kinetics exist between the tarsal plate and the cornea, then patients and doctors may take comfort in knowing that the lower concentrations of latanoprost that actually do get absorbed[143] appear to have no effect on cell viability.

Consistent with the hypothesis was BAK's dose-dependent effect on cell viability, a phenomenon already well-described.[117,123,126,127,146] BAK operates through a detergent mechanism, disrupting cell membranes and triggering lysis.[116] Since embarking on this research project, two other groups have evaluated the effects of BAK on HMGECs, and all reports are in agreement: BAK is toxic to HMGECs.[127,128] The more interesting question related to these BAK-related cell viability experiments was whether the combination of latanoprost and BAK, as is formulated pharmaceutically, provided an additive or synergistic toxic effect. As a reassuring finding for clinicians, it appears that the combination is no more lethal than its most lethal component: there is no added concern of cell death, at least for HMGECs, beyond the already known effects of BAK.

The story of how latanoprost and BAK alter the HMGEC lipidome is far more complex and somewhat speculative, opening doors for future experimentation. It appears

as though latanoprost elicited a weaker overall effect relative to $PGF_{2\alpha}$, at least based on the number of CEs and TAGs that responded to each. Latanoprost altered 8% of CEs and 10% of TAGs, while $PGF_{2\alpha}$ altered 18% and 16%, respectively. These experiments, unfortunately, are not amenable to inference testing to ascertain whether these are truly significant differences, but assuming they are, then there may be a difference in how $PGF_{2\alpha}$ and latanoprost inflict their effects on HMGECs. Despite this potential difference, the more interesting observation is what $PGF_{2\alpha}$ and latanoprost have in common: a low-dose suppression followed by a quasi-dose-dependent increase in several CEs and TAGs. This pattern was discussed at length in Chapter Five and postulated to be secondary to FP-mediated inhibition of PPARγ[141] at low doses that is overwhelmed by positive-feedback upregulation of endogenously produced prostaglandins[142,147,148] known to activate PPARγ[149] at higher doses. It also cannot be ruled out that these observations could be secondary to random variations in enormous datasets; however, the consistency suggests that these are true relationships resulting from what is currently an ill-defined mechanism. Further experimentation is necessary to elucidate the pathways accounting for these patterns.

When initially undertaking this project, BAK's effects on the HMGEC lipidome was anticipated to be non-specific and associated with its dose-dependent toxicity. Upon completion, however, a greater appreciation was developed for BAK's ability to modulate physiology at sublethal concentrations. It is much more functionally active than presumed and more than just a proverbial grenade to the ocular surface. The most striking observation was that nearly one-third of all CEs detected were affected by BAK. With a more targeted search of the literature, it was found that BAK has a known influence on

the regulation of sterol biosynthesis.[150] Further, in this dissertation project, BAK mostly downregulated polyunsaturated CEs and upregulated saturated or monounsaturated CEs, including those with chain lengths of at least 20 carbons—a clinical paradox to say the least. A molecule presumed to be highly toxic and mostly lethal appears to be modulating the HMGEC lipid profile to be *more similar* to normal human meibum. Even latanoprost exhibited this pattern, albeit to a lesser extent. Assuming these are real relationships that translate into clinical care, clinicians should remain mindful of the numerous other effects that BAK exerts on other parameters (degradation of tight junctions, inflammatory cell infiltration, induction of epitheliopathy, etc)[117,120,123-127,146] on a variety of ocular surface tissues. Even beyond its biological effects, BAK has extensive physiochemical influence on the tear film lipid layer that cannot be ignored.[151] The bulk of the literature supports a plethora of adverse events associated with BAK, even if the potential for promoting a favorable CE expression profile truly exists.

PITFALLS AND TROUBLESHOOTING

While progressing through this work, a few challenges were met, most of which were attributed to naïveté with immunostaining, fluorescent microscopy, and image processing. To facilitate imaging, HMGECs were cultured on 8-well chambered slides. Despite sufficient seeding initially, few cells remained when it became time to initiate the immunostaining protocol. It was assumed that media aspiration had been performed too vigorously throughout the cell culture steps. Repeated attempts avoided vacuum aspiration and utilized gentler, manual aspiration with an improvement in cell number.

The first attempt at immunostaining followed a protocol that recommended an air-tight seal created by paraffin film around the chamber slide while incubating with the primary antibody overnight at 4°C. Following the incubation, the antibody diluent had evaporated; therefore, the decision to cease that particular experimental replicate was made out of concern for high levels of non-specific staining and high false positives. To address this pitfall, the immunostaining protocol was modified to incorporate a humidified chamber for incubation, which successfully prevented any further problems with evaporation.

The last challenge that was encountered required greater troubleshooting. The image quality was subpar during early attempts, so a series of modifications were taken to improve quality. Through an iterative process, images were improved by adding z stacks, increasing intensity of the channel sensitive to the secondary antibody fluor, increasing exposure duration of the same channel, utilizing an autofocus plug-in to identify the best focus, binning adjacent pixels, and deconvolving all images. These modifications ultimately led to significantly increased image quality sufficient for publication standards.

LIMITATIONS

This dissertation project has two main limitations that could interfere with generalizability. The first is the possibility for confounding effects between rosiglitazone and FP-mediated signaling on PPARγ, as originally described in Chapter Five. With effects that converge on one particular nuclear receptor, it can be difficult to discern exactly how $PGF_{2\alpha}$ and latanoprost affect lipid synthesis. A series of follow-up

experiments are described below in the section titled Forward-Looking Statements that could help parse out these pathways.

The second limitation is one that is commonly raised in response to this particular cell line: is the HMGEC line representative of meibomian glands *in vivo*? It was described in the Introduction and in Chapters Two, Three, and Four that the lipid profiles between the two are vastly different. The HMGEC lipidome is high in phospholipids yet comparatively low in CEs and WEs, the inverse of the meibum lipidome.[40,77,78,132] To address this overarching question, what is known about these cells must be revisited. It is known that these cells are resident to the tarsal plate and that they exhibit a morphology consistent with an epithelial cell.[53] It is known that these cells produce lipids[40,53,77,78,135] and that they increase their lipid production in response to known lipogenic substances.[53,82,152] Indisputably, the field can likely agree that these cells are lipogenic epithelial cells that reside in the tarsal plate. Claiming that these are specifically acinar versus ductal cells—or some other epithelial source—is based only on preliminary, yet encouraging, work that shows that HMGECs under growth and differentiating conditions express biomarkers of progenitor and differentiated meibomian gland epithelial cells.[76] Further replication and corroboration of these findings would provide strong evidence that these cells are indeed derived from the meibomian gland acinar units.

Hampel proposed that the immortalization process of HMGECs inherently prevents terminal differentiation.[78] Both Chen et al.[39] and Sullivan et al.[40] proposed that phospholipid recycling occurs across the ductal epithelium *in vivo*. Therefore, expecting mature meibum to be expressed from HMGECs may be unrealistic and unattainable. Admittedly, the lack of wax ester expression is a concern, though other research groups

have detected small amounts.[40,53,77] Regardless of this cell's true identity, the extent to which it differentiates, or whether other cell types contribute to meibum production, the *changes* that are observed from stimulated HMGECs likely represent a change that would occur *in vivo* under similar conditions. HMGECs remain as a useful component of the MGD research portfolio, representing an important preclinical platform for testing very specific hypotheses that can guide translational and clinical research downstream.

FORWARD-LOOKING STATEMENTS

Like all good research, the search for answers often yields additional questions. The next most immediate step in this research is to analyze the lipid extracts from HMGECs stimulated with PGE_2, $PGF_{2\alpha}$, and latanoprost in the presence of EP- and FP-type receptor inhibitors. The outcome will provide insight into FP's role in lipid metabolism and isolate rosiglitazone as the only agent acting on PPARγ. Future directions include treating with $PGF_{2\alpha}$ and/or latanoprost and measuring downstream events: upregulation of second messengers, phosphorylation of PPARγ, and upregulation of PPARγ-regulated lipogenic gene products. Introducing cyclooxygenase inhibitors and measuring other synthesized prostaglandins will also elucidate whether a positive-feedback loop is promoting increased prostaglandin production.

A second research direction pursues the conjecture that oxidative stress stimulates lipid synthesis in latanoprost- and BAK-treated HMGECs, as presented in Chapter Six. As a simple, proof-of-concept experiment, HMGECs could be exposed to oxidative stress, and lipid accumulation could be measured by LipidTox staining. If lipids do indeed accumulate, subsequent experiments would be aimed to evaluate the lipidomic

response to oxidative stress, quantify oxidative stress markers in response to latanoprost and BAK treatment, and interrogate antioxidant mechanisms in HMGECs.

Drawing upon clinical experience and harnessing skills as a clinician-scientist, a human subjects-based research project is worthy of exploration. As has been reviewed extensively throughout this dissertation, there are known links between PGAs, BAK, and ocular surface disease (OSD). There is also evidence that OSD leads to worse treatment outcomes in glaucoma. To date, there is no known report of an adequately powered, prospective, randomized, controlled, clinical trial evaluating a preserved and nonpreserved PGA on long-term glaucomatous outcomes. If the adverse effects of preserved PGAs are confirmed in a well-designed clinical trial, then there may be enough compelling evidence to warrant a paradigm shift in the medical management of glaucoma.

TRANSLATION INTO CLINICAL CARE AND CONCLUSION

The development of OSD in patients treated with preserved PGAs is a topic of recent interest. Historically, OSD was viewed as no more than a nuisance, but clinicians are now beginning to gain the perspective that OSD may be a blinding eye condition when it interferes with successful glaucoma therapy.[1,20] While clinicians are encouraged to avoid overgeneralization of research from cell culture systems, the following comprise a list of clinical applications and low-risk recommendations supported by this body of work. First, the concentration of latanoprost that is likely to reach the meibomian glands after a single instillation is probably not lethal. It is unknown whether there is a cumulative effect with repeated daily dosing. Second, both latanoprost and BAK appear

to modify the lipid content from meibomian glands; therefore, clinicians should be aware that instilling these drops may change the composition of the tear film. BAK may change it more than latanoprost. Using a BAK-free or a non-preserved formulation, when feasible, may be prudent. Third, the benefits of latanoprost (excellent IOP-lowering efficacy, convenient dosing schedule, low systemic side effect profile, and affordability) outweigh the risk of latanoprost-induced tear film alterations. Fourth, proactive clinicians may choose to supplement latanoprost therapy with the use of non-preserved, lipid-based artificial tears even in asymptomatic patients with a healthy ocular surface.

Ongoing research that further elucidates the mechanisms for how OSD develops in the presence of PGAs and BAK can inform future drug engineering endeavors, leading to optimization of therapeutic effects and minimization of adverse events. With improved pharmaceuticals, patients treated for glaucoma may have better visual outcomes, ultimately prolonging the quality and duration of their sight.

GENERAL LIST OF REFERENCES

1. Batra R, Tailor R, Mohamed S. Ocular surface disease exacerbated glaucoma: optimizing the ocular surface improves intraocular pressure control. J Glaucoma. 2014;23(1):56-60.

2. Ghosh S, O'Hare F, Lamoureux E, Vajpayee RB, Crowston JG. Prevalence of signs and symptoms of ocular surface disease in individuals treated and not treated with glaucoma medication. Clin Exp Ophthalmol. 2012;40(7):675-681.

3. Kim JH, Shin YU, Seong M, Cho HY, Kang MH. Eyelid Changes Related to Meibomian Gland Dysfunction in Early Middle-Aged Patients Using Topical Glaucoma Medications. Cornea. 2018;37(4):421-425.

4. Lee SM, Lee JE, Kim SI, Jung JH, Shin J. Effect of topical glaucoma medication on tear lipid layer thickness in patients with unilateral glaucoma. Indian J Ophthalmol. 2019;67(8):1297-1302.

5. Uzunosmanoglu E, Mocan MC, Kocabeyoglu S, Karakaya J, Irkec M. Meibomian Gland Dysfunction in Patients Receiving Long-Term Glaucoma Medications. Cornea. 2016;35(8):1112-1116.

6. Cho WH, Lai IC, Fang PC, et al. Meibomian Gland Performance in Glaucomatous Patients With Long-term Instillation of IOP-lowering Medications. J Glaucoma. 2018;27(2):176-183.

7. Mocan MC, Uzunosmanoglu E, Kocabeyoglu S, Karakaya J, Irkec M. The Association of Chronic Topical Prostaglandin Analog Use With Meibomian Gland Dysfunction. J Glaucoma. 2016;25(9):770-774.

8. Cunniffe MG, Medel-Jimenez R, Gonzalez-Candial M. Topical antiglaucoma treatment with prostaglandin analogues may precipitate meibomian gland disease. Ophthalmic Plast Reconstr Surg. 2011;27(5):e128-129.

9. Tham YC, Li X, Wong TY, Quigley HA, Aung T, Cheng CY. Global prevalence of glaucoma and projections of glaucoma burden through 2040: a systematic review and meta-analysis. Ophthalmology. 2014;121(11):2081-2090.

10. Quigley HA, Broman AT. The number of people with glaucoma worldwide in 2010 and 2020. Br J Ophthalmol. 2006;90(3):262-267.

11. Foster PJ, Johnson GJ. Glaucoma in China: how big is the problem? Br J Ophthalmol. 2001;85(11):1277-1282.

12. Weinreb RN, Aung T, Medeiros FA. The pathophysiology and treatment of glaucoma: a review. JAMA. 2014;311(18):1901-1911.

13. Quigley HA, McKinnon SJ, Zack DJ, et al. Retrograde axonal transport of BDNF in retinal ganglion cells is blocked by acute IOP elevation in rats. Invest Ophthalmol Vis Sci. 2000;41(11):3460-3466.

14. Quigley HA, Addicks EM, Green WR, Maumenee AE. Optic nerve damage in human glaucoma. II. The site of injury and susceptibility to damage. Arch Ophthalmol. 1981;99(4):635-649.

15. Vrabec JP, Levin LA. The neurobiology of cell death in glaucoma. Eye (Lond). 2007;21 Suppl 1:S11-14.

16. Agnifili L, Brescia L, Oddone F, et al. The ocular surface after successful glaucoma filtration surgery: a clinical, in vivo confocal microscopy, and immune-cytology study. Sci Rep. 2019;9(1):11299.

17. Schwab IR, Linberg JV, Gioia VM, Benson WH, Chao GM. Foreshortening of the inferior conjunctival fornix associated with chronic glaucoma medications. Ophthalmology. 1992;99(2):197-202.

18. Liesegang TJ. Conjunctival changes associated with glaucoma therapy: implications for the external disease consultant and the treatment of glaucoma. Cornea. 1998;17(6):574-583.

19. Tauber J, Melamed S, Foster CS. Glaucoma in patients with ocular cicatricial pemphigoid. Ophthalmology. 1989;96(1):33-37.

20. Broadway DC, Grierson I, O'Brien C, Hitchings RA. Adverse effects of topical antiglaucoma medication. II. The outcome of filtration surgery. Arch Ophthalmol. 1994;112(11):1446-1454.

21. Milla E, Stirbu O, Rey A, et al. Spanish multicenter tafluprost tolerability study. Br J Ophthalmol. 2012;96(6):826-831.

22. Baudouin C, Riancho L, Warnet JM, Brignole F. In vitro studies of antiglaucomatous prostaglandin analogues: travoprost with and without benzalkonium chloride and preserved latanoprost. Invest Ophthalmol Vis Sci. 2007;48(9):4123-4128.

23. Wolff E. The muco-cutaneous junction of the lid margin and the distribution of the tear fluid. Trans Ophthalmol Soc U K. 1946;66:291-308.

24. Holly FJ, Lemp MA. Tear physiology and dry eyes. Surv Ophthalmol. 1977;22(2):69-87.

25. Willcox MDP, Argueso P, Georgiev GA, et al. TFOS DEWS II Tear Film Report. Ocul Surf. 2017;15(3):366-403.

26. Gipson IK, Argueso P. Role of mucins in the function of the corneal and conjunctival epithelia. Int Rev Cytol. 2003;231:1-49.

27. Spurr-Michaud S, Argueso P, Gipson I. Assay of mucins in human tear fluid. Exp Eye Res. 2007;84(5):939-950.

28. Dartt DA. Control of mucin production by ocular surface epithelial cells. Exp Eye Res. 2004;78(2):173-185.

29. Mishima S, Gasset A, Klyce SD, Jr., Baum JL. Determination of tear volume and tear flow. Invest Ophthalmol. 1966;5(3):264-276.

30. Braun R. Dynamics of the tear film. Annu Rev Fluid Mech. 2012;44:267-297.

31. Schuett BS, Millar TJ. An investigation of the likely role of (O-acyl) omega-hydroxy fatty acids in meibomian lipid films using (O-oleyl) omega-hydroxy palmitic acid as a model. Exp Eye Res. 2013;115:57-64.

32. Craig JP, Willcox MD, Argueso P, et al. The TFOS International Workshop on Contact Lens Discomfort: report of the contact lens interactions with the tear film subcommittee. Invest Ophthalmol Vis Sci. 2013;54(11):TFOS123-156.

33. Knop E, Knop N, Millar T, Obata H, Sullivan DA. The international workshop on meibomian gland dysfunction: report of the subcommittee on anatomy, physiology, and pathophysiology of the meibomian gland. Invest Ophthalmol Vis Sci. 2011;52(4):1938-1978.

34. Sirigu P, Shen RL, Pinto da Silva P. Human meibomian glands: the ultrastructure of acinar cells as viewed by thin section and freeze-fracture transmission electron microscopies. Invest Ophthalmol Vis Sci. 1992;33(7):2284-2292.

35. Nicolaides N, Kaitaranta JK, Rawdah TN, Macy JI, Boswell FM, 3rd, Smith RE. Meibomian gland studies: comparison of steer and human lipids. Invest Ophthalmol Vis Sci. 1981;20(4):522-536.

36. Olami Y, Zajicek G, Cogan M, Gnessin H, Pe'er J. Turnover and migration of meibomian gland cells in rats' eyelids. Ophthalmic Res. 2001;33(3):170-175.

37. Linton RG, Curnow DH, Riley WJ. The Meibomian Glands: An Investigation into the Secretion and Some Aspects of the Physiology. Br J Ophthalmol. 1961;45(11):718-723.

38. Josephson J. Appearance of the preocular tear film lipid layer. Am J Optom Physiol Opt. 1983;60:883-887.

39. Chen J, Green-Church KB, Nichols KK. Shotgun lipidomic analysis of human meibomian gland secretions with electrospray ionization tandem mass spectrometry. Invest Ophthalmol Vis Sci. 2010;51(12):6220-6231.

40. Sullivan DA, Liu Y, Kam WR, et al. Serum-induced differentiation of human meibomian gland epithelial cells. Invest Ophthalmol Vis Sci. 2014;55(6):3866-3877.

41. Bai Y, Nichols JJ. Advances in thickness measurements and dynamic visualization of the tear film using non-invasive optical approaches. Prog Retin Eye Res. 2017;58:28-44.

42. Olsen T. Reflectometry of the precorneal film. Acta Ophthalmol (Copenh). 1985;63(4):432-438.

43. Fogt N, King-Smith PE, Tuell G. Interferometric measurement of tear film thickness by use of spectral oscillations. J Opt Soc Am A Opt Image Sci Vis. 1998;15(1):268-275.

44. King-Smith PE, Fink BA, Fogt N, Nichols KK, Hill RM, Wilson GS. The thickness of the human precorneal tear film: evidence from reflection spectra. Invest Ophthalmol Vis Sci. 2000;41(11):3348-3359.

45. King-Smith PE, Bailey MD, Braun RJ. Four characteristics and a model of an effective tear film lipid layer (TFLL). Ocul Surf. 2013;11(4):236-245.

46. King-Smith PE, Reuter KS, Braun RJ, Nichols JJ, Nichols KK. Tear film breakup and structure studied by simultaneous video recording of fluorescence and tear film lipid layer images. Invest Ophthalmol Vis Sci. 2013;54(7):4900-4909.

47. Hamano H, Hori M, Mitsunaga S. Measurement of evaporation rate of water from the precorneal tear film and contact lenses. Contacto. 1981;25(2):7-15.

48. Nichols JJ, Mitchell GL, King-Smith PE. Thinning rate of the precorneal and prelens tear films. Invest Ophthalmol Vis Sci. 2005;46(7):2353-2361.

49. Thai LC, Tomlinson A, Doane MG. Effect of contact lens materials on tear physiology. Optom Vis Sci. 2004;81(3):194-204.

50. Cox SM, Nichols JJ. The neurobiology of the meibomian glands. Ocul Surf. 2014;12(3):167-177.

51. Chung CW, Tigges M, Stone RA. Peptidergic innervation of the primate meibomian gland. Invest Ophthalmol Vis Sci. 1996;37(1):238-245.

52. Jester JV, Rife L, Nii D, Luttrull JK, Wilson L, Smith RE. In vivo biomicroscopy and photography of meibomian glands in a rabbit model of meibomian gland dysfunction. Invest Ophthalmol Vis Sci. 1982;22(5):660-667.

53. Liu S, Hatton MP, Khandelwal P, Sullivan DA. Culture, immortalization, and characterization of human meibomian gland epithelial cells. Invest Ophthalmol Vis Sci. 2010;51(8):3993-4005.

54. Truong S, Cole N, Stapleton F, Golebiowski B. Sex hormones and the dry eye. Clin Exp Optom. 2014;97(4):324-336.

55. Suzuki T, Schirra F, Richards SM, Jensen RV, Sullivan DA. Estrogen and progesterone control of gene expression in the mouse meibomian gland. Invest Ophthalmol Vis Sci. 2008;49(5):1797-1808.

56. Schaumberg DA, Buring JE, Sullivan DA, Dana MR. Hormone replacement therapy and dry eye syndrome. JAMA. 2001;286(17):2114-2119.

57. Nichols KK, Foulks GN, Bron AJ, et al. The international workshop on meibomian gland dysfunction: executive summary. Invest Ophthalmol Vis Sci. 2011;52(4):1922-1929.

58. Nelson JD, Shimazaki J, Benitez-del-Castillo JM, et al. The international workshop on meibomian gland dysfunction: report of the definition and classification subcommittee. Invest Ophthalmol Vis Sci. 2011;52(4):1930-1937.

59. Korb DR, Henriquez AS. Meibomian gland dysfunction and contact lens intolerance. J Am Optom Assoc. 1980;51(3):243-251.

60. Gutgesell VJ, Stern GA, Hood CI. Histopathology of meibomian gland dysfunction. Am J Ophthalmol. 1982;94(3):383-387.

61. Green-Church KB, Butovich I, Willcox M, et al. The international workshop on meibomian gland dysfunction: report of the subcommittee on tear film lipids and lipid-protein interactions in health and disease. Invest Ophthalmol Vis Sci. 2011;52(4):1979-1993.

62. Chen J, Nichols KK. Comprehensive shotgun lipidomics of human meibomian gland secretions using MS/MS(all) with successive switching between acquisition polarity modes. J Lipid Res. 2018;59(11):2223-2236.

63. Chen J, Green KB, Nichols KK. Quantitative profiling of major neutral lipid classes in human meibum by direct infusion electrospray ionization mass spectrometry. Invest Ophthalmol Vis Sci. 2013;54(8):5730-5753.

64. Butovich IA, Uchiyama E, McCulley JP. Lipids of human meibum: mass-spectrometric analysis and structural elucidation. J Lipid Res. 2007;48(10):2220-2235.

65. Butovich IA. Cholesteryl esters as a depot for very long chain fatty acids in human meibum. J Lipid Res. 2009;50(3):501-513.

66. Butovich IA. Fatty acid composition of cholesteryl esters of human meibomian gland secretions. Steroids. 2010;75(10):726-733.

67. Butovich IA. Lipidomic analysis of human meibum using HPLC-MSn. Methods Mol Biol. 2009;579:221-246.

68. Butovich IA, Uchiyama E, Di Pascuale MA, McCulley JP. Liquid chromatography-mass spectrometric analysis of lipids present in human meibomian gland secretions. Lipids. 2007;42(8):765-776.

69. Mudgil P, Torres M, Millar TJ. Adsorption of lysozyme to phospholipid and meibomian lipid monolayer films. Colloids Surf B Biointerfaces. 2006;48(2):128-137.

70. McCulley JP, Shine W. A compositional based model for the tear film lipid layer. Trans Am Ophthalmol Soc. 1997;95:79-88; discussion 88-93.

71. Cory CC, Hinks W, Burton JL, Shuster S. Meibomian gland secretion in the red eyes of rosacea. Br J Dermatol. 1973;89(1):25-27.

72. Mathers WD, Lane JA. Meibomian gland lipids, evaporation, and tear film stability. Adv Exp Med Biol. 1998;438:349-360.

73. Dass C. Fundamentals of contemporary mass spectrometry. John Wiley & Sons; 2007.

74. Simons B, Duchoslav E, Burton L, Bonner R. Molecular characterization and quantitation of lipids with high resolution accurate mass tandem MS techniques. In. Vol 4430211-01. Framingham, MA: SCIEX; 2011:1-5.

75. Murphy RC, Gaskell SJ. New applications of mass spectrometry in lipid analysis. J Biol Chem. 2011;286(29):25427-25433.

76. Xie HT, Sullivan DA, Chen D, Hatton MP, Kam WR, Liu Y. Biomarkers for Progenitor and Differentiated Epithelial Cells in the Human Meibomian Gland. Stem Cells Transl Med. 2018;7(12):887-892.

77. Hampel U, Schroder A, Mitchell T, et al. Serum-induced keratinization processes in an immortalized human meibomian gland epithelial cell line. PLoS One. 2015;10(6):e0128096.

78. Hampel U, Garreis F. The human meibomian gland epithelial cell line as a model to study meibomian gland dysfunction. Exp Eye Res. 2017;163:46-52.

79. Liu Y, Kam WR, Ding J, Sullivan DA. Effect of azithromycin on lipid accumulation in immortalized human meibomian gland epithelial cells. JAMA Ophthalmol. 2014;132(2):226-228.

80. Liu Y, Kam WR, Ding J, Sullivan DA. One man's poison is another man's meat: using azithromycin-induced phospholipidosis to promote ocular surface health. Toxicology. 2014;320:1-5.

81. Jester JV, Potma E, Brown DJ. PPARgamma Regulates Mouse Meibocyte Differentiation and Lipid Synthesis. Ocul Surf. 2016;14(4):484-494.

82. Kim SW, Xie Y, Nguyen PQ, et al. PPARgamma regulates meibocyte differentiation and lipid synthesis of cultured human meibomian gland epithelial cells (hMGEC). Ocul Surf. 2018;16(4):463-469.

83. Kim SW, Brown DJ, Jester JV. Transcriptome analysis after PPARgamma activation in human meibomian gland epithelial cells (hMGEC). Ocul Surf. 2019;17(4):809-816.

84. Janani C, Ranjitha Kumari BD. PPAR gamma gene--a review. Diabetes Metab Syndr. 2015;9(1):46-50.

85. Dozsa A, Dezso B, Toth BI, et al. PPARgamma-mediated and arachidonic acid-dependent signaling is involved in differentiation and lipid production of human sebocytes. J Invest Dermatol. 2014;134(4):910-920.

86. McDermott AM, Baidouri H, Woodward AM, et al. Short Tandem Repeat (STR) Profiles of Commonly Used Human Ocular Surface Cell Lines. Curr Eye Res. 2018;43(9):1097-1101.

87. Almeida JL, Cole KD, Plant AL. Standards for Cell Line Authentication and Beyond. PLoS Biol. 2016;14(6):e1002476.

88. Ricciotti E, FitzGerald GA. Prostaglandins and inflammation. Arterioscler Thromb Vasc Biol. 2011;31(5):986-1000.

89. Sugimoto Y, Narumiya S. Prostaglandin E receptors. J Biol Chem. 2007;282(16):11613-11617.

90. Sugimoto Y, Yamasaki A, Segi E, et al. Failure of parturition in mice lacking the prostaglandin F receptor. Science. 1997;277(5326):681-683.

91. Breyer RM, Bagdassarian CK, Myers SA, Breyer MD. Prostanoid receptors: subtypes and signaling. Annu Rev Pharmacol Toxicol. 2001;41:661-690.

92. Schachtschabel U, Lindsey JD, Weinreb RN. The mechanism of action of prostaglandins on uveoscleral outflow. Curr Opin Ophthalmol. 2000;11(2):112-115.

93. Mukhopadhyay P, Bian L, Yin H, Bhattacherjee P, Paterson C. Localization of EP(1) and FP receptors in human ocular tissues by in situ hybridization. Invest Ophthalmol Vis Sci. 2001;42(2):424-428.

94. Woodward DF, Regan JW, Lake S, Ocklind A. The molecular biology and ocular distribution of prostanoid receptors. Surv Ophthalmol. 1997;41 Suppl 2:S15-21.

95. Schlotzer-Schrehardt U, Zenkel M, Nusing RM. Expression and localization of FP and EP prostanoid receptor subtypes in human ocular tissues. Invest Ophthalmol Vis Sci. 2002;43(5):1475-1487.

96. Chen W, Tsai SJ, Wang CA, Tsai JC, Zouboulis CC. Human sebocytes express prostaglandin E2 receptors EP2 and EP4 but treatment with prostaglandin E2 does not affect testosterone production. Br J Dermatol. 2009;161(3):674-677.

97. Heller S, Cable C, Penrose H, et al. Intestinal inflammation requires FOXO3 and prostaglandin E2-dependent lipogenesis and elevated lipid droplets. Am J Physiol Gastrointest Liver Physiol. 2016;310(10):G844-854.

98. Hollo G. The side effects of the prostaglandin analogues. Expert Opin Drug Saf. 2007;6(1):45-52.

99. Ocklind A. Effect of latanoprost on the extracellular matrix of the ciliary muscle. A study on cultured cells and tissue sections. Exp Eye Res. 1998;67(2):179-191.

100. Hoy SM. Latanoprostene Bunod Ophthalmic Solution 0.024%: A Review in Open-Angle Glaucoma and Ocular Hypertension. Drugs. 2018;78(7):773-780.

101. Inan UU, Ermis SS, Orman A, et al. The comparative cardiovascular, pulmonary, ocular blood flow, and ocular hypotensive effects of topical travoprost, bimatoprost, brimonidine, and betaxolol. J Ocul Pharmacol Ther. 2004;20(4):293-310.

102. Hedner J, Everts B, Moller CS. Latanoprost and respiratory function in asthmatic patients: randomized, double-masked, placebo-controlled crossover evaluation. Arch Ophthalmol. 1999;117(10):1305-1309.

103. Waldock A, Snape J, Graham CM. Effects of glaucoma medications on the cardiorespiratory and intraocular pressure status of newly diagnosed glaucoma patients. Br J Ophthalmol. 2000;84(7):710-713.

104. Feldman RM. Conjunctival hyperemia and the use of topical prostaglandins in glaucoma and ocular hypertension. J Ocul Pharmacol Ther. 2003;19(1):23-35.

105. Johnstone MA. Hypertrichosis and increased pigmentation of eyelashes and adjacent hair in the region of the ipsilateral eyelids of patients treated with unilateral topical latanoprost. Am J Ophthalmol. 1997;124(4):544-547.

106. Niggemann B, Weinbauer G, Vogel F, Korte R. A standardized approach for iris color determination. Int J Toxicol. 2003;22(1):49-51.

107. Alm A, Schoenfelder J, McDermott J. A 5-year, multicenter, open-label, safety study of adjunctive latanoprost therapy for glaucoma. Arch Ophthalmol. 2004;122(7):957-965.

108. Parrish RK, Palmberg P, Sheu WP, Group XLTS. A comparison of latanoprost, bimatoprost, and travoprost in patients with elevated intraocular pressure: a 12-week, randomized, masked-evaluator multicenter study. Am J Ophthalmol. 2003;135(5):688-703.

109. Suominen S, Valimaki J. Bilateral anterior uveitis associated with travoprost. Acta Ophthalmol Scand. 2006;84(2):275-276.

110. Wand M, Shields BM. Cystoid macular edema in the era of ocular hypotensive lipids. Am J Ophthalmol. 2002;133(3):393-397.

111. Taketani Y, Yamagishi R, Fujishiro T, Igarashi M, Sakata R, Aihara M. Activation of the prostanoid FP receptor inhibits adipogenesis leading to deepening of the upper eyelid sulcus in prostaglandin-associated periorbitopathy. Invest Ophthalmol Vis Sci. 2014;55(3):1269-1276.

112. Kam WR, Liu Y, Ding J, Sullivan DA. Do Cyclosporine A, an IL-1 Receptor Antagonist, Uridine Triphosphate, Rebamipide, and/or Bimatoprost Regulate Human Meibomian Gland Epithelial Cells? Invest Ophthalmol Vis Sci. 2016;57(10):4287-4294.

113. Tu EY. Balancing antimicrobial efficacy and toxicity of currently available topical ophthalmic preservatives. Saudi J Ophthalmol. 2014;28(3):182-187.

114. Steven DW, Alaghband P, Lim KS. Preservatives in glaucoma medication. Br J Ophthalmol. 2018;102(11):1497-1503.

115. Freeman P, Kahook M. Preservatives in topical ophthalmic medications: historical and clinical perspectives. Expert Rev Ophthalmol. 2009;4:59-64.

116. Pereira B, Tagkopoulos I. Benzalkonium chloride: uses, regulatory status, and microbial resistance. Applied and Environmental Microbiology. 2019;85(13):1-13.

117. Tripathi BJ, Tripathi RC, Kolli SP. Cytotoxicity of ophthalmic preservatives on human corneal epithelium. Lens Eye Toxic Res. 1992;9(3-4):361-375.

118. Chen W, Hu J, Zhang Z, et al. Localization and expression of zonula occludins-1 in the rabbit corneal epithelium following exposure to benzalkonium chloride. PLoS One. 2012;7(7):e40893.

119. Baudouin C, Labbe A, Liang H, Pauly A, Brignole-Baudouin F. Preservatives in eyedrops: the good, the bad and the ugly. Prog Retin Eye Res. 2010;29(4):312-334.

120. Pauly A, Meloni M, Brignole-Baudouin F, Warnet JM, Baudouin C. Multiple endpoint analysis of the 3D-reconstituted corneal epithelium after treatment with benzalkonium chloride: early detection of toxic damage. Invest Ophthalmol Vis Sci. 2009;50(4):1644-1652.

121. Guenoun JM, Baudouin C, Rat P, Pauly A, Warnet JM, Brignole-Baudouin F. In vitro comparison of cytoprotective and antioxidative effects of latanoprost, travoprost, and bimatoprost on conjunctiva-derived epithelial cells. Invest Ophthalmol Vis Sci. 2005;46(12):4594-4599.

122. Guenoun JM, Baudouin C, Rat P, Pauly A, Warnet JM, Brignole-Baudouin F. In vitro study of inflammatory potential and toxicity profile of latanoprost, travoprost, and bimatoprost in conjunctiva-derived epithelial cells. Invest Ophthalmol Vis Sci. 2005;46(7):2444-2450.

123. Brasnu E, Brignole-Baudouin F, Riancho L, Guenoun JM, Warnet JM, Baudouin C. In vitro effects of preservative-free tafluprost and preserved latanoprost, travoprost, and bimatoprost in a conjunctival epithelial cell line. Curr Eye Res. 2008;33(4):303-312.

124. Pisella PJ, Debbasch C, Hamard P, et al. Conjunctival proinflammatory and proapoptotic effects of latanoprost and preserved and unpreserved timolol: an ex vivo and in vitro study. Invest Ophthalmol Vis Sci. 2004;45(5):1360-1368.

125. Liang H, Pauly A, Riancho L, Baudouin C, Brignole-Baudouin F. Toxicological evaluation of preservative-containing and preservative-free topical prostaglandin analogues on a three-dimensional-reconstituted corneal epithelium system. Br J Ophthalmol. 2011;95(6):869-875.

126. Baudouin C, de Lunardo C. Short-term comparative study of topical 2% carteolol with and without benzalkonium chloride in healthy volunteers. Br J Ophthalmol. 1998;82(1):39-42.

127. Rath A, Eichhorn M, Trager K, Paulsen F, Hampel U. In vitro effects of benzalkonium chloride and prostaglandins on human meibomian gland epithelial cells. Ann Anat. 2019;222:129-138.

128. Chen X, Sullivan DA, Sullivan AG, Kam WR, Liu Y. Toxicity of cosmetic preservatives on human ocular surface and adnexal cells. Exp Eye Res. 2018;170:188-197.

129. Folch J, Lees M, Sloane Stanley GH. A simple method for the isolation and purification of total lipides from animal tissues. J Biol Chem. 1957;226(1):497-509.

130. Bi H, Krausz KW, Manna SK, Li F, Johnson CH, Gonzalez FJ. Optimization of harvesting, extraction, and analytical protocols for UPLC-ESI-MS-based metabolomic analysis of adherent mammalian cancer cells. Anal Bioanal Chem. 2013;405(15):5279-5289.

131. Teng Q, Huang W, Collette T, Ekman D, Tan C. A direct cell quenching method for cell-culture based metabolomics. Metabolomics. 2009;5:199-208.

132. Ziemanski JF, Chen J, Nichols KK. Evaluation of Cell Harvesting Techniques to Optimize Lipidomic Analysis from Human Meibomian Gland Epithelial Cells in Culture. Int J Mol Sci. 2020;21(9).

133. Xia J, Psychogios N, Young N, Wishart DS. MetaboAnalyst: a web server for metabolomic data analysis and interpretation. Nucleic Acids Res. 2009;37(Web Server issue):W652-660.

134. Riss TL, Moravec RA, Niles AL, et al. Cell Viability Assays. In: Sittampalam GS, Grossman A, Brimacombe K, et al., eds. Assay Guidance Manual. Bethesda (MD)2016.

135. Liu Y, Kam WR, Ding J, Sullivan DA. Effect of azithromycin on lipid accumulation in immortalized human meibomian gland epithelial cells. JAMA Ophthalmology. 2013.

136. Liu Y, Ding J. The combined effect of azithromycin and insulin-like growth factor-1 on cultured human meibomian gland epithelial cells. Invest Ophthalmol Vis Sci. 2014;55(9):5596-5601.

137. Stetten D, Schoenheimer R. The Conversion of Palmitic Acid into Stearic and Palmitoleic Acids in Rats. J Biol Chem. 1940;133:329-345.

138. Asano N, Hampel U, Garreis F, et al. Differentiation Patterns of Immortalized Human Meibomian Gland Epithelial Cells in Three-Dimensional Culture. Invest Ophthalmol Vis Sci. 2018;59(3):1343-1353.

139. Woodward DF, Liang Y, Krauss AH. Prostamides (prostaglandin-ethanolamides) and their pharmacology. Br J Pharmacol. 2008;153(3):410-419.

140. Casimir DA, Miller CW, Ntambi JM. Preadipocyte differentiation blocked by prostaglandin stimulation of prostanoid FP2 receptor in murine 3T3-L1 cells. Differentiation. 1996;60(4):203-210.

141. Reginato MJ, Krakow SL, Bailey ST, Lazar MA. Prostaglandins promote and block adipogenesis through opposing effects on peroxisome proliferator-activated receptor gamma. J Biol Chem. 1998;273(4):1855-1858.

142. Ueno T, Fujimori K. Novel suppression mechanism operating in early phase of adipogenesis by positive feedback loop for enhancement of cyclooxygenase-2

expression through prostaglandin F2alpha receptor mediated activation of MEK/ERK-CREB cascade. FEBS J. 2011;278(16):2901-2912.

143. Sjoquist B, Stjernschantz J. Ocular and systemic pharmacokinetics of latanoprost in humans. Surv Ophthalmol. 2002;47 Suppl 1:S6-12.

144. Shen JW, Shan M, Peng YY, Fan TJ. Cytotoxic Effect of Latanoprost on Human Corneal Stromal Cells in vitro and its Possible Mechanisms. Curr Eye Res. 2017;42(4):534-541.

145. Walsh K, Jones L. The use of preservatives in dry eye drops. Clin Ophthalmol. 2019;13:1409-1425.

146. Chang C, Zhang AQ, Kagan DB, Liu H, Hutnik CM. Mechanisms of benzalkonium chloride toxicity in a human trabecular meshwork cell line and the protective role of preservative-free tafluprost. Clin Exp Ophthalmol. 2015;43(2):164-172.

147. Maldve RE, Kim Y, Muga SJ, Fischer SM. Prostaglandin E(2) regulation of cyclooxygenase expression in keratinocytes is mediated via cyclic nucleotide-linked prostaglandin receptors. J Lipid Res. 2000;41(6):873-881.

148. Yousufzai SY, Ye Z, Abdel-Latif AA. Prostaglandin F2 alpha and its analogs induce release of endogenous prostaglandins in iris and ciliary muscles isolated from cat and other mammalian species. Exp Eye Res. 1996;63(3):305-310.

149. Yu K, Bayona W, Kallen CB, et al. Differential activation of peroxisome proliferator-activated receptors by eicosanoids. J Biol Chem. 1995;270(41):23975-23983.

150. Herron JM, Hines KM, Tomita H, Seguin RP, Cui JY, Xu L. Multi-omics investigation reveals benzalkonium chloride disinfectants alter sterol and lipid homeostasis in the mouse neonatal brain. Toxicol Sci. 2019.

151. Georgiev GA, Yokoi N, Ivanova S, Krastev R, Lalchev Z. Surface chemistry study of the interactions of pharmaceutical ingredients with human meibum films. Invest Ophthalmol Vis Sci. 2012;53(8):4605-4615.

152. Hampel U, Kruger M, Kunnen C, Garreis F, Willcox M, Paulsen F. In vitro effects of docosahexaenoic and eicosapentaenoic acid on human meibomian gland epithelial cells. Exp Eye Res. 2015;140:139-148.